# Dpp dispersal in the *Drosophila melanogaster* wing disc

**Inauguraldissertation**
zur
Erlangung der Würde eines Doktors der Philosophie
vorgelegt der
Philosophisch-Naturwissenschaftlichen Fakultät
der Universität Basel
von

Niklas Simon

aus Karlsruhe, Deutschland

Basel, 2024

Genehmigt von der Philosophisch-Naturwissenschaftlichen Fakultät

auf Antrag von

Prof. Dr. Markus Affolter

Prof. Dr. Peter Scheiffele

Prof. Dr. Jean-Paul Vincent

Dr. Shinya Matsuda

Basel, den 20/09/2022

Prof. Dr. Marcel Mayor

Dekan

# Table of Contents

# 1 Acknowledgment

First of all, I want to thank Shinya Matsuda for hiring me and giving me this great opportunity to work on this project. He taught me all the basics about fly work and Dpp whereof I had no idea when I started this PhD. Also thanks for pushing me to work as scientifically correct as possible and for long discussions about the project, pushing me to think and engage more on the science behind it.

I want to thank Prof. Markus Affolter for taking me in his great lab and supporting me during this PhD. His enthusiasm about science is really infectious and scientific discussions with him always leaves you more motivated to continue on your project.

I thank the members of my scientific committee, Prof. Peter Scheiffele and Prof. Jean-Paul Vincent for their time and scientific input.

I would like to thank Giorgos Pyrowolakis for his generosity in sharing his fly stocks with me throughout my whole PhD. Generating all these stocks myself would have needed the time of a second PhD.

Of course I thank all the current and former members of the Affolter lab. In particular Gustavo Aguilar for being an awesome friend and scientist who was always there for me to discuss my results and give great advice about how to interpret and analyze data and on how to have some gluten-free beer for closing time. Also special thanks to Sheida (for moral support), Milena (for all the walks to Coop), Cindy (for the talks in the morning when no one else was around), Daniel (for loosening up the daily lab routine with some football talk), Maria (for distracting me from work to talk about all kind of things) and Ludovico (for always spreading good mood).

I would also like to thank all the members of the Imaging core facility and the Biozentrum kitchen for all the things we take for granted, if it is washed beakers or functioning microscopes. Also many thanks to Helen for taking care of all our non-scientific problems and to Martin for taking care of all the scientific and technical problems in the lab.

At this point I truly want to thank my family for always being there for me and supporting me during all these years.

Last, but not least, I want to thank Antonia for being awesome and always supportive in everything I do. I'm truly happy to have you in my life.

# 2 List of Abbreviations

| | |
|---|---|
| Aa | Amino acid |
| Ap | Apterous |
| A/P | Anterior/Posterior |
| Bam | Bag of marbels |
| BMP | Bone morphogenetic protein |
| Botv | Brother of tout-velu |
| Brk | Brinker |
| Btl | Breathless |
| Ci | Cubitus interruptus |
| Co-Smad | Common-mediator Smad |
| Dad | Daugthers against Dpp |
| Dally | Division abnormally delayed |
| Dlp | Dally-like protein |
| D/V | Dorsal/Ventral |
| Dpp | Decapentaplegic |
| ECM | Extracellular Matrix |
| EGFR | Epidermal growth factor receptor |
| En | Engrailed |
| FCS | Fluorescent correlation spectroscopy |
| FGF | Fibroblast growth factor |
| Flp | Flippase |
| FRAP | Fluorescence Recovery After Photobleaching |
| FRT | Flippase recognition site |
| GAG | Glycosaminoglycan |
| Gbb | Glass bottom boat |
| GFP | Green fluorescent protein |

| | |
|---|---|
| GPC | Glypican |
| GPI | Glycosylphosphatidylinositol |
| GSC | Germline stem cell |
| HA | Hemagglutinin |
| Hb | Hunchback |
| Hh | Hedgehog |
| HS | Heparan sulfate |
| HSPG | Heparan sulfate Proteoglycan |
| ISC | Intestinal stem cells |
| Mad | Mothers agains Dpp |
| mRNA | messenger ribonucleic acid |
| NGS | Normal goat serum |
| Omb | Optomotor blind |
| PBS | Phosphate Buffered Saline |
| PCR | Polymerase chain reaction |
| PFA | Paraformaldehyde |
| pMad | Phospho-mothers against Dpp |
| Ptc | Patched |
| Put | Punt |
| R-Smad | Regulatory Smad |
| Sal | Spalt |
| ScFv | Single chain variable Fragment |
| Scw | Srew |
| Sfl | Sulfateless |
| Sgl | Sugarless |
| Shh | Sonic Hedgehog |
| Shi | Shibire |
| Shn | Schnurri |
| Sna | Snail |
| Sog | Short gastrulation |

| | |
|---|---|
| Sotv | Sister of tout-velu |
| TGF | Transforming growth factor |
| Tkv | Thickveins |
| Ts | Temperature |
| Tsg | Twisted gastrulation |
| Ttv | Tout-velu |
| UAS | Upstream activation sequence |
| Vg | Vestigial |
| Vn | Vein |
| Wg | Wingless |
| Wnt | Wingless-related integration site |
| Wt | Wild-type |
| YFP | Yellow fluorescent protein |

# 3 Abstract

Bone morphogenetic proteins (BMPs) are members of the transforming growth factor beta (TGF-β) superfamily and have been shown to be important for many developmental processes (Balemans & Van Hul, 2002; Shi & Massagué, 2003). In the fruit fly *Drosophila melanogaster*, many investigations focus on the BMP2/4 orthologue Decapentaplegic (Dpp). In the Drosophila wing imaginal disc, Dpp is secreted in an anterior stripe at the anterior/posterior compartment border and disperses to form a concentration gradient (Lecuit et al., 1996). This gradient is disturbed in mutants encoding Heparan Sulfate (HS) modifying enzymes, such as Sulfateless (Sulf) (Belenkaya et al., 2004) and Sugarless (Sgl) (Bornemann et al., 2004). HS chains are part of the Heparan Sulfate Proteogylcans (HSPGs) and important for their function.

In the Drosophila wing imaginal disc, two glypicans, Division abnormally delayed (Dally) and Dally-like (Dlp) are present on the cell surface. Both have been demonstrated to be important for morphogen function, however, how the distinct glypicans control Dpp distribution and signaling through HS remains largely unknown. In the present study, the roles of the glypicans for Dpp function was analyzed by classical means and extended by novel approaches.

I first found that, although glypicans are modified by HS, only Dally is required for Dpp gradient formation and signaling through interaction of its core protein with Dpp. I then found that Dally is largely dispensable for transporting or recycling of Dpp, but it is required for Dpp stability on the cell surface through antagonizing Tkv-mediated internalization trough the HS chains. Interestingly I found that direct interaction of Dally and Dpp appears to be largely dispensable.

Taken together, these result provide new insights into how glypicans control morphogen functions during development.

# Introduction

# 4 Introduction

## 4.1 Developmental Biology

Cells are what distinguish living things like humans, trees or mushrooms from non-living things like stones or cars. All living things consist of cells, the smallest one of one single cell, more complex ones out of billions of cells. Every multicellular organism consists of a variety of different cell types, which communicate with each other, execute different functions and make up an entire organism out of one single cell during development. For decades, scientists came to consider the issue of how animals develop from an embryo to a fully grown adult. Even Aristotle tried to explain how a morphological form is achieved in the offspring, although he did not know yet the concept of a cell (Aristotle and Peck, 1965.). Yet, it took until 1604 when Fabricius published the first illustrated text about embryology (Adelman, 1967) and another 47 years to publish the first unified principle of development and reproduction by William Harvey (Chauvois and Harvey, 1957). However, all these books were written before Antoni van Leeuwenhoek discovered and described the cell in 1665 (Dobell, 1960).

The prevailing idea during the middle age was that the future structure is already present in the embryo just in a smaller form and then grows bigger during development. This perception changed in the 19th century with scientists starting to rank related species and the theory of evolution by Charles Darwin. The idea of fixed species and creationism lost ground to the concept of epigenesis. In 1888, an embryologist named Wilhelm Roux performed an experiment in which he killed one cell of a two cell-stage frog embryo (Roux, 1888). The remaining cell developed into half a frog, which lead to the conclusion that different structures were already specified in the fertilized egg and its early progeny. On the contrary, when Hans Driesch performed a similar experiment in 1891 with sea urchin embryos by separating a two-cell embryo into two individual cells, he obtained perfectly formed sea urchins, just smaller in size, showing that embryo cells are not as predestined as one would have thought (Driesch, 1891). A key experiment to overcome the concept of preformation was conducted in 1924 by Spemann and Mangold who transplanted a piece from the upper blastopore lip of *Triturus cristatus* into a ventral region of the presumptive epidermis of a *Triturus taeniatus* embryo undergoing gastrulation. In this setup, the transplanted cells instructed the surrounding cells to form a second embryo, showing that a piece of the upper blastopore lip transplanted to

another embryo is sufficient to instruct the formation of a partial second embryo (Spemann & Mangold, 1924). These experiments indicated that cells must communicate with each other. In the 1930s, scientists claimed there would be gradients of molecules, acting very much like hormones. Joseph Needham labeled these molecules `morphogenetic hormone` (Needham, 1942).

## 4.2 Morphogens

In an experiment performed by the American embryologist Thomas Hunt Morgan, a connection between polarity and protein gradients was proposed. When Morgan cut earthworms, he observed that heads would regenerate slower the further back the cut was performed. He concluded there must be some kind of "head material" which declines from anterior to posterior and by that, forms a gradient, which is important for head development. Nonetheless, he was unable to explain how such a gradient would generate differentiated patterns and cell fates during development (Rewieved in Rogers & Schier, 2011a). In 1952, the famous mathematician, Alan Turing came up with the theoretical framework of how secreted molecules can instruct differentiated patterns (Turing, 1990). He stated that simple diffusion through a tissue could be sufficient to build a gradient, and also proposed to call such diffusing substances morphogens.

In 1969, Lewis Wolpert published a paper entitled "Positional Information and the Spatial Pattern of Cellular Differentiation", in which he introduced the French flag problem (Wolpert, 1969). In this analogy, the pattern of the French flag (the blue, white and red) stands for the pattern of a tissue in an organism. He wondered how such lines of cells of the same colour develop the French flag and how such patterns could develop irrespective of the number of cells in the line (Fig. 4.1). As an answer to these questions, he proposed that cells could read out their position from a gradient whose concentration is fixed at the start and the end. A diffusible morphogen is produced locally at the source and diffuses through the tissue, generating a gradient, which can provide the positional information for the cells. In 1970, Francis Crick extended the model by introducing the source-sink model (Crick, 1970). In this model, the morphogen is produced in a source of cells, spreads through the tissue and on the way gets degraded by the receiving cells, thereby forming a gradient.

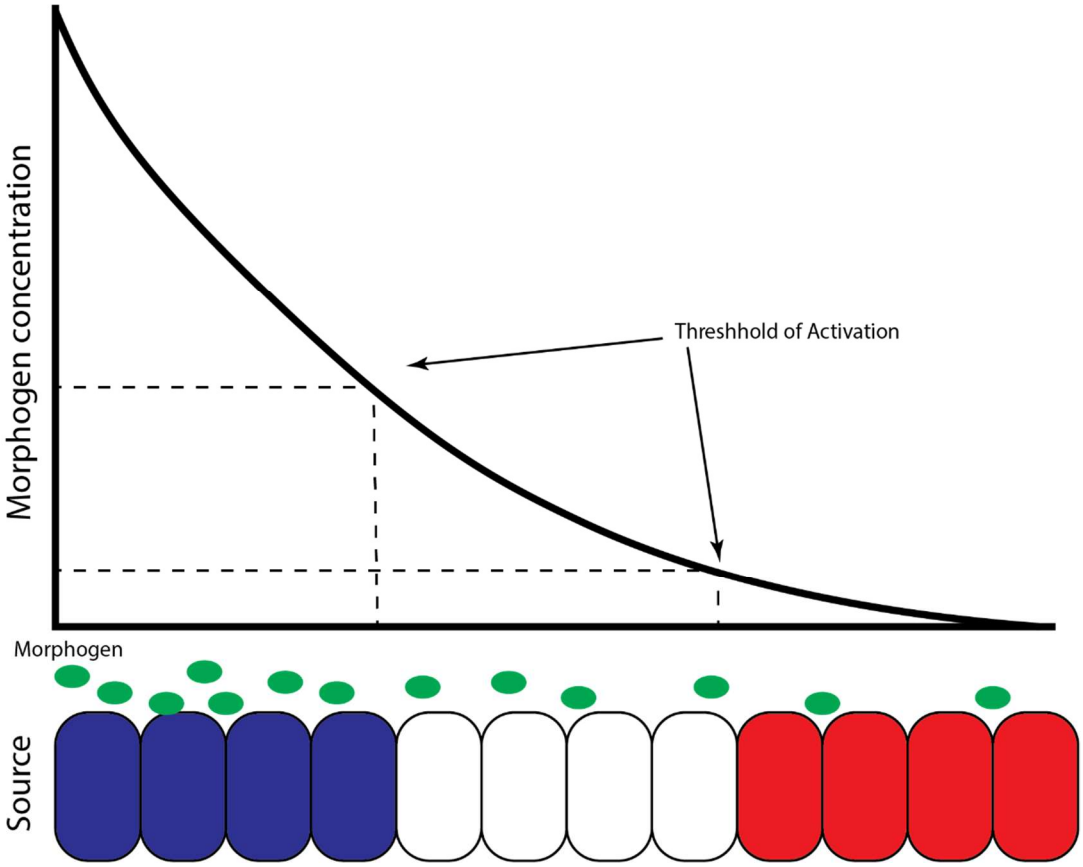


***Figure 4.1: French Flag model.***
*From the producing cells (source) on the left side, the morphogen (green) spreads to the surrounding tissue to form a concentration gradient. The cells on the way can sense the concentration and adopt distinct cell fates in a threshold response. In the French flag model of Wolpert, cells close to the source sense high concentrations of morphogen and adopt a blue fate, cells in a medium distance sense less morphogen and adopt a white fate and cells far away from the source sense low morphogen levels and adopt a red fate. Modified from Hamaratoglu et al., 2011.*

A lot of theoretical work has been published on morphogens, but the proof for the existence of morphogens and their importance in gradient formation was still missing, until in 1988 Wolfgang Driever and Christiane Nüsslein-Volhard described the first morphogen, Bicoid in Drosophila (Driever & Nüsslein-Volhard, 1995). Bicoid protein is translated from anteriorly localized mRNA transcripts in the drosophila embryo, forms an anterior to posterior gradient and by doing so, activates *hunchback* transcription in the anterior region where Bicoid concentration is high. Although Bicoid disperses and forms a gradient, it is not considered as a classical morphogen, since it is a transcription factor, which is unlikely to have access to the extracellular space. It is important to mention that Bicoid acts in the embryonic syncytium, where no cells are present and Bicoid can thus reach the nuclei directly. Nowadays, many secreted morphogens, such as Bone morphogenetic proteins (BMPs), Hedgehog (Hh), Wingless-related integration site (Wnt), Fibroblast growth factor (Fgf) or retinoic acid are

known (Heyman et al., 1992; Nusse & Varmus, 1982; Nüsslein-Volhard & Wieschaus, 1980; Ornitz & Itoh, 2001; Spencer et al., 1982).

Furthermore, it remains unclear whether and how morphogen gradients adapt to tissue growth. How do morphogens regulate the matching of patterns to size? Scaling is an old subject in biology and still not fully understood. How can two individuals of the same species have different sizes, but with patterns identical in proportions? Scaling of patterns with tissue size can be observed between the same tissues of one species with different genetic or environmental background and also between the same tissue from different species with different size (Akiyama & Gibson, 2015). Since it is known that the patterning of many body parts depends on morphogen function, they too, must be scaled appropriately. The scaling of the morphogens is not addressed in the French flag model and, to date, it remains unclear how it is achieved at the molecular level.

Anyhow, morphogens are most often locally produced, secreted signaling molecules that act over long distances and control growth and patterning within a region of tissue in a concentration dependent manner (Sagner & Briscoe, 2017). Their concentration can subdivide cells into different cell types, leading to pattern formation and eventually to differential tissue architecture.

Although morphogens are widely studied, there remain open questions in the field, such as: how do morphogens control patterning, how do morphogen gradients control uniform growth, how are patterning and growth coordinated and how are gradients formed?

To form a proper morphogen gradient, three main steps are crucial: production, dispersal and removal of the morphogen. The relationship between these different parameters can be described in the following formula:

$$c(x)=c_0 e^{-\frac{x}{\lambda}} \qquad c_0=\frac{j0}{\sqrt{Dk}} \qquad \lambda=\sqrt{\frac{D}{k}}$$

c(x)=concentration at distance x, $c_0$=concentration at x=0, $j_0$=flux at source boundary, D=diffusion constant, k=degradation rate and λ=decay length. The size of the morphogen gradient depends on the concentration on the source boundary ($c_0$) and the gradient decay length (λ). The decay length λ depends on the diffusion constant D and the degradation rate k. If degradation is decreased, the gradient decay length will increase and the gradient will flatten. However, if the diffusion constant D is decreased, the gradient will be shorter. If the

production, or the concentration at the source boundary, $c_0$ is decreased, the gradient will be shortened (formula from Wartlick et al., 2009). This illustrates that to ensure proper development, the morphogen gradient needs to be regulated at many levels. Although all the levels were considered, the focus of this thesis lies in morphogen transport, thus the next chapter will elucidate in more detail how morphogens are transported in developing tissues.

## 4.3 Mechanisms of Morphogen gradient formation

Today we can distinguish two ways of how a morphogen gradient is formed. In the first scenario, the morphogen is present throughout the tissue before it accumulates in a specific area (Fig. 4.2A). This happens in the case of Decapentaplegic (Dpp) in the Drosophila embryo (Fig. 4.2B). Dpp is secreted from cells in the entire dorsal side of the embryo, but is then shuttled to the dorsal midline and accumulates there (Mizutani et al., 2005; Sawala et al., 2012; Shimmi et al., 2005). Moreover, in Xenopus, BMP4 is produced in the animal cap and ventrolateral marginal zone and then shuttled to the ventral pole (Hawley et al., 1995) (Fig. 4.2C).

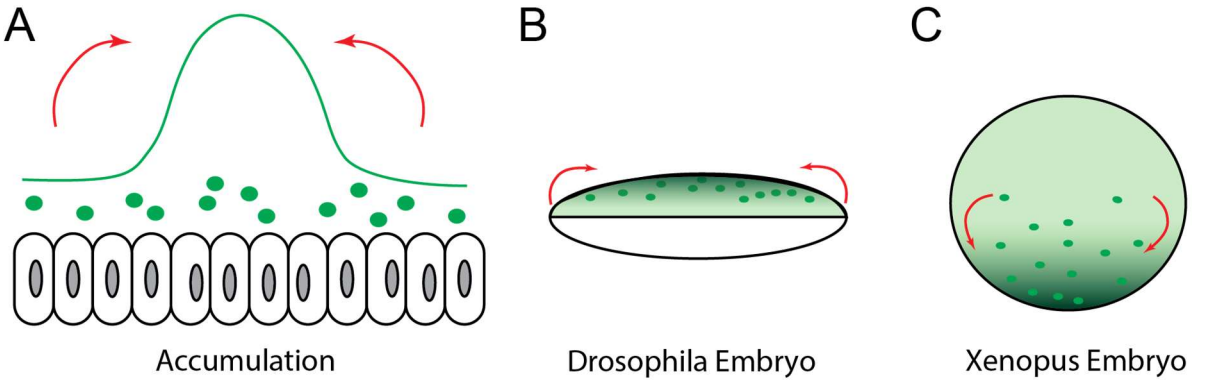


***Figure 4.2: Morphogen gradient formation by accumulation.***
*One way to establish a morphogen gradient is through accumulation of the morphogen in a specific area. The morphogen is widely produced in the tissue and then accumulated in a specific area. By transporting and accumulating the morphogen in one area, a concentration gradient is established.*

In the second scenario, the morphogen is produced in a local source and spreads from the source to the surrounding tissue to form a concentration gradient (Fig. 4.3A). A classic example is Dpp in the Drosophila wing disc, in which Dpp is produced in the anterior part of the wing disc close to the compartment boundary and spreads to form two gradients (Matsuda & Affolter, 2017; Teleman & Cohen, 2000) (Fig.4.3B). Furthermore, in the vertebrate limb bud,

Sonic Hedgehog (Shh) is produced in the posterior side and spreads to the surrounding anterior tissue to specify future digit regions (Tickle & Towers, 2017) (Fig. 4.3C).

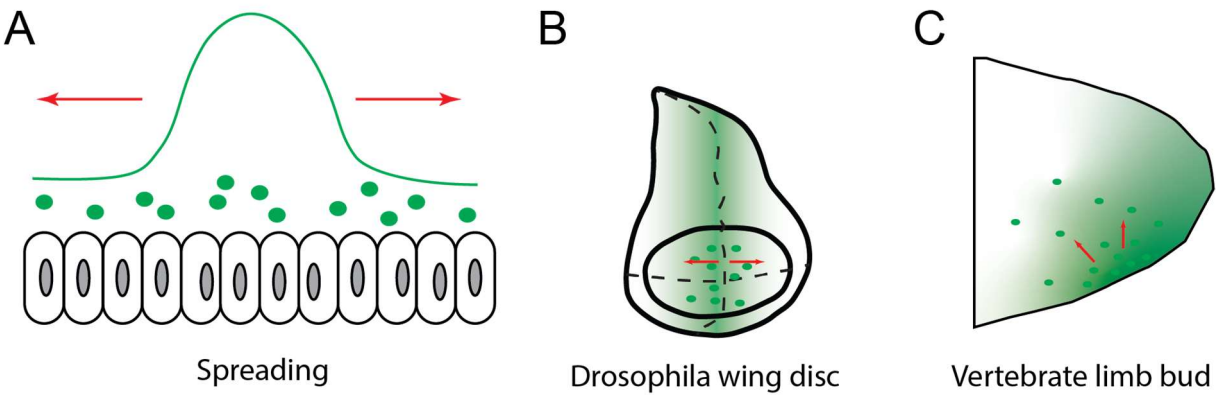


***Figure 4.3: Morphogen gradient formation by spreading.***
*The morphogen gradient can be established by spreading from a source to the surrounding tissue. In this model, the morphogen is produced in a specific source and spreads to the sourrounding cells. By spreading a concentration gradient is established.*

While these are two different scenarios of how a gradient can be formed, they do not explain how the morphogen itself diffuses or disperses through the tissue to form a concentration gradient. Over the years, many different ways of how morphogens spread through tissues have been discovered, proven and disproven again.

Morphogen dispersal models can be divided into two categories: cell-based and diffusive. While cell-based models always contain a cellular mechanism to transport the morphogen, the diffusive models predict morphogens to diffuse freely via a random walk through the tissue (Muller et al., 2013). To date five major models for morphogen dispersal have been proposed. Three cell-based models (facilitated transport, transcytosis and cytonemes) and two diffusive models (free diffusion and hindered diffusion).

### *4.3.1 Free diffusion*

Free diffusion is the simplest and most straight forward concept for morphogen dispersal (Fig. 4.4A). In this model the morphogen disperses freely, without help of other molecules. The movements are random and not directed and the diffusion speed is modified by the viscosity of the surrounding medium, the temperature and the size of the morphogen. However, freely diffusing substances would not form a gradient, but would rather disperse to form a uniform distribution. To form a gradient, a "sink" needs to be in place, which could be achieved by receptor-mediated degradation. Anyhow, free diffusing particles in the extracellular matrix

are considered to be fast. The measured diffusion coefficient for GFP in water is roughly 80$\mu m^2 sec^{-1}$ (Petrášek & Schwille, 2008), which would be sufficiently fast for gradient formation during development. Yet, it has been shown that a secreted form of GFP fails to form a gradient (Entchev et al., 2000), which raises the question whether these measurements of GFP diffusion speed represent any useful information which can be used to interpret morphogen dispersal *in vivo*. Furthermore, studies in the zebrafish neural tube with fluorescently tagged fibroblast growth factor 8, yielded high diffusion speeds of 50–90 $\mu m^2$ $sec^{-1}$, consistent with free diffusion (Yu et al., 2009). However, the measured diffusion speed of a GFP-tagged version of Dpp in Drosophila yielded diffusion speeds of only 0.1 $\mu m^2$ $sec^{-1}$ (Kicheva et al., 2007), arguing against free diffusion. Anyhow, it remains unclear whether free diffusion can form a gradient with the precision and robustness needed for patterning (Kerszberg & Wolpert, 2007). This difficulty could be solved with a feedback regulation of the extracellular morphogen distribution (Umulis, 2009).

### *4.3.2 Hindered diffusion*

The extracellular matrix contains many molecules, either floating or bound to cell surfaces (Fig. 4.4B). In the "Hindered diffusion" model, the morphogen spreads freely but interacts with some of these molecules, in contrast to the free diffusion model, in a reversible manner. This interaction blocks or slows down morphogen dispersal. Slowing down the dispersal of a morphogen can enhance the steepness of the gradient by concentrating it close to the source. This has been shown in the vertebrate neural tubes where the Shh range is modulated and enhanced by binding to Proteoglycans, thereby slowing down the transport (Saha & Schaffer, 2006).

### *4.3.3 Facilitated transport*

In the facilitated transport model, the morphogen requires another molecule to generate a concentration gradient. These molecules, called facilitators, can be bound to the cell surface or freely floating in the extracellular matrix. The facilitator enables morphogen mobility; in their absence the morphogen is not mobile or its mobility is at least strongly affected. There are different ways a facilitator can act on the morphogen. Shuttling of the morphogen is one way for facilitated transport (Fig. 4.4D). Shuttling can result in the overall oriented transport of an otherwise randomly dispersing molecule, eventually building up a gradient. In another

way the facilitator and the extracellular binding molecule compete for the binding of the morphogen (Fig. 4.4C). Without the facilitator, the morphogen remains bound and immobile. It is assumed that the diffusion speed of the morphogen should be slow compared to free diffusion. Measurements conducted in the Drosophila wing imaginal disc, regarding the diffusion speed of Dpp, using Fluorescent correlation spectroscopy (FCS), revealed a diffusion speed faster than that predicted for hindered diffusion (Zhou et al., 2012). Anyhow, since FCS measures the changes of fluorescence intensity on a single molecule scale, it needs to be considered that possibly not all morphogen is bound and a small portion of unbound, free diffusing Dpp can lead to misleading results (Takada et al., 2018; Yu et al., 2009). Furthermore, experiments in the wing disc using Fluorescence Recovery After Photobleaching (FRAP) to measure Dpp diffusion speed produced relatively slow diffusion speeds (Kicheva et al., 2007), consistent with facilitated Diffusion.

Further support for the facilitated transport model comes from experiments in HSPG mutants. In mutant clones of GAG biosynthetic enzymes encoded by *sulfateless* (*sfl)*, tout-velu (*ttv)*, *brother of tout-velu* (*botv)* or sister of tout-velu (*sotv)*, BMP signaling and distribution are significantly reduced (Belenkaya et al., 2004; Bornemann et al., 2004). Leading to the assumption that HSPGs are facilitating BMP dispersal.

### *4.3.4 Transcytosis*

During gradient formation via transcytosis, morphogens travel through the cells in vesicles via repeated internalization and exocytosis (Fig. 4.4F). The ligand is internalized by endocytosis in the receiving cell, recycled via exocytosis and internalized by endocytosis by the neighboring cell. This cycle repeats until the ligand is eventually degraded in one of the receiving cells. For several years, this model was used to explain the dispersal of the Drosophila morphogen Wingless (Wg) in the wing imaginal disc. Because of the hydrophobic properties of Wg, transcytosis was a plausible way to explain Wg movement in an aqueous environment. Nonetheless, new studies found that Dally-like plays an important role in shielding the hydrophobic moiety of Wg and thereby helps it to travel through the extracellular matrix (McGough et al., 2020). Trancytosis was also considered to be the case in Dpp dispersal (Entchev et al., 2000). In the wing imaginal disc, it was shown that Dpp dispersal was dependent on dynamin-mediated endocytosis. In this experiment, the researchers blocked dynamin function in clones using a temperature sensitive *shibire* (*shi*) mutant. In these clones,

they found the endocytosis was inhibited and the Dpp gradient was reduced (Entchev et al., 2000). Furthermore, a study using FRAP also showed dynamin-dependent dispersal of GFP-tagged Dpp (Kicheva et al., 2007). However, another study showed dynamin-mediated endocytosis to be neglect-able for Dpp dispersal. The authors did not find a reduction in Dpp signaling behind *shi* mutant clones, arguing that Dpp can cross these clones (Belenkaya et al., 2004). Furthermore, a study investigating the receptor-mediated transcytosis model found no change in Dpp intensity behind receptor mutant clones in the wing imaginal disc, arguing against this model (Schwank et al., 2011).

### *4.3.5 Cytonemes*

Cytonemes are specialized, actin rich, filopodia-like cell protrusions. They can form towards morphogen producing centers, where they pick up the morphogen directly to initiate the signaling response in the receiving cell (W. Chen et al., 2017; Ramírez-Weber & Kornberg, 1999) (Fig. 4.4E). Cytonemes were first connected with signaling events in the Drosophila wing imaginal disc, where a special type of filopodia was noticed to uniformly orient towards the anterior/posterior border of the disc (Ramírez-Weber & Kornberg, 1999). Later, cytonemes were proposed to transport non-soluble morphogens such as Hh or Wnt proteins and overcome the problem of a hydrophobic protein in an aqueous environment. Cytonemes can be found in numerous organism, for example in Drosophila (Ramírez-Weber & Kornberg, 1999), zebrafish (Waghmare & Page-Mccaw, 2021), chick (Sanders et al., 2013) and even human organoids (Mattes et al., 2018). Cytonemes can be produced by the source cells, but more often cytonemes or cytoneme-like structures are produced in the receiving cells and reach out for the morphogen source. The cytonemes contain the receptor of the morphogen to allow binding and signaling induced at the place of contact (Hsiung et al., 2005). In the Drosophila air sac primordium, a precursor of the dorsal thoracic air sac, which acts directly to oxygenate the Drosophila flight muscle and is connected to the Drosophila wing imaginal disc in the larval stage, cytonemes have been proposed to pick up the morphogen FGF directly at the source in the wing disc. These cytonemes contain the FGF receptor Breathless (Btl), to enable morphogen binding (Du et al., 2018). Another example of cytoneme-mediated morphogen dispersal is the formation of the Hh gradient in the Drosophila wing disc. Here, Hh travels in vesicles along cytonemes, but also the receiving cells form cytonemes, containing the receptor Patched (Ptc), and pick up Hh from the source cells. Hh reception takes place at

membrane contact points between cytonemes produced by the source cells and cytonemes produced by the receiving cells (González-Méndez et al., 2017).

### *4.3.6 Others*

For the sake of completeness, it should be mentioned that morphogens might disperse without spreading from cell to cell. The ligand might form a gradient by cell movement or simple tissue growth. This mode of movement was demonstrated in the Drosophila embryo, where Wg moves in part by the division and roaming of Wg producing cells (Pfeiffer et al., 2000).

Furthermore, morphogens can disperse in a tissue with the help of lipophorins. Lipophorins are an assembly of lipids and proteins, which forms a spherical structure (Van der Horst & Ryan, 2005). Since lipid-modified proteins are hydrophobic, they cannot disperse freely in the extracellular space. The idea is that these proteins are transported inside of the lipophorins. Indeed, morphogens such as Hh and Wg in *Drosophila*, which are covalently modified by a lipid, have been shown to co-localize with lipophorins (Callejo et al., 2008; Panáková et al., 2005). Furthermore, a knockdown of lipophorin in Drosophila affects the function of Hh and Wg signaling, demonstrating some role in morphogen function (Panáková et al., 2005). In a more recent study on Wg in Drosophila, GFP-Wg was trapped using a membrane-tethered anti GFP nanobody and while GFP-Wg was accumulated on cells expressing this nanobody, lipophorin was not accumulated, leading to the assumption that Wg is not transported by lipophorin (McGough et al., 2020).

Exosomes have been shown to be able to conduct several signaling events in the lymphocyte lineage (Denzer et al., 2000). Knowing this function of budded vesicles, previous studies investigated the involvement of vesicles in morphogen gradient formation. They found membranous particles, which they called argosomes, to co-localize with the morphogen Wg in the Drosophila wing imaginal disc, which lead to the conclusion that argosomes are important for Wg dispersal in the wing disc (Greco et al., 2001). Further, it has been shown that HSPGs are necessary for Wg to co-localize with the argosomes (Greco et al., 2001).

Furthermore, argosomes and lipophorin might act as a kind of facilitator for morphogen dispersal, making this a form of facilitated transport.

It is Important to mention that not all morphogens must use the same mechanism, maybe some morphogens disperse differently than others. So all these models might reflect mechanisms at work *in vivo*, but not for the same morphogen. Yet, all models are not necessarily exclusive. Some of these different mechanisms may work together to form a gradient of a particular morphogen.

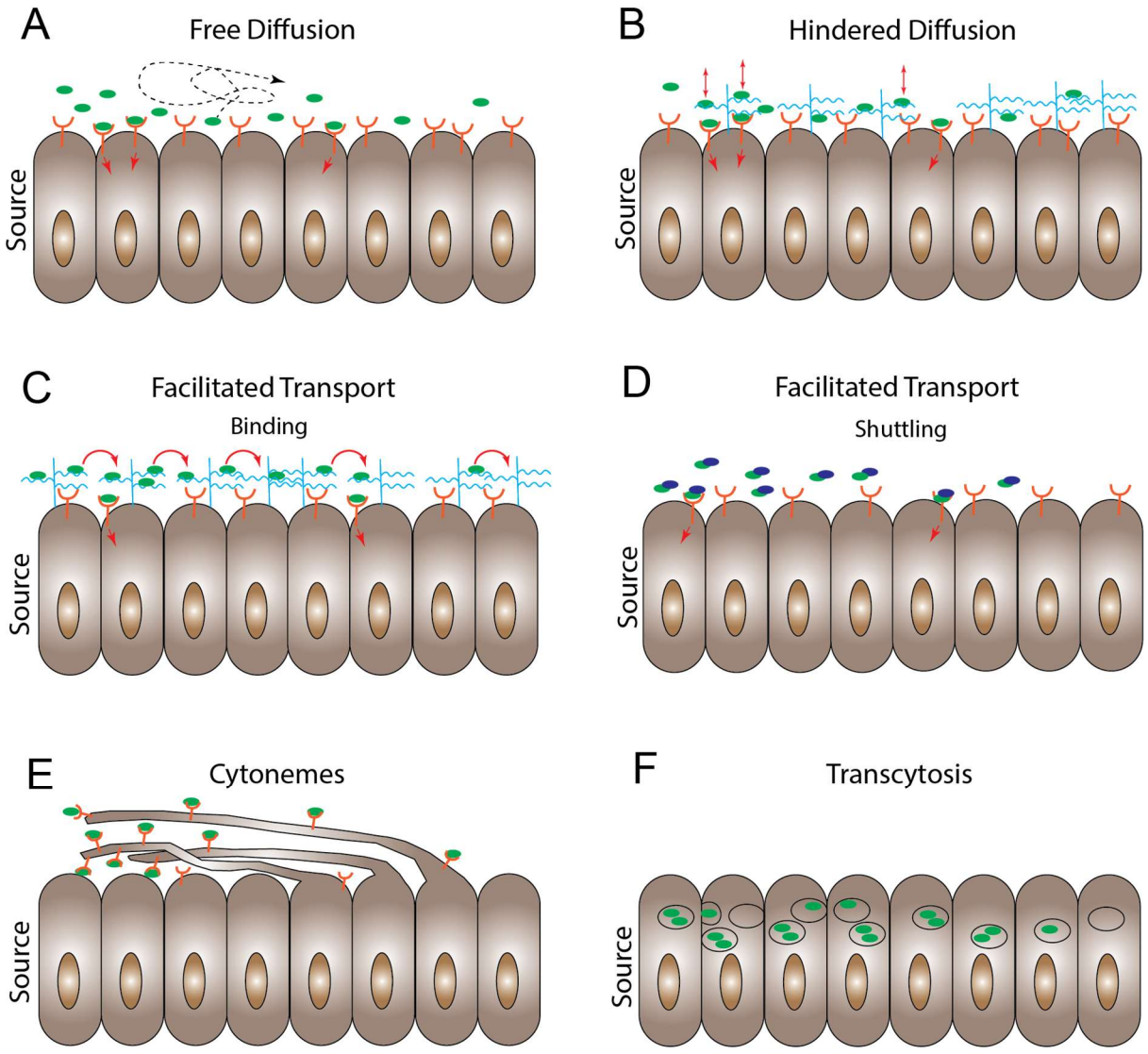


***Figure 4.4: Different models of morphogen transport.***
*(**A**) Free Diffusion model. The morphogen (green) disperses by free, random movements (dashed line) through the tissue without interacting with other molecules until they encounter a receptor (orange) and bind to it. (**B**) Hindered diffusion model. This model predicts free diffusion of the morphogen, but with occasional attachment and detachment to cell surface molecules (blue) other than receptors. In this model, on a small scale, the morphogen is diffusing fast and free, but on a larger scale, diffusion should be slow. (**C-D**) Facilitated transport model. In the facilitated transport model, the morphogen requires another molecule to spread. The facilitated transport model can be divided in two different mechanisms. In the binding model (**C**), the morphogen transport is mediated by a cell surface molecule. In the shuttling model (**D**), a shuttling molecule binds to the morphogen to facilitate the transport. (**E**) Cytonemes. The morphogen is picked up from the source by filopodia like extrusion,*

*called cytonemes, produced by the receiving cells. Some evidence also points to some systems with cytonemes being produced by the source cells and reaching out to the receiving cells to form a concentration gradient. (**F**) Transcytosis. In the transcytosis model, the morphogen travels through the cells via repeated internalization and exocytosis. The ligand is internalized by endocytosis in the receiving cell, recycled via exocytosis and taken up by the next cell again. This cycle repeats until the ligand gets degraded in one of the receiving cells.*

## 4.4 Regulation of Morphogen gradients

As morphogens move between the cells, they interact with different molecules and some of these molecules are able to alter the morphogen gradient. This regulation can be through binding leading to degradation of the morphogen, by shuttling of the morphogen or by binding of the morphogen leading to its stabilization. Many molecules interact in some way with morphogens, but the most important ones will be summarized in this chapter.

### *4.4.1 Receptors*

As morphogens move through the tissue, they can bind to receptors. This receptor-ligand binding is crucial for extracellular molecules to signal inside the cell, and provides a connection between the intra- and extracellular space. How the cells interpret morphogen signaling provided by the receptors is still a matter of debate, but two main theories are widely accepted nowadays. The cells could either measure absolute numbers of ligand-occupied receptors or the ratio of bound to unbound receptors to determine the morphogen concentration and translate it into distinct gene expression patterns. For most morphogens, absolute numbers of morphogen-bound receptors are thought to determine morphogen-responsive gene expression in the cell (Rogers & Schier, 2011b). In a study in Xenopus blastula cells, it was found that regardless of the number of receptors, a cell-bound version of the morphogen Activin can cause cells to switch gene expression over time, demonstrating that Activin signaling levels are measured in absolute numbers of morphogen-bound receptors (Dyson & Gurdon, 1998). Nevertheless, the signaling levels of a morphogen can regulate the expression of the morphogens receptor itself, which, in addition to the signal transduction, can also regulate morphogen gradient formation via receptor-mediated endocytosis. It is important to mention that the signal provided by the morphogen can lead to a higher receptor production or to a decreased receptor production. In the case of the Hh receptor Ptc, Hh signaling leads to an upregulation of receptor levels, leading to more receptors close to the source of Hh, and thereby to a shorter range of the morphogen (Y. Chen & Struhl, 1996; Li et al., 2018). For Dpp and Wg, higher signal leads to reduced receptor expression. Lower receptor

levels on the cell surface results in less receptor mediated-endocytosis and degradation of the morphogen and a wider gradient (Akiyama et al., 2008).

In summary, feedback loops can modulate the expression of receptors and thereby modulate the morphogen gradient. These feedback loops lead to more robustness of the gradient against fluctuations in morphogen production or secretion (Eldar et al., 2003; Morimura et al., 1996).

### *4.4.2 Heparan sulfate proteoglycans*

Previous studies indicate that the heparan sulfate proteoglycans (HSPGs) play important roles in morphogen gradient formation. HSPGs are cell-surface macromolecules with at least one glycosaminoglycan (GAG) chain attached to the core protein (Häcker et al., 2005; Sarrazin et al., 2011). They can be found on all cell types in an animals' body and all classes of HSPG possess at least 2 GAG chains attached to the core protein, while the extracellular matrix proteoglycans mostly hold chondroitin sulfate (CS) chains, the membrane-bound HSPGs mostly hold heparan sulfate (HS) chains. GAG chains are long, unbranched polysaccharide chains synthesized in the Golgi apparatus, where they are attached to a serine residue on the core protein (Häcker et al., 2005). In glypicans, these HS chains can be rather conserved (Lawrence et al., 2008). However, various GAG modifying enzymes are known, for example EXT1 and EXT2 in mammals, to catalyze the assembly of the 25-100 repeating disaccharide units of the GAG chains (Annaval et al., 2020). The EXT1 and EXT2 enzymes, together with other enzymes involved in the biosynthesis of GAG, are highly conserved in animals (Bornemann et al., 2004). Thus, mutations in these enzymes in different model organisms resulted in disrupted morphogen function (Bellaiche et al., 1998; Shieh et al., 2014; Wiweger et al., 2012). Furthermore, after assembly of the GAG chains, the latter are further processed by sulfation through sulfotransferases. These sulfation patterns have been proven critical for morphogen-HS interaction (Sarrazin et al., 2011). In a study of the FGF pathway in mice, overexpression of heparanase resulted in a higher HSPG turnover and upregulation of sulfation. More sulfation of the GAG chains resulted in more FGF ligand-receptor complexes, which promoted FGF signaling (Escobar, Galvis et al., 2007). In this case, HSPGs act as co-receptors by binding to ligand and receptor to form a ternary complex.

We can further categorize HSPGs into three different classes: the membrane-bound HSPGs like Syndecans, Glypicans or Betaglycan, the secretory vesicle HSPGs, such as Serglycin and the extracellular matrix (ECM) Proteoglycans such as Perlecan, Agrin and Collagen XVIII.

Depending on their class and their localization, respectively, the role of the HSPGs in morphogen function can vary. While ECM Proteoglycans are mostly found in the ECM, including the basement membrane, where they act as a kind of barrier and/or reservoir for morphogens, secretory vesicle HSPGs are secreted and thereby support ligand movement (Sarrazin et al., 2011). Membrane-bound HSPGs are anchored to the cell membrane through either a transmembrane domain (syndecan), or a glycosylphosphatidylinositol (GPI) anchor (Glypicans). Through their proximity to the cell membrane, they can act as co-receptors and mediators of endocytosis. Furthermore, it is also thought that these membrane-bound HSPGs are able to retain the ligand close to the cell surface and act as a barrier to avoid ligand leakage from the tissue. However, membrane-bound HSPGs can also be cleaved by a sheddase, leading to a distribution throughout the ECM, giving them the potential to actively shuttle ligands through the ECM (Park et al., 2000).

HSPG function in ligand distribution can be either supportive or disruptive for gradient formation. In the zebrafish, for example, the glypican Knypek is required for Wnt11 signaling (Topczewski et al., 2001). Additionally, Glypican 3 is known to interact with Wnt and its receptor Frizzled to activate the canonical Wnt pathway (M. Capurro et al., 2014). Furthermore, a loss of the Drosophila EXT1/2 homolog Ttv in the wing imaginal disc, results in inhibited Hh movement (The et al., 1999). Yet, mice mutant for EXT1 had a larger Indian Hedgehog gradient during chondrocyte differentiation, leading to more expression of Parathyroid hormone related hormone (Koziel et al., 2004).

HSPGs do not only provide an interface for morphogens to bind directly, they can also bind to many cell-surface molecules which can be important components of the signaling pathway. Examples include Ihog, a co-receptor for Hh (McLellan et al., 2006; Yao et al., 2006), the Shifted lipoprotein, which can bind Hh (Eugster et al., 2007; Glise et al., 2005; Gorfinkiel et al., 2005), and Crossveinless2, which can bind Dpp (Serpe et al., 2008). Furthermore, the interaction between HSPGs and antagonists can also be important for morphogen function. Twisted Gastrulation (Tsg), for example, enhances the inhibitory activity of Chordin on BMP. Tsg can interact with HSPGs only after it is bound to Chordin. Therefore, HSPG-Tsg binding might be essential for the antagonism of BMP signaling by Chordin (Jasuja et al., 2004).

### *4.4.3 Others*

In the classical exocytosis pathway, proteins pass through the Golgi apparatus before they are secreted (Vitale & Denecke, 1999). This also applies for most morphogens. In the Golgi all kinds of post translational modifications, like phosphorylation or glycosylation, take place (Wang & Huang, 2017). Previous studies demonstrated the importance of these post translational modifications for morphogen function (Negreiros et al., 2018; Willert et al., 2003). N-linked glycosylation of Short gastrulation (Sog) does affect the extracellular levels and distribution of Sog in the Drosophila longitudinal veins, posterior crossvein and embryo (Negreiros et al., 2018). However, glycosylation of Sog does not only affect its own range, but also the range of the morphogen Dpp, with an inhibitory effect of Sog glycosylation mutants on Dpp signaling (Negreiros et al., 2018). Furthermore, the morphogen Wnt was demonstrated to be palmitoylated. Cell culture and *in vivo* experiments in Drosophila confirmed this attachment of fatty acids to be important for Wnt signaling (Willert et al., 2003). Furthermore, a study demonstrated the importance of N-glycosylation of BMP6 for the interaction with its receptor ActR-I (Saremba et al., 2008).

## 4.5 Drosophila melanogaster and the wing imaginal disc as a model

Since all multicellular animals are believed to have arisen from a common ancestor, the fundamental principles underlying their development are thought to be very similar. Due to this, findings in one organism can lead to a broader understanding of all life forms. That is the reason why in biology and particularly in basic research, model organisms are applied. Model organisms usually have some traits that make them easy to work with and simple to experimentally manipulate in order to address a certain topic. In bacteria, most research is done in *Escherichia coli*, which is easy to cultivate on agar plates. In eucaryotes, the simplest model organism ought to be yeast, *Saccharomyces cerevisae*, which is easy to cultivate and grow. However, bacteria are procaryotes and yeast is unicellular, which makes the investigation of development rather challenging. Mice and zebrafish are powerful eucaryotic, multicellular model organisms, but their developmental period is long and their genetics and the tools to manipulate their genes are complicated or not as advanced as in the fruit fly *Drosophila melanogaster.* The big advantages of *D. melanogaster* are the relatively short life cycle of about 10 days at 25°C and the small genome consisting of four chromosomes, 140 Mbp of DNA and about 14.000 genes. To date, many fundamentals of basic genetics have been unraveled in the fruit fly *Drosophila melanogaster*.

To study the function of morphogens in patterning and growth, the Drosophila imaginal discs (Fig. 4.5A), the precursors of the fly appendages and the majority of the fly epidermis of the head and thoracic segments, are widely used. These imaginal discs share the big advantage of a very predictable development proceeding always according to the book, but at the same time they are very reactive to genetic manipulations.

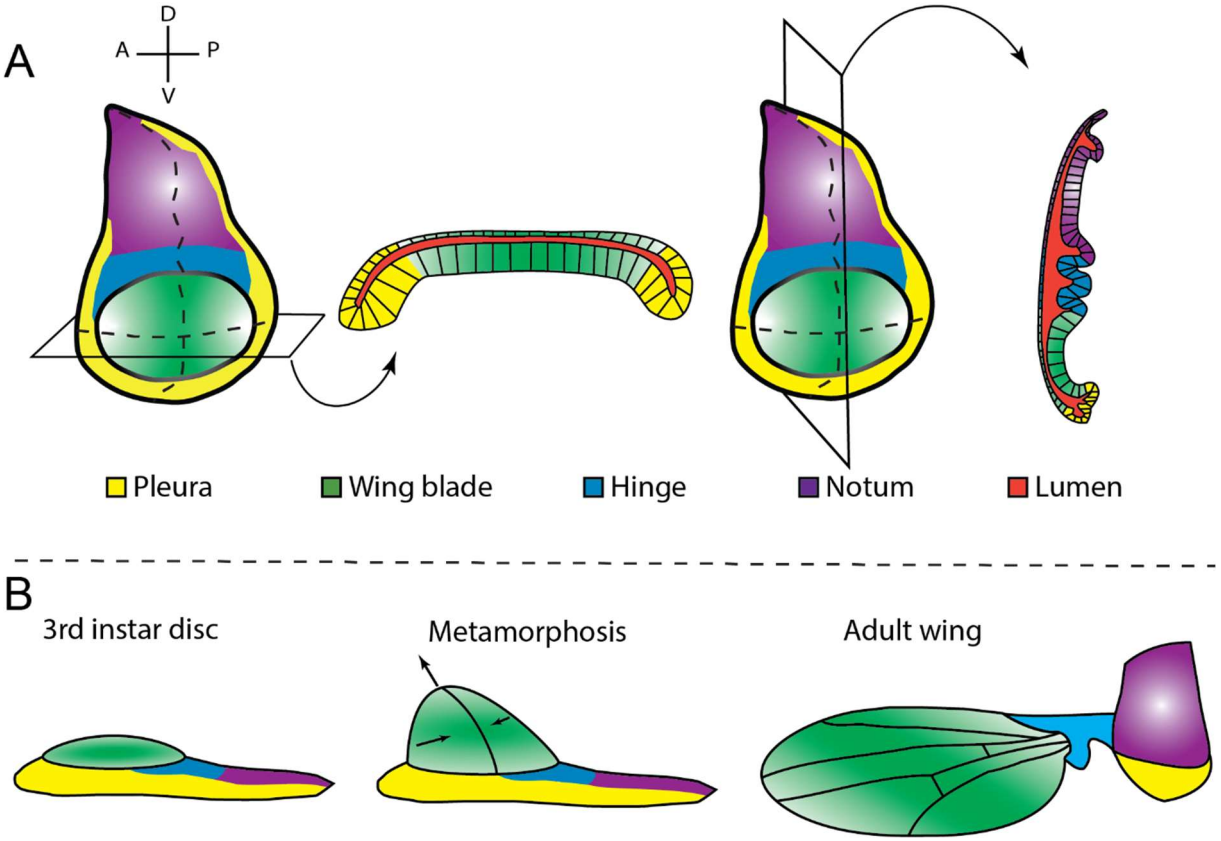


***Figure 4.5: Wing disc architecture and wing development.***
*(**A**) Schematic of a third instar larval wing disc top view and horizontal and vertical cross section. The wing blade is coloured in green, the pleura in yellow, the hinge region in blue, the notum in purple and the lumen in dark orange. The anterior/posterior and the dorsal/ventral borders are indicated by a dashed line. (**B**) During metamorphosis, the wing blade evaginates until the dorsal and ventral part of the pouch merge and form a two-cell-layered wing. The hinge connects the wing with the flies' thorax. The notum and pleura make up the part of the thorax, which is connected to the hinge and the wing blade.*

In addition, altering of gene expression can lead to specific phenotypes in the adult fly, leading to easier interpretation and analysis (Molnar et al., 2011). Furthermore, the wing discs provide the opportunity to investigate different developmental processes such as cell proliferation and cell death, cell growth and cell differentiation, pattern formation and tissue mechanics underlying morphogenesis as well as their molecular mechanisms in one and the same model

system. All these characteristics makes the wing imaginal disc a perfect tissue which has been used in multiple studies in developmental biology.

In the larval body, the imaginal discs grow without function for the survival of the larva, their only function is to provide the cellular populations required for the formation of the adult body. Wing imaginal discs in newly hatched first instar larva contain about 20-70 cells and grow to about 10000-50000 cells in 3$^{rd}$ instar larva (Mandaravally Madhavan & Schneiderman, 1977). The wing imaginal discs are known not only to form the wing in the adult fly but also to form all metathoracic structures; only cells located in the wing pouch within the wing disc form the wing proper. During metamorphosis, the wing pouch becomes the wing by excrescence of the monolayered pouch to form a two layered wing blade (Fig. 4.5B).

In the developing embryo, the wing imaginal discs form a cluster of cells at stage 12, in the T2 segment. This cell differentiation is triggered by the expression of *vestigial* (*vg*) and *snail* (*sna*) (Diaz de la Loza & Thompson, 2017). To subdivide the wing imaginal discs into dorsal/ventral and anterior/posterior compartments, different mechanisms are at play. To establish the Dorsal/Ventral (D/V) polarity in the early disc, the EGFR ligand *vein* (*vn*) is expressed proximal and *wg* is expressed distal. The EGFR pathway triggers the expression of *apterous* (*ap*) (Milán & Cohen, 2000). Ap defines the signaling boundary of Notch, whose signal is activated in-between cells expressing *ap* and cells not expressing *ap*. Notch, in turn, drives the expression of *vg*, which specifies the wing pouch and, eventually gives rise to the adult wing (Williams et al., 1991, 1993). Furthermore, Notch induces *wg* transcription at the D/V boundary in the wing pouch.

From the early stages of the development of the disc primordia, the latter contains two cell lineages with different cell fate, an anterior and a posterior cell lineage. This Anterior/Posterior (A/P) polarity is already set up in the T2 embryonic segment (Martinez-Arias & Lawrence, 1985). The posterior identity is given by the expression of the selector gene *engrailed* (*en*) (Hama et al., 1990). En activates *hh* expression in the posterior compartment. However, Hh cannot function in the posterior compartment due to the lack of Cubitus interruptus (Ci), which is repressed by En (Von Ohlen et al., 1997). Hh spreading into the anterior compartment activates the expression of the TGF-β superfamily member, *dpp*.

## 4.6 BMPs

One of the best studied families of morphogens are the Bone-morphogenic proteins (BMPs). BMPs are part of the transforming growth factor beta (TGF-β) superfamily, and to date over 20 members have been identified in humans alone. BMPs were originally identified in bone extracts (Urist et al., 2009), and were later shown to regulate a multitude of developmental processes, such as growth, apoptosis, and cell differentiation. Dysregulated BMP can lead to numerous malfunctions, such as cancer (Canalis et al., 2003; Singh & Morris, 2010). Due to known sequence and functional similarities, BMPs can be subdivided into four groups: BMP2/4, BMP5/6/7/8a/8b, BMP9/10, and BMP12/13/14 (Von Bubnoff & Cho, 2001). BMPs consists of a 400-600 amino acids large protein divided into a N-terminal pro- and a C-terminal mature domain. All BMPs are synthesized as precursors and then cleaved so that the mature domain is released. Furthermore, every BMP contains seven cysteins, with six of them forming a cysteine knot and the seventh being used for dimerization with a second BMP monomer (Nohe et al., 2004). After dimerization, the prodomain is cleaved and the mature domain is released. The function of the prodomain is thought to be the coordination of the proper folding for the mature domain (Sieber et al., 2009). BMPs bind to type II and type I serine/threonine kinase receptors with a single transmembrane domain and a intracellular serine/threonine kinase domain (Ashique et al., 2002). The serine/threonine domain of the type II receptor is constitutively active and phosphorylates the type I receptor upon ligand binding. This activated type I receptor phosphorylates Regulatory Smads (R-Smads). The phosphorylated R-Smads recruit the Common Smad (Co-Smad) to form a complex. This complex migrates into the nucleus and activates the transcription of target genes (Heldin et al., 1997).

## 4.7 Decapentaplegic

In the fruit fly *Drosophila melanogaster*, three BMP-type ligands, Dpp, Glass bottom boat (Gbb) and Screw (Scw), act as homo- and/or heterodimers. Dpp is one of the best characterized BMP ligands and is known to be involved in multiple processes during drosophila development, such as imaginal disc development, germline maintenance, as well as establishing dorsal-ventral polarity and midgut formation in the embryo (Harris & Ashe, 2011; Ma et al., 2019; Matsuda et al., 2016). Dpp is the vertebrate BMP 2/4 homolog in Drosophila and can be divided into prodomain and mature ligand domain. The Dpp protein possesses

three processing sites between the pro- and mature domain, which can be cleaved by Furin. Upon processing through cleavage, Dpp can generate two secreted isoforms (Künnapuu et al., 2009). The mature ligand domain forms the Dpp gradient and signals to activate the target genes of Dpp; the role of the prodomain, however, remains unclear.

Dpp plays many important roles in different developmental stages during Drosophila development. In the embryo, Dpp is vital for dorsal-ventral polarity. To achieve this polarity, Dpp is shuttled to the dorsal side of the embryo to form a concentration gradient from high concentration (dorsal) to lower concentrations (ventral). In order to be properly shuttled, Dpp forms a heterodimer with another BMP-type ligand, Screw. Catalyzed by CollagenIV, a complex is formed consisting of the BMP heterodimer, Sog and Tsg. This complex is shuttled and relocated to the dorsal side of the embryo and the ligands are released via cleavage of the complex through the protease Tolloid (Tld) (O'Connor et al., 2006; Sawala et al., 2012). In the germline stem cell (GSC) niche, Dpp function is required to repress the expression of *bag of marbles* (*bam*) (D. Chen & McKearin, 2003; Song et al., 2004). This repression results in the cells to remain stem cells (Song et al., 2004). Once *bam* is expressed, the stem cells differentiate to cystoblasts. Overexpression of Dpp in the GSC niche prevents *bam* expression and GSC differentiation (D. Chen & McKearin, 2003). In this system, Dpp acts as a short-range signal to repress *bam* and prevent differentiation of GSC to cystoblasts.

Furthermore, in the adult fly midgut, adult intestinal stem cells (ISC) are present in the basal membrane. ISCs differentiate into enteroblasts via asymmetric division (Micchelli & Perrimon, 2006). Dpp signaling is known to negatively regulate ISC proliferation and, with that, midgut homeostasis (Ma et al., 2019).

All these different systems underline the importance of Dpp for Drosophila development and survival. However, Dpp gradient formation and the signaling pathway are different in these systems, making it difficult to determine a general way of Dpp function. Hence, to unravel Dpp function, focusing on only one of these systems is helpful. Consequently, in this thesis, Dpp gradient formation in the wing imaginal disc was investigated.

### *4.7.1 Dpp pathway in the wing imaginal disc*

In the Drosophila wing imaginal disc, Dpp can form homo- or heterodimers with another BMP family member, Glass bottom boat (Gbb), and is secreted from an anterior stripe of cells to

form a concentration gradient (Bangi & Wharton, 2006) (Fig. 4.6A,B). Loss of *dpp* expression in the wing disc results in small wing rudiments while ectopic expression of *dpp* can lead to the formation of wing duplications and/or overgrowth (Zecca et al., 1995). The Dpp signaling pathway is triggered by binding of Dpp to the type I receptor Thickveins (Tkv) and less efficiently to the type I receptor Saxophone (Brummel et al., 1994; Inoue et al., 1998). Upon binding, a heterotetrameric complex of two type I receptors and two type II receptors (Punt) is formed (Ruberte et al., 1995). The type II receptor Punt phosphorylates Tkv. This phosphorylation activates the serine/threonine kinase domain in Tkv, which phosphorylates the Smad1 homologue Mothers against Dpp (Mad) (Fig. 4.6C,G). Phosphorylated Mad (pMad) then forms a complex with the Smad4 homologue Medea, translocates to the nucleus and binds to the GC-rich regulatory regions of genes such as *spalt* (*sal*) or *daughters against dpp* (*dad*) to control their transcription. The pMad/Medea complex also binds to the silencer elements of the *brinker* (*brk*) locus, which recruits another transcription factor, Schnurri (Shn) (Marty et al., 2000). This complex represses the transcription of *brk* and *pentagone* (*pent*) (Vuilleumier et al., 2011). The repression of *brk* leads to a Brk protein gradient reverse of pMad in the wing imaginal disc (Jaźwińska et al., 1999). Brk is known as a repressor of Dpp target genes, such as *optomotor blind* (*omb) sal*, or *dad* (Fig. 4.6D,E,G). The patterning genes *omb* and *sal* play crucial roles in patterning the longitudinal vein 2 (L2) and 5 (L5) (Spencer et al., 1982). While L2 is specified in the anterior compartment by the border of *sal* expression, L5 is specified by cells that express *omb*, but lack *sal* (Cook et al., 2004). The position of L3 and L4 are determined by Hh signaling (Biehs et al., 1998). Dad is known to be an antagonist of Dpp. When overexpressed, Dad blocks Dpp activity; this blockade is accomplished by blocking the access of Mad to the receptor complex and prevent the phosphorylation of Mad (Tsuneizumi et al., 1997). Consistent with Dad blocking Dpp function, wing cell growth and cell division is slower in *dad* overexpression clones. Similar results are seen in cells mutant for *tkv*.

Support for the role of Dpp in disc growth comes from experiments with a constitutive active form of the Dpp receptor Tkv ($Tkv^{Q253D}$). Ectopic expression of $Tkv^{Q253D}$ activates the Dpp signaling pathway with high levels of pMad, Omb and Sal (Martín-Castellanos & Edgar, 2002). Reduction of *brk*, on the other hand, results in overgrowth of the wing imaginal disc (Jaźwińska et al., 1999). However, the disc still overgrows in *brk*/*dpp* loss-of function mutant discs, leading to the assumption that Dpp-instructed wing disc growth is mediated by the repression of *brk* and not the graded activity of the Dpp signaling pathway (Schwank et al., 2008).

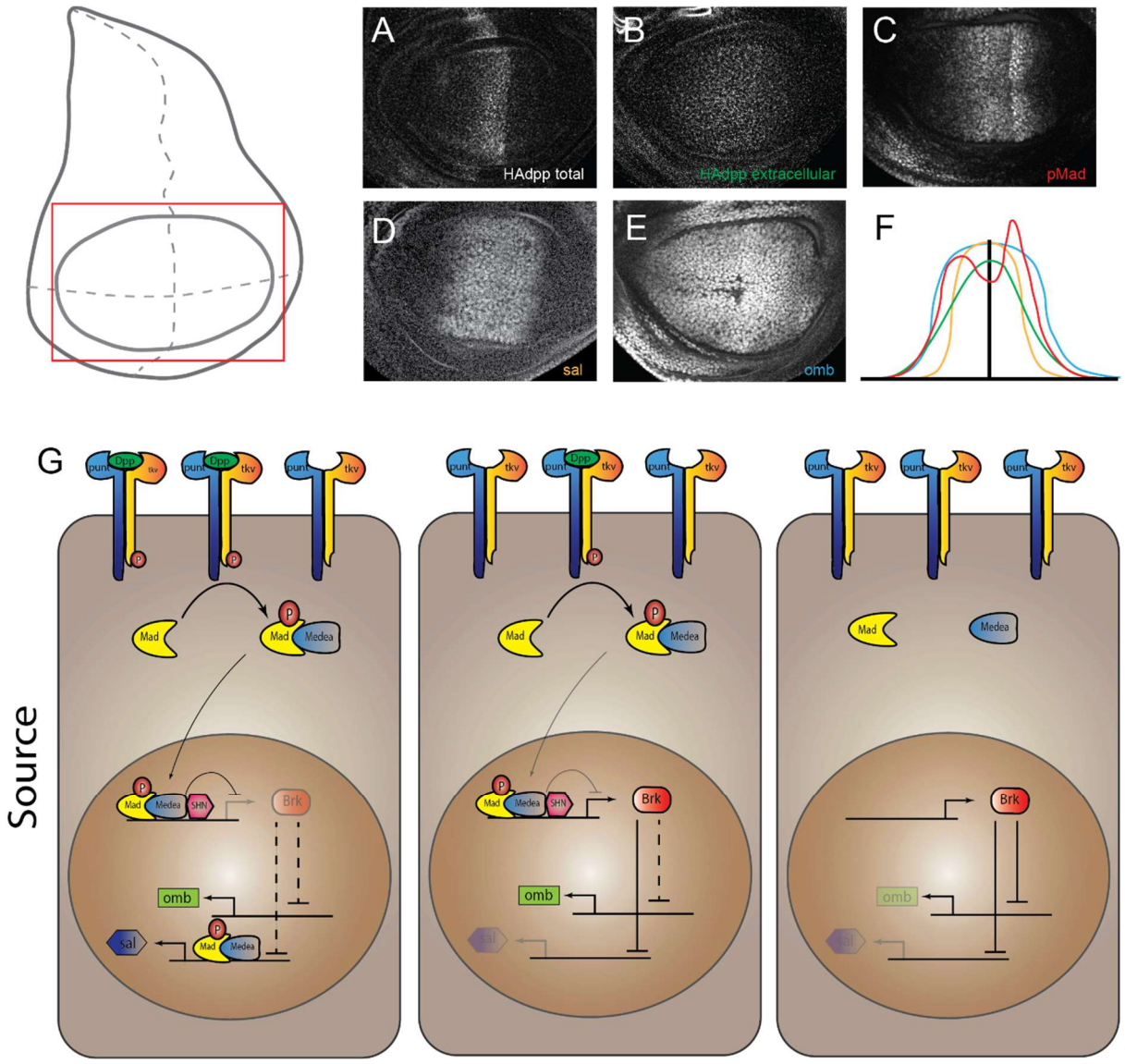


***Figure 4.6: Dpp pathway in the Drosophila melanogaster wing disc.***
*(**A-F**) The third instar wing imaginal disc and expression patterns of dpp and dpp target genes in the wing pouch. Dpp is expressed in a stripe in the anterior side adjacent to the anterior/posterior border. When Dpp is stained extracellularly, a concentration gradient can be observed with high concentrations at the A/P border and lower concentration laterally. pMad expression is highest in the center and declines to the more lateral sides of the pouch. The pMad intensity is drastically reduced in a center stripe adjacent to the A/P border due to reduced levels of the Dpp receptor Tkv. While spalt expression is restricted to a broad stripe in the center of the pouch, optomotor blind is expressed broader than sal. (**G**) The graded distribution of Dpp leads to different activation levels of the tkv-punt receptor complex with high activation close to the source and low activation in the periphery. This leads to a graded distribution of phosphorylated Mad. Once Mad is phosphorylated by Tkv, Medea is recruited to form a complex with pMad. This complex translocates in the nucleus and together with Schnurri (Shn), represses the expression of brk. This causes a brinker gradient opposed to the gradient of pMad. Since brk acts as a repressor of the genes omb and sal, and high pMad represses brk, omb and sal are expressed close to the source. The transcription of omb and sal is activated by unknown factors, but pMad-Medea can enhance sal expression. All the way in the periphery of the wing pouch, Dpp signaling is absent and brinker expression high, causing the suppression of sal and omb.*

### *4.7.2 Dpp dispersal in the wing imaginal disc*

Due to a lack of a good antibody against the mature domain of Dpp, the direct study of the extracellular gradient of Dpp was not possible for a long time. The first time an Dpp extracellular gradient was visualized was in the year 2000 by two separate groups using a GFP-Dpp fusion protein (Entchev et al., 2000; Teleman & Cohen, 2000). In these cases, overexpression of GFP-Dpp was able to partially rescue the Dpp function in the wing imaginal disc and the adult wing. To visualize the endogenous Dpp gradient, a new way to tag endogenous dpp, using the shortened peptide tags HA and Ollas, was developed (Bosch et al., 2017; Inoue et al., 1998; Matsuda et al., 2021). Flies tagged endogenously with HA and/or Ollas tag are homozygous viable and show no phenotypes, showing that these tags do not affect the function of Dpp (Matsuda et al., 2021). With this new method, we are now able to visualize the endogenous Dpp gradient. But how the Dpp gradient forms remains still controversial, and after much work on Dpp gradient formation has been done over the years, different models for gradient formation have been proposed. Among the proposed models are the before-mentioned free diffusion, facilitated transport, cytonemes and transcytosis (Belenkaya et al., 2004; Hsiung et al., 2005; Kicheva et al., 2007; Kornberg & Roy, 2014; Kruse et al., 2004; Zhou et al., 2012). In support of the transcytosis model, in a hypomorphic Drosophila *α-adaptin* allele, the wings showed similar phenotypes to hypomorphic *dpp* mutants (González-Gaitán & Jäckle, 1999). Furthermore, the *sal* expression domain was reduced in *α-adaptin* mutant wing discs, leading to the assumption that impaired endocytosis shortens the range of Dpp signaling. Furthermore, in discs mutant for *shi* (encoding the Drosophila Dynamin homologue) in the receiving cells, GFP-Dpp was not able to form a proper gradient and was only found at low levels close to the source cells. When clones mutant for *shi* were generated, a region with reduced GFP-Dpp signal was observed distal to the clone, called “shadow effect”. This shadow effect is only observed for a limited amount of time; after several hours, GFP-Dpp and *sal* activation was recovered behind the clones (Entchev et al., 2000). The authors argued that this GFP-Dpp was able to move behind the clones from lateral and downstream neighboring cells (Entchev et al., 2000). However, mutant clones of a temperature sensitive allele of *shibire* ($shi^{ts}$) showed pMad distal of the clone and in some cases even higher pMad signal than in control cells outside the clone (Entchev et al., 2000). Furthermore, in wild type cells surrounded by $shi^{ts}$ mutant clones, pMad staining was observed, arguing against transcytosis (Entchev et al., 2000). GFP-Dpp could travel over and

beyond the clones and was not reduced on the wild type cells behind or adjacent to *shi$^{ts}$* mutant clones. In *shi$^{ts}$* mutant wing imaginal discs, GFP-Dpp was observed to form a normal gradient, demonstrating that Dynamin-mediated endocytosis is not necessary for Dpp dispersal in the wing imaginal disc (Entchev et al., 2000). However, in mosaic clones mutant for *sfl*, pMad was reduced. pMad levels were also reduced behind the clones, suggesting HSPGs regulate Dpp signaling and movement. Also, Dpp distribution was affected behind *dally/dally-like (dlp)* mutant clones, suggesting that HSPGs play an important role in Dpp movement (Belenkaya et al., 2004). Furthermore, *dally* hypomorphic mutants showed a shrunk gradient of pMad, with high levels in the central domain but a sudden steep slope outside of the central region, suggesting Dally to be a crucial part for Dpp to form a gradient (Fujise, 2003) and supporting the model of facilitated transport.

Nevertheless, the group of Thomas Kornberg found directional cytonemes in the Drosophila wing pouch, non-directed cytonemes in the notum and no cytonemes in the hinge (Hsiung et al., 2005). Since Dpp signaling is essential for pouch and notum formation, Dpp dispersal is only essential in the wing pouch and dispensable in the hinge, they argued that these region-specific cytonemes are essential for Dpp dispersal. Moreover, they observed over twofold more cytonemes and these cytonemes were not oriented to the A/P border anymore in *dpp* mutant discs than in wild type discs. Additionally, when GFP-Tkv was present in the cells, the cytonemes contained GFP-Tkv. These results, however, only show that cytonemes sense and respond to Dpp, but not that they actually transport it.

It should also be possible to determine important aspects of the transport mechanisms of Dpp by measuring the diffusion speed of Dpp. Dpp dispersal should be slower in a cell-based dispersal model or in a hindered diffusion model than if it were to disperse through free diffusion. Kicheva et al., measured a dispersal rate of 0.1 µm2 sec−1 for GFP-Dpp, using FRAP (Kicheva et al., 2007). These dispersal speeds are consistent with a dispersal through one of the cell-based dispersal models or through hindered diffusion. Usually, when transport rates are gained from FRAP kinetics, spreading of the ligand is the only factor that influences the recovery of ligand during the observation time (Sprague et al., 2004). However, other processes, such as binding to extracellular molecules or degradation can influence the FRAP kinetics measurements. In this case, the FRAP results do not tell us much about the actual transport of a molecule (Zhou et al., 2012). Experiment-based calculations came to the result

that only about 3% of the total Dpp correspond to free, unbound Dpp (furthermore, only about 1% is visualized by fluorescence imaging) (Kicheva et al., 2007; Teleman & Cohen, 2000; Zhou et al., 2012). In this case, even with Dpp dispersing in a fast and free manner, the observed FRAP kinetics would be slow, due to the huge amount of bound Dpp. To overcome this weakness of the FRAP approach and answer the question of Dpp dispersal in the wing disc, fluorescence spreading after photoactivation, spatial FRAP, FCS, and pair correlation function microscopy were carried out (Zhou et al., 2012). The results of all four of these experimental procedures supported free diffusion as a major dispersal route for Dpp.

## 4.8 Glypicans

One class of HSPGs are the glypicans. Together with the syndecans, glypicans are the two major cell surface HSPGs. While syndecans are anchored in the cell membrane by a transmembrane domain, glypicans possess a GPI anchor, which targets and anchors them to the outer membrane (Filmus et al., 2009) (Fig. 4.7). The GPI anchor can be cleaved and the glypican released from the cell surface by a lipase called Notum, leading to glypicans shedding into the extracellular environment (Traister et al., 2008). These shed glypicans have been shown to play a role in the transport of Wnts and Hh for the purpose of morphogen gradient formation (Fujise, 2003; Han et al., 2004; Kirkpatrick et al., 2006). However, a more recent study provided evidence against the idea of Notum to cleave the GPI anchor of glypicans, but Notum deacylating (Wnt) proteins with the help of glypicans to suppress signaling activity (Kakugawa et al., 2015).

Mammals express six different glypicans: glypican 1-6 (GPC1-GPC6). These GPCs can be divided into two subfamilies: GPC1/2/4/6 and GPC3/5. In polarized cells, glypicans are, like most GPI-anchored proteins, located mostly apically, but also basolateral (Mertens et al., 1996). This basolateral localization seems to be determined by the HS chains, since glypicans without these chains are sorted more apically (Mertens et al., 1996).

Two glypicans, the GPC3/5 homolog Dally and the GPC1/2/4/6 homolog Dlp are present in Drosophila. Dlp is larger than Dally with 626 amino acids for Dally and 939 amino acids for Dlp (Nakato et al., 1995; Paine-Saunders et al., 1999).

Attached to all glypican core proteins are two to four Glycosaminoglycan (GAG) chains of the HS type. These HS chains in glypicans are very conserved between the glypican groups (Lawrence et al., 2008), but also between vertebrates and Drosophila (Toyoda et al., 2000).

The core proteins, however, do not show much homology and seem not to have any domains with close homology to structurally characterized proteins. Yet, all core proteins share 14 conserved cysteine residues, suggesting the three dimensional structure of glypicans to be very similar (Veugelers et al., 1999). Additionally, all glypicans contain two to four Ser-Gly sequences, which serve as a GAG chain attachment side, close to the carboxyl terminus, placing them close to the cell surface and allowing these chains to interact with other cell surface molecules, such as receptors. Glypicans in mammals and Drosophila are known to modulate the activity of a large number of protein ligands, with more than 100 proteins being reported to interact with their HS chains (Hufnagel et al., 2006; Vallet et al., 2021). Further hints for glypican involvement in morphogenesis come from experiments investigating the timely expression patterns of glypicans; glypican expression changes over time, with high expression during development and less expression in later stages (Litwack et al., 1998).

Most of the *in vivo* evidence points to glypicans main functions being the regulation of signaling via Wnts, Hhs, FGFs, and BMPs (Ohkawara et al., 2003; Topczewski et al., 2001; Tsuda et al., 1999).

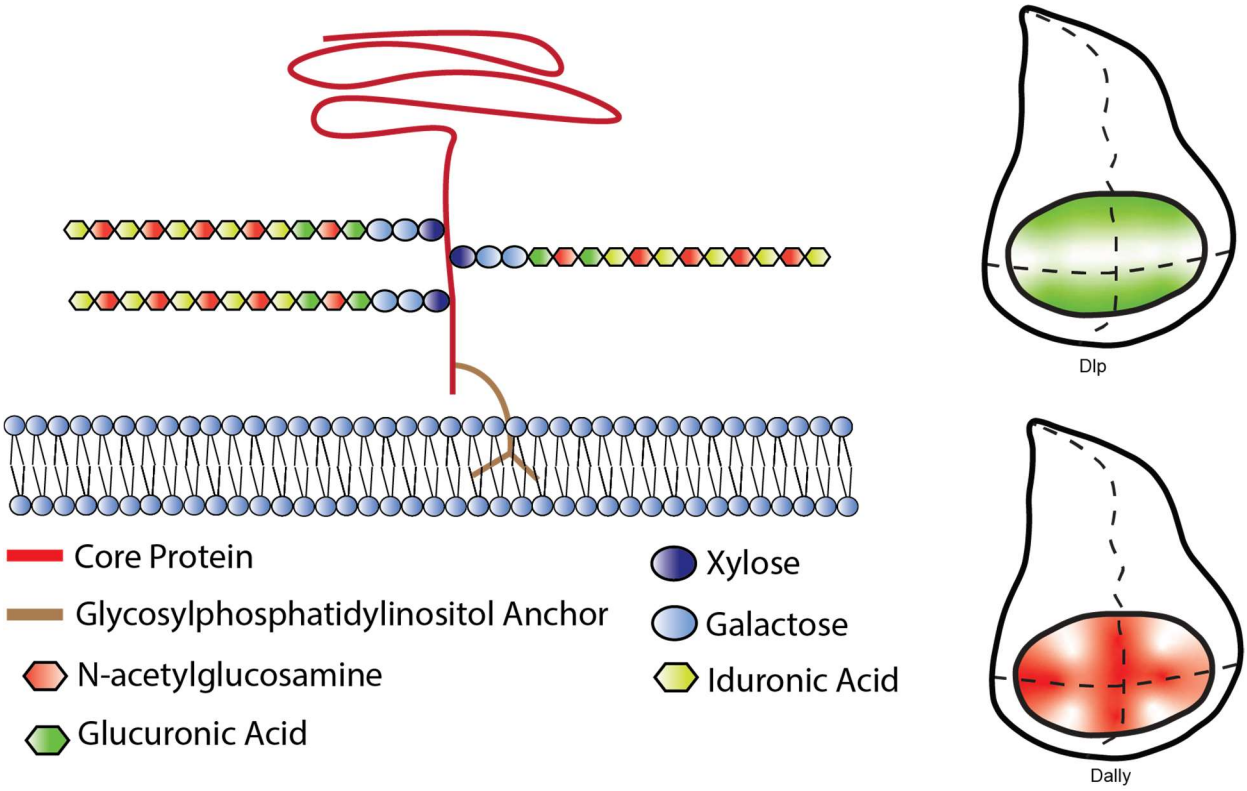


*Figure 4.7: Schematic representation of a glypican and expression patterns of Dally and Dlp in the wing pouch.*

*The Glypican core protein (red) contains two-four serine-glycine sequences where the HS chains are attached. All HS chains start with a Xylose attachted to the serine residue, followed by two Galactoses and a Glucuronic Acid. The rest of the chain is a linear polysaccharide comprised of repeating disaccharide units with a signature repeat of N-acetylglucosamine and Iduronic Acid. The HS chains can become 100 or more sugar units long and are modified by different Sulfotransferases to generate distinct sulfation patterns. The core protein is C-terminally attached to the external cell membrane by a Glycosylphosphatidylinositol (GPI)-anchor, which can be cleaved by lipase activity.*

### *4.8.1 Division abnormally delayed (Dally)*

One of the best characterized glypicans in Drosophila is Dally (Fig. 4.7). Dally was discovered due to its requirement for cell division patterning during postembryonic development (Nakato et al., 1995). *dally* mutants show phenotypes in a number of patterning events of different tissues, like the eye, brain, antenna, genitalia and the wing (Jackson et al., 1997a; Nakato et al., 2002). Furthermore, Dally is also known to be required for Dpp signaling in the Drosophila wing disc. But the effect of Dally on Dpp is not limited to the wing disc. It was shown that the eye, genital, and antennal phenotypes of *dally* mutants are a consequence of a reduction of Dpp function (Jackson et al., 1997a). *dally* expression is gone in *smoothened* mutant clones and dramatically increased in *en* mutant clones (Alcedo et al., 1996; Fujise, 2003), indicating that Hh signaling increases and *en* expression decreases *dally* expression. Furthermore, *dally* expression is also regulated by Dpp signaling as the Dpp receptor Tkv together with Dally regulates Dpp signaling, this forms a negative feedback loop. In the lateral sides of the wing pouch, less Dpp leads to higher levels of Tkv and Dally (Fujise, 2003). Even with Dally being the best-characterized glypican in Drosophila, how Dally affects Dpp distribution and/or signaling remains unclear. To shed light on this question, different ectopic expression and genetic experiments were conducted in the past. When *dally* is ectopically expressed in clones, pMad signaling is enhanced, suggesting Dally to serve as a co-receptor for Dpp. Furthermore, in *dally,dlp*-mutant clones, the Dpp levels were significantly reduced (Belenkaya et al., 2004). While the enhancement of pMad upon ectopic expression of *dally* points to a function as a co-receptor (Fig. 4.8D), the reduced levels of Dpp in *dally* mutants can be interpreted in a way that Dally is required for Dpp movement or Dpp stability (Fig. 4.8A,B). It has been proposed that Dally serves to stabilize Dpp on the cell surface by inhibiting receptor mediated endocytosis to support Dpp gradient formation (Akiyama et al., 2008).The similar pMad patterns in *dally* mutants and *tkv* overexpressing wing discs support this idea (Fujise, 2003; Lecuit & Cohen, 1998; Tanimoto et al., 2000) suggesting that either Dally downregulates *tkv* expression or stabilizes Dpp through a Tkv-dependent process. Furthermore, a recent study

proposed Dally together with Pent to be involved in scaling of Dpp through recycling of Dpp back to the extracellular space (Romanova-Michaelides et al., 2022) (Fig. 4.8C).

However, how Dally acts in Dpp gradient formation and signaling remains unclear. Previous studies provided evidence for all four mechanisms, co-receptor function, stabilizing Dpp on the cell surface, recycling and transporting Dpp (Akiyama et al., 2008; Fujise, 2003; Romanova-Michaelides et al., 2022) (Fig. 4.8). Anyhow, these mechanisms are not mutually exclusive and might as well act together to enable Dpp function.

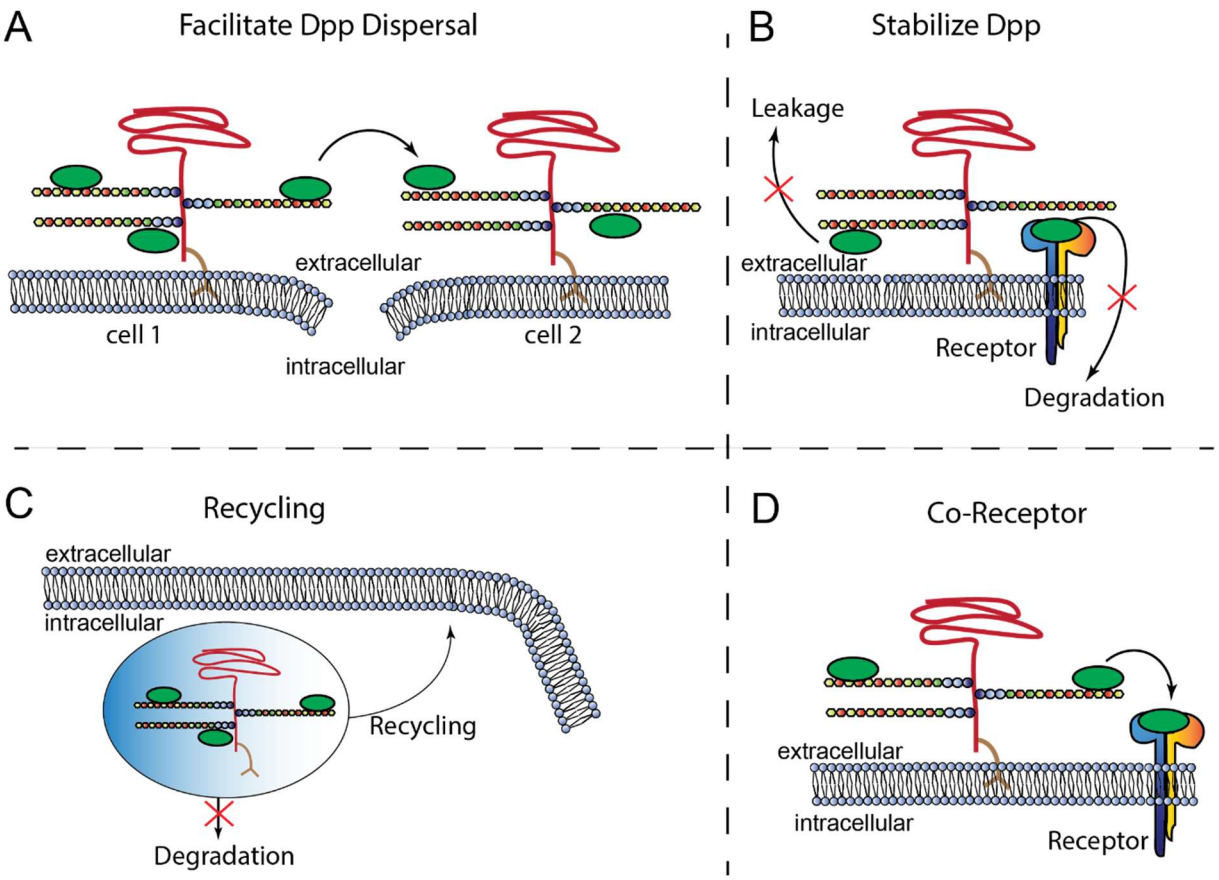


***Figure 4.8: Proposed modes of Dally function in the Dpp pathway.***
*(A) Facilitate Dpp dispersal through active transport of Dpp along the cell surface. (B) Stabilize Dpp on the cell surface by blocking receptor mediated endocytosis or leakage of Dpp from the tissue (C) Recycle Dpp back to the cell surface after internalization. (D) Co-receptor by facilitating Dpp-receptor interaction.*

Dally also regulates Wg and Hh activity. Some evidence for these functions comes from *slf* and *sgl* mutant embryos, which develop cuticle defects with a similar phenotype to *wg* or *hh* mutants (Häcker et al., 1997). Furthermore, mutations in genes encoding the HS chain modifying EXT proteins, Ttv, Sotv and Botv, lead to reduced extracellular Wg protein levels

and reduced expression of *wg* target genes (Wodarz & Nusse, 1998). In the Drosophila wing disc, *dally* mutants show wing margin defects similar to the ones observed in *wg* mutants, suggesting a role of Dally in Wg signaling and/or dispersal (Lin & Perrimon, 1999). Like Wg, Hh is a key mediator in many developmental processes in Drosophila and HSPGs are known to control its function (M. I. Capurro et al., 2008). In the wing disc, it was shown that Ttv is required for proper Hh movement in the anterior compartment (Bellaiche et al., 1998). It is proposed that, in the wing disc, Dally and Dlp act redundant in Hh movement (Han et al., 2004).

The simple question of what is the basis of the selectivity of Dally (and Dlp) in the regulation of the different pathways of morphogens in different tissues still remains unanswered.

### *4.8.2 Core protein versus HS GAG Chains*

Since the HS chains on Glypicans have a strong negative charge, HSPGs can interact with proteins that display positively charged domains of cell surface and secreted molecules (Vallet et al., 2021). On this basis, it was originally thought that the HS chains were essential for glypican activity. However, several lines of evidence point to the direction that the HS chains represent only one part of the proteins characteristics required for the function of glypicans in Hh, Wnt and BMP signaling (Kirkpatrick et al., 2006).

The core protein of GPC3 has been shown to directly bind Shh with high affinity and inhibit its signaling activity (M. I. Capurro et al., 2008). Another study showed the ability of the GPC3 core protein to bind to several Wnt members and thereby stimulate Wnt signaling (M. I. Capurro et al., 2005). Hence, the GPC3 core protein can impact different morphogens in a positive or negative manner. Also in Drosophila, a recent study demonstrated the ability of the Dlp core protein to bind to the lipid moiety of Wg and modulate the extracellular gradient via this interaction (McGough et al., 2020).

When preincubated with heparin, BMP4 was still capable to associate with Dally, suggesting some involvement of the core protein. Furthermore, Co-IP studies showed that a form of Dally, in which the HS chains were removed, still retained some ability to bind Dpp (Kirkpatrick et al., 2006).

### *4.8.3 DppΔDally*

Since Dally has been shown to act on many different cell surface molecules, trying to unravel the function of Dally on one single pathway is challenging by investigating *dally* mutants. *dally* mutants affect several pathways, which might cause unwanted phenotypes or make it difficult to interpret the results obtained. To investigate the interaction of HSPGs with BMPs, a previous study determined the binding site of Xenopus BMP4 to HS (Ohkawara et al., 2002). The authors identified a N-terminal region in the mature domain of BMP containing a stretch of basic amino acids. This region of basic amino acids was shown to be highly conserved in the animal kingdom, giving rise to the assumption that they are essential for BMP function. A few years later, $Dpp^{\Delta N}$ was generated, a form of Dpp which lacks seven basic amino acids in the N-terminal region of the mature domain (Akiyama et al., 2008). This mutated Dpp showed the same properties *in vitro* as the wild type Dpp, but it had a shorter half-life and less signaling activity *in vivo*, causing the authors to suggest that interaction of the N-terminal basic amino acids of Dpp and the HS chains of Dally is important for Dpp stability. These experiments were done using an overexpression essay and it remains open how $Dpp^{\Delta N}$ behaves under endogenous conditions.

## 4.9 Protein binders

While previous studies on proteins and their functions relied on RNA interference and mutants, recent advances in the field of synthetic tools based on protein binders made new techniques available and applicable. Protein binders such as single chain variable fragments, nanobodies, Design Ankyrin Proteins and others have been applied in developmental biology to unravel the functions of proteins, by directly targeting the protein of interest *in vivo*. These synthetic tools have been used in many different ways, such as to allow for protein visualization (Gross et al., 2013; Rothbauer et al., 2006), protein degradation (Caussinus et al., 2011), protein relocalization (Harmansa et al., 2017), and post-translational modification (Roubinet et al., 2017). Furthermore, recent studies demonstrated the power of protein binders in unraveling the functions of extracellular morphogen gradients by trapping morphogens on the cell surface (Harmansa et al., 2015; Matsuda et al., 2021). By fusing the GFP nanobody to a transmembrane domain, it was possible to trap GFP-tagged proteins. This system was originally generated to manipulate GFP-Dpp gradient formation in Drosophila, but has since been applied in different systems, like Zebrafish, Xenopus and *C. elegans* (Almuedo-Castillo et al., 2018; Mii et al., 2021; Pani & Goldstein, 2018). More recently, an anti-HA scFv

was fused to a transmembrane domain to trap endogenous HA-tagged Dpp and manipulate Dpp gradient formation *in vivo* (Matsuda et al., 2021). Using this method, it is possible to directly investigate the requirement for dispersal of the morphogen without manipulating receptors or other pathway components. Another way to manipulate dispersal of a morphogen is by fusing a transmembrane domain directly to the protein and thereby tethering the morphogen to the cell membrane. This approach has been used successfully to tether Wg to the cell membrane and hinder its dispersal (Alexandre et al., 2014). These new methods open up new possibilities to investigate morphogens and their function in development and might help to answer old questions in the field by looking at them using this novel approach.

# 5 Aim of the study

Although the formation of morphogen gradients has been extensively studied in the past, it remains unclear how most morphogens disperse and form a gradient. One example is Dpp, for which many different modes of transport have been proposed, depending on the tissue studied. However, even within a single tissue, in this case the Drosophila wing imaginal disc, many different models have been proposed to account for gradient formation.

Mutations in genes encoding Drosophila glypicans show defects in Dpp morphogen signaling and distribution, leading to the assumption that glypicans are important for Dpp gradient formation and signaling. However, how glypicans achieve this function remains unclear. Previous studies propose different scenarios of how glypicans control Dpp gradient formation in the wing imaginal disc. Four different main ideas have emerged: glypicans transport Dpp directly by handing it from glypican to glypican; glypicans interfere with Dpp dispersal by binding Dpp; glypicans stabilize Dpp on the cells surface and glypicans control Dpp endocytosis and recycling.

Here, I aimed to further characterize glypican function in Dpp morphogen signaling in the Drosophila wing imaginal disc. To do so, I used newly generated glypican mutants as well as protein binder approaches; furthermore, I made use of endogenously tagged *dpp* to investigate the extracellular Dpp gradient. In order to better understand the function of the Drosophila glypicans, I overexpressed different glypican mutant proteins, with and without their HS chains attached and with parts of their core protein being truncated. Furthermore, we generated and studied a Dpp construct which lacks the Dally-binding site and expressed it for the first time from the endogenous *dpp* locus. Additionally, I expressed a synthetic HA trap to investigate Dpp dispersal *in vivo* in the presence or absence of glypicans and finally, I used tethered Dpp constructs to investigate glypican function with regard to Dpp independent of its transport.

My aim is to gain a better understanding of how glypicans shape morphogen gradients and in particular how they affect Dpp gradient formation and signaling at the molecular level.

# Materials & Methods

# 6 Materials and Methods

## 6.1 Drosophila husbandry and genetics

Flies for experiments were kept at 25°C in standard fly vials containing polenta and yeast. Stocks or crosses during experiments were flipped in new vials containing fresh food every day. To be able to distinguish homozygous from heterozygous flies and larvae, stocks were usually generated to contain balancers CyODfd or TM6Tb.

### *6.1.1 Fly stocks*

| Number | Genotype | Origin |
|---|---|---|
| 1 | *tkv-RNAi* | Bloomington 40937 |
| 2 | *dally-RNAi* | VDRC 14136 |
| 3 | *dlp-RNAi* | VDRC 106568 |
| 4 | UAS-GFP-HA-Dally | Suzanne Eaton |
| 5 | UAS-YFP-Dally | This study |
| 6 | UAS-YFP-DallyΔHS | This study |
| 7 | UAS-YFP-DallyΔcoreprotein | This study |
| 8 | UAS-YFP-DallyΔHSΔcoreprotein | This study |
| 9 | UAS-YFP-DallyΔ390bp1 | This study |
| 10 | UAS-YFP-DallyΔ390bp2 | This study |
| 11 | UAS-YFP-DallyΔ390bp3 | This study |
| 12 | UAS-YFP-DallyΔNterminalAA | This study |
| 13 | UAS-TdppTLR4 | This study |
| 14 | UAS-TdppΔDallyTLR4 | This study |
| 15 | tkvmcherry | Akiyama et al., 2018 |
| 16 | tkvHA | Giorgos Pyrowolakis |
| 17 | Dally(ko;attB) | Giorgos Pyrowolakis |
| 18 | Dlp(ko;attB) | Giorgos Pyrowolakis |
| 19 | HA-dppΔdally | This study |
| 20 | Ollas-HA-dppΔdally | This study |
| 21 | Ollas-dppΔdally | This study |
| 22 | HA-dppchangedAA | This study |

| | | |
|---|---|---|
| **23** | HA-dppchangedAAΔdally | This study |
| **24** | OllasProdomainHAdpp | Milena Bauer |
| **25** | TehtProV5DppollasDpp | This study |
| **26** | TehtProV5DppollasDppΔdally | This study |
| **27** | secGFP | Gustavo Aguilar |
| **28** | secGFPDallybs | This study |
| **29** | UAS-GPC3 | JP Vincent |
| **30** | UAS-GPC4 | JP Vincent |
| **31** | UAS-GPC5 | JP Vincent |
| **32** | UAS-GPC6 | JP Vincent |
| **33** | DppBMPDally | This study |
| **34** | DppDallyBMP | This study |
| **35** | yw | Affolter stock |
| **36** | dppHA-3NQ | Antonio Galeone et al., 2020 |
| **37** | dppHA-N529Q | Shinya Matsuda |
| **38** | ap-Gal4 | Affolter stock |
| **39** | hh-Gal4 | Dr. Manolo Calleja |
| **40** | ptc-Gal4 | Bloomington 2017 |
| **41** | UAS-HA-trap | Shinya Matsuda |
| **42** | Hb-lacZ | M. Llimargas |
| **43** | ywHSFlp; act>y$^{+}$>LHG | Affolter stock |
| **44** | HSFlp; tub>CD2>Gal4 | Affolter stock |
| **45** | Morphotrap | Harmansa et al., 2015 |
| **46** | Dally$^{32}$ | Franch-Marro et al., 2005 |

**Table 6.1: Fly stocks used in this study**

## 6.2 Immunofluorescent stainings

### *6.2.1 Total staining*

Wing discs from third instar Larvae were dissected and stored temporarily in Phosphate Buffered Saline (PBS) (gibco) on ice until enough samples were collected. The discs were then fixed in 4% Paraformaldehyde in PBS for 30min on the shaker at room temperature (25°C). After fixation the discs were rinsed three times quickly with PBS and three times for 15min

with PBS at 4°C. Wing discs were permeabilised in PBST (0.3% Triton-X in PBS) and then blocked in 5% normal goat serum (NGS) in PBST for at least 30min. Primary Antibodies were added for incubation over night at 4°C. The next day, the primary Antibody was removed carefully (primary Antibody could be reused multiple times to achieve stainings with less background signal) and the samples were rinsed three times quickly in PBST and three times 15min at room temperature in PBST. Discs were incubated in secondary Antibody and covered in aluminum foil for 2h at room temperature. Afterwards the samples were washed again three times quickly and three times 15min in PBST at room temperature. After the final washing the PBST was rinsed with PBS, then the PBS was removed completely and the samples were mounted in VECTORSHIELD on glass slides. For HS stainings, wing discs were dissected as prescribed before. After fixation discs were washed and blocked, then treated with Heparinase III (Sigma-Aldrich) for 1.5h at 37°C. Afterwards the discs were blocked again and staining continued according to protocol.

### *6.2.2 Extracellular staining*

Wing discs from third instar Larvae were dissected and stored temporarily in Schneider's Drosophila medium (S2) on ice until enough samples were collected. The discs were then blocked in cold 5% NGS in S2 medium on ice for 10min. The blocking solution was removed carefully and the primary Antibody added for 1h on ice. During the 1h staining period, the tubes were tapped carefully every 15min, to make sure the Antibody is distributed evenly. After 1h incubation on ice the Antibody was removed and the samples were washed at least 6 times with cold S2 medium and another two times with cold PBS to remove excess primary Antibody. Wing discs were fixed with 4% Paraformaldehyde in PBS for 30min on the shaker at room temperature (25°C). After fixation the discs were rinsed three times quickly with PBS and three times for 15min with PBS at 4°C. To have a total staining with another primary Antibody in these wing discs, the staining continued as in the total staining protocol when the PBST was added. Otherwise, the wing discs were washed three times 5min in PBST at room temperature, then blocked in blocking solution over night at 4°C. The next day secondary Antibody was added for 2h at room temperature. Afterwards the samples were washed again three times quickly and three times 15min in PBST at room temperature. After the final washing the PBST was rinsed with PBS, then the PBS was removed completely and the samples were mounted in VECTORSHIELD (H-1000, Vector Laboratories) on glass slides.

### *6.2.3 Embryo staining*

Embryos were collected over night (or dependent on desired stage, shorter or longer) at 25°C on grape juice plates with some yeast on top of it. Collected embryos were dechorionated in 50% bleach (Sodium hypochloride) in $H_2O$ for 1.5min. Dechorionated embryos were poured through a funnel with mesh and collected in a collection tube with a smaller mesh. These embryos were washed with $H_2O$ to get rid of excess bleach. Embryos were transferred from the mesh to an Eppendorf tube containing fixing solution (1:1 heptane: 4%Paraformaldehyde in PBS. The Heptane is needed for the $H_2O$ based PFA to penetrate the hydrophobic vitelline membrane of the Embryo). The embryos were fixed for 20-30min on the shaker at room temperature. After fixing the tubes were vortexed shortly to allow more embryos to settle to the bottom of the tube. The fixing solution divided into two phases, top (Heptane) and bottom phase (PFA). The bottom phase was removed and replaced by the same amount of MeOH to remove the vitelline membrane. The tubes were shaken by hand for 1min. The devitellinized Embryos settle to the bottom, embryos that remained in the Heptane were removed together with the Heptane. Embryos were washed 4 times with MeOH at room temperature. Afterwards embryos were rehydrated in 1:1 PBS:MeOH at room temperature on the shaker for 5min, then they were washed quickly in PBS. To permeabilise the embryos, they were washed four times 15min with PBST on the shaker at room temperature and afterwards blocked in 5% NGS in PBST for at least 30min at room temperature. Samples were incubated over night with primary Antibody at 4°C. The following day, samples were washed two times quickly and four times 15min in PBST at room temperature before the secondary Antibody was added. Tubes were covered in aluminium foil and left on a shaker for 2h at room temperature. Embryos were washed two times quickly and four times 15min in PBST at room temperature. Afterwards they were rinsed in PBS, PBS was replaced with VECTORSHIELD (H-1000, Vector Laboratories) and the embryos were mounted on a glass slide.

### *6.2.4 Imaging*

Samples were imaged using a Leica SP5-II-MATRIX confocal microscope and Leica LAS AF and Images were analyzed using ImageJ (version v1.53c). Figures were optained using Omero (version 5.7.0) and Adobe Illustrator (version v26.4.1).

### *6.2.5 Quantification*

Images were analyzed using ImageJ. Each analyzed Image was a composite of three z-stacks from which a signal intensity profile along the A/P (or for wg D/V) axis was extracted. Each measure point was collected in Excel and aligned based on the A/P compartment boundary determined by anti-ptc staining. These points were plotted and averaged by a script provided by Etienne Schmelzer (Scripts are available at https://etiennees.github.io/Wing_disc-alignment/) . The resulting graphs were generated in prism.

### *6.2.6 Antibodies*

Primary Antibodies: rb- anti-phospho-Smad1/5 (41D10, Cell Signaling, #9516; 1:200), m-anti-wg (4D4, DSHB, University of Iowa; total staining: 1:120, extracellular staining: 1:20), m-anti-ptc (DSHB, University of Iowa; total staining: 1:40), rat-anti-HA (3F10, Roche, 11867423001; total staining: 1:300, extracellular staining: 1:20), rat-anti-Ollas (L2, Novus Biologicals, NBP1-06713; total staining: 1:300, extracellular staining: 1:20) , rb-anti-sal (Schuh, Reinhard, University of Göttingen; toal staining: 1:40), m-anti-β-Galactosidase (Promega Z378825580610; total staining: 1:10), rb-anti-GFP (Torrey pines biolab, Lot: 042704; extracellular staining: 1:200), m-anti-V5 (Invitrogen; total staining: 1:5000), m-anti-HS (F69-3G10, amsbio; total staining: 1:100).

The following secondary antibodies were used at 1:500 dilutions in this study. Goat anti-rabbit 488 (A11008 Thermo Fischer), goat anti-rabbit 568 (A11011 Thermo Fischer), goat anti-rabbit 680 (A21109 Thermo Fischer), goat anti-rat 568 (A11077 Thermo Fischer), goat anti-mouse 568 (A11004 Thermo Fischer), goat anti-rat Fcγ fragment specific 488 (ab97089 abcam), goat anti-mouse Fcγ fragment specific (115625071 Jackson Immuno Research).

## 6.3 Isolation of genomic DNA from flies

### *6.3.1 Preparation of DNA from single flies*

Solutions: Squishing Buffer: 10µL 1M Tris-HCl (pH 7.5), 5µL 500mM EDTA (pH 8.0), 5µL 5M NaCl, 10µL Proteinase K (20mg/ml), up to 1mL with ddH2O.

Single flies were euthanized with CO2, transferred into a PCR tube and put on ice for 15min. The flies were mashed with a pipet tip. Afterwards, 50ml of squishing buffer was added and the mashed flies and the buffer were mixed well. The samples were incubated at 37°C for

30min and 5min at 95°C to deactivate the Proteinase K. In a 25ul PCR reaction, 1ul of single fly prep was used as a template.

### *6.3.2 Polymerase Chain Reaction (PCR)*

Protocol for OneTaq® 2X Master Mix with Standard Buffer

For 25ul reaction:

12.5ul one Taq 2x Master Mix Polymerase

0.5ul Forward Primer (10uM)

0.5ul Reverse Primer (10uM)

1ul Template DNA (>1000ng)

5.5ul nuclease free $H_2O$

PCR Program:

94°C 30s

94°C 20s
45-68°C 1m } 30cycles

68°C 1m/kb

68°C 5m

4°C ∞

Protocol for Phusion/Q5 Polymerase

For 25ul reaction:

0.25ul Phusion DNA Polymerase/Q5 DNA Polymerase

0.5ul dNTPs (10mM)

1.25ul Forward Primer (10uM)

1.25ul Reverse Primer (10uM)

Xul Template DNA (~50ng)

5x Reaction Buffer (Phusion or Q5)

Xul Nuclease free $H_2O$

PCR Program:

98°C 30s

98°C 10s
45-72°C 30s } 30cycles
72°C 30s/kb

72°C 2m

4°C ∞

The PCR products were cleaned up directly or, after determination of the right size of the DNA strand, from an Agarose gel by using the NucleoSpin® Gel and PCR Clean-up Kit (Macherey-Nagel) according to the manufacturer's protocol.

### *6.3.3 Sequencing*

To be able to identify the correct fly genotypes or cloned minipreps, DNA was sequenced. To sequence Plasmids, 0.7ug of Plasmid was mixed with a suitable primer and complemented with nuclease free $H_2O$ to a final volume of 15ul. To sequence PCR products a DNA concentration of 1.5ng/ul per 100bp was used and mixed with a suitable primer and complemented with nuclease free $H_2O$ up to 15ul. Sequencing was performed by Microsynth AG 9436 Balgach, Switzerland.

## 6.4 Molecular cloning methods

### *6.4.1 Restriction Ligation Digestion*

Plasmids (table xxx) suitable for the desired cloning results were chosen to be digested using restriction enzymes (table xxx) and the following protocol:

- Restriction Enzyme: 0.5ul
- Restriction Buffer: 2ul
- Plasmid : 1.5-2ug
- H2O : up to 20ul

The solution was mixed in a PCR tube and heated up to 37°C over night. Restriction enzymes were deactivated the next day, using the appropriate temperature for 30min.

If the Plasmid was cut two times with the same enzyme, 2.5ul phosphatase together with 5ul dephosphorylation buffer was added after 1h of reaction time.
The digested DNA was run on an agarose gel, bands of the correct size were cut and the DNA was isolated via gel purification, using the NucleoSpin® Gel and PCR Clean-up Kit (Macherey-Nagel) according to the manufacturer's protocol. Then DNA concentration was determined using a Nanotrop Photospectrometer.
Some of the Inserts used in this study were single stranded Oligonucleotides and were not isolated from an existing Plasmid, but ordered (table xxx). To be able to ligate these into the receiving Plasmid they needed to be annealed first. The following protocol was used to do so:

- 1ul Forward oligo
- 1ul Reverse Oligo
- 1ul 10x Ligation Buffer
- 1ul T4 Polynuclease Kinase
- 6ul $H_2O$

The solution was mixed in a PCR tube and heated up to 37°C for 30min, then up to 95°C for 5min and 1 hour at room temperature to slowly cool down.

### *6.4.2 Ligation*

Next, a ligation was conducted to fuse the insert to the recipient plasmid. To calculate the amount of insert and vector used for ligation, a ligation calculator program was used (http://www.insilico.uni-duesseldorf.de/Lig_Input.html). The vector:insert ratio used for all ligation reaction in this study was 1:3. The Ligation was conducted according the following protocol:

- Xul insert
- Xul vector
- 1ul Buffer
- 0.5ul Ligase
- Xul $H_2O$ (up to 10ul)

The Ligation was put at 18°C over night. The next day, the ligation could be transformed into bacteria.

| Primer Number | Sequence |
|---|---|
| 1 | ATTCGGAATTCATGGCGGCCAGGAGCGTGC |
| 2 | CGAATGAATTCTTAACTACAGCTACTAAAGAGCAT |
| 3 | GGCCGGAACAAGCGGCAGCCGAACCACGACGACCTAGGG |
| 4 | TCCTCTAGACTATCGACAGCCACAGCCCACC |
| 5 | TGGGAATTCAGTTGCAAGCGACCATGCGC |
| 6 | CGGCTGCCGCTTGTTCCGGCC |
| 7 | ATTCGCACCACCATCGC |
| 8 | AGGTGTCGTCGTGGTTC |
| 9 | GGCCTACGAGGCGCAAGAACCACGACGACACCTGCCGGCGCCACTCGCTC |
| 10 | ACCAAACAGCATTTGATGCTCTCTCGCTCGCGATTTCCCATCGCATCCACTCGGTTGAG TGGATGGCGTGGTATGGTGCGATGGTGGTGCGAATTCAGCGGCACCCACATC |
| 11 | CAGACGGCCTACGAGGCGCAAGGGTAC |
| 12 | CCTTGCGCCTCGTAGGCCGTCTGGTAC |
| BMPDpp UTRF2 | GATGGTAGTAGAGGGATGTGGGTGCCGCTGAATTCGCACCACCATCGCACCATAC |
| BMPbs Dpp-R | CTGTGAGTGATGCTTAGGGCTCCGCTTGTTCCGGCCGCCCTTGCC |

**Table 6.2: List of Primers**

| Number | Description | Cloning Method |
|---|---|---|
| 1 | PBSATTBollasdppdeltaDally | pBattBHADppΔDally plasmid was used as a template and digested using XhoI and NheI. The insert was generated from pBattBollasDpp plasmid by digestion with XhoI and NheI. The resulting fragments were ligated. |
| 2 | PBSATTBollasHAdppdeltadally | pBattBOllasHAdpp plasmid was used as a template and digested using XhoI and BspEI. For the insert pBattBHAdppΔdally was digested with the same restriction enzymes. The two fragments were ligated. |
| 3 | PUASATTBHATdppDallyCD8TLR4 | pUASattB-Dpp plasmid was used as a template and digested using AgeI and KpnI. The insert was ordered from Genewiz ligated with the linearized vector using Gibson assembly. |
| 4 | PUASATTBHATdppdeltaDallyCD8TLR4 | pUASattB-Dpp plasmid was used as a template and digested using AgeI and KpnI. The insert was ordered from Genewiz ligated with the linearized vector using Gibson assembly. |
| 5 | PUASATTBHATDppdeltadallyTLR4 | pUASattB-Dpp plasmid was used as a template and digested using AgeI and KpnI. The insert was ordered from Genewiz ligated with the linearized vector using Gibson assembly. |
| 6 | PUASATTBHATdppDallyTLR4 | pUASattB-Dpp plasmid was used as a template and digested using AgeI and KpnI. The insert was ordered from Genewiz ligated with the linearized vector using Gibson assembly. |
| 7 | UASDppGFPdeltaDally | eGFP::Dpp was used as a template. The primers 3 and 4 were used to amplify one fragment. A second fragment was amplified using 6 and 5. Both fragments were combined by a PCR using the primers Dpp-F and GFP-R. This fragment was cloned into a TOPO vector. The TOPO vector and the eGFP::Dpp plasmid were digested using |

| | | |
|---|---|---|
| | | EcoRI and XbaI. The fragment from the TOPO vector was used as an insert and ligated into the eGFP::Dpp vector. |
| **8** | HADppdeltaprocessingBAA | Generated by Genewiz |
| **9** | HADppdeltaProcessingBAAdeltaDally | Generated by Genewiz |
| **10** | HADppchangedProcessing | Generated by Genewiz |
| **11** | HADppdeltaDallychangedprocessing | Generated by Genewiz |
| **12** | pBSATTBDppBMPDally | pBSattB-wtDpp plasmid was used as a template. PCR was run using BMPbsDpp-R and BMPDppUTRF2 as primers. The Insert Fragment was ordered at Genewiz and aligned with the PCR product using Gibson assembly. |
| **13** | pBSATTBDppDallyBMP | pBSattB-wtDpp plasmid was used as a template. PCR was run using 7 and 8 as primers. The Insert Fragment was ordered at Genewiz and another PCR was run with this Fragment and the primers 9 and 10. The two PCR products were combined using Gibson assembly. |
| **14** | PBSATTB_ProV5TehtDppOllasDpp | pBsattB-ollasdpp plasmid was used as a template and digested with BspEI and XhoI. The inserted fragment was ordered at Genewiz and also digested with BspEI and XhoI before ligation. |
| **15** | PBSATTB_ProV5TehtDppOllasDppDeltaDally | pBsattB-ollasdpp plasmid was used as a template and digested with BspEI and XhoI. The inserted fragment was ordered at Genewiz and also digested with BspEI and XhoI before ligation. |
| **16** | PBSATTB_ProV5TehtDppOllasDppDeltaaaDeltaDally | pBsattB-ollasdpp plasmid was used as a template and digested with BspEI and XhoI. The inserted fragment was ordered at Genewiz and also digested with BspEI and XhoI before ligation. |

| | | |
|---|---|---|
| **17** | pUAStattBsecGFPDallybs | pUASattBsecGFP was used as a template and digested using KpnI. The insert consisted of two annealed oligos (11 and 12), which were also digested with KpnI. Insert and vector where ligated. |
| **18** | RIV FRTDallyVenusFRT | RIVFmcspAFmcs3paxCHE and RIVwhiteDallyVenus were used as templates and digested with EcoRI and KpnI restriction enzymes. The DallyVenus part was then inserted into the RIVFmcspAFmcs3paxCHE vector by ligation. |
| **19** | pUASattP UAS-YFP-Dally | Was constructed using YFP-Dally flies (from Giorgos Pyrowolakis) as a template. To amplify the YFP-Dally sequence the two primers 1 and 2 were used. The amplified DNA sequence was cloned into the plasmid vector pUASattB using EcoRI restriction enzymes. |
| **20** | pUASattP UAS-YFP-DallydeltaHS | Was constructed using YFP-Dally$^{\Delta HS}$ flies (from Giorgos Pyrowolakis) as a template. To amplify the YFP-Dally$^{\Delta HS}$ sequence the two primers 1 and 2 were used. The amplified DNA sequence was cloned into the plasmid vector pUASattB using EcoRI restriction enzymes. |
| **21** | pUASattBDallyYFPdeltaHSdelta390bp1 | Generated by Genewiz |
| **22** | pUASattBDallyYFPdeltaHSdelta390bp2 | Generated by Genewiz |
| **23** | pUASattBDallyYFPdeltaHSdelta390bp3 | Generated by Genewiz |
| **24** | pUASattBDallyYFPdeltacore Protein | Generated by Genewiz |
| **25** | pUASattBDallyYFPdeltaHSdeltacoreProtein | Generated by Genewiz |
| **26** | pUASattBDallyYFPdeltaHSdeltaNterminalAA | Generated by Genewiz |

**Table 6.3: Plasmids generated during this study**

### *6.4.3 Gibson Assembly*

The strength of Gibson Cloning is that it allows for multiple DNA fragments, regardless their length or compatibility to be assembled together. In this study, multiple Plasmids were generated using this method (table xxx). To perform the Gibson assembly, a plasmid of choice was digested, using restriction enzymes (see Digestion) to linearize the plasmid. Insert Fragments were amplified using PCR. Oligos were designed to have 15-20bp homology distal and proximal with the vector, or the adjoined insert Oligo, depending on the number of inserts. To assemble vector and inserts, the following protocol was used:

- Xul insert
- Xul Vector
- 10ul Gibson Assembly Master Mix
- Xul H2O (up to 20ul)

To calculate the amount of Insert and vector the subsequent formula was used:

pmol=1000xng/bpx650

Cloning success is highest with 50-100ng of vector and 2-3 fold molar excess of insert. Since the Gibson Assembly Master Mix contains exonuclease to generate single stranded 3` overhangs, a polymerase and a Ligase to ligate the fragments, the solution could be transformed (see xxx) right incubation at 50°C for 1h.

## 6.5 Generation of transgenic flies

### *6.5.1 Preparation of electro-competent E.coli bacteria*

To generate electro-competent bacteria for transformation, the desired bacteria strain was added to 50ml LB medium without salt, including the proper Antibiotic, and placed at 37°C over night. The next morning, the culture was diluted 1:100 in 1l of LB medium without salt and without Antibiotic. These culture were grown until an $OD_{600}$ of 0.6-0.8. Once the correct $OD_{600}$ was reached, the bacteria were placed on ice to avoid further growth. From now on every step was conducted on ice or in cooled conditions. The cultures were put into bottles for the SLA-3000 rotor and centrifuged for 10min at 4°C. The supernatant was discarded and

the pellet re-suspended in 10% Glycerol. The re-suspended bacteria were distributed to 2ml Eppendorf tubes and centrifuged again at 4°C. The pellet was re-suspended again in 10% glycerol and then distributed as 50ul aliquots and shock cooled in liquid nitrogen. The bacteria were stored at -80°C until use.

### *6.5.2 Transformation*

For transformation, generated electro-competent E.coli bacteria were taken from -80°C freezer and put on ice. In the meantime, the salt concentration in the solution containing the DNA was reduced by dialyzing against H2O on a 0.025µm membrane filter paper (Millipore®) for 10 min. After dialyzing, 1ul of DNA solution was mixed with the bacteria and transfered into a 1 mm Gene Pulser cuvette. Transformation was executed on a Biorad Micropulser™. After Transformation, the bacteria were transferred quickly to 500ul of LB medium and kept at 37°C for 1h in a shaker. Then the bacteria were centrifuged for 30s at XXXrpm and 300ul of supernatant was discarded and the pellet resuspended in the remaining 200ul. Hereinafter, the bacteria were platted on LB Agar plates with the subsequent Antibiotic and left at 37°C over night.

### *6.5.3 Mini Preps*

Single colonies of transformed E.coli bacteria were picked from the LB Agar Plates with 200ul Pipet tips and grown in 5ml LB medium with respective Antibiotics over night at 37°C on a shaker. The next day, DNA was isolated using protocol 5.1 of NucleoSpin® Plasmid Kit (Machery-Nagel). Positive candidates were determined with restriction digests or directly via sequencing. Left over mini prep culture could be stored at 4°C for several days.

### *6.5.4 Midi Preps*

Once the correctness of the mini prep was determined, 5ul of the left over culture was taken and grown in 100ml of LB medium with the respective Antibiotic at 37°C over night on a shaker. Plasmid DNA was isolated using protocol 8.1 and 8.3 of NucleoBond® Xtra Midi EF (Macherey-Nagel). After purification, the concentration of DNA was determined using a Nanotrop Photospectrometer.

### *6.5.5 Injection*

Fly lines to be injected were set up in fly cages with grape-juice agar plates containing a fresh drop of yeast. Grape-juice agar plates were changed to fresh ones 3-4 times a day for 3 days until the flies laid enough eggs for injection. Embryos were collected over 30min, dechorionated in 30% Sodium hypochloride solution for 1min and collected in a container equipped with a fine-mashed net. After, Embryos were washed with water and transferred to an agar block to be aligned under a binocular. The aligned Embryos were picked up with a microscope slide containing embryo glue (adhesive tape dissolved in heptane). Next, the Embryos were dried using a cold hair dryer for 5min and covered with Voltalef PCTFE oil (Atofina). Then the Embryos were injected with Plasmid solution containing 300ng/ul DNA in 25ul of 10% 10xPBS. Injected Embryos were kept at 18°C for 2 days, switched to 25°C over night and collected the next morning. Survivors were collected in conventional fly vials containing polenta and yeast. Adult flies were collected and crossed with $y^{-}w^{-}$ flies and offspring was screened for positives. Single positives were crossed again to obtain balanced stocks.

### *6.5.6 Generating dpp endogenous mutants*

Dpp genomic fragments were injected into yw M{vas-int.Dm}zh-2A; dppMI03752/Cyo, P23 flies. Embryos were collected and after hatching crosses with themselves. The offspring was screened for a loss of y, which was inserted between attP sites in the mimic transposon line. This mimic fragment should be exchanged with the inserted dpp mutant fragment. Positive flies were single crossed with balancer flies to establish a stock. The orientation of the insert was tested with PCR. In these flies, the endogenous dpp was still present. To remove the endogenous dpp, male flies with the right orientation of the insert were crossed to hsFLP; al, Pbac{RB}e00178 /SM6, al, sp and heat shocked every day for 1h until they hatched. Since both flies contain FRT sites, a FRT mediated recombination appeared. Upon recombination the inserted dpp fragment is followed by a FRT site and $w^{+}$. Males positive for w were corssed with the balancer stock yw; al, b, c, sp/ SM6, al, sp. The offspring from this cross was screened for $w^{+}$, no al and no mcherry. Flies positive for all three selection criteria were single crossed again to yw; al, b, c, sp/ SM6, al, sp and a stock was established with their offspring.

### *6.5.7 UAS/Gal4 System*

The UAS/Gal4 system is a useful system derived from yeast to ectopically switch genes on or off in specific regions of an organism. This system is commonly used in Drosophila to drive tissue specific expression of a gene of interest. In this study the system was used to ectopically express or knock down genes using RNAi. Gal4 is a transcription factor which binds to the Upstream Activating Sequence, short UAS. This binding activates an upstream situated gene. Nowadays exists many UAS and Gal4 lines in Drosophila. This allows for many possible combinations to activate or knock out different genes in different places within Drosophila. In order to be able to activate your gene of interest temporally, the Gal80ts can be used. Gal80 represses the function of Gal4 and by that blocks the activation of UAS activated genes. Since Gal80ts is temperature sensitive and is deactivated at 29°C, the expression of a gene of interest can be temporally regulated.

### *6.5.8 Generation of mitotic recombination clones*

Flystocks with the genotypes *HA-dppΔDallyFRT w+/Sm6* and *hsflp;armlacZ M(2) FRT/CyO* were crossed with each other and offspring collected over night. Collected larvae were kept at 18°C for 48h, before they were transferred to 37°C for 1h of heatshock. Larvae were dissected after another 6-7 days at 18°C. Clones were identified by a lack of lacZ expression.

*Genewiz Fragments*

HATdppΔdallyTLR4

AGCACGGACACGGTGAGCCTCGATGTCCAGCCGGCCGTGGACCGGTGGCTGGCGAGTCCGCAGCGCAACTACGGACTGCTGGTGGAGGTGCGGACGGT
CCGCTCCCTGAAGCCGGCCCCACACCATCACGTACGCCTGCGCCGCAGCGCGGACGAGGCGCACGAGCGGTGGCAGCACAAGCAGCCGCTCCTGTTCACC
TACACGGACGACGGGCGGCACAAGGCGCGCTCCATTCGGGACGTGTCTGGCGGAGAGGGCGGTGGCAAGGGCGGCCGGAACAAGCGGCAGCCGAACC
ACGACGACCTCGAGTACCCATACGATGTTCCAGATTACGCCGGAGGTGGATCAGGCGGAGGCTCAGGGGGAGGTTCGACCATCATTGGTGTGTCGGTCCT
CAGTGTGCTTGTAGTATCTGTTGTAGCAGTTCTGGTCTATGGCGGAGGCTCTGGAGGAGGTTCTCGAACAATTATCGGGGTATCGGTACTAAGCGTACTTG
TTGTCTCTGTCGTTGCAGTCCTGGTATATGGTGGTGGCTCCGGCGGTGGATCGGCTAGCACCTGCCGGCGGCACTCGCTGTACGTGGACTTCTCGGACGTG
GGCTGGGACGACTGGATTGTGGCGCCTCTGGGCTACGATGCGTACTACTGCCACGGGAAGTGCCCCTTCCCGCTGGCCGACCACTTCAACTCGACCAATCA
CGCCGTGGTGCAGACCCTGGTCAACAATATGAATCCCGGCAAGGTGCCGAAGGCGTGCTGCGTGCCCACGCAACTGGACAGCGTGGCCATGCTCTATCTC
AACGACCAAAGTACGGTGGTGCTGAAGAACTACCAGGAGATGACCGTGGTGGGCTGTGGCTGTCGATAGGGTACCTCTAGAGGATCTTTGTGAAGGAAC
CTTACTTCTGTGGTGT

HATdppTLR4

AGCACGGACACGGTGAGCCTCGATGTCCAGCCGGCCGTGGACCGGTGGCTGGCGAGTCCGCAGCGCAACTACGGACTGCTGGTGGAGGTGCGGACGGT
CCGCTCCCTGAAGCCGGCCCCACACCATCACGTACGCCTGCGCCGCAGCGCGGACGAGGCGCACGAGCGGTGGCAGCACAAGCAGCCGCTCCTGTTCACC
TACACGGACGACGGGCGGCACAAGGCGCGCTCCATTCGGGACGTGTCTGGCGGAGAGGGCGGTGGCAAGGGCGGCCGGAACAAGCGGCAGCCGAACC
ACGACGACCTCGAGTACCCATACGATGTTCCAGATTACGCCGGAGGTGGATCAGGCGGAGGCTCAGGGGGAGGTTCGACCATCATTGGTGTGTCGGTCCT

CAGTGTGCTTGTAGTATCTGTTGTAGCAGTTCTGGTCTATGGCGGAGGCTCTGGAGGAGGTTCTCGAACAATTATCGGGGTATCGGTACTAAGCGTACTTG
TTGTCTCTGTCGTTGCAGTCCTGGTATATGGTGGTGGCTCCGGCGGTGGATCGAGACGGCCTACGAGGCGCAAGGCTAGCACCTGCCGGCGGCACTCGCT
GTACGTGGACTTCTCGGACGTGGGCTGGGACGACTGGATTGTGGCGCCTCTGGGCTACGATGCGTACTACTGCCACGGGAAGTGCCCCTTCCCGCTGGCC
GACCACTTCAACTCGACCAATCACGCCGTGGTGCAGACCCTGGTCAACAATATGAATCCCGGCAAGGTGCCGAAGGCGTGCTGCGTGCCCACGCAACTGG
ACAGCGTGGCCATGCTCTATCTCAACGACCAAAGTACGGTGGTGCTGAAGAACTACCAGGAGATGACCGTGGTGGGCTGTGGCTGTCGATAGGGTACCTC
TAGAGGATCTTTGTGAAGGAACCTTACTTCTGTGGTGT

## HATdppΔdallyCD8TLR4

AGCACGGACACGGTGAGCCTCGATGTCCAGCCGGCCGTGGACCGGTGGCTGGCGAGTCCGCAGCGCAACTACGGACTGCTGGTGGAGGTGCGGACGGT
CCGCTCCCTGAAGCCGGCCCCACACCATCACGTACGCCTGCGCCGCAGCGCGGACGAGGCGCACGAGCGGTGGCAGCACAAGCAGCCGCTCCTGTTCACC
TACACGGACGACGGGCGGCACAAGGCGCGCTCCATTCGGGACGTGTCTGGCGGAGAGGGCGGTGGCAAGGGCGGCCGGAACAAGCGGCAGCCGAACC
ACGACGACCTCGAGTACCCATACGATGTTCCAGATTACGCCGGAGGTGGATCAGGCGGAGGCTCAGGGGGAGGTTCGATTTACATCTGGGCACCCTTGGC
CGGAATCTGCGTGGCCCTTCTGCTGTCCTTGATCATCACTCTCATCTGCTACGGCGGAGGCTCTGGAGGAGGTTCTCGAACAATTATCGGGGTATCGGTACT
AAGCGTACTTGTTGTCTCTGTCGTTGCAGTCCTGGTATATGGTGGTGGCTCCGGCGGTGGATCGGCTAGCACCTGCCGGCGGCACTCGCTGTACGTGGACT
TCTCGGACGTGGGCTGGGACGACTGGATTGTGGCGCCTCTGGGCTACGATGCGTACTACTGCCACGGGAAGTGCCCCTTCCCGCTGGCCGACCACTTCAA
CTCGACCAATCACGCCGTGGTGCAGACCCTGGTCAACAATATGAATCCCGGCAAGGTGCCGAAGGCGTGCTGCGTGCCCACGCAACTGGACAGCGTGGCC
ATGCTCTATCTCAACGACCAAAGTACGGTGGTGCTGAAGAACTACCAGGAGATGACCGTGGTGGGCTGTGGCTGTCGATAGGGTACCTCTAGAGGATCTT
TGTGAAGGAACCTTACTTCTGTGGTGT

## HATdppCD8TLR4

AGCACGGACACGGTGAGCCTCGATGTCCAGCCGGCCGTGGACCGGTGGCTGGCGAGTCCGCAGCGCAACTACGGACTGCTGGTGGAGGTGCGGACGGT
CCGCTCCCTGAAGCCGGCCCCACACCATCACGTACGCCTGCGCCGCAGCGCGGACGAGGCGCACGAGCGGTGGCAGCACAAGCAGCCGCTCCTGTTCACC
TACACGGACGACGGGCGGCACAAGGCGCGCTCCATTCGGGACGTGTCTGGCGGAGAGGGCGGTGGCAAGGGCGGCCGGAACAAGCGGCAGCCGAACC
ACGACGACCTCGAGTACCCATACGATGTTCCAGATTACGCCGGAGGTGGATCAGGCGGAGGCTCAGGGGGAGGTTCGATTTACATCTGGGCACCCTTGGC
CGGAATCTGCGTGGCCCTTCTGCTGTCCTTGATCATCACTCTCATCTGCTACGGCGGAGGCTCTGGAGGAGGTTCTCGAACAATTATCGGGGTATCGGTACT
AAGCGTACTTGTTGTCTCTGTCGTTGCAGTCCTGGTATATGGTGGTGGCTCCGGCGGTGGATCGAGACGGCCTACGAGGCGCAAGGCTAGCACCTGCCGG
CGGCACTCGCTGTACGTGGACTTCTCGGACGTGGGCTGGGACGACTGGATTGTGGCGCCTCTGGGCTACGATGCGTACTACTGCCACGGGAAGTGCCCCT
TCCCGCTGGCCGACCACTTCAACTCGACCAATCACGCCGTGGTGCAGACCCTGGTCAACAATATGAATCCCGGCAAGGTGCCGAAGGCGTGCTGCGTGCCC
ACGCAACTGGACAGCGTGGCCATGCTCTATCTCAACGACCAAAGTACGGTGGTGCTGAAGAACTACCAGGAGATGACCGTGGTGGGCTGTGGCTGTCGAT
AGGGTACCTCTAGAGGATCTTTGTGAAGGAACCTTACTTCTGTGGTGT

## ProV5tehtDpp

GAGGCTCATGCACTTGATCCTCCGGATTGTACGGTTTTATTCGCTGATTCCGATTTCAGGTGGATAAAGCAGACAGCTGGAAGTGGGCTGTTTTTTAGAACC
ACCTATAAAAAGATGGAATGTGCTAAAGTCCTTTTTTTAGATTCATTAGCCAAGTTCCTATGATTTATTTGCTCCAAACTCACCCGCAATATCCTTCTTTTCCG
TTTGCTTGCAGATAGTAAAATCGACGATCGATTTCCGCACCACCATCGGTTTCGGCTGCACTTCGACGTGAAGAGCATTCCCGCCGACGAGAAGCTGAAGG
CGGCGGAGCTGCAGCTGACCCGGGACGCACTCAGTCAACAGGTGGTGGCCAGCAGATCGTCGGCGGGTAAGCCTATCCCTAACCCTCTCCTCGGTCTCGA
TTCTACGGACGTCGGAGGTGGCTCAGGCGGAGGATCAGGGGGAGGATCGACCATTATAGGCGTAAGCGTACTGAGCGTGCTTGTGGTCAGCGTCGTGGC
AGTACTGGTGTATGGAGGAGGCTCTGGCGGAGGTTCTCGAACAATTATCGGGGTATCGGTACTAAGCGTACTTGTTGTCTCTGTCGTTGCAGTCCTGGTAT
ATGGTGGTGGCTCCGGCGGTGGATCGAGATCTAATCGGACGCGCTACCAGGTGCTTGTCTACGACATCACGCGCGTCGGGGTGCGTGGTCAGCGGGAGC
CGAGCTATCTGCTGTTGGACACCAAGACGGTCCGGCTTAACAGCACGGACACGGTGAGCCTCGATGTCCAGCCGGCCGTGGACCGGTGGCTGGCGAGTCC
GCAGCGCAACTACGGACTGCTGGTGGAGGTGCGGACGGTCCGCTCCCTGAAGCCGGCCCCACACCATCACGTACGCCTGCGCCGCAGCGCGGACGAGGC
GCACGAGCGGTGGCAGCACAAGCAGCCGCTCCTGTTCACCTACACGGACGACGGGCGGCACAAGGCGCGCTCCATTCGGGACGTGTCTGGCGGAGAGG
GCGGTGGCAAGGGCGGCCGGAACAAGCGGCAGCCGAGACGGCCTACGAGGCGCAAGAACCACGACGACCTCGAGTACCCATACG

### ProV5tehtDppΔdally

GAGGCTCATGCACTTGATCCTCCGGATTGTACGGTTTTATTCGCTGATTCCGATTTCAGGTGGATAAAGCAGACAGCTGGAAGTGGGCTGTTTTTTAGAACC
ACCTATAAAAAGATGGAATGTGCTAAAGTCCTTTTTTTAGATTCATTAGCCAAGTTCCTATGATTTATTTGCTCCAAACTCACCCGCAATATCCTTCTTTTCCG
TTTGCTTGCAGATAGTAAAATCGACGATCGATTTCCGCACCACCATCGGTTTCGGCTGCACTTCGACGTGAAGAGCATTCCCGCCGACGAGAAGCTGAAGG
CGGCGGAGCTGCAGCTGACCCGGGACGCACTCAGTCAACAGGTGGTGGCCAGCAGATCGTCGGCGGGTAAGCCTATCCCTAACCCTCTCCTCGGTCTCGA
TTCTACGGACGTCGGAGGTGGCTCAGGCGGAGGATCAGGGGGAGGATCGACCATTATAGGCGTAAGCGTACTGAGCGTGCTTGTGGTCAGCGTCGTGGC
AGTACTGGTGTATGGAGGAGGCTCTGGCGGAGGTTCTCGAACAATTATCGGGGTATCGGTACTAAGCGTACTTGTTGTCTCTGTCGTTGCAGTCCTGGTAT
ATGGTGGTGGCTCCGGCGGTGGATCGAGATCTAATCGGACGCGCTACCAGGTGCTTGTCTACGACATCACGCGCGTCGGGGTGCGTGGTCAGCGGGAGC
CGAGCTATCTGCTGTTGGACACCAAGACGGTCCGGCTTAACAGCACGGACACGGTGAGCCTCGATGTCCAGCCGGCCGTGGACCGGTGGCTGGCGAGTCC
GCAGCGCAACTACGGACTGCTGGTGGAGGTGCGGACGGTCCGCTCCCTGAAGCCGGCCCCACACCATCACGTACGCCTGCGCCGCAGCGCGGACGAGGC
GCACGAGCGGTGGCAGCACAAGCAGCCGCTCCTGTTCACCTACACGGACGACGGGCGGCACAAGGCGCGCTCCATTCGGGACGTGTCTGGCGGAGAGG
GCGGTGGCAAGGGCGGCCGGAACAAGCGGCAGCCGAACCACGACGACCTCGAGTACCCATACG

### ProV5tehtDppΔAAΔdally

GAGGCTCATGCACTTGATCCTCCGGATTGTACGGTTTTATTCGCTGATTCCGATTTCAGGTGGATAAAGCAGACAGCTGGAAGTGGGCTGTTTTTTAGAACC
ACCTATAAAAAGATGGAATGTGCTAAAGTCCTTTTTTTAGATTCATTAGCCAAGTTCCTATGATTTATTTGCTCCAAACTCACCCGCAATATCCTTCTTTTCCG
TTTGCTTGCAGATAGTAAAATCGACGATCGATTTCCGCACCACCATCGGTTTCGGCTGCACTTCGACGTGAAGAGCATTCCCGCCGACGAGAAGCTGAAGG
CGGCGGAGCTGCAGCTGACCCGGGACGCACTCAGTCAACAGGTGGTGGCCAGCAGATCGTCGGCGGGTAAGCCTATCCCTAACCCTCTCCTCGGTCTCGA
TTCTACGGACGTCGGAGGTGGCTCAGGCGGAGGATCAGGGGGAGGATCGACCATTATAGGCGTAAGCGTACTGAGCGTGCTTGTGGTCAGCGTCGTGGC
AGTACTGGTGTATGGAGGAGGCTCTGGCGGAGGTTCTCGAACAATTATCGGGGTATCGGTACTAAGCGTACTTGTTGTCTCTGTCGTTGCAGTCCTGGTAT
ATGGTGGTGGCTCCGGCGGTGGATCGAGATCTAATCGGACGCGCTACCAGGTGCTTGTCTACGACATCACGCGCGTCGGGGTGCGTGGTCAGCGGGAGC
CGAGCTATCTGCTGTTGGACACCAAGACGGTCCGGCTTAACAGCACGGACACGGTGAGCCTCGATGTCCAGCCGGCCGTGGACCGGTGGCTGGCGAGTCC
GCAGCGCAACTACGGACTGCTGGTGGAGGTGCGGACGGTCCGCTCCCTGAAGCCGGCCCCACACCATCACGTACGCCTGCGCCGCAGCGCGGACGAGGC
GCACGAGCGGTGGCAGCACAAGCAGCCGCTCCTGTTCACCTACACGGACGACGGGCGGCACAAGGCGCGCTCCATTCGGGACGTGTCTGGCGGAGAGG
GCGGTGGCGACGACCTCGAGTACCCATACG

### DppDallyBMP

CGGCGCCACTCGCTCTATGTGGACTTCAGCGATGTGGGCTGGAATGACTGGATTGTGGCCCCACCAGGCTACCAGGCCTTCTACTGCCATGGGGACTGCCC
CTTTCCACTGGCTGACCACCTCAACTCAACCAACCATGCCATTGTGCAGACCCTGGTCAATTCTGTCAATTCCAGTATCCCCAAAGCCTGTTGTGTGCCCACT
GAACTGAGTGCCATCTCCATGCTGTACCTGGATGAGTATGATAAGGTGGTACTGAAAAATTATCAGGAGATGGTAGTAGAGGGATGTGGGTGCCGCTGA

### DppBMPDally

AGCCCTAAGCATCACTCACAGCGGGCCAGGAAGAAGAATAAGAACTGCCGGCGCCACTCGCTCTATGTGGACTTCAGCGATGTGGGCTGGAATGACTGG
ATTGTGGCCCCACCAGGCTACCAGGCCTTCTACTGCCATGGGGACTGCCCCTTTCCACTGGCTGACCACCTCAACTCAACCAACCATGCCATTGTGCAGACC
CTGGTCAATTCTGTCAATTCCAGTATCCCCAAAGCCTGTTGTGTGCCCACTGAACTGAGTGCCATCTCCATGCTGTACCTGGATGAGTATGATAAGGTGGTA
CTGAAAAATTATCAGGAGATGGTAGTAGAGGGATGTGGGTGCCGCTGA

# Results

# 7 Results

## 7.1 Paper manuscript

# Dally is not essential for Dpp spreading or internalization but for Dpp stability by antagonizing Tkv-mediated internalization of Dpp

Niklas Simon*[1], Abu Safyan *[2,3,4], Giorgos Pyrowolakis[2,3,4], Shinya Matsuda[1]

1. Growth & Development, Biozentrum, Spitalstrasse 41, University of Basel, 4056 Basel, Switzerland
2. Institute for Biology I, Faculty of Biology, University of Freiburg, 79104 Freiburg, Germany.
3. CIBSS – Centre for Integrative Biological Signalling Studies, University of Freiburg, 79104 Freiburg, Germany.
4. Center for Biological Systems Analysis, University of Freiburg, Habsburgerstrasse 49, 79104 Freiburg, Germany.

* These authors contributed equally.

For correspondence:

shinya.matsuda@unibas.ch

g.pyrowolakis@biologie.uni-freiburg.de

**Abstract**

Dpp/BMP acts as a morphogen to control cell fates and tissue growth during development. Two glypicans, Division abnormally delayed (Dally) and Dally-like (Dlp) have been proposed to interact with Dpp through their heparan sulfate (HS) chains and control Dpp gradient formation by facilitating Dpp transport, stabilizing Dpp on the cell surface, or recycling Dpp in the Drosophila wing disc. However, how these distinct glypicans control Dpp/BMP gradient formation remains largely unknown. Here we generate genome engineering platforms for glypicans and found that Dally, but not Dlp, is critical for Dpp gradient formation through interaction of its core protein with Dpp. We show that HS of Dally is essential but its direct interaction with Dpp is largely dispensable for Dpp gradient formation and signaling. We provide evidence that, while largely dispensable for transporting or recycling Dpp, HS of Dally is required for stabilizing Dpp on the cell surface through antagonizing Tkv-mediated Dpp internalization. These results provide new insights into how glypicans control dispersal and signaling of distinct morphogens during development.

**Introduction**

Morphogens are signaling molecules that are secreted from localized source cells and control cell fates in a concentration dependent manner during development. Evolutionarily conserved signaling molecules have been proposed to act as morphogens in a variety of developing tissues (Briscoe et al., 2001; Lecuit et al., 1996; Nellen et al., 1997; Neumann & Cohen, 1997; Strigini & Cohen, 1996). Among them, *Decapentaplegic* (*dpp*), the vertebrate BMP2/4 homolog. How Dpp acts as a morphogen in the Drosophila wing imaginal disc (wing precursor) has served as an excellent model to investigate how morphogens spread, establish a morphogen gradient, control and coordinate tissue patterning and growth (Hamaratoglu et al., 2014). In the Drosophila wing disc, Dpp spreads from an anterior stripe of cells along the anterior-posterior compartment boundary to act as a morphogen to control nested target gene expressions and growth in the wing disc. Dpp binds to the Type I receptor Tkv to induce the tetrameric receptor complex consisting of Tkv and type II receptor Punt. Tkv then phosphorylates the downstream transcription factor Mad, resulting into the graded phosphorylated Mad (pMad) distribution that reflects Dpp signaling activity in the wing disc. The pMad gradient then regulates nested target gene expressions (ex, Sal and Omb) mainly through generating an inverse gradient of a transcription repressor Brk repressed by Dpp. The nested target gene expression patterns are thought to position the future adult wing veins such as L2 and L5. Dpp signal controls also growth of the wing through repressing Brk as complete lack of wing disc tissue in *dpp* mutants is rescued by removing *brk*.

While the endogenous Dpp is indeed distributed in a graded manner (Matsuda et al., 2021), how the gradient arises is controversial. A class of molecules that controls Dpp gradient formation are the glypicans, a family of GPI-anchored heparan sulfate proteoglycans (HSPGs) that consist of a core protein and haparan sulfate (HS) chains covalently attached to them (Filmus et al., 2009). Previous genetic studies showed that two Drosophila glypicans, Division abnormally delayed (Dally) and Dally-like (Dlp), are involved in regulating a variety of signaling pathways such as Hh, Wg, and Dpp (Belenkaya et al., 2004; Han et al., 2004; McGough et al., 2020). In the case of Dpp, glypicans are proposed to act as co-receptors and regulate Dpp morphogen distribution and signaling (Belenkaya et al., 2004; Fujise, 2003). Indeed, upon GFP-Dpp overexpression, extracellular Dpp distribution and pMad signal was reduced when the two, Dally and Dlp, were removed (Belenkaya et al., 2004). Similar phenotypes were observed in mutant clones for *sulfateless* (*sfl*), a heparan sulfate N-deacetylase/N-sulfotransferase required for HS biosynthesis (Baeg et al., 2001; Lin & Perrimon, 1999). Given that Dpp binds to heparin (Akiyama et al., 2008), it has been generally thought that interaction of Dpp with the HS chains of glypicans is essential for their function to regulate Dpp gradient formation and signaling.

Several models have been proposed on how glypicans control Dpp morphogen gradient formation. First, glypicans are proposed to transport Dpp by handing it over from one cell to the next cells in a “bucket brigade” manner (Kerszberg & Wolpert, 1998). Consistent with the so-called "restricted diffusion” model, FRAP assay using overexpression of GFP-Dpp revealed a low diffusion coefficient of Dpp ($D=0.1\pm0.05\mu m^2/s$). Indeed, pMad signal and Dpp distribution has been shown to be reduced not only in the glypican mutant clones but also in the surrounding wild type cells located further to the Dpp producing cells (so-called “shadow” effect), indicating that Dpp spreading requires glypicans.

Second, glypicans are proposed to interfere with Dpp spreading. The “hindered diffusion” model postulates that Dpp spreads freely and transient interaction of Dpp with cell surface molecules such as glypicans and receptors can hinder Dpp spreading (Muller et al., 2013). It has recently been shown that Pentagon (Pent), a secreted feedback factor, crucial for expanding the Dpp gradient, can internalize and degrade glypicans (Norman et al., 2016). The Dpp signaling gradient expanded upon loss of glypicans in the peripheral regions, where pent is expressed, indicating that Pent degrades glypicans in the peripheral region to allow Dpp to spread (Zhu et al., 2020).

Third, glypicans are proposed to stabilize Dpp on the cell surface (Akiyama et al., 2008). Dpp lacking the N-terminal HS binding site is less stable than wild type Dpp, indicating that Dally regulates Dpp distribution by stabilizing Dpp on the cell surface (Akiyama et al., 2008). Given that genetic interaction showed that Dally antagonizes Tkv, which is thought to internalize and

degrade Dpp, Dally has been proposed to stabilize Dpp by blocking Tkv-mediated internalization and degradation of Dpp.

Forth, glypicans and Pent are proposed to control endocytosis of Dpp followed by its recycling and secretion, which is critical for Dpp spreading and thereby scaling of the Dpp gradient (Romanova-Michaelides et al., 2022). Surprisingly, although receptor-mediated endocytosis is thought to be the mechanism to clear morphogens from the exptracellular space, the same study showed that Dpp can be internalized in *tkv* mutant clones, indicating that Tkv is not the receptor to internalize Dpp.

In this study, to better understand the function of glypicans, we generated genome engineering platforms to manipulate two glypicans, Dally and Dlp. Together with recently generated endogenously tagged *dpp* alleles and protein binder tools to visualize and manipulate the endogenous Dpp morphogen gradient (Matsuda et al., 2021), we first found that Dally, but not Dlp, is critical for Dpp gradient formation through interaction of its core protein with Dpp. Surprisingly, we found that while HS of Dally is essential for Dally's function, *dpp* mutants that lack interaction with HS display minor phenotypes, indicating that the interaction of HS of Dally with Dpp is largely dispensable for Dpp gradient formation and signaling. We provide evidence that, HS of Dally is not essential for Dpp internalization or spreading but rather antagonizes Tkv-mediated internalization of Dpp to stabilize Dpp on the cell surface. These results provide new insights into how glypicans control dispersal and signaling of distinct morphogens during development.

**Results**

**Dally but not Dlp interacts with Dpp**

Previous genetic studies showed that Drosophila Glypicans Dally and Dlp are involved in extracellular Dpp distribution and signaling through the interaction of Dpp with HS chains on Dally and Dlp (Belenkaya et al., 2004). However, the relative contribution of each Glypicans on Dpp distribution and signaling remains unclear. To address this, we first compared the ability of Dally and Dlp to activate Dpp signaling and trap Dpp in the wing disc. We found that expression of Dally in the dorsal compartment of the wing disc using *ap*-Gal4 induced a larger pMad gradient compared with that of the control ventral compartment (Fig. 7.1.1A, B). In contrast, expression of Dlp using ap-Gal4 did not expand the pMad gradient (Fig. 7.1.1C, D). To visualize endogenous extracellular Dpp distribution, we utilized a functional *Ollas-dpp* allele (Bauer et al., 2022) as well as an *HA-dpp* allele (Matsuda et al., 2021). We found that Dally expression broadly expanded extracellular Ollas-Dpp distribution, although Dpp signal reached to the background level at the peripheral region (Fig. 7.1.1E, F), indicating that the majority of trapped Dpp is sequestered by Dally. In contrast, Dlp expression did not expand but rather reduced extracellular Ollas-Dpp distribution (Fig. 7.1.1G, H). Instead, consistent with

a previous report (Han et al., 2005), Dlp, but not Dally, expanded extracellular Wg distribution (Fig. 7.1.1I-L). These results suggest that each HSPG has ligand preference; Dally interacts with Dpp and Dlp interacts with Wg.

**Dally, but not Dlp, is required for the Dpp gradient formation and signaling**

To compare the relative contribution of Dally and Dlp for Dpp distribution and signaling, we then generated null mutants for *dally* and *dlp* (*dally*$^{KO}$ and *dlp*$^{KO}$ respectively) by inserting an attP site via CRISPR. Although there is no good anti-Dally antibody, comparison of *dally*$^{KO}$ and *dally*$^{32}$ (a null allele) showed that defects in pMad signal in *dally*$^{KO}$ wing discs are similar to that in *dally*$^{32}$ wing discs (Fig. 7.1.2A-C,E). Consistently, in the adult wing, defects in growth and patterning (partial loss of L5) in *dally*$^{KO}$ mutants mimic that in *dally*$^{32}$ mutants (Fig. 7.1.2F-H, J). In contrast, immunostaining for Dlp revealed that Dlp expression is completely lost in *dlp*$^{KO}$ wing disc (Fig. 7.1.S1). Thus, we confirmed that they are null alleles respectively. These null alleles also serve as a platform to insert a tag or introduce mutations into *dally* or *dlp* locus.
We then compared the two null alleles and found that, while severely shrunk in the *dally*$^{KO}$ wing disc, pMad signal was not affected in *dlp*$^{KO}$ wing disc (Fig. 7.1.2C, D). In the rare mutant adult wings, patterning defects linked to defects in Dpp signaling (truncated L5) were seen in *dally*$^{KO}$ mutants (Fig. 7.1.2H). In contrast, distal tip of L3 was close toward L4 in *dlp*$^{KO}$ mutants (see arrows in Fig. 7.1.2I), which is indicative of Hh signaling defects. Although both *dally*$^{KO}$ and *dlp*$^{KO}$ adult wings are smaller than control (Fig. 7.1.2J), *dally*$^{KO}$ adult wings, but not *dlp*$^{KO}$ adult wings, are narrower along the A-P axis (Fig. 7.1.S2). Consistently, while severely shrunk in the *dally*$^{KO}$ wing discs, extracellular Dpp distribution was not affected in *dlp*$^{KO}$ wing disc (Fig. 7.1.2K-N). These results suggest that Dally, but not Dlp, is required for Dpp signaling-mediated wing patterning and growth along the A-P axis.

To test if the functions of the two glypicans are exchangeable, we first generated *YFP-dally* and *3xHA-dlp* respectively. *YFP-dally* rescued pMad defects in the wing disc (Fig. 7.1.2O-Q, S) and adult wing patterning and growth defects in *dally*$^{KO}$ mutants (Fig. 7.1.2T-V, Z). *3xHA-dlp* showed no growth defects in the adult wing (Fig. 7.1.2W, X, Z). Furthermore, both alleles have no obvious defects in external morphology and can be maintained as homozygous stocks, confirming that each allele is functional. We then inserted *3xHA-dlp* into *dally*$^{KO}$ and found that *3xHA-dlp* inserted into *dally*$^{KO}$ could not rescue pMad defects (Fig. 7.1.2P, R, S) or adult wing patterning and growth defects in *dally*$^{KO}$ mutants (Fig 7.1.2U, Y, Z), indicating that Dlp cannot replace Dally.

Taken together, these results suggest that *dally*, but not *dlp*, is required for Dpp distribution and signaling.

**Interaction of core protein of Dally with Dpp**

How can only Dally be involved in Dpp distribution and signaling if HS is attached to both HSPGs (Filmus et al., 2009)? It has been implicated that Dally interacts with Dpp *in vitro* not only through HS but also through the core protein (Kirkpatrick et al., 2006). Thus, we wondered if the core protein of Dally can interact with Dpp in the wing disc. To test this, we compared the ability of overexpressed Dally and Dally$^{\Delta HS}$, a *dally* mutant lacking all three HS attachment sites, to trap Dpp on the cell surface of the wing disc. We first confirmed that HS levels do not increase upon *dally$^{\Delta HS}$* expression (Fig.7.1.S3) (ref). We found that GFP-Dally$^{\Delta HS}$ expression in the dorsal compartment trapped endogenous Ollas-Dpp higher than GFP-HA-Dally expression (Fig. 7.1.3A, D). However, since GFP-Dally$^{\Delta HS}$ expression was higher than Dally expression (Fig. 7.1.3A, C inset), we measured the relative Dpp accumulation against Dally expression (Fig. 7.1.3E). We found that relative Dpp accumulation upon *dally$^{\Delta HS}$* expression is slightly reduced compared with that upon *dally* expression (Fig. 7.1.3E). These results suggest that Dally can interact with Dpp through HS but mainly through the core protein of Dally in the wing disc. Interestingly, while expanded upon Dally expression (Fig. 7.1.3F, G), pMad signal was rather narrowed upon *dally$^{\Delta HS}$* expression despite broad Dpp accumulation (Fig.7.1.3 H, I), indicating that HS of Dally is required for co-receptor function of Dally.

**HS of Dally is critical for Dally function**

It has been proposed that HS is essential for Dpp distribution and signaling (Belenkaya et al., 2004). However, the interaction of the core-protein of Dally with Dpp raises the question about if and how HS of Dally is involved in Dpp distribution and signaling. To test this, we generated *YFP-dally$^{\Delta HS}$* alleles. We found that pMad signaling and extracellular Dpp distribution were severely affected in the *dally-YFP$^{\Delta HS}$* wing discs similar to *dally$^{KO}$* mutant phenotypes (Fig. 7.1.3J-N). These results suggest that, although the core protein of Dally can sufficiently interact with Dpp in the wing disc (Fig.7.1.3C), HS of Dally is required for Dpp signaling and Dpp distribution in the wing disc.

**Interaction of HS of Dally with Dpp is largely dispensable for Dpp distribution and signaling**

A previous study showed that basic amino acids at the N-terminal of the Dpp mature domain is crucial to interact with heparin and Dally but is dispensable for interaction with receptors (Akiyama et al., 2008), indicating that the interaction of HS of Dally with Dpp through the basic amino acids at the N-terminal of Dpp is critical for Dally function. To test the importance of this interaction *in vivo*, we generated *dpp$^{\Delta N}$*, in which N-terminal basic amino acids were deleted from the Dpp mature domain (Akiyama et al., 2008). We first found that the *dpp$^{\Delta N}$* allele is embryonic lethal likely because the heparin binding domain is also a collagen binding site and

the interaction of Dpp with Collagen IV is important for shuttling Dpp toward the dorsal midline of the early embryo (Sawala et al., 2012).

To bypass this embryonic lethality, we utilized a transgene that contains the genomic region of *dpp* (JAX) that rescues the early lethality of *dpp* mutants (Hoffmann & Goodman, 1987). The transgene does not rescue the wing phenotypes of *dpp* disc alleles (Fig. 7.1.S4), thus making the transgene ideal to bypass the embryonic lethality without affecting the wing disc development. Indeed, early lethality of *HA-dpp$^{\Delta N}$* was greatly rescued in *JAX; HA-dpp$^{\Delta N}$*, allowing us to study the effects of the absence of the basic amino acids in later stages. We found that pMad and extracellular Dpp distribution were slightly reduced in *JAX; HA-dpp$^{\Delta N}$* mutant wing discs compared with the control *JAX; HA-dpp* wing disc (Fig. 7.1.4A-D), but overall phenotypes were much milder than *dally$^{KO}$* (Fig. 7.1.2) or *dally$^{\Delta HS}$* mutants (Fig. 7.1.3). Consistently, patterning and growth defects in *JAX; HA-dpp$^{\Delta N}$* adult wings were much milder than dally adult wing (Fig. 7.1.4E-G).

To test the interaction of Dpp$^{\Delta N}$ with Dally, we compared the ability of Dally to trap endogenously expressed Dpp or Dpp$^{\Delta N}$. We found that Dally expression trapped Dpp$^{\Delta N}$ less efficiently than Dpp (Fig. 7.1.4H-J), consistent with the interaction of basic amino acids of Dpp with Dally (Akiyama et al., 2008). The remaining interaction of Dally and Dpp$^{\Delta N}$ could be mediated by the interaction of HS of Dally with Dpp outside the basic amino acids, which may explain the mild phenotypes of *JAX; HA-dpp$^{\Delta N}$*. To test this, we then compared the ability of Dally and Dally$^{\Delta HS}$ to trap endogenous HA-Dpp$^{\Delta N}$. We found that HA-Dpp$^{\Delta N}$ accumulated in both cases (Fig. 7.1.4K, L). Although the extent of *HA-dpp$^{\Delta N}$* accumulation differs in two conditions due to different Dally expression level (small box Fig. 7.1.4K, L inset), normalized HA-Dpp$^{\Delta N}$ accumulation against Dally expression level was comparable between two (Fig. 7.1.4M). This suggest that Dpp$^{\Delta N}$ indeed lacks interaction with HS of Dally in the wing disc. The remained accumulation of Dpp$^{\Delta N}$ upon Dally$^{\Delta HS}$ expression suggests that the core protein of Dally can interact with Dpp outside the basic amino acids. Furthermore, Dally expression, but not Dally$^{\Delta HS}$ expression, activated pMad signal in *JAX; HA-dpp$^{\Delta N}$* (Fig. 7.1.4K`,L`,N,O), indicating that HS of Dally can activate pMad signaling without interacting with Dpp. Taken together, these results suggest that, despite the critical role of HS of Dally for Dpp singaling and distribution (Fig.7.1.3), direct interaction of HS of Dally with Dpp is not as important as previously thought.

**Trapping Dpp using HA trap reveals decrease of extracellular Dpp in *dally* mutants**

How is Dally required for Dpp distribution through HS? While expanded upon overexpression of Dally (Fig. 7.1.1E, 3A), extracellular Dpp gradient was shrunk in *dally* mutants (Fig. 7.1.2K, 7.1.3K'). This appears to be consistent with the roles of Dally in transporting or stabilizing Dpp but not with that in blocking Dpp spreading or internalizing Dpp, since extracellular Dpp

distribution should “expand” or “increase” in the latter two cases. However, if Dally is also essential for Dpp to bind to the cell surface, unbound extracellular Dpp could be lost, since the unbound Dpp is thought to be washed away in the current extracellular staining protocol. Thus, the reduced extracellular Dpp distribution in *dally* mutants may be also consistent with the latter two scenarios.

To distinguish these scenarios, we induced clones of cells expressing “HA trap”, a membrane tethered anti-HA scFv (Matsuda et al., 2021), to trap endogenous Ollas-HA-Dpp. Expression of HA trap clones in the posterior compartment resulted in cell surface accumulation of Ollas-HA-Dpp, which is otherwise washed away (Fig. 7.1.5A, B). We reasoned that upon loss of *dally* in the posterior compartment the amount of extracellular Dpp trapped by HA trap reduces in the first two scenarios and increases (or at least not decreases) in the last two cases. We found that the accumulated Ollas-HA-Dpp by HA trap is rather reduced in *hh>dallyRNAi* discs (Fig. 7.1.5C, D), supporting the first two scenarios.

**Dally is not critical for Dpp spreading but for Dpp stability through Tkv**

If *dally* is not required for internalization of Dpp, then what internalizes Dpp? It has been generally thought that receptor-mediated endocytosis is the main mechanism to internalize and remove morphogens from the extracellular space. To test this possibility, we knocked down *tkv* by RNAi in the dorsal compartment and visualized endogenous extracellular Dpp distribution. We found that extracellular Dpp increased and expanded under this condition (Fig. 7.1.6A, D), indicating that Tkv is required to internalize Dpp. Interestingly, when *tkv* is knocked down by RNAi in the dorsal compartment, pMad is lost from the dorsal compartment but is upregulated in the ventral compartment along the dorsal-ventral compartment boundary (arrow, Fig. 7.1.6G). This observation is consistent with the idea that, when Tkv-mediated Dpp internalization is blocked, Dpp derived from the dorsal compartment can reach further and binds to Tkv and activate Dpp signaling in the ventral compartment. In contrast, this phenotype was not seen when *dally* was knocked down (Fig 7.1.6H). Taken together, these results suggest that, Tkv, but not Dally, is a cell surface receptor to internalize Dpp.

To test if Dally regulates Dpp spreading or stability, we asked if the defects in Dpp distribution in *dally* mutants is rescued by knocking down *tkv* by RNAi. If Dpp spreading is lost in *dally* mutants, blocking internalization of Dpp would not rescue the Dpp distribution. If Dpp can spread but is removed from the extracellular space by Tkv-mediated endocytosis in *dally* mutants, blocking internalization of Dpp would rescue the Dpp distribution. We found that, when *tkv is* knocked down by RNAi in the dorsal compartment in a *dally* mutant, the extracellular Dpp gradient was expanded in the dorsal compartment (Fig. 7.1.6C, D). Similar results were obtained when *tkv* was knocked down by RNAi in *dally*$^{\Delta HS}$ mutant (Fig. 7.1.6E, F). These results indicate that HS of Dally stabilizes Dpp on the cell surface by antagonizing Tkv-

mediated Dpp internalization. Furthermore, Dpp distribution in the absence of *dally* and *tkv* suggest that Dally is not required for Dpp spreading.

## Discussion

It has long been thought that Glypicans are critical for Dpp/BMP morphogen gradient formation and signaling in the Drosophila wing disc. However, it remained largely unknown how Glypicans control Dpp distribution and signaling. In this study, we generated genome engineering platforms to manipulate Glypicans in Drosophila and utilized a recently generated genome engineering platform and protein binder tools to visualize and manipulate endogenous Dpp distribution (Matsuda et al., 2021) to revisit this question.

### *Dally vs Dlp*

We first found that Dally, but not Dlp, is critical for Dpp distribution and signaling, although both are modified with HS. We found that Dally interacts with Dpp mainly through its core protein, which can explain selective interaction of Dally with Dpp. Consistently, we found that the interaction of HS of Dally with Dpp is relatively minor and largely dispensable for Dally's function (Fig. 7.1.4). Nevertheless, since an increase of HS levels by overexpressing dlp could not sufficiently accumulate Dpp (Fig.7.1.1G), interaction of HS of Dally with Dpp is likely dependent of its core-protein.

It has recently been shown that the core protein of Dlp shields the lipid moiety of Wg (McGough et al., 2020). Thus, each glypican appears to acquire ligand specificity through its core protein. In contrast to Wg, Dpp has no lipid modification and is diffusible. Indeed, our results suggest that Dally is not essential for Dpp spreading (Fig.7.1.6C). Given a partial rescue of the *dally* mutant phenotypes by overexpression of the core-protein of Dally (Kirkpatrick et al., 2006), it has been proposed that the core-protein of Dally may have HS-independent roles. However, we found that dally$^{\Delta HS}$ mimicked dally$^{KO}$ phenotypes (Fig. 7.1.3K,K',L,L'), indicating that the core-protein of Dally is not sufficient to regulate Dpp distribution and signaling . Since HS is critical but not sufficient for Dally's function (Fig. 7.1.3; 7.1.1), we speculate that the interaction of the core protein of Dally with Dpp is prerequisite for HS of Dally to control Dpp distribution and signaling.

### *Dally stabilizes Dpp on the cell surface by blocking Tkv mediated Dpp internalization*

Among the proposed models, our results are consistent with the model in which HS of Dally stabilizes Dpp on the cell surface by antagonizing Tkv-mediated internalization of Dpp. Consistently, pulse-chase experiments showed that Dpp is less stable in dally mutants (Akiyama et al., 2008) and in pent mutants (Vuilleumier et al., 2010). Dally has been proposed to control Dpp stability through direct interaction of HS of Dally with a trech of basic amino

acids in Dpp, However, relatively minor phenotypes in $dpp^{\Delta N}$, and severe phenotypes in $dally^{\Delta HS}$ (Fig. 7.1.3; 7.1.4) indicate that HS of Dally stabilizes Dpp independent of a direct interaction with Dpp. It remains unknown how HS of Dally antagonizes Tkv-mediated Dpp internalization but the simplest possibility is that HS of Dally interacts with Tkv to stabilize Dpp on the cell surface. Consistent with this possibility, it has been shown that heparin binds to BMPR (Kanzaki et al., 2008).

*Internalization of Dpp*

Internalization of Dpp by Tkv but not Dally is consistent with the widely accepted notion that morphogens are removed from the extracellular space via receptor-mediated endocytosis. However, our results contradict a recent report, in which Dally, but not Tkv, internalizes and recycles Dpp to control Dpp morphogen scaling (Romanova-Michaelides et al., 2022). How can we explain the discrepancy?

First, the authors showed that internalization of overexpressed GFP-Dpp is not affected in tkv mutant clones, proposing that Tkv is not required for Dpp internalization. However, the effects on internalization of Dpp in tkv mutants could be easily missed by internalization of overexpressed GFP-Dpp via other factors. Indeed, we found that Dpp can bind to the cell surface without Tkv, raising a possibility that other factors can internalize Dpp in the absence of Tkv (Fig. 7.1.6C). Furthermore, the increase of extracellular Dpp upon blocking Dpp internalization could be also missed if extracellular Dpp is saturated due to its high expression. Indeed, while overexpressed extracellular GFP-Dpp distribution did not increase in tkv mutant clones (Schwank et al., 2011), we found that endogenous Dpp distribution expanded and increased upon knocking down of Tkv by RNAi (Fig. 7.1.6A). Second, the authors found that internalized Dpp is reduced upon knocking down sfl by RNAi or upon cleaving HSPGs by PI-PLC. However, since extracellular Dpp distribution is reduced in these conditions due to reduced Dpp stability, it would not be surprising that internalization of Dpp is also affected in these conditions.

Thus, we argue against Dally-mediated recycling and re-secretion of Dpp as a scaling mechanism. Instead, our results raise a possibility that Dally controls scaling through stabilizing Dpp on the cell surface. Alternatively, recycling of Dpp can contribute to the extracellular Dpp gradient formation independent of Dally. For example, internalized Dpp through Tkv may be recycled back to the cell surface to contribute to Dpp gradient formation. In this scenario, since Dpp-Tkv interaction is irreversible, recycling does not contribute to the spreading but rather stability of Dpp on the cell surface. Alternatively, Dpp may be internalized through other factors and be recycled and re-secreted as we showed that Dpp can interact with other cell surface molecules in the absence of Tkv and Dally.

*Dpp spreading mechanisms*

Our results suggest that Dally is not essential for Dpp spreading, arguing against the “facilitated transport” model, where Dpp is handed over via Glypicans. The reduced extracellular Dpp pool in dally mutants seems also inconsistent with the “hindered diffusion” model, where Dpp spreads freely and interaction of Dpp with Dally hinders effective Dpp spreading. However, enhanced Dpp spreading in dally mutants could be missed if Dpp is rapidly internalized via Tkv in the absence of Dally. Thus, to address the role of Dally in hindering Dpp spreading, it would be important in the future to measure parameters of the endogenous Dpp gradient in the presence or absence of Dally in a tkv mutant background. Interestingly, our results suggest that there are factors other than Tkv and Dally that bind to Dpp on the cell surface, which may hinder or facilitate Dpp spreading in the absence of Tkv and Dally.

*Comparison with a synthetic morphogen system*

It is interesting to compare our results with the recent attempt to create a synthetic morphogen system using an inert secreted GFP in the wing disc (Stapornwongkul et al., 2020). Secreted GFP is constantly leaked from the wing disc and the graded distribution could not be established in the absence of cell surface receptors. By replacing the Dpp morphogen system with this synthetic morphogen system, the authors noticed that a high affinity signaling receptor alone (corresponding to Tkv) is not sufficient to mimic the endogenous Dpp signaling gradient due to the leakage of GFP and increasing the level of high affinity signaling receptor (corresponding to Tkv) cannot reduce the leakage without shortening the gradient. The authors found that the additional non-signaling receptor with low binding affinity (corresponding to Dally) can reduce the leakage of Dpp to improve the gradient formation if the non-signaling receptors can spread in the tissue to assist Dpp spreading.

There are a couple of differences between the natural morphogen system and a synthetic morphogen system. First, we found that leakage of Dpp did not take place significantly without Tkv and Dally (Fig. 7.1.6C), indicating anothercell surface molecule to keep Dpp in the wing epithelium. Second, Dally can interact with Dpp through its core-protein, but this interaction was not sufficient to maintain the Dpp gradient and signaling even if Dally can spread in the tissue (Fig.7.1.3K,K’,L,L’). Third, Dally is not essential for Dpp spreading itself (Fig. 7.1.6). Our results rather suggest that Tkv compromises the long-range action of Dpp through internalization of Dpp, and Dally contributes to the gradient formation by blocking this process rather than blocking leakage of Dpp or assisting spreading of Dpp. It is not surprising that a natural morphogen system utilizes different mechanisms from the engineered gradient system to establish a morphogen gradient. It would be interesting to compare the mechanisms used in nature and in the synthetic system to gain insights into critical requirements to achieve robust and scalable morphogen gradient formation.

## Materials and Methods

### Data reporting

No statistical methods were used to predetermine sample size. The experiments were not randomized, and investigators were not blinded to allocation during experiments and outcome assessment.

### Fly stocks

Flies for experiments were kept at 25°C in standard fly vials containing polenta and yeast. The following fly lines were used: yw (Affolter stock), *tkv-RNAi* (Bloomington 40937), *dally-RNAi* (VDRC 14136), *dlp-RNAi* (VDRC106568), Ollas-dpp (Bauer et al., 2022), *UAS-GFP-HA-Dally* (Suzanne Eaton), UAS-dlp (Baeg et al., 2001), HA-dpp (Mastuda et al., 2021), HA-dppΔN (this study), dlp [ko;attB] (this study), dally [ko;attB] (this study), dally [YFP-dallyΔHS;attP] (this study), dally [HA-dlp;attP] (this study), *ap-Gal4* (Markus Affolter), JAX (Hoffmann & Goodman, 1987), UAS-YFP-dally (this study), UAS-YFP-dallyΔHS (this study), Ollas-HA-dppΔN (this study), hh-Gal4 (Gift from Dr Manolo Calleja), ywhsFlp, Ollas-HA-dpp (Matsuda et al., 2021), LexAop-HA-trap (Matsuda et al., 2021), dally$^{32}$ (Franch-Marro et al., 2005).

### Genotypes by figures

| | |
|---|---|
| Fig 7.1.1A, E, J<br>Fig 7.1.3A, F | *ap-Gal4, Ollas-dpp/+ ; UAS-GFP-HA-Dally/+* |
| Fig 7.1.1C, G, K | *ap-Gal4, Ollas-dpp/+ ; UAS-Dlp/+* |
| Fig 7.1.1I | *ap-Gal4, Ollas-dpp/+ ; +/Tm6Tb* |
| Fig 7.1.2A, F, O, T | *yw* |
| Fig 7.1.2B, G | *dally$^{32}$/dally$^{32}$* |
| Fig 7.1.2C, H, P, U | *dally[KO;attB]/dally[KO;attB]* |
| Fig 7.1.2D, I, W | *dlp[KO;attB]/dlp[KO;attB]* |
| Fig 7.1.2K | *HA-dpp/CyO, Dfd:YFP* |
| Fig 7.1.2K | *HA-dpp/CyO, Dfd:YFP; dally[KO;attB]/dally[KO;attB]* |
| Fig 7.1.2M | *HA-dpp/HA-dpp* |

| | |
|---|---|
| Fig 7.1.2M | *HA-dpp/HA-dpp ; dlp[KO;attB]* |
| Fig 7.1.2Q,V | *Dally[YFP-dally;attP]* |
| Fig 7.1.2R,Y | *Dally[HA-dlp;attP]* |
| Fig 7.1.2X | *Dlp[HA-dlp;attP]* |
| Fig 7.1.3C, H | *ap-Gal4, Ollas-dpp/+ ; UAS-GFP-Dally$^{\Delta HS}$* |
| Fig 7.1.3J, J' | *HA-dpp/HA-dpp* |
| Fig 7.1.3K, K' | *HA-dpp/HA-dpp ; dally[KO;attB]/dally[KO;attB]* |
| Fig 7.1.3L, L' | *HA-dpp/HA-dpp ; dally[YFP-dally$^{\Delta HS}$;attP] w$^{+}$/ dally[YFP-dally$^{\Delta HS}$;attP] w$^{+}$* |
| Fig 7.1.4A, A', E | *JAX; HA-dpp/HA-dpp* |
| Fig 7.1.4B, B', F | *JAX; HA-dpp$^{\Delta N}$/; HA-dpp$^{\Delta N}$* |
| Fig 7.1.4H | *JAX; Ollas-HA-dpp/HA-dpp ; hh-Gal4/UAS-GFP-HA-Dally* |
| Fig 7.1.4I | *JAX; Ollas-HA-dpp$^{\Delta N}$/HA-dpp$^{\Delta N}$ ; hh-Gal4/UAS-GFP-HA-Dally* |
| Fig 7.1.4K, K' | *JAX; ap-Gal4,Ollas-HA-dpp$^{\Delta N}$/HA-dpp$^{\Delta N}$; UAS-GFP-HA-Dally/+* |
| Fig 7.1.4L, L' | *JAX; ap-Gal4,Ollas-HA-dpp$^{\Delta N}$/HA-dpp$^{\Delta N}$; UAS-GFP-Dally$^{\Delta HS}$/+* |
| Fig 7.1.5A, A', A'' | *ywhsFlp/+ ; act>y+>LHG, Ollas-HA-dpp/+ ; LexAop-HAtrap, hh-Gal4/+* |
| Fig 7.1.5C, C', C'' | *ywhsFlp/+ ; act>y+>LHG, Ollas-HA-dpp/+ ; LexAop-HAtrap, hh-Gal4/UAS-dallyRNAi* |
| Fig 7.1.6A, G | *ap-Gal4, Ollas-dpp/UAS-tkvRNAi* |
| Fig 7.1.6C | *ap-Gal4, Ollas-dpp/UAS-tkvRNAi ; dally[KO;attB]/dally[KO;attB]* |
| Fig 7.1.6E | *ap-Gal4, Ollas-dpp/UAS-tkvRNAi ; dally[YFP-dally$^{\Delta HS}$;attP]/dally[YFP-dally$^{\Delta HS}$;attP]* |
| Fig 7.1.6H | *ap-Gal4, Ollas-dpp/UAS-dallyRNAi* |
| Supplement Fig 7.1.1A | *dlp[Ko;attB]/+* |

| | |
|---|---|
| Supplement Fig 7.1.1B | *dlp[Ko;attB]/ dlp[Ko;attB]* |
| Supplement Fig 7.1.3A | *ap-Gal4/+; UAS-YFP-Dally/+* |
| Supplement Fig 7.1.3B | *ap-Gal4/+; UAS-YFP-Dally$^{\Delta HS}$/+* |
| Supplement Fig 7.1.4A, C, E | *dpp$^{d8}$/dpp$^{d12}$* |
| Supplement Fig 7.1.4B, D, F | *JAX; dpp$^{d8}$/dpp$^{d12}$* |

**DNA contructs**

UAS-YFP-Dally and UAS-YFP-Dally$^{\Delta HS}$ were constructed using YFP-dally or YFP-dally$^{\Delta HS}$ flies as a template. To amplify the YFP-dally sequence the two primers ATTCGGAATTCATGGCGGCCAGGAGCGTGC and CGAATGAATTCTTAACTACAGCTACTAAAGAGCAT were used. The amplified DNA sequence was cloned into the plasmid vector pUASattB, using EcoRI restriction enzymes.

HA-dpp$^{\Delta N}$ – Generated by Shinya Matsuda.

Ollas-HA-dpp$^{\Delta N}$ was constructed by using the already existing HA-dpp$^{\Delta N}$ plasmid and the Ollas-HA-dpp plasmid as templates. Both plasmids were digested using XhoI and BspEI as restriction enzymes. The small fragment from the HA-dpp$^{\Delta N}$ plasmid and the large fragment from the Ollas-HA-dpp plasmid were used for ligation.

Dally$^{KO}$/Dlp$^{KO}$ – Generated by Abu Safyan.

**Immunohistochemistry**

Total stainings

Wing discs from third instar larvae were dissected and stored temporarily in Phosphate Buffered Saline (PBS) (Gibco) on ice until enough samples were collected. The discs were then fixed in 4% Paraformaldehyde (PFA) in PBS for 30min on the shaker at room temperature

(25°C). After fixation, the discs were rinsed three times quickly with PBS and three times for 15 min with PBS at 4°C. Wing discs were permeabilised in PBST (0.3% Triton-X in PBS) and then blocked in 5% normal goat serum (NGS) in PBST for at least 30min. Primary antibodies were added in 5% normal goat serum (NGS) in PBST for incubation over night at 4°C. The next day, the primary antibodies were carefully removed and the samples were rinsed three times quickly in PBST and three times 15 min at room temperature in PBST. Discs were incubated in secondary antibody for 2h at room temperature. Afterwards the samples were washed again three times quickly and three times 15 min in PBST at room temperature. After the final washing the PBST was rinsed with PBS, then the PBS was removed completely and the samples were mounted in VECTORSHIELD on glass slides. For HS stainings, wing discs were dissected as described above. After fixation, discs were washed in PBS and blocked in 5% NGS in PBST, then treated with Heparinase III (Sigma-Aldrich) for 1.5h at 37°C. Afterwards the discs were blocked again in 5% NGS in PBST and stained as described above.

Extracellular stainings

Wing discs from third instar larvae were dissected and stored temporarily in Schneider's Drosophila medium (S2) on ice until enough samples were collected. The discs were then blocked in cold 5% NGS in S2 medium on ice for 10min. The blocking solution was removed carefully and the primary antibody was added for 1h on ice. During the 1h incubation period, the tubes were tapped carefully every 15min, to make sure the antibody is distributed evenly. After 1h incubation on ice, the antibody was removed and the samples were washed at least 6 times with cold S2 medium and another two times with cold PBS to remove excess primary antibody. Wing discs were then fixed with 4% PFA in PBS for 30min on the shaker at room temperature (25°C). After fixation the protocol continued as described in total stainings.

Antibodies

Primary antibodies: rabbit-anti-phospho-Smad1/5 (41D10, Cell Signaling, #9516; 1:200), mouse-anti-Wg (4D4, DSHB, University of Iowa; total staining: 1:120, extracellular staining: 1:120), mouse-anti-Ptc (DSHB, University of Iowa; total staining: 1:40), rat-anti-HA (3F10, Roche, 11867423001; total staining: 1:300, extracellular staining: 1:20), rat-anti-Ollas (L2, Novus Biologicals, NBP1-06713; total staining: 1:300, extracellular staining: 1:20), mouse-anti-HS (F69-3G10, amsbio; 1:100)

The following secondary antibodies were used at 1:500 dilutions in this study. Goat anti-rabbit IgG (H+L) Alexa Fluor™ 488 (A11008 Thermo Fischer), goat anti-rabbit IgG (H+L) Alexa Fluor™ 568 (A11011 Thermo Fischer), goat anti-rabbit IgG (H+L) Alexa Fluor™ 680 (A21109 Thermo Fischer), goat anti-rat IgG (H+L) Alexa Fluor™ 568 (A11077 Thermo Fischer), goat anti-mouse IgG (H+L) Alexa Fluor™ 568 (A11004 Thermo Fischer), goat anti-rat IgG Fc 488

(ab97089 abcam), goat anti-mouse IgG Fc Alexa Fluor™ 680 (115625071 Jackson Immuno Research).

**Imaging**

Samples were imaged using a Leica SP5-II-MATRIX confocal microscope and Leica LAS AF and Images were analyzed using ImageJ. Figures were obtained using Omero and Adobe Illustrator.

**Quantification of pMad and extracellular staining**

From each z-stack image, signal intensity profile along A/P axis was extracted from average projection of three sequential images using ImageJ (v.2.0.0-rc69/1.52p ). Each signal intensity profile collected in Excel (Ver. 16.51) was aligned along A/P compartment boundary (based on anti-Ptc staining or pMad staining) and average signal intensity profile from different samples was generated and plotted by the script (wing_disc-alignment.py). The average intensity profile from control and experimental samples was then compared by the script (wingdisc_comparison.py). Both scripts can be obtained from https://etiennees.github.io/Wing_disc-alignment/. The resulting signal intensity profiles (mean with SD) were generated by Prism (v.8.4.3(471)). Figures were prepared using Omero (ver5.9.1) and Illustrator (24.1.3).

**Quantification of adult wing size**

The A/P compartment boundary of the adult wings were approximated by L4 position. The size of each compartment was measured using ImageJ (v.2.0.0-rc69/1.52p) and collected in Excel (Ver. 16.51). Scatter dot plots (mean with SD) were generated by Prism (v.8.4.3(471)). Figures were prepared using Omero (ver5.9.1) and Illustrator (24.1.3).

**Figures**

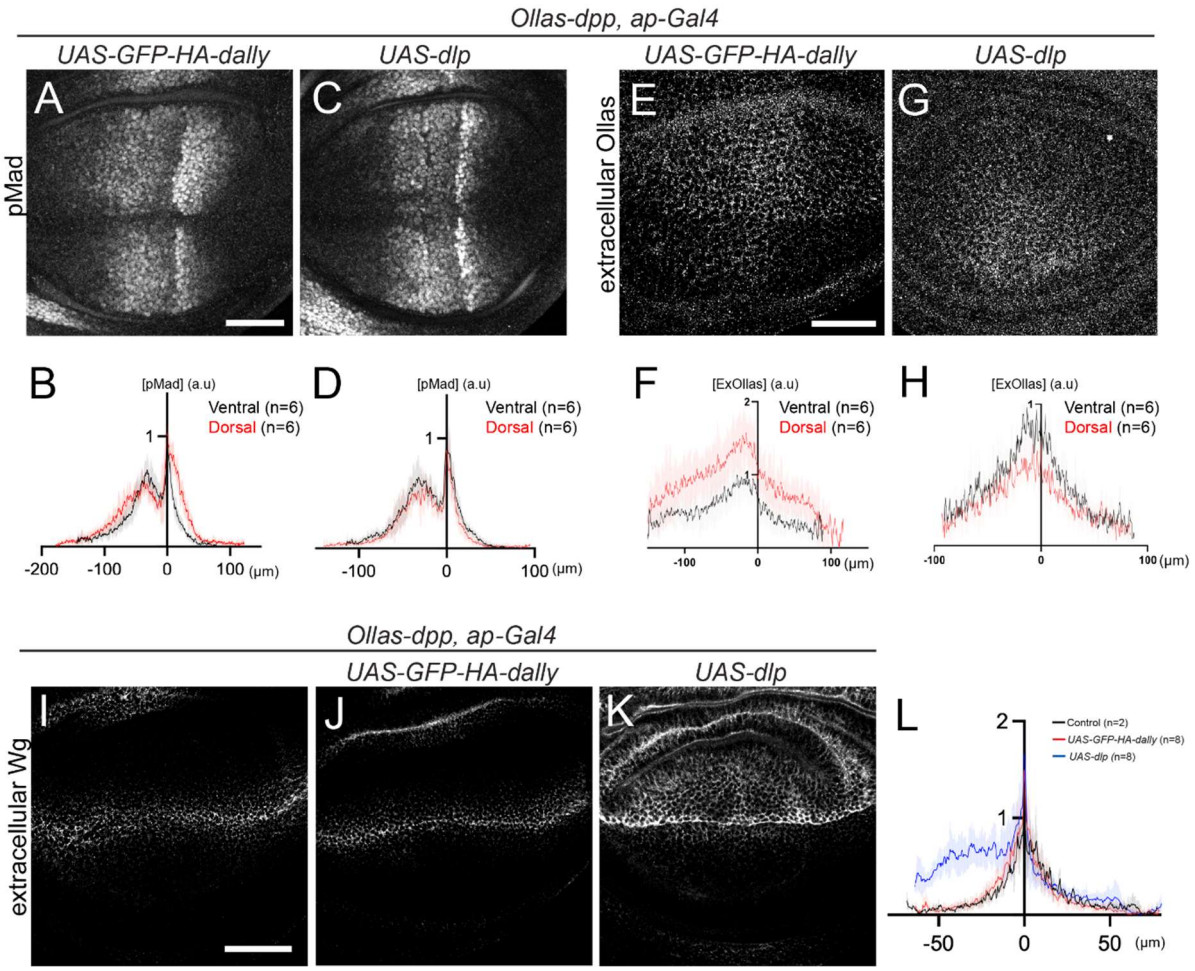


***Figure 7.1.1: Overexpression of dally, but not dlp, accumulates Dpp.***
***A-B*** *α-pMad staining (***A***) and average fluorescence intensity profile (***B***) of Ollas-dpp/+, ap>GFP-HA-dally disc. Data are presented as mean +/- SD.* **C-D** *α-pMad staining (**C**) and average fluorescence intensity profile (**D**) of Ollas-dpp/+, ap>dlp disc. Data are presented as mean +/- SD.* **E-F** *extracellular α-Ollas staining (**E**) and average fluorescence intensity profile (**F**) of Ollas-dpp/+, ap>GFP-HA-dally disc. Data are presented as mean +/- SD.* **G-H** *extracellular α-Ollas staining (**G**) and average fluorescence intensity profile (**H**) of Ollas-dpp/+, ap>dlp disc. Data are presented as mean +/- SD.* ***I-K*** *extracellular α-Wg staining of Ollas-dpp/+, ap>+ (control) (**I**), Ollas-dpp/+, ap>GFP-HA-dally (**J**) and Ollas-dpp/+, ap>dlp (**K**).* **L** *Average fluorescence intensity profile of extracellular α-Wg staining of* ***I-K****. Data are presented as mean +/- SD. Scale bar: 50µm.*

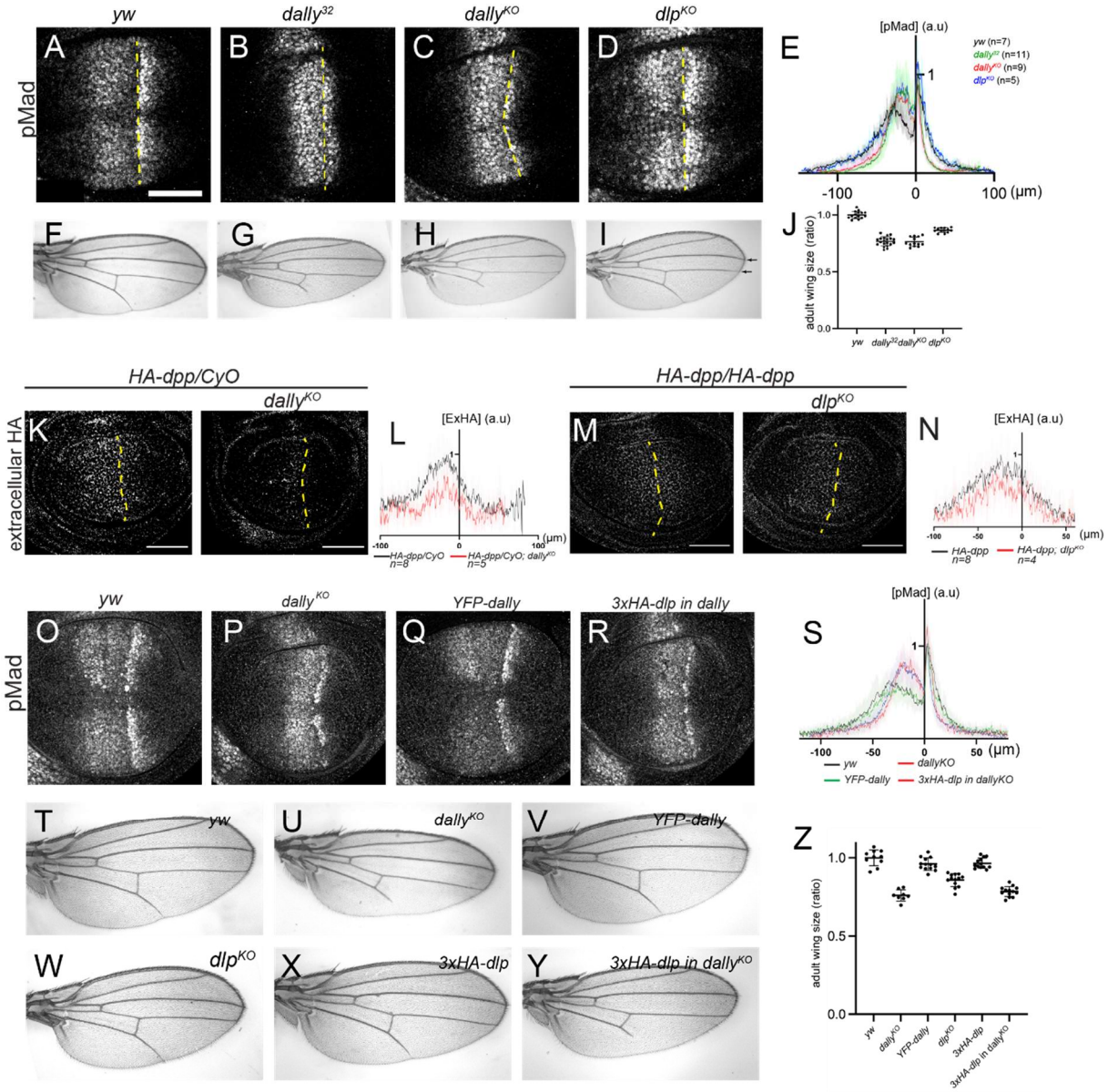


***Figure 7.1.2: Dally, but not Dlp, is required for the Dpp gradient formation and signaling***

***A-D*** *pMad staining of yw (control) (**A**), dally$^{32}$ (**B**), dally$^{KO}$ (**C**) and dlp$^{KO}$ (**D**) discs.* ***E*** *Average fluorescence intensity profiles of pMad staining of (**A-D**). Data are presented as mean +/- SD.* ***F-I*** *Adult wings of yw (**F**), dally$^{32}$ (**G**), dally$^{KO}$ (**H**) and dlp$^{KO}$ (**I**).* ***J*** *Adult wing size comparison of (**F-I**). Data are presented as mean +/- SD.* ***K*** *extracellular α-HA staining of HA-dpp/CyO; dallyKO/Tm6Tb (control) (**left**) and HA-dpp/CyO; dally$^{KO}$ discs (**right**).* ***L*** *Average fluorescence intensity profile of extracellular α-HA staining of (**K**). Data are presented as mean +/- SD.* ***M*** *extracellular α-HA staining of HA-dpp/HA-dpp (control) (**left**) and HA-dpp/HA-dpp; dlp$^{KO}$ disc (**right**).* ***N*** *Average fluorescence intensity profile of extracellular α-HA staining of **M**. Data are presented as mean +/- SD.* ***O-R*** *α-pMad staining of yw (**O**), dally$^{KO}$ (**P**), YFP-dally (**Q**) and 3xHA-dlp in dally$^{KO}$ (**R**) discs.* ***S*** *Average fluorescence intensity profile of α-pMad staining of (**O-R**). Data are presented as mean +/- SD.* ***T-Y*** *Adult wing of yw (**T**), dally$^{KO}$ (**U**), YFP-dally (**V**), dlp$^{KO}$ (**W**), 3xHA-dlp (**X**) and 3xHA-dlp in dally$^{KO}$ (**Y**).* ***Z*** *Adult wing size comparison of (**T-Y**). Data are presented as mean +/- SD. Scale bar: 50µm.*

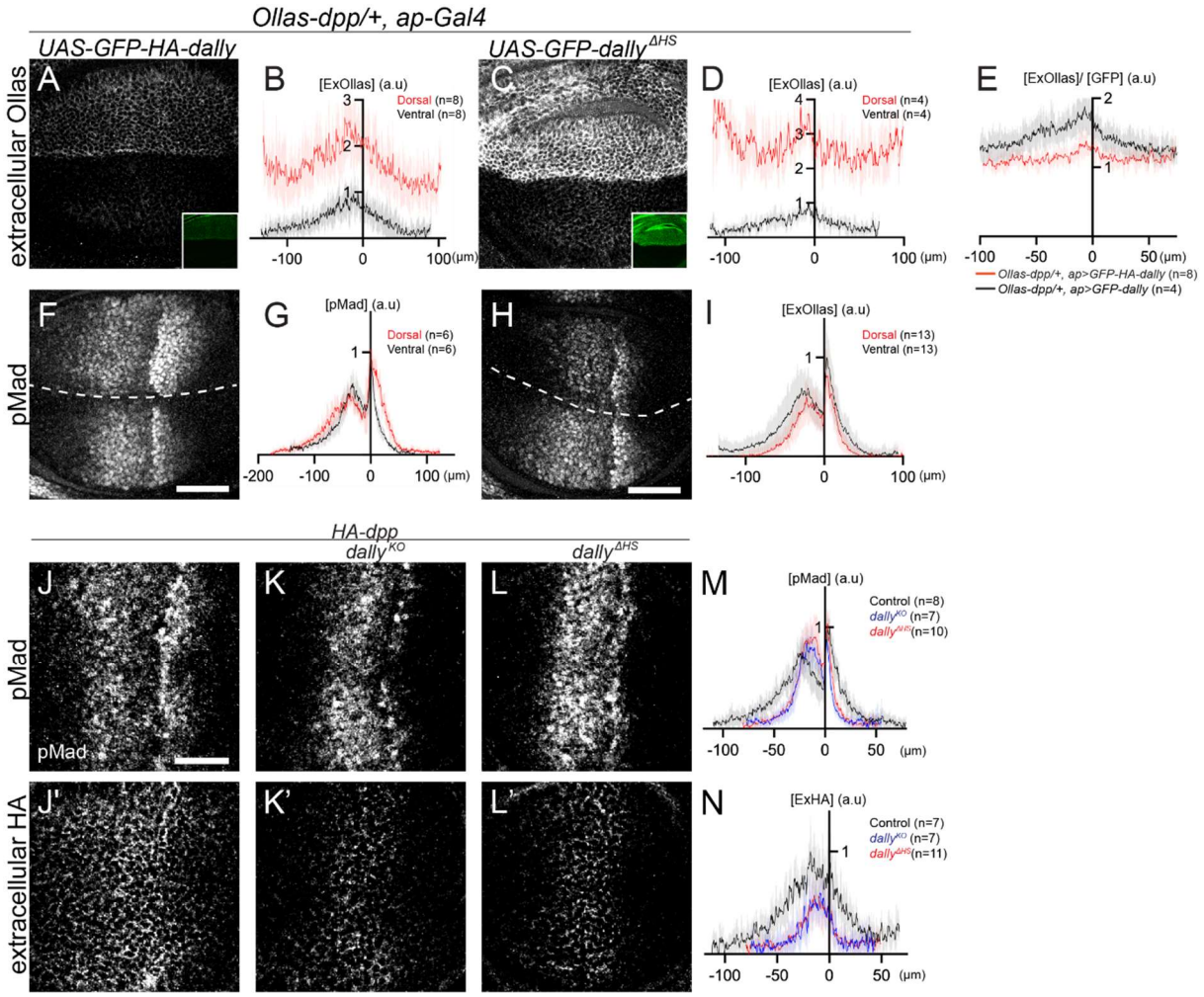


***Figure 7.1.3: Core protein of Dally can interact with Dpp but HS of Dally is critical for Dally function***

***A-B*** *extracellular α-Ollas staining and GFP signal (inset) (**A**) and average fluorescence intensity profile (**B**) of Ollas-dpp, ap>GFP-HA-dally. Data are presented as mean +/- SD.* ***C-D*** *extracellular α-Ollas staining and GFP signal (inset) (**C**) and average fluorescence intensity profile (**D**) of Ollas-dpp, ap>GFP-HA-dally$^{\Delta HS}$ discs. Data are presented as mean +/- SD.* ***E*** *Relative average extracellular α-Ollas staining intensity profile against GFP of **A, D**. Data are presented as mean +/- SD.* ***F-G*** *α-pMad staining (**F**) and average fluorescence intensity profile (**G**) of Ollas-dpp, ap>GFP-HA-dally discs. Data are presented as mean +/- SD.* ***H-I*** *α-pMad staining (**H**) and average fluorescence intensity profile (**I**) of Ollas-dpp, ap>GFP-HA-dally$^{\Delta HS}$ discs. Data are presented as mean +/- SD.* ***J-L*** *α-pMad (**J-L**) and extracellular α-HA (**J'-L'**) staining of HA-dpp (**J, J'**), HA-dpp;dally$^{KO}$ (**K, K'**) and HA-dpp;dally$^{\Delta HS}$ (**L, L'**).* ***M*** *Average fluorescence intensity profile of α-pMad staining of **J-L**. Data are presented as mean +/- SD.* ***N*** *Average fluorescence intensity profile of extracellular α-HA staining of **J'-L'**. Data are presented as mean +/- SD. Scale bar: 50µm*

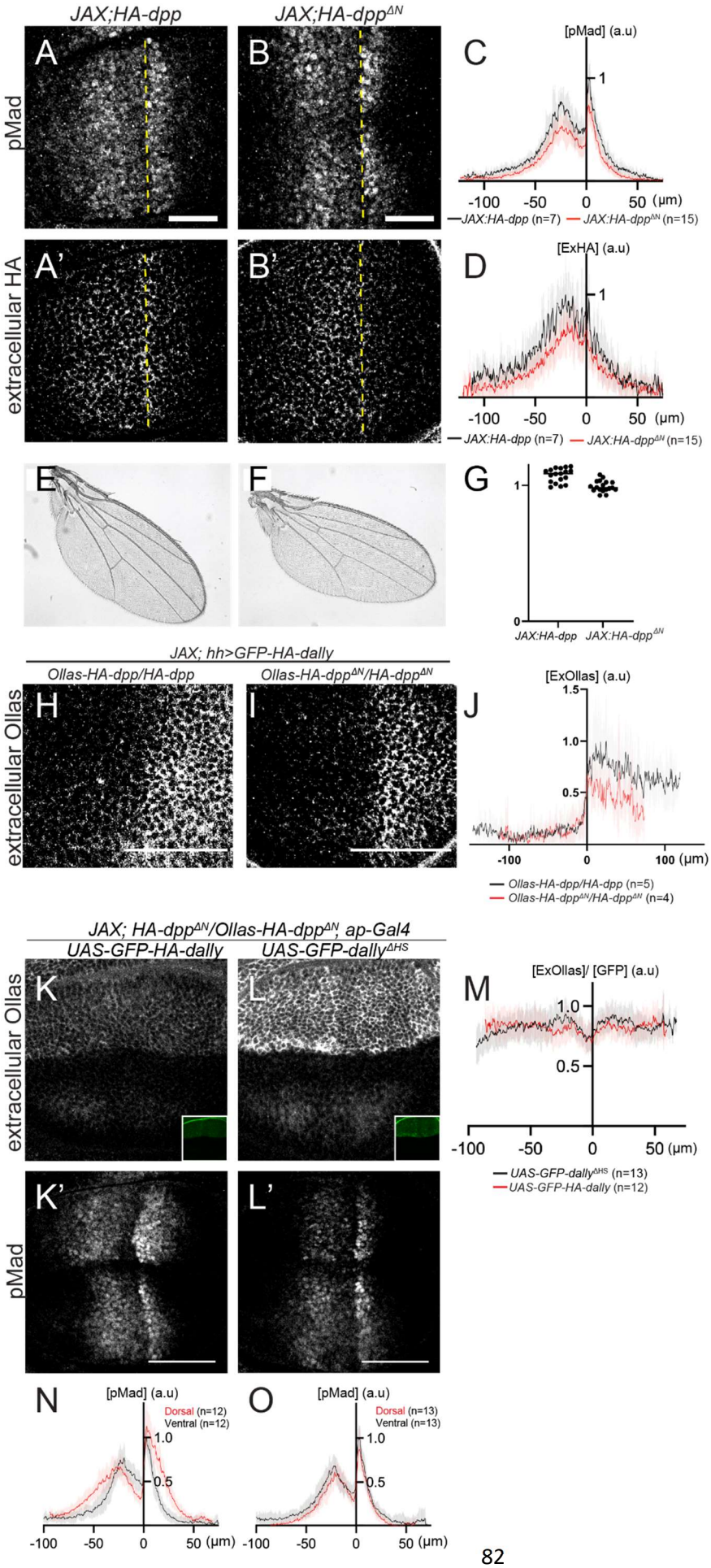
JAX;HA-dpp
JAX;HA-dpp^ΔN
pMad
extracellular HA
A
B
A'
B'
C
D
[pMad] (a.u)
[ExHA] (a.u)
-100 -50 0 50 (μm)
JAX:HA-dpp (n=7)
JAX:HA-dpp^ΔN (n=15)
E
F
G
JAX:HA-dpp
JAX:HA-dpp^ΔN
JAX; hh>GFP-HA-dally
Ollas-HA-dpp/HA-dpp
Ollas-HA-dpp^ΔN/HA-dpp^ΔN
extracellular Ollas
H
I
J
[ExOllas] (a.u)
-100 0 100 (μm)
Ollas-HA-dpp/HA-dpp (n=5)
Ollas-HA-dpp^ΔN/HA-dpp^ΔN (n=4)
JAX; HA-dpp^ΔN/Ollas-HA-dpp^ΔN; ap-Gal4
UAS-GFP-HA-dally
UAS-GFP-dally^ΔHS
K
L
M
[ExOllas]/ [GFP] (a.u)
-100 -50 0 50 (μm)
UAS-GFP-dally^ΔHS (n=13)
UAS-GFP-HA-dally (n=12)
K'
L'
N
O
[pMad] (a.u)
Dorsal (n=12)
Ventral (n=12)
Dorsal (n=13)
Ventral (n=13)
-100 -50 0 50 (μm)

***Figure 7.1.4: Interaction of HS of Dally with Dpp is largely dispensable for Dpp distribution and signaling***
***A-B*** *α-pMad (**A-B**) and extracellular α-HA (**A'-B'**) staining of JAX;HA-dpp (**A, A'**) and JAX;HA-dpp$^{\Delta N}$ (**A', B'**). **C** Average fluorescence profile of α-pMad staining of (**A-B**). Data are presented as mean +/- SD. **D** Average fluorescence profile of extracellular α-HA staining of (**A'-B'**). Data are presented as mean +/- SD. **E-F** Adult wing of JAX;HA-dpp (**E**) and JAX;HA-dpp$^{\Delta N}$ (**F**). **G** Size comparison of adult wing of (**E-F**). Data are presented as mean +/- SD. Two-tailed unpaired t-test was used for comparison of the wing sizes ($p < 0.0001$). **H-I** Extracellular α-Ollas staining of JAX;Ollas-HA-dpp/HA-dpp, hh>GFP-HA-dally (**H**) and JAX;Ollas-HA-dpp$^{\Delta N}$/HA-dpp$^{\Delta N}$, hh>GFP-HA-dally (**I**). **J** Average fluorescence profile of extracellular α-Ollas staining of (**H-I**). Data are presented as mean +/- SD. **K-L** Extracellular α-Ollas staining and GFP signal (inset) (**K-L**) and pMad (**K'-L'**) staining of JAX;Ollas-HA-dpp$^{\Delta N}$/HA-dpp$^{\Delta N}$, hh>GFP-HA-dally (**k**) and JAX;Ollas-HA-dpp$^{\Delta N}$/HA-dpp$^{\Delta N}$, hh>GFP-dally$^{\Delta HS}$ (**L**). **M** Average fluorescence profile of extracellular α-Ollas staining of (**K-L**). Data are presented as mean +/- SD. **N-O** Average fluorescence intensity profile of pMad staining of (**K'-L'**). Data are presented as mean +/- SD. Scale bar: 50µm*

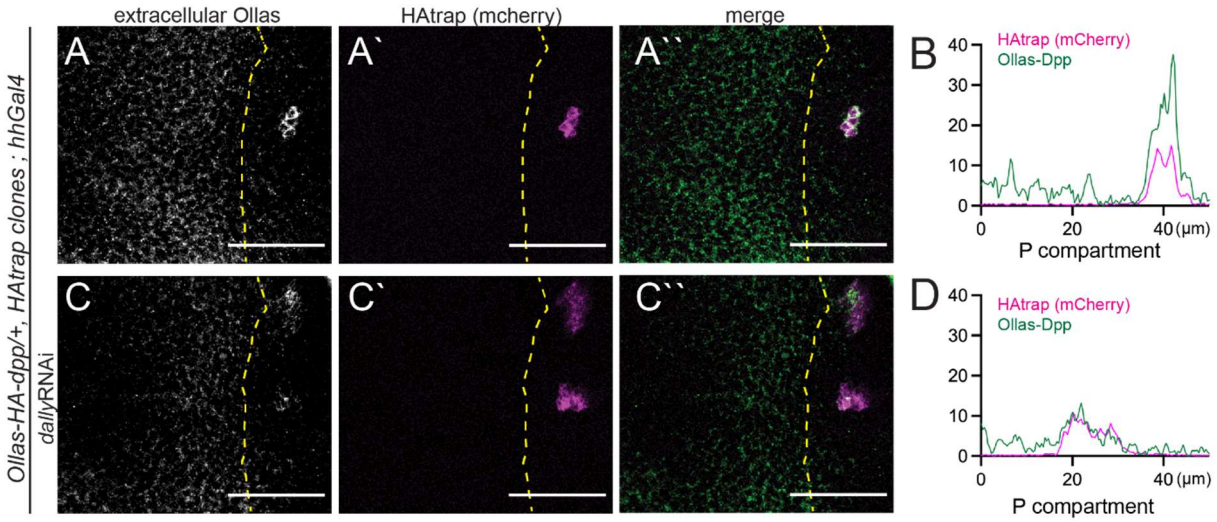


***Figure 7.1.5: Trapping Dpp using HA trap reveals decrease of extracellular Dpp in dally mutants***
***A-A"*** *extracellular α-Ollas staining (**A**), HAtrap (mCherry) signal (**A'**) and merge (**A"**) of yw, hSFlp; act>y+>LHG, Ollas-HA-dpp; hh>+ (control) discs.* ***B*** *Fluorescence intensity profile of extracellular α-Ollas and HAtrap (mCherry) signal.* ***C-C"*** *extracellular α-Ollas staining (**C**), HAtrap (mCherry) signal (**C'**) and merge (**C"**) of yw, hsFlp; act>y+>LexAop-HAtrap, Ollas-HA-dpp; hh>dallyRNAi discs.* ***D*** *Fluorescence intensity profile of extracellular α-Ollas and HAtrap (mCherry) signal. Scale bar: 25µm.*

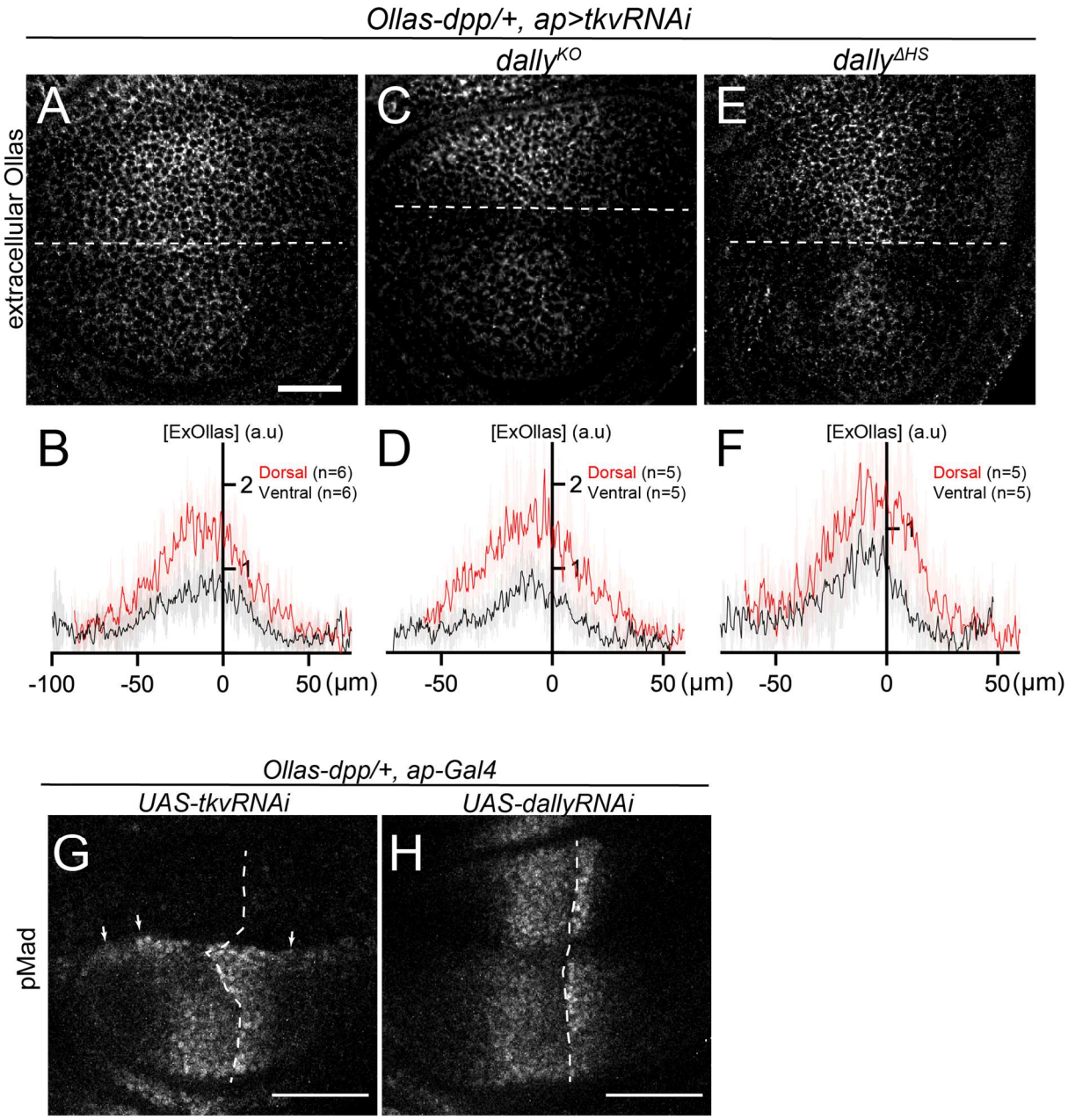


***Figure 7.1.6: Dally is critical for Dpp stability by antagonizing Tkv-mediated Dpp internalization but not for Dpp spreading***

***A*** *extracellular α-Ollas staining of Ollas-dpp, ap>tkvRNAi disc.* ***B*** *Average fluorescence profile of extracellular α-Ollas staining of Ollas-dpp, ap>tkvRNAi discs. Data are presented as mean +/- SD.* ***E*** *extracellular α-Ollas staining of Ollas-dpp, ap> tkvRNAi, dally$^{KO}$ disc.* ***F*** *Average fluorescence profile of extracellular α-Ollas staining of* ***E****.* ***G*** *extracellular α-Ollas staining of Ollas-dpp, ap> tkvRNAi, dally$^{\Delta HS}$ disc.* ***H*** *Average fluorescence profile of extracellular α-Ollas staining of* ***H****. Data are presented as mean +/- SD. Scale bar: 50µm.*

**Supplement Figures**

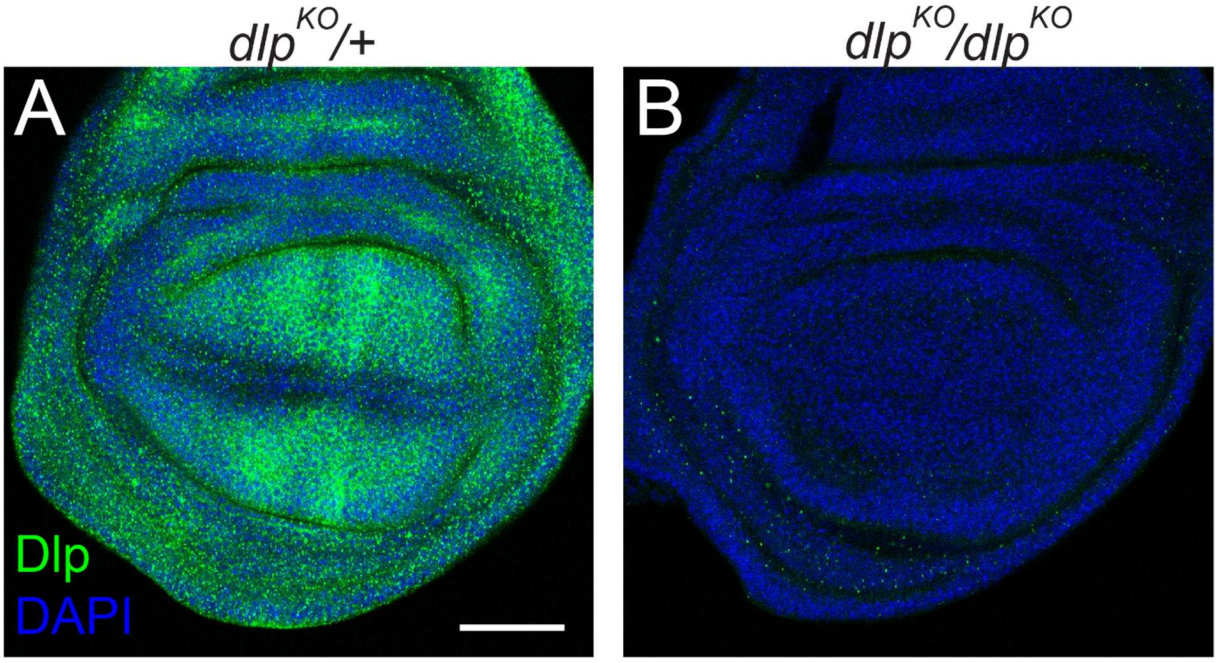


***Supplement Figure 7.1.1: Dlp staining is gone in dlp$^{KO}$ wing discs.***
***A*** *α-dlp staining and DAPI dye in dlp$^{KO}$/+ wing disc.* ***B*** *α-dlp staining and DAPI dye in dlp$^{KO}$/dlp$^{KO}$ wing disc.*

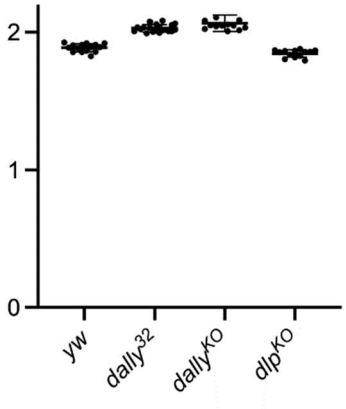


***Supplement Figure 7.1.2:*** **Wing size comparison along the A/P axis of yw, dally32, dally$^{KO}$ and dlp$^{KO}$ adult wings.**

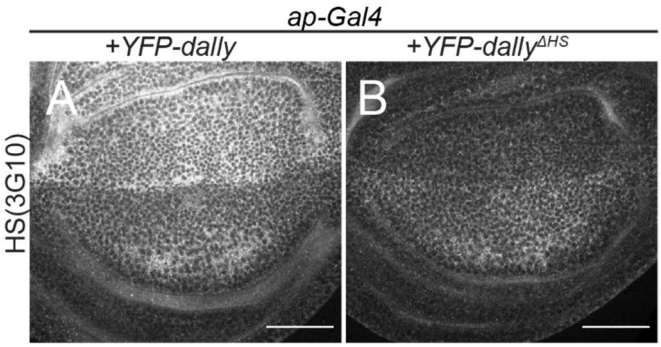


***Supplement Figure 7.1.3: Dally$^{\Delta HS}$ does not enhance the HS intensity when expressed in the dorsal compartment.***
***A*** *α-HS staining of ap-Gal4>UAS-YFP-Dally wing disc.* ***B*** *α-HS staining of ap-Gal4>UAS-YFP-DallyΔHS wing disc. Scale bar: 50µm.*

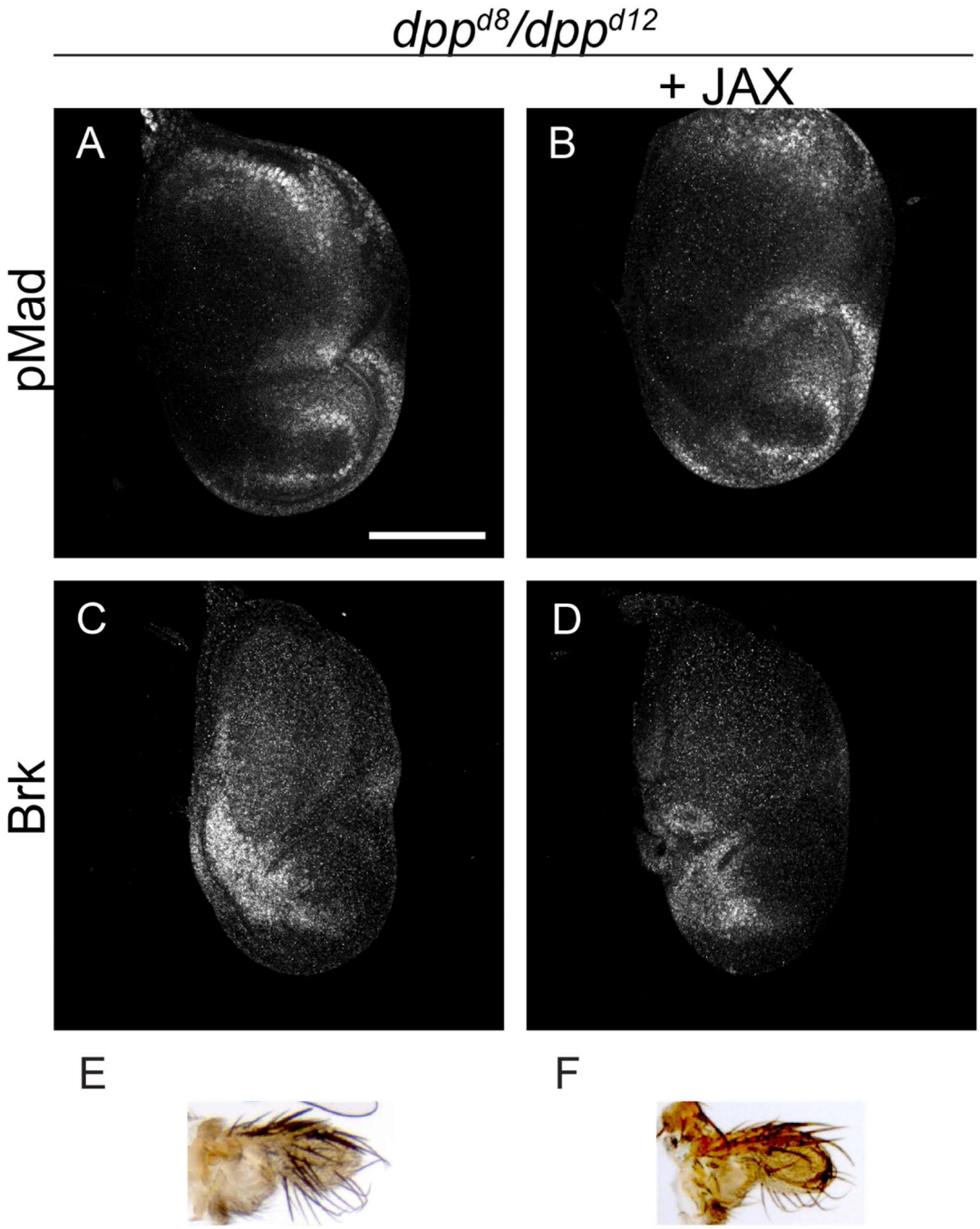


***Supplement Figure 7.1.4: JAX does not rescue the dpp mutant wing disc phenotype.***
***A*** *α-pMad staining of dpp$^{d8}$/dpp$^{d12}$ wing disc.* ***B*** *α-pMad staining of JAX; dpp$^{d8}$/dpp$^{d12}$ wing disc.* ***C*** *α-brk staining of dpp$^{d8}$/dpp$^{d12}$ wing disc.* ***D*** *α-brk staining of JAX; dpp$^{d8}$/dpp$^{d12}$ wing disc.* ***E*** *Adult wing of dpp$^{d8}$/dpp$^{d12}$ fly.* ***F*** *Adult wing of JAX; dpp$^{d8}$/dpp$^{d12}$ fly.*

## 7.2 Additional Results

### *7.2.1 Dally*

In chapter 7.1 I saw that mostly Dally and not Dlp is involved in Dpp function. In *dally* mutants the pMad and the extracellular Dpp gradient is shrunk. However, in the previous chapter I unravelled a role of the core protein of Dally for Dpp function as well as a mechanism for Dally to antagonize Tkv mediated endocytosis of Dpp. Anyhow, there might be other roles of Dally for Dpp function in place. To further investigate these possibilities, I performed additional experiments.

*Changes in Dpp signaling in dally mutants are not through downstream changes*

When affecting a component of a signaling pathway, the resulting downstream signal and consequently the downstream responses are disturbed. In the case of Dpp, changing the intensity of the Dpp signal changes the expression of Dpp and also the expression of the receptor Tkv (Fujise, 2003). These changes in expression might in turn cause the changes in pMad and Dpp range and intensity. To further investigate this possibility, I stained pMad in *dally/brk* double mutants. Under this condition, the discs overgrow, however the pMad gradient remained small, similar to the *dally* mutant (Fig. 7.2.1). Based on this result, I conclude that the effect of Dally on Dpp is not due to a downstream effect caused by a change in signaling.

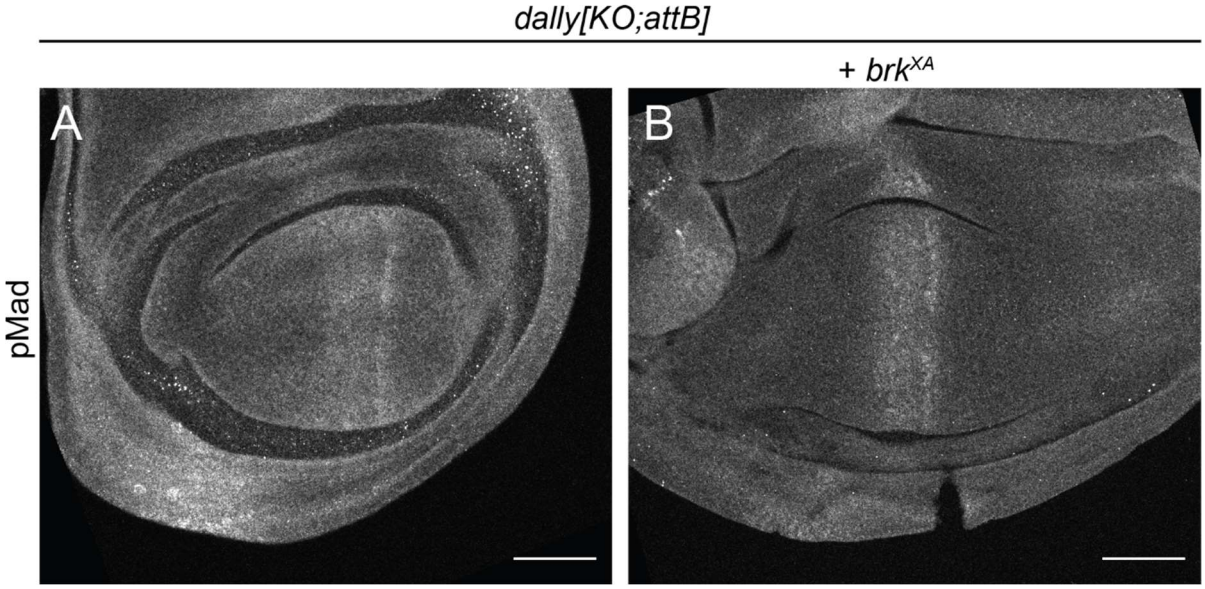


***Figure 7.2.1: Removing brk additionally to dally does not restore the pMad gradient.***
***A*** *α-pMad staining of dally$^{KO}$ mutant wing disc.* ***B*** *α-pMad staining of dally$^{KO}$+brk$^{XA}$ mutant wing disc. Scale bar: 50µm.*

The role of Dally on Dpp function could be indirect through the effect of Dally on Hh (M. I. Capurro et al., 2008; Han et al., 2004). In the HA-trap experiment presented in 7.1, I observed less Dpp trapped in the HA-trap clones when *dally*RNAi was expressed (Fig 7.1.5). This could be due to less stability or less efficient transport of Dpp through the posterior compartment where Dally is gone. However, another possibility is that there is less Dpp entering the posterior compartment due to an effect of the loss of Dally on Hh. To test this possibility, and to see how much Dpp enters the posterior compartment, I endogenously expressed Ollas-HA-dpp and the HA trap with and without *dally*RNAi in the posterior compartment (Fig. 7.2.2A,B). In this setup, the Dpp entering the posterior compartment will be trapped immediately by the HA-trap, giving me the possibility to assess the levels of Dpp entering the posterior compartment. When the HA-trap was expressed in the posterior compartment, the extracellular staining of HA showed high accumulation of signal adjutant to the Dpp source (Fig. 7.2.2C,E). When *dally*RNAi was expressed together with the HA-trap, the extracellular signal was less accumulated (Fig 7.2.2D,E), indicating that less Dpp reaches the posterior compartment. Anyhow, it might be that a reduction of Dally leads to less stable Dpp even when Dpp is trapped to the HA-trap.

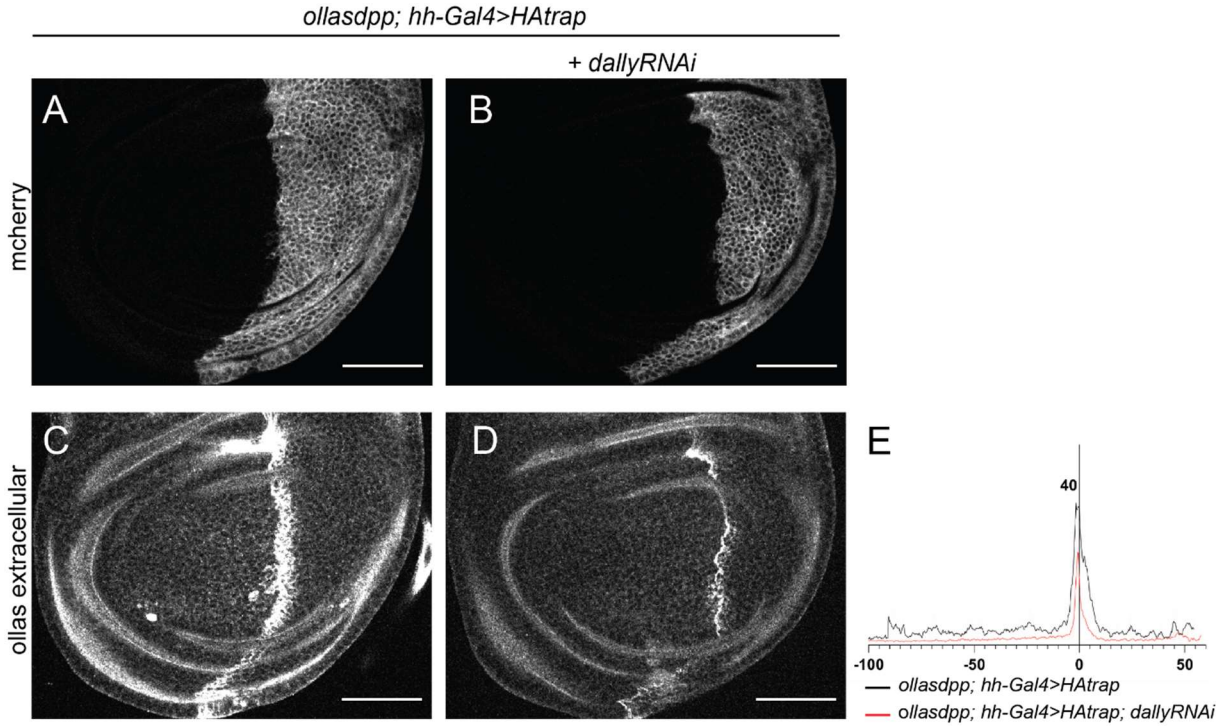


***Figure 7.2.2: Trapping HA-Dpp in the posterior compartment together with dallyRNAi.***
***A,B*** *mcherry signal in Ollas-dpp; hh-Gal4 (**A**) andOllas-dpp;hh-Gal4>dallyRNAi (**B**) wind disc (**B**).* ***C,D*** *Extracellular α-Ollas staining in Ollas-dpp; hh-Gal4 (**C**) andOllas-dpp;hh-Gal4>dallyRNAi (**D**) wind disc.* ***E*** *Average intensity profile of extracellular α-Ollas staining in Ollas-dpp; hh-Gal4 andOllas-dpp;hh-Gal4>dallyRNAi wing discs. Scale bar: 50µm.*

Moreover, when I looked at Dpp-lacZ flies together with *dally*RNAi, the intensity of lacZ staining was only slightly reduced when compared to Dpp-lacZ alone (Fig. 7.2.3). This result is consistent with previous studies showed reduced levels of Dpp-lacZ in the Dpp source abutting *dally* mutant clones in the posterior compartment (Ayers et al., 2010).

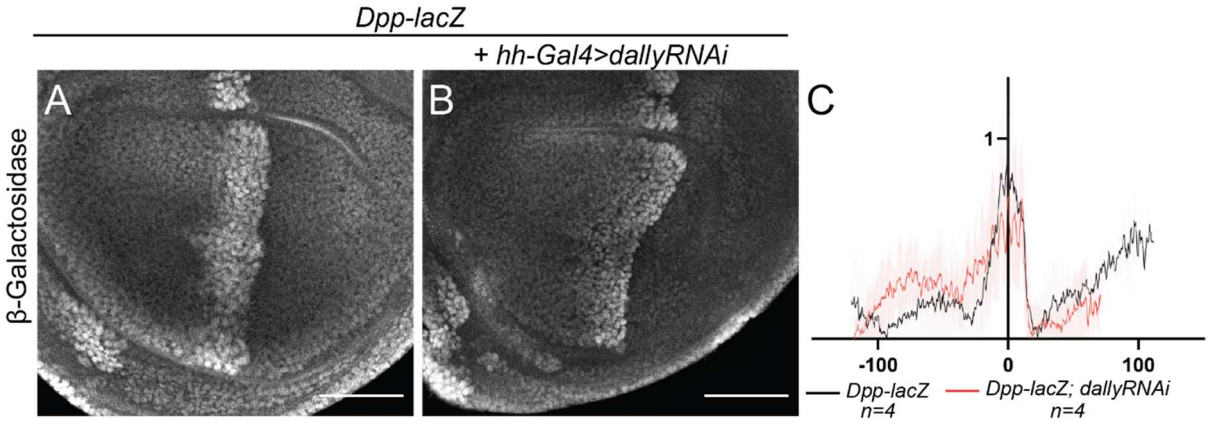


***Figure 7.2.3: Dpp-lacZ expression is slightly reduced when dally is removed from the posterior compartment**. **A,B** α-ß-Galactosidase staining in Dpp-lacZ (**A**) and Dpp-lacZ; hhGal4>dallyRNAi(**B**) wing discs. **C** Average intensity profile of α-ß-Galactosidase staining in Dpp-lacZ and Dpp-lacZ; hhGal4>dallyRNAi wing discs. Scale bar: 50µm.*

*Trapping of YFP-Dally in the posterior compartment increases pMad signal in the wing disc*

Previous studies proposed that cleavage of Dally is important for the long-range gradient formation of different morphogens (Ayers et al., 2010; Eugster et al., 2007; Han et al., 2004; Takeo et al., 2005). Anyhow, the role of Dally being shed from the cell surface in Dpp dispersal remains unclear (Han et al., 2005). To test this role, I expressed morphotrap in the posterior compartment in wing discs expressing YFP-Dally at an endogenous level (Fig 7.2.4). The morphotrap in combination with the YFP-Dally should prevent any Dally movement in the posterior compartment if Dally is shed from the cell surface. Under that condition I observed high accumulation of YFP signal where the morphotrap is expressed (Fig. 7.2.4B), indicating accumulation of YFP-Dally in this region. The pMad intensity in these discs is higher, compared to the YFP-Dally control (Fig. 7.2.4D,E,F). However, the pMad intensity is higher in the whole disc and not just the posterior compartment where morphotrap is expressed. Furthermore, the discs expressing morphotrap together with YFP-Dally showed cytoneme-like structures with high accumulation of YFP-Dally in the basal part of the disc (Fig. 7.2.4C).

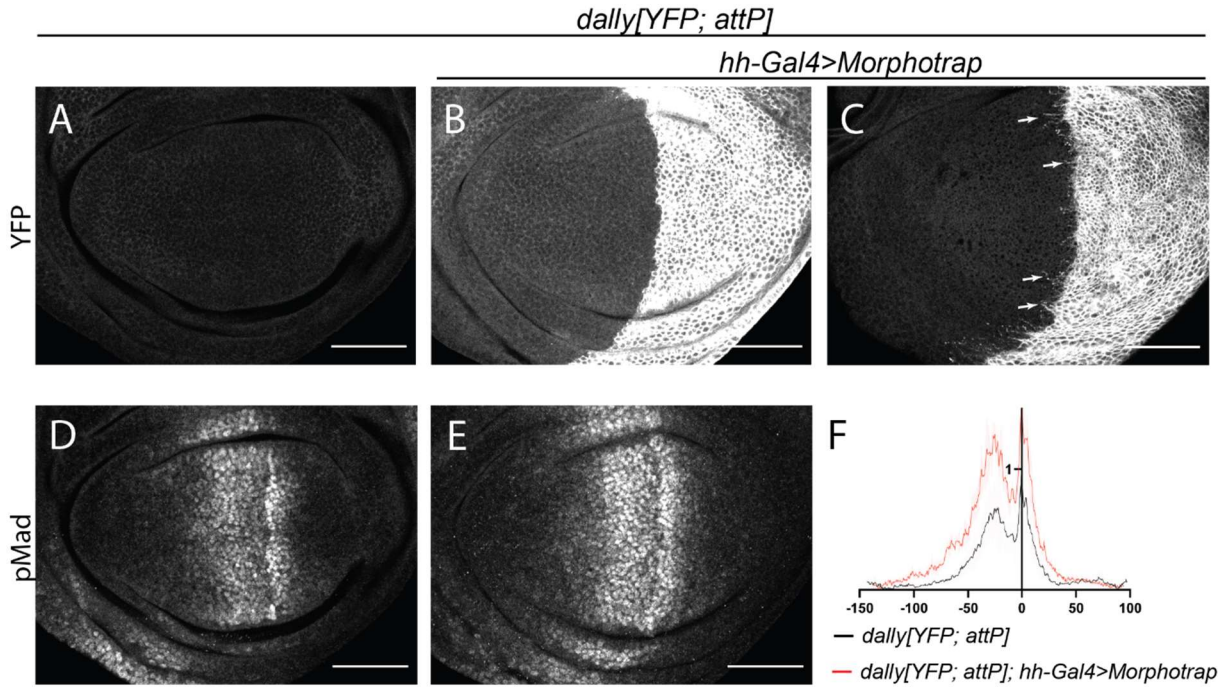


***Figure 7.2.4: Trapping YFP-Dally using the morphotrap in the posterior compartment leads to higher levels of pMad and high accumulations of Dally in the posterior compartment.***
***A*** *YFP-Dally expression pattern.* ***B*** *YFP-Dally + Morphotrap.* ***C*** *YFP-Dally + Morphotrap. Arrows point to potential Cytonemes reaching in the anterior compartment.* ***D*** *pMad gradient in a wing disc expressing endogenous amounts of YFP-Dally.* ***E*** *pMad gradient when additionally to YFP-Dally the morphotrap is expressed in the posterior compartment.* ***F*** *Average Intensity profiles of α-pMad staining in YFP-Dally and YFP-Dally + Morphotrap condition. Scale bar: 50µm.*

*Dally does not upregulate Dpp signaling cell-autonomously*

Although there are different mechanisms that have been proposed regarding the function of Dally, to date the exact role of Dally remains unclear. So far I showed that Dally is important to stabilize Dpp on the cell surface and most likely does not act as an active transporter of Dpp. However, Dally might act in multiple ways in parallel. Since Dally was also proposed to be a co-receptor for Dpp (Belenkaya et al., 2004), I wanted to test this possibility. I ectopically expressed clones of GFP-HA-Dally to examine the co-receptor function of Dally. Clones were induced using *tub*-Gal4 under the control of a heatshock-inducible Flp. In small clones not in contact with the source of Dpp, the signal should still be enhanced. However, I could not detect enhanced signaling levels in these clones (Fig 7.2.5). This result is in line with a previous study where clones of ectopic Dally were generated and the authors could not detect enhanced pMad signal in the clones in the periphery (Fujise, 2003). However, in clones close to the source cells, the authors could detect enhanced pMad intensity. Lower pMad levels in the peripheral clones expressing *dally* may just reflect the low amounts of Dpp present and does not necessarily argue against the co-receptor model of Dally.

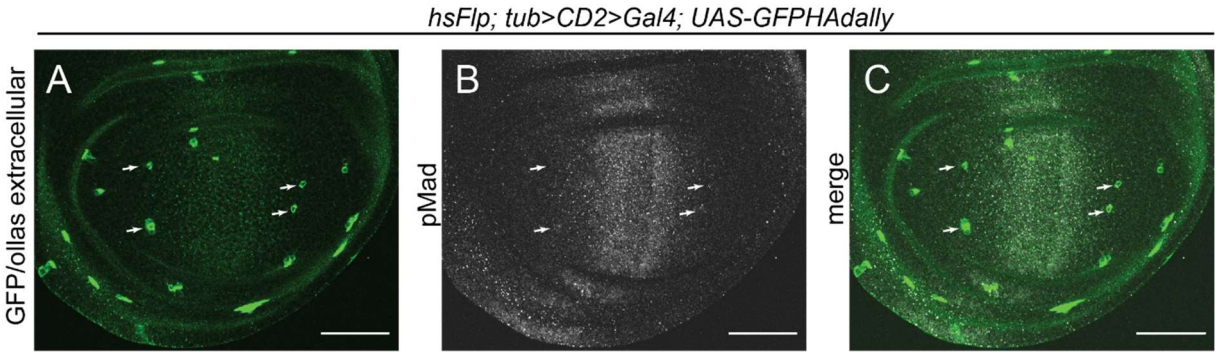


***Figure 7.2.5: Clonal expression of UAS-GFP-HA-Dally does not enhance pMad locally.***
***A*** *Clones expressing UASGFPHADally, seen by GFP in the Dally construct.* ***B*** *α-pMad staining in wing disc expressing clones of Dally (white arrows).* ***C*** *merge of GFP signal and α-pMad staining. Scale bar: 50µm.*

To further test the co-receptor function of Dally in Dpp signaling, I generated a membrane-tethered form of Dpp (Tdpp). To do so, I added two transmembrane domains of the human Toll-like receptor4 (TLR4) to the N-terminus of the mature domain of Dpp (Fig. 7.2.6A,B). Additionally, an HA tag was added N-terminally of the inserted TM domains and I certained that the Dally binding site (Dallybs) was N-terminally to the TM domains together with the mature domain in order to exclude possible phenotypes due to inaccessibility of the Dallybs or disruption of its function due to the distance to the mature domain. Staining for the HA tag confirmed the presence of the Tdpp construct when Gal4 was expressed under the *ap* driver (Fig. 7.2.6C).

The Tdpp construct was expressed together with *dally*RNAi (Fig. 7.2.6H) or an UAS-GFP-HA-Dally (Fig. 7.2.6E) construct. With this setup, eliminating the possibility that changes in pMad intensity are due to altered Dpp dispersal and focusing on the effect of Dally on Dpp signaling only. Tethering Dpp to the cell surface leads to high accumulation of pMad in the region where Tdpp is expressed (Fig. 7.2.6D,G). When GFP-HA-Dally was expressed in the presence of Tdpp, the pMad intensity was reduced compared to Tdpp alone (Fig. 7.2.6E,F). *dally*RNAi expressed together with Tdpp enhanced the pMad intensity when compared to Tdpp alone (Fig. 7.2.6H,I). If Dally was an important co-receptor for Dpp signaling, higher signal could be expected when more Dally is present and lower signal when Dally is removed. However, my experiments suggest the opposite to be the case. This might be due to differences in stability of the Tdpp constructs when Dally is present or not. With more Dally on the cell surface, less Tdpp might be internalized and able to signal, with Dally removed from the cell surface, more Dpp might be internalized and able to signal.

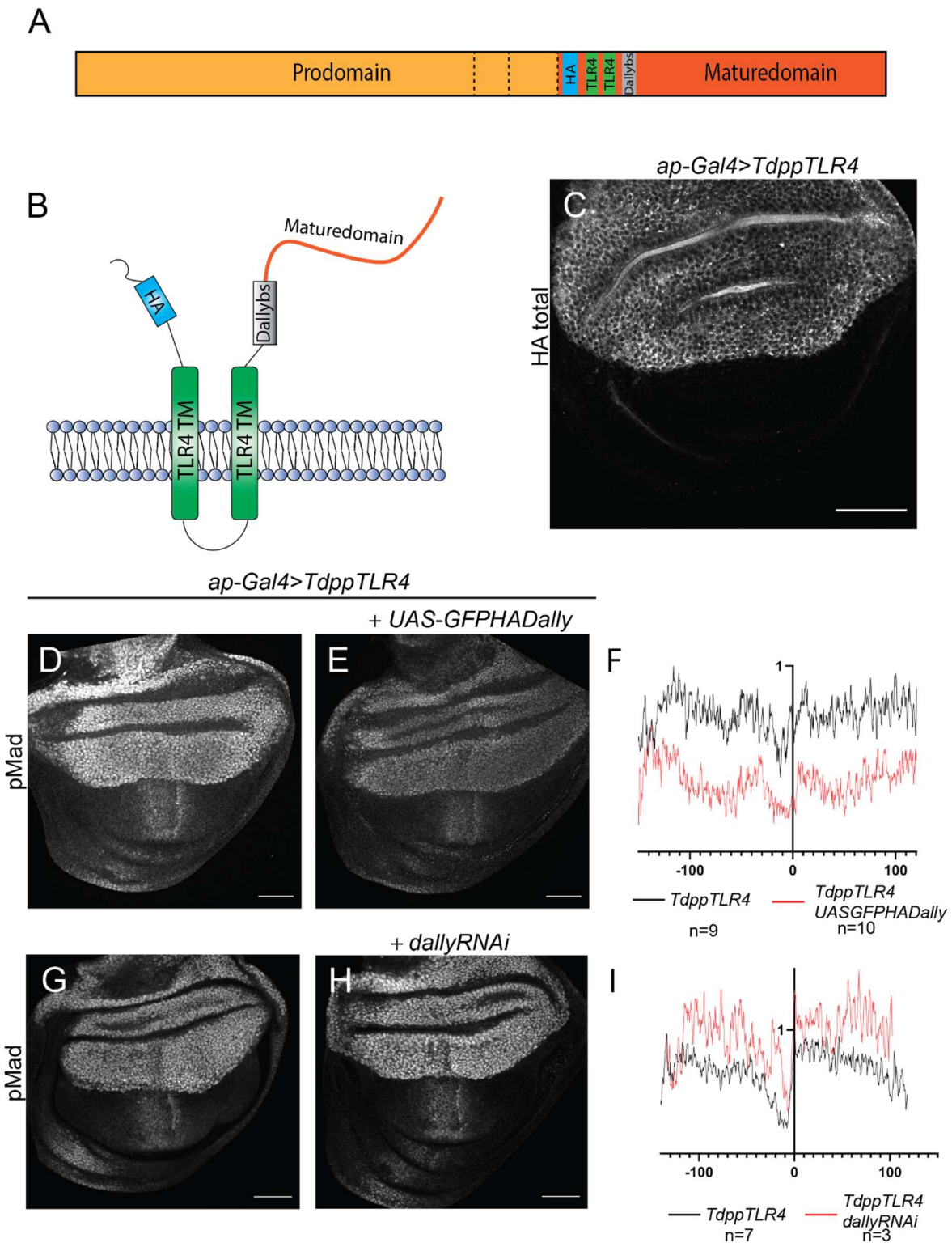


***Figure 7.2.6: Tethered Dpp (Tdpp) in the wing disc.***
***A-B*** *Schematic view of the Tethered Dpp construct. Two TLR4 transmembrane domains (green) were added to the N-terminus of the Dpp maturedomain together with an HA tag (blue). The Dally binding site (grey) was left C-terminally of the transmembrane domains to be in close proximity to the maturedomain.* ***C*** *α-HA staining in ap-Gal4>TdppTLR4 wing disc.* ***D,G*** *α-pMad staining in ap-Gal4>TdppTLR4 wing disc.* ***E*** *α-pMad staining in ap-Gal4>TdppTLR4,UASGFPHADally wing disc.* ***F*** *Average intensity profile of α-pMad staining in ap-Gal4>TdppTLR4 and ap-Gal4>TdppTLR4,UASGFPHADally wing discs.* ***H*** *α-pMad staining in ap-Gal4>TdppTLR4,dallyRNAi wing disc.* ***I*** *Average intensity profile of α-pMad staining of ap-Gal4>TdppTLR4 and ap-Gal4>TdppTLR4,dallyRNAi wing discs. Scale bar: 50µm.*

*Levels of Tkv are different in dallyRNAi and UASGFPDally conditions*

I showed in chapter 7.1 that Dally stabilizes Dpp through a receptor mediated process. When Tkv was removed using RNAi, the Dpp gradient observed was enhanced (Fig. 7.1.6).

To look further into this enlarged gradient and confirm this result, I used the HA trap expressing clones, to trap HA-Dpp far from the source when *tkv*RNAi was expressed. When *tkv*RNAi was expressed under the control of Hh-Gal4, the wing disc was divided by a fold through the centre where the A/P border is supposed to be (Fig. 7.2.7B-B``). Anyways, we could observe the expression of clones of HA trap. As expected, when *tkv*RNAi was expressed, the accumulation of Dpp was higher in the HA trap clones compared to the control clones where no RNAi was expressed (Fig. 7.2.7). This supports the observed enlargement of the Dpp gradient when only *tkv*RNAi was expressed. However, the fold at the A/P compartment boundary makes this result hard to interpret, since the Dpp source might be affected directly. Furthermore, the spreading of Dpp might be impaired by the additional fold.

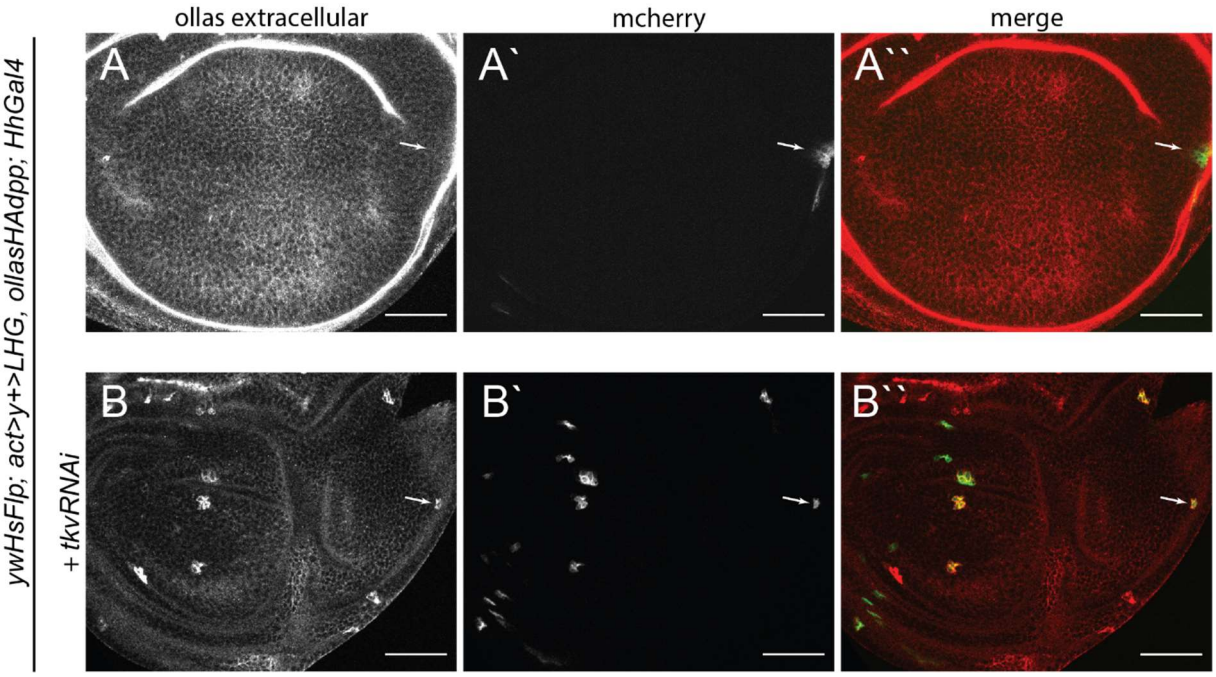


***Figure 7.2.7: Removing Tkv from the posterior compartment does enhance the size of the Dpp gradient.***
***A,B*** *Extracellular α-Ollas staining in wing discs expressing HA trap clones in the whole disc (**A**) and additionally tkvRNAi in the posterior compartment (**B**).* ***A`,B`*** *mcherry intensity in wing discs expressing HA trap clones in the whole disc (**A`**) and additionally tkvRNAi in the posterior compartment (**B`**).* ***A``,B``*** *merge of extracellular α-Ollas and mcherry. Scale bars: 50µm.*

However, I still do not know the mechanism behind the stabilization of Dpp through Dally. To see if Dally influences Tkv levels directly, I looked at Tkv in *dally* overexpression and *dally*RNAi conditions. To monitor Tkv levels directly, I used two differently, endogenously tagged Tkv; Tkv tagged with a mCherry (Fig. 7.2.8) and Tkv tagged with an HA tag (Fig. 7.2.9). When Dally

was overexpressed in the posterior compartment using Hh-Gal4, I could observe a slightly weaker signal intensity of mCherry-tagged Tkv in the posterior compartment (Fig. 7.2.8).

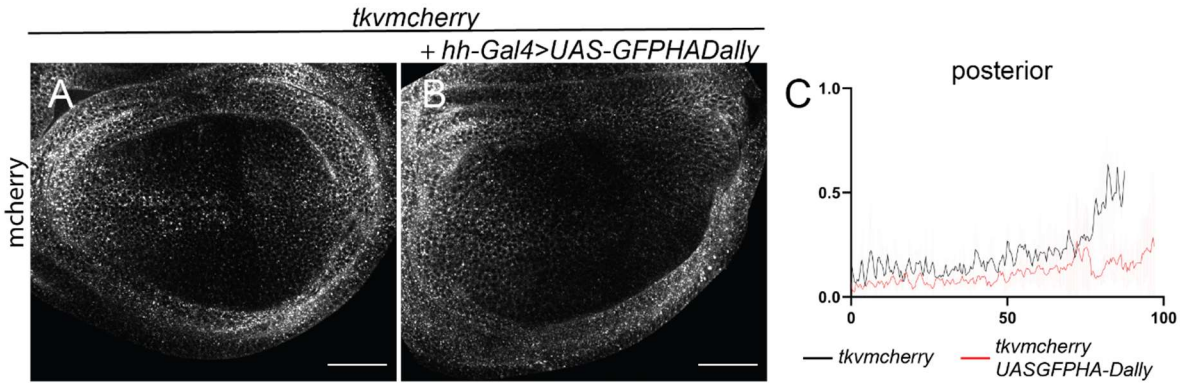


***Figure 7.2.8: Expression of Dally reduces Tkv.***
***A*** *tkvmcherry intensity in the wing disc.* ***B*** *tkvmcherry intensity together with hh-Gal4>UASGFPHADally in the wing disc.* ***C*** *Average Intensity profile of tkvmcherry in the posterior compartment in wing discs expressing tkvmcherry with and without overexpression of UAS-GFP-HA-Dally. Scale bars: 50µm.*

Moreover, when Dally was removed using *dally*RNAi expressed in the dorsal compartment by *ap*-Gal4, the intensity of HA-tagged Tkv was reduced in the dorsal compartment (Fig. 7.2.9). Anyhow, by removing Dally from the dorsal compartment, the whole compartment was shrunk when compared to the ventral side of the wing disc (Fig. 7.2.9), making this result hard to interpret.

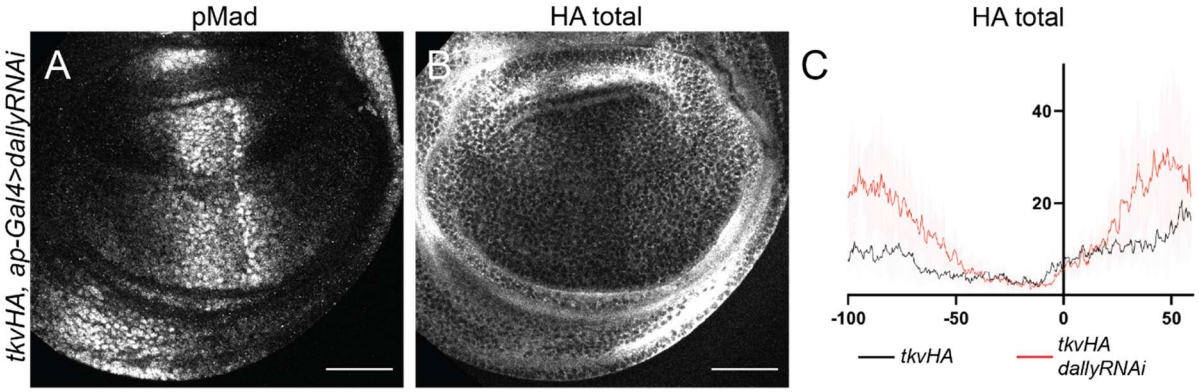


***Figure 7.2.9: Loss of dally leads to higher amounts of Tkv.***
***A*** *α-pMad staining of tkvHA, ap-Gal4>dallyRNAi wing disc.* ***B*** *Intensity pattern of tkvHA in the wing disc expressing dallyRNAi under the ap-Gal4 driver.* ***C*** *Average intensity profile of the ventral and the dorsal compartment in tkvHA, ap-Gal4>dallyRNAi wing discs. Scale bars: 50µm.*

*Removing parts of the Dally core protein*

In chapter 7.1 I showed that Dpp can bind to the core protein of Dally. Next, I wanted to know how important this binding of Dpp to the core protein of Dally is for proper Dpp function. Therefore, I generated my own Dally construct, a Dally lacking the core protein, but still containing the HS attachment sites (Dally$^{\Delta coreprotein}$) and another Dally lacking both, core

protein and HS attachment sites (Dally$^{\Delta HS\Delta coreprotein}$) (Fig. 7.2.10). To remove the HS attachment sites, the serine in position 549, 569 and 573 were changed to alanine (TCC-> GCC) (indicated by a red cross in Fig. 7.2.10).

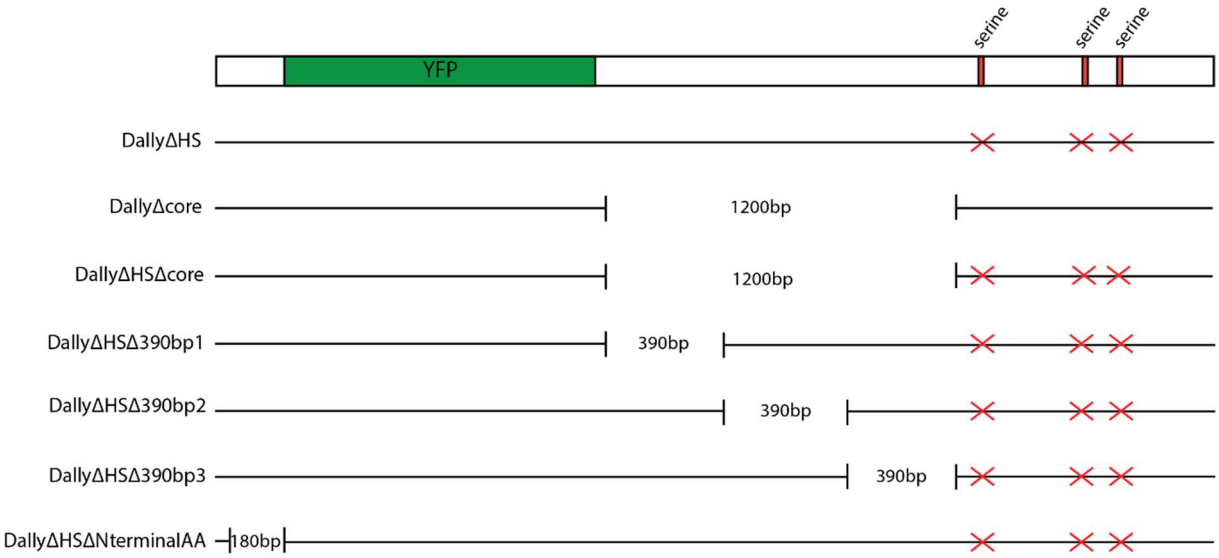


***Figure 7.2.10: Dally core protein deletion constructs generated in this study.***
*In this study, eight different UAS-Dally constructs were generated. All constructs contained a N-terminal YFP-tag to visualize the construct after expression. Six of the constructs had the three C-terminal serine residues changed to alanine (TCC->GCC), indicated by the red crosses. DallyΔcore and DallyΔHSΔcore had a sequence of 1200bp removed from the core protein. DallyΔHSΔ390bp1, DallyΔHSΔ390bp2 and DallyΔHSΔ390bp3 had smaller sequences of 390bp, adjacent to each other, removed. DallyΔHSΔNterminalAA had a small sequence of 180bp N-terminally of the YFP-tag removed.*

The Dally overexpression construct confirmed results we obtained with the constructs used in previous experiments, namely a broader pMad signal and an accumulation of extracellular Dpp in the whole dorsal compartment (Fig. 7.1.1A, 7.2.11A). When YFP-Dally$^{\Delta HS\Delta core}$ was expressed, pMad was not enhanced and Dpp did not accumulate (Fig. 7.2.11C,C'). Furthermore, YFP-Dally$^{\Delta core}$ did not enhance pMad levels nor accumulate Dpp (Fig. 7.2.11B,B'). This indicates the importance of the Dally core protein for interacting with Dpp. However, in these mutants, I deleted a big part of the core protein in Dally. This might disrupt more functions than just the interaction with Dpp. To test whether these constructs are present on the cell surface I stained discs expressing these constructs using an Antibody against GFP and stained extracellularly for the YFP Tag. The same intensity of extracellular YFP could be detected in all Dally constructs (Fig. 7.2.12D-F), suggesting that the secretion of these constructs is not perturbed, or that the protein encoded by these constructs are produced and retained on the cell surface. To test if YFP-Dally$^{\Delta core}$ possess HS chains, I stained discs expressing these constructs using an antibody against HS. As expected, HS staining showed a

clear accumulation of HS in the dorsal compartment when my Dally construct was expressed (Fig. 7.2.11G,G'). However, when YFP-Dally$^{\Delta core}$ and YFP-Dally$^{\Delta HS\Delta core}$, were expressed, no difference between dorsal and ventral signal intensity was observed (Fig. 7.2.11H,H',I,I'). This shows that the core protein of Dally is required for HS addition. Thus it was not possible to test if the HS of Dally can bind to Dpp independent of the core protein. To try and determine the binding location of Dpp and the importance of Dpp binding to the core protein, I generated an additional three constructs by subdividing the large deletion of the Dally$^{\Delta core}$ into three smaller deletions of 390bp each, with all three constructs also lacking the HS attachment site (Fig. 7.2.10). The hope was to not disrupt the protein folding by deleting smaller parts of the core protein, yet big enough to either retain or affect the binding of Dpp. As expected, when I expressed these constructs in the dorsal compartment using *ap*-Gal4, none of these construct lead to an accumulation of pMad (Fig. 7.2.13F-H). However, Dpp was not accumulated where the constructs were expressed, the staining intensity was rather decreased by all three constructs (Fig. 7.2.13B-D). This might be because the whole core protein is needed for Dpp binding, however, since the three smaller deletions still lack 130 aa of the core protein, this could also severely affect the function of the core protein.

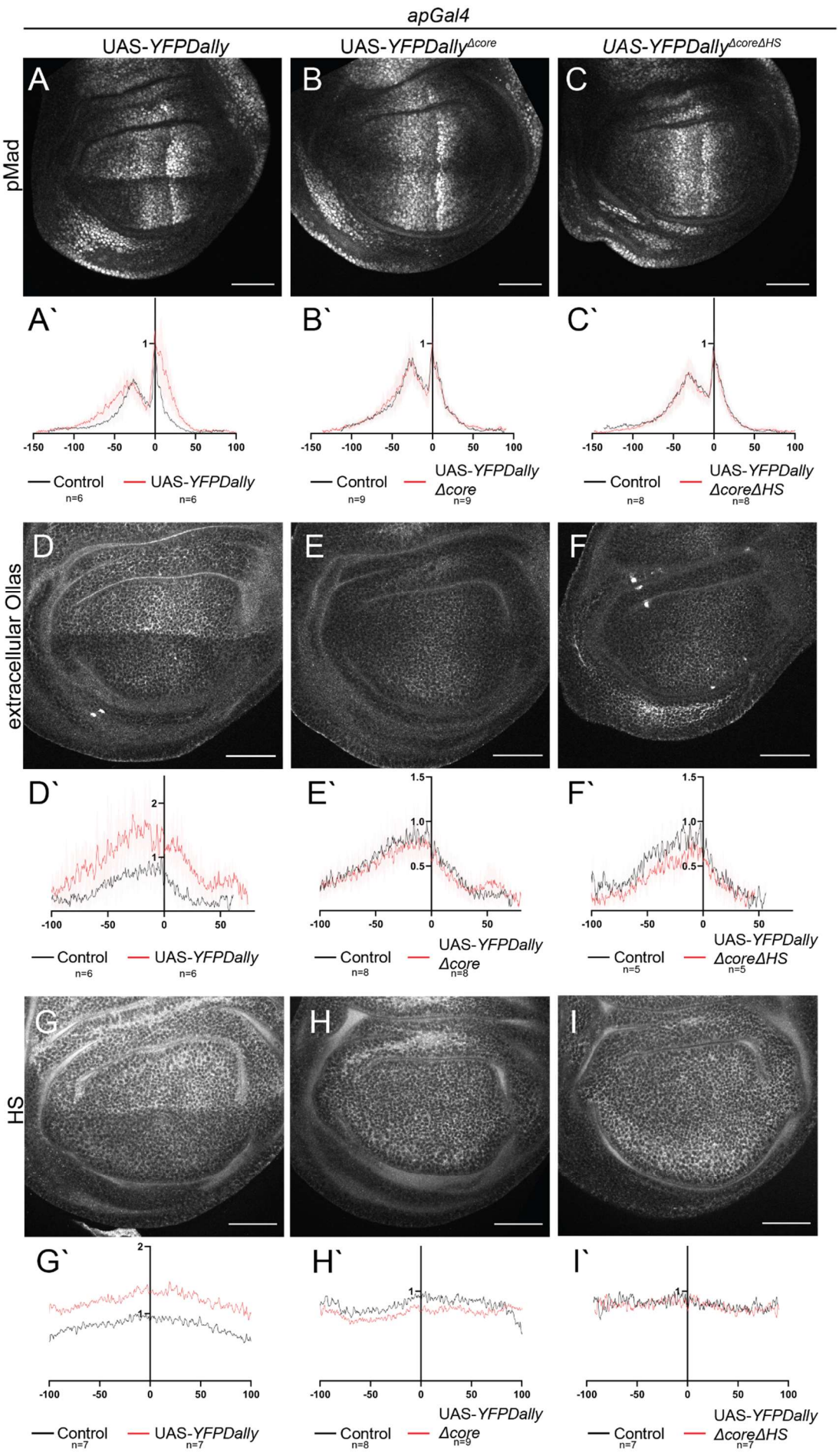
apGal4
UAS-YFPDally
UAS-YFPDally^Δcore
UAS-YFPDally^ΔcoreΔHS
pMad
extracellular Ollas
HS
A
B
C
A`
B`
C`
D
E
F
D`
E`
F`
G
H
I
G`
H`
I`
Control
UAS-YFPDally
UAS-YFPDally Δcore
UAS-YFPDally ΔcoreΔHS
n=6
n=9
n=8
n=5
n=7

***Figure 7.2.11: The core protein deletion constructs do not accumulate Dpp.***
***A-C*** *α-pMad staining of ap-Gal4>UAS-YFP-Dally (**A**), ap-Gal4>UAS-YFP-Dally$^{\Delta coreprotein}$ (**B**) and ap-Gal4>UAS-YFP-Dally$^{\Delta coreproteinΔHS}$ (**C**) wing discs. **A`-C`** Average intensity profiles of ventral (control) vs. dorsal α-pMad staining in ap-Gal4>UAS-YFP-Dally (**A`**), ap-Gal4>UAS-YFP-Dally$^{\Delta coreprotein}$ (**B`**) and ap-Gal4>UAS-YFP-Dally$^{\Delta coreproteinΔHS}$ (**C`**) wing discs. **D-F** Extracellular α-Ollas staining of ap-Gal4>UAS-YFP-Dally (**D**), ap-Gal4>UAS-YFP-Dally$^{\Delta coreprotein}$ (**E**) and ap-Gal4>UAS-YFP-Dally$^{\Delta coreproteinΔHS}$ (**F**) wing discs. **D`-F`** Average intensity profiles of ventral (control) vs. dorsal extracellular α-Ollas staining in ap-Gal4>UAS-YFP-Dally (**D`**), ap-Gal4>UAS-YFP-Dally$^{\Delta coreprotein}$ (**E`**) and ap-Gal4>UAS-YFP-Dally$^{\Delta coreproteinΔHS}$ (**F`**) wing discs. G-I α-HS staining of ap-Gal4>UAS-YFP-Dally (**G**), ap-Gal4>UAS-YFP-Dally$^{\Delta coreprotein}$ (**H**) and ap-Gal4>UAS-YFP-Dally$^{\Delta coreproteinΔHS}$ (**I**) wing discs. G`-I` Average intensity profiles of ventral (control) vs. dorsal α-HS staining in ap-Gal4>UAS-YFP-Dally (**G`**), ap-Gal4>UAS-YFP-Dally$^{\Delta coreprotein}$ (**H`**) and ap-Gal4>UAS-YFP-Dally$^{\Delta coreproteinΔHS}$ (**I`**) wing discs. Scale bars: 50µm.*

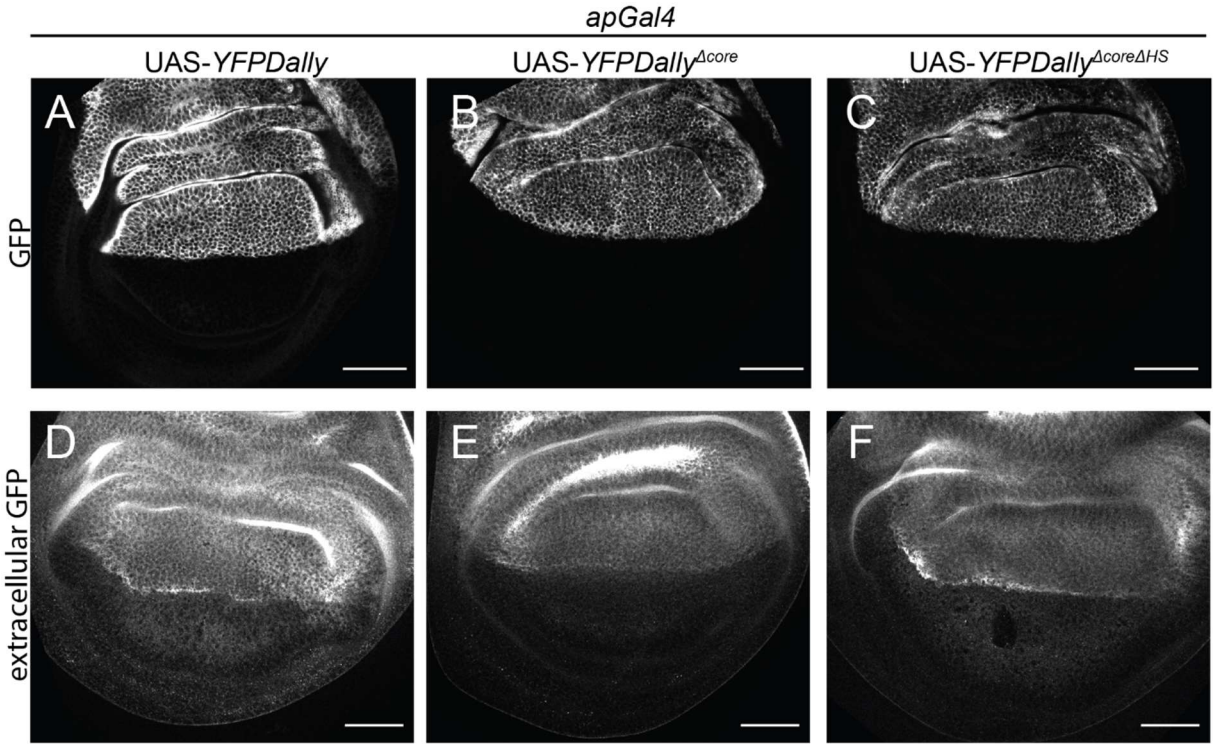


***Figure 7.2.12: The Dally core protein deletion constructs are expressed and present on the cell surface.***
***A-C*** *GFP intensity of ap-Gal4>UAS-YFP-Dally (**A**), ap-Gal4>UAS-YFP-Dally$^{\Delta coreprotein}$ (**B**) and ap-Gal4>UAS-YFP-Dally$^{\Delta coreproteinΔHS}$ (**C**) wing discs. **D-F** Extracellular α-GFP staining of ap-Gal4>UAS-YFP-Dally (**D**), ap-Gal4>UAS-YFP-Dally$^{\Delta coreprotein}$ (**E**) and ap-Gal4>UAS-YFP-Dally$^{\Delta coreproteinΔHS}$ (**F**) wing discs. Scale bars: 50µm.*

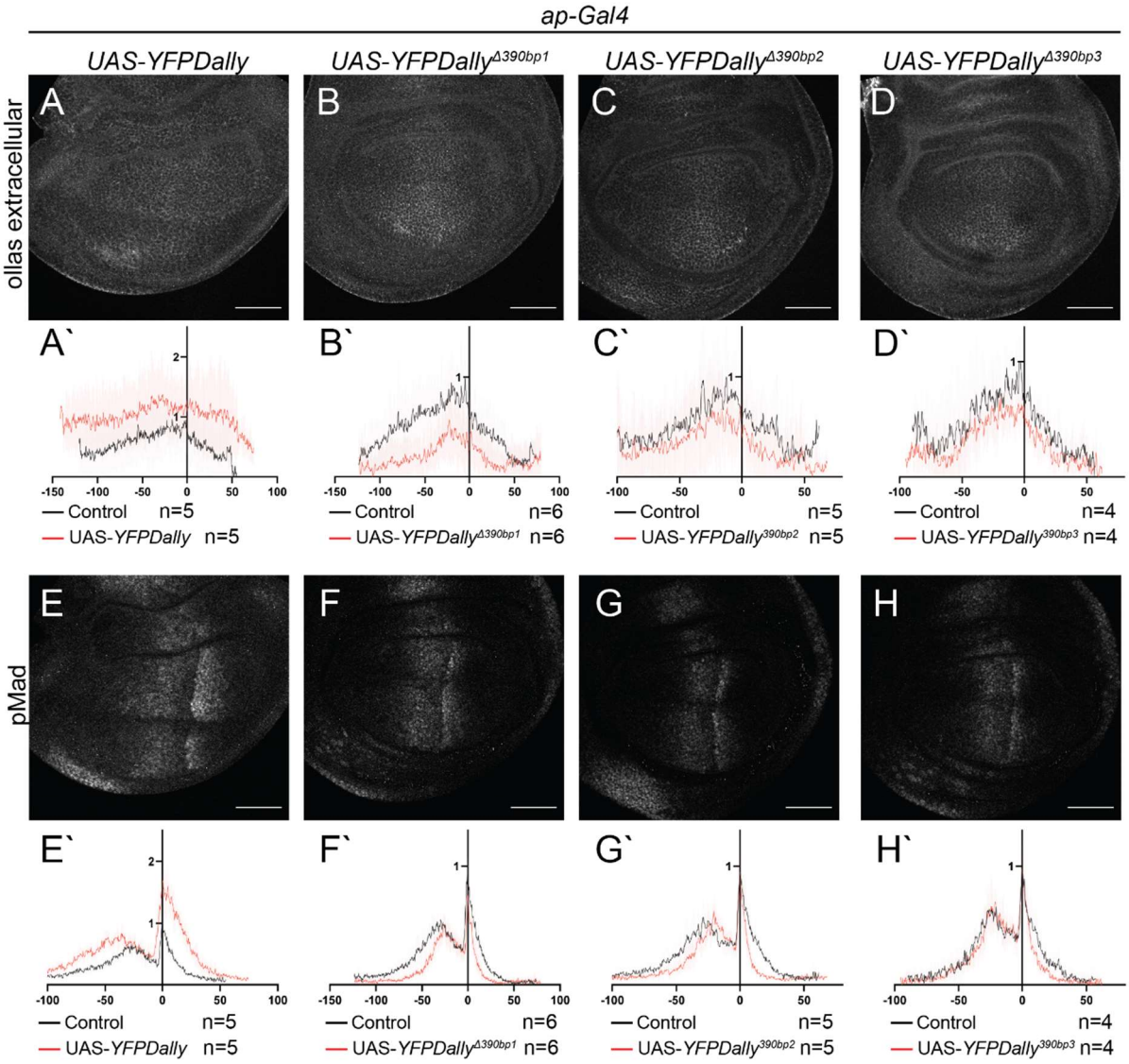


***Figure 7.2.13: The smaller deletion constructs do not accumulate Dpp.***
***A-D*** *Extracellular α-Ollas staining of ap-Gal4>UAS-YFP-Dally (**A**), ap-Gal4>UAS-Dally$^{\Delta HS\Delta 390bp1}$ (**B**), ap-Gal4>UAS-Dally$^{\Delta HS\Delta 390bp2}$ (**C**) and ap-Gal4-UAS-YFP-Dally$^{\Delta HS\Delta 390bp3}$ (**D**) wing discs. **A`-D`** Average intensity profiles of of ventral (control) vs. dorsal extracellular α-Ollas staining in ap-Gal4>UAS-YFP-Dally (**A`**) ap-Gal4>UAS-Dally$^{\Delta HS\Delta 390bp1}$ (**B`**), ap-Gal4>UAS-Dally$^{\Delta HS\Delta 390bp2}$ (**C`**) and ap-Gal4-UAS-YFP-Dally$^{\Delta HS\Delta 390bp3}$ (**D`**) wing discs. **E-H** α-pMad stainings of ap-Gal4>UAS-YFP-Dally (**E**), ap-Gal4>UAS-Dally$^{\Delta HS\Delta 390bp1}$ (**F**), ap-Gal4>UAS-Dally$^{\Delta HS\Delta 390bp2}$ (**G**) and ap-Gal4-UAS-YFP-Dally$^{\Delta HS\Delta 390bp3}$ (**H**) wing discs. **E`-H`** Average intensity profiles of of ventral (control) vs. dorsal extracellular α-pMad staining in ap-Gal4>UAS-YFP-Dally (**E`**) ap-Gal4>UAS-Dally$^{\Delta HS\Delta 390bp1}$ (**F`**), ap-Gal4>UAS-Dally$^{\Delta HS\Delta 390bp2}$ (**G`**) and ap-Gal4-UAS-YFP-Dally$^{\Delta HS\Delta 390bp3}$ (**H`**) wing discs. Scale bars: 50µm.*

### *7.2.2 An endogenous Dpp lacking the binding site for Dally*

Dally controls not only Dpp function but also the function of other morphogens. To tackle the multifunctionality problem of Dally in Drosophila and to investigate Dally function, a form of Dpp lacking seven basic amino acid residues (Dpp$^{\Delta N}$) necessary for BMP-HSPG interaction was generated by Akiyama et al. (Akiyama et al., 2008; Ohkawara et al., 2002). S2 cells treated with Dpp$^{\Delta N}$ induced the same level of pMad as wild type Dpp (wtDpp). Overexpressing an HA-tagged version of Dpp$^{\Delta N}$ in the wing disc showed reduced extracellular distribution compared

to wtDpp. This study was conducted in cell culture and in overexpressing condition and may not reflect a physiological condition. For this reason, Shinya Matsuda generated flies which produce Dpp lacking the seven basic amino acid residues together with an HA-tag (HA-dpp$^{\Delta dally}$) from the endogenous locus (Fig. 7.2.14A) (See also chapter 7.1 (Dpp$^{\Delta N}$).

*HA-Dpp$^{\Delta dally}$ homozygous mutants are embryonic lethal*

*HA-Dpp$^{\Delta dally}$* homozygous flies died during early embryonic development and were not viable. This was surprising since *dally* mutant flies are homozygous viable. A previous study found that the seven amino acid residues which were removed in these mutants not only bind to Dally, but also to Collagen IV, an important component during dorsal-ventral patterning of the early embryo (Sawala et al., 2012).To distinguish homozygous from heterozygous individuals, the flies were combined with *hunchback*-lacZ (Hb-lacZ). *hb* is expressed in the anterior part of the early embryo, giving me the possibility to distinguish homo- from heterozygous individuals in an early stage. β-Galactosidase and pMad stainings were performed. Embryos with and without β-Galactosidase staining were observed (Fig. 7.2.14B,D), indicating the presence of homo- and heterozygous individuals in the stock. Consistent with the previously mentioned model (Sawala et al., 2012), pMad was completely lost in *HA-Dpp$^{\Delta dally}$* embryos (Fig. 7.2.14C). However, in heterozygous *HA-Dpp$^{\Delta dally}$*, the dorsal pMad stripe was observed (Fig 7.2.14E).

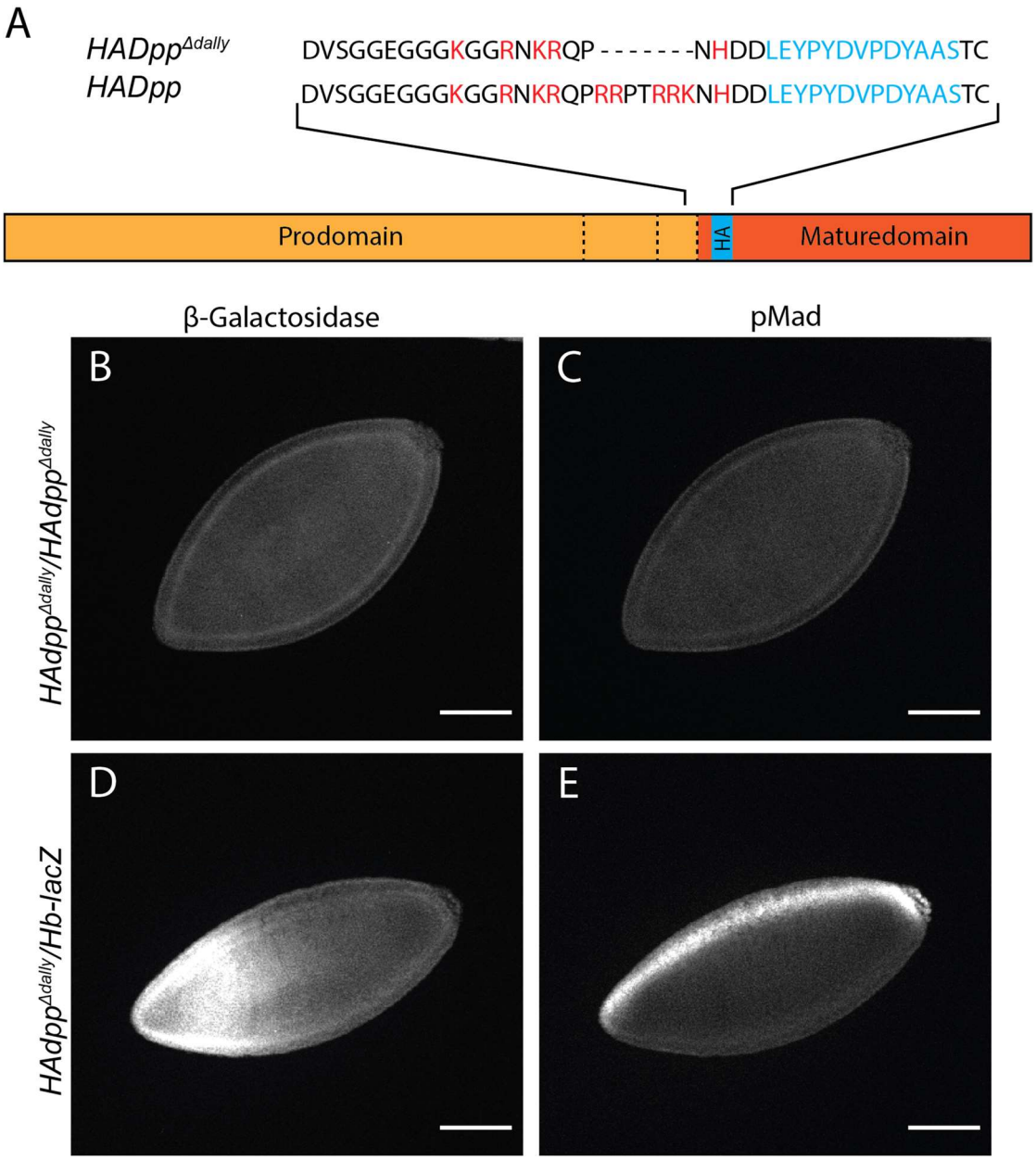


***Figure 7.2.14: Scheme of the HA-Dpp$^{\Delta Dally}$ construct and mutant embryos stained for pMad.***
*A N-terminal amino acid sequence of HA-Dpp$^{\Delta Dally}$ and HA-Dpp. The basic amino acids are marked in red and the HA tag in blue. The seven basic amino acids removed from the construct are in the mature domain of Dpp (dark orange) close to one of the processing sides (dashed line). B β-Galactosidase staining of HA-dpp and HA-dpp$^{\Delta Dally}$ embryos. C pMad staining in the same embryos. Scale bars: 100µm.*

### *HA-Dpp$^{\Delta dally}$ phenotype is mild in the wing disc and adult wing*

To be able to examine *HA-Dpp$^{\Delta dally}$* wing discs, I generated flies with homozygous mutant clones, using Flp/FRT-induced mitotic recombination with the *minute* technique. Absence of *arm*-lacZ marks the mutant clones. Clones with one copie of *minute* will grow slower due to the growth retardation effect of *minute*, causing the *HA-Dpp$^{\Delta dally}$* clones to outgrow the surrounding cells, which ultimately produces larger *HA-Dpp$^{\Delta dally}$* homozygous clones (Fig. 7.2.15A). To get homozygous clones, a heatshock @37°C was given 48h after egg laying for

90min. In these discs, I looked for clones big enough to cover the Dpp producing region in the centre of the disc (Fig. 7.2.15C-C''). In these wing discs, the pMad intensity was slightly reduced compared to control discs (Fig. 7.2.15B-D). Since it is not always easy to obtain the right clones in the right position and size, I looked for another way to overcome the early lethality of the *HA-Dpp$^{\Delta ddally}$* flies. To do so, I provided them with a transgene (JAX), which leads to *dpp* expression during the early stages of *Drosophila* development, but not later during imaginal wing disc development (Hoffmann & Goodman, 1987).

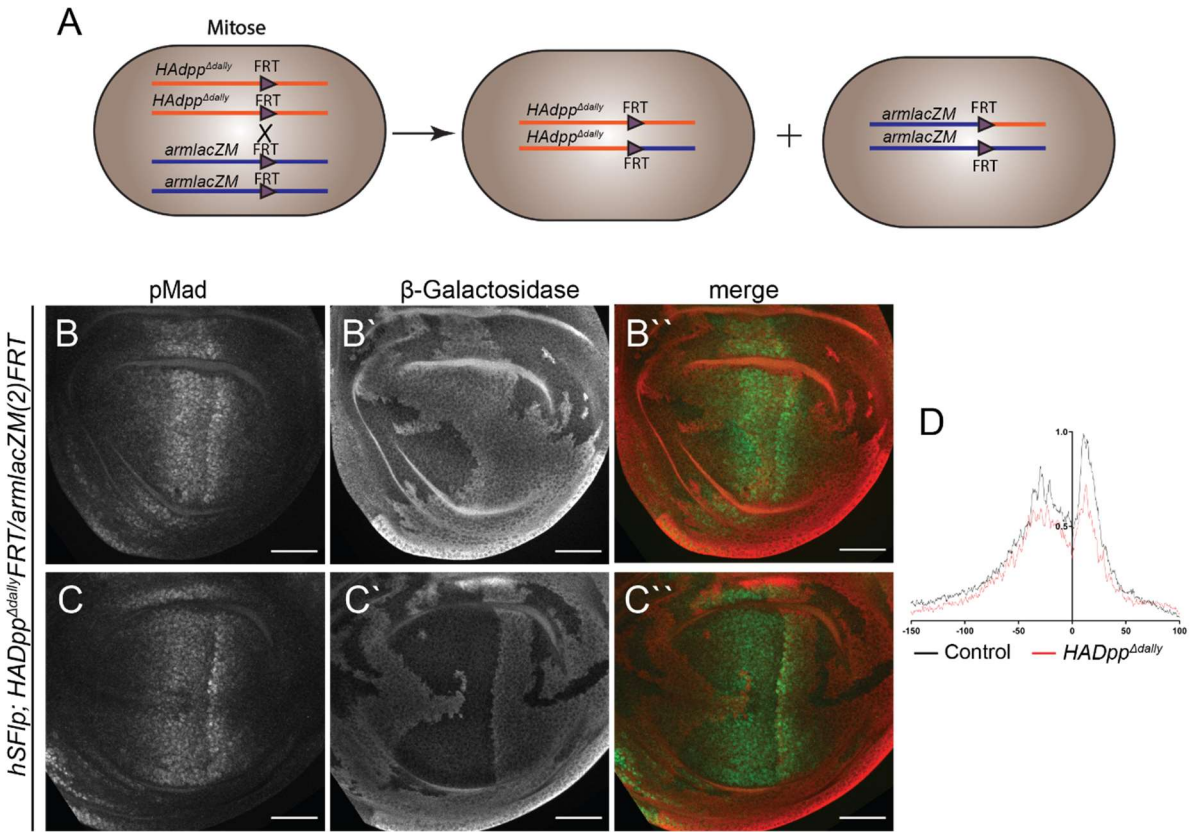


***Figure 7.2.15: Clones of HA-dpp$^{\Delta Ddally}$ show reduced pMad.***
***A*** *Schmeatic view of the generation of homozygous clones using the Flp-FRT system. Upon heat shock during mitosis, the flp recombinase directs site directed recombination between the FRT sites, creating clones of homozygous HA-dpp$^{\Delta Ddally}$ and armlacZM. Clones of interest can be distinguished by staining of ß-Galactosidase.* ***B-B``*** *α-pMad (**B**), α-ß-Galactosidase (**B`**) and merge (**B``**) of a wing disc with clones not in the source of Dpp thereby with wild type Dpp. C-C`` α-pMad (**C**), α-ß-Galactosidase (**C`**) and merge (**C``**) of a wing disc with a clones covering the whole source of Dpp thus leading to all the Dpp being HA-Dpp$^{\Delta Ddally}$ mutant.* ***D*** *Intensity profile of the pMad in the two wing discs. Scale bars: 50µm.*

I found that *HA-Dpp$^{\Delta ddally}$* flies combined with JAX are homozygous viable, survive until adulthood and are fertile. In the wing disc, I found that pMad and extracellular HA-dpp was slightly reduced in these *HA-Dpp$^{\Delta ddally}$* alleles (Fig. 7.1.4). When I looked at the expression of the Dpp target genes, the high-threshold target Sal showed a slightly increased expression

domain (Fig. 7.2.16A-A'') and the omb expression domain was unchanged when compared to a *HA-Dpp* control disc (Fig. 7.2.16B-B'').

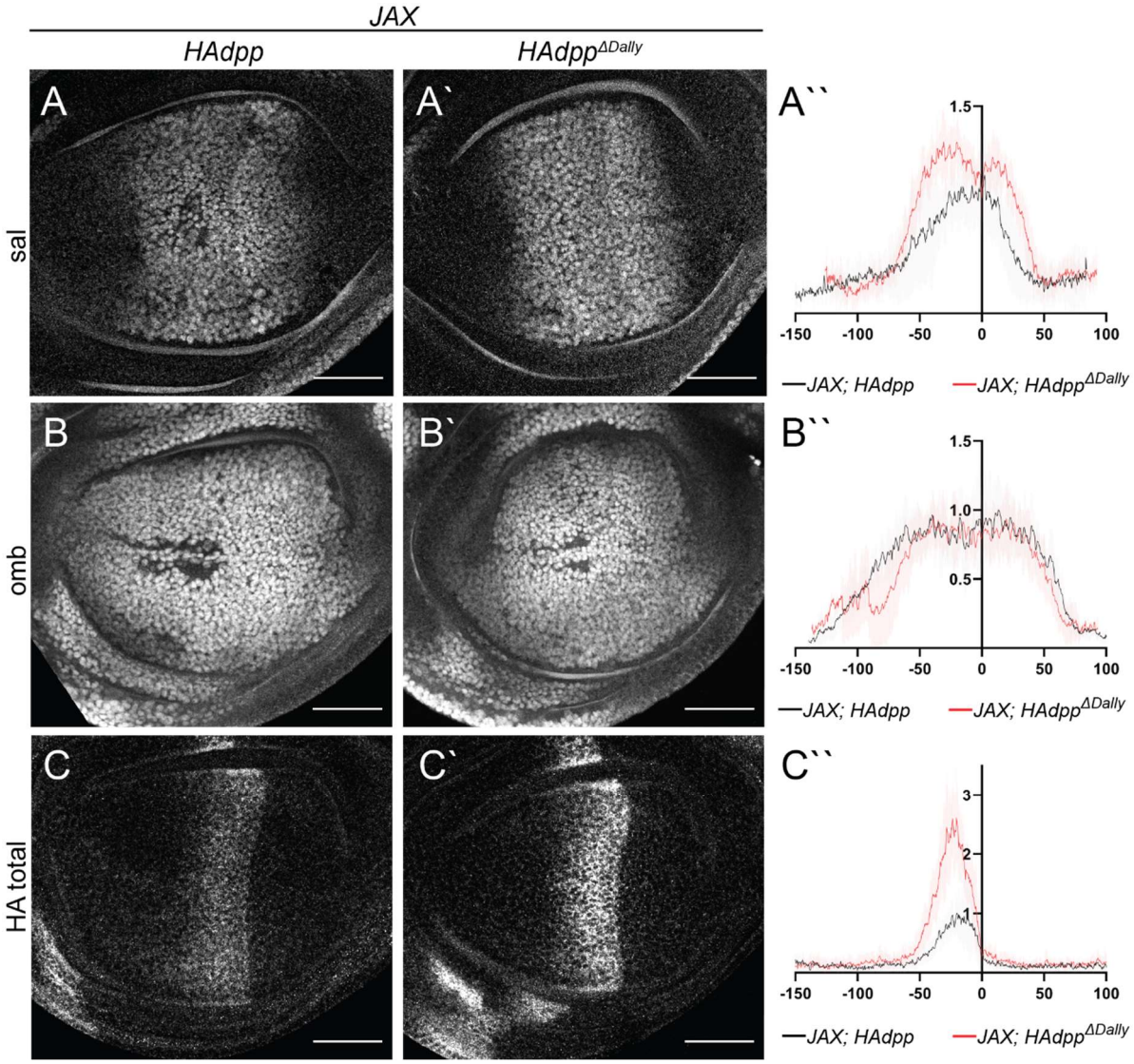


***Figure 7.2.16: JAX;HA-Dpp$^{\Delta Dally}$ in the wing disc.***
*A,A` α-sal staining in JAX;HA-dpp (A) and JAX;HA-dpp$^{\Delta Dally}$ (A`) wing disc. A`` Average iIntensity profile of the α-sal staining in JAX;HA-dpp and JAX;HA-dpp$^{\Delta Dally}$ wing disc. B,B` α-omb staining of JAX; HA-dpp (B) and JAX;HA-dpp$^{\Delta Dally}$ (B`) wing disc. B`` Average intensity profile of α-omb staining in JAX;HA-dpp and JAX;HA-dpp$^{\Delta Dally}$ wing discs. C,C` α-HA staining of JAX;HA-dpp (C) and JAX;HA-dpp$^{\Delta Dally}$ (C`) wing discs. C`` Average intensity profiles α-HA staining of JAX;HA-dpp and JAX;HA-dpp$^{\Delta Dally}$ wing discs. Scale bars: 50µm.*

To my surprise, when I conducted a total staining of HA-Dpp and HA-Dpp$^{\Delta dally}$, the staining intensity was much higher in the *HA-dpp$^{\Delta dally}$* mutants (Fig. 7.2.16C-C''). However, when I compared the wings of *HA-Dpp$^{\Delta dally}$* and *HA-Dpp* adult flies, I could not observe any phenotype in the patterning, although the wings of *HA-Dpp$^{\Delta dally}$* mutant flies were significantly smaller (Fig. 7.1.4E-G). Anyhow, even though the wing blade size in *HA-Dpp$^{\Delta dally}$* flies was smaller, the size difference when compared to the control, was minor.

In a study, researchers found that a version of BMP which lacks the heparin binding side together with a GPC without HS chains was able to activate mad phosphorylation. However, normal BMP together with a GPC without HS chains was not able to activate phosphorylation of mad. They concluded that the heparin binding side of BMP is blocking the BMP-receptor interaction and that the HS chains of the Glypican interrupts this function (Kuo et al., 2010). To test this idea, I expressed *HA-Dpp$^{\Delta dally}$* in *dally* mutants. In this condition, the size of the gradient was still reduced, like in the *dally* mutant (Fig. 7.2.17), arguing against their model.

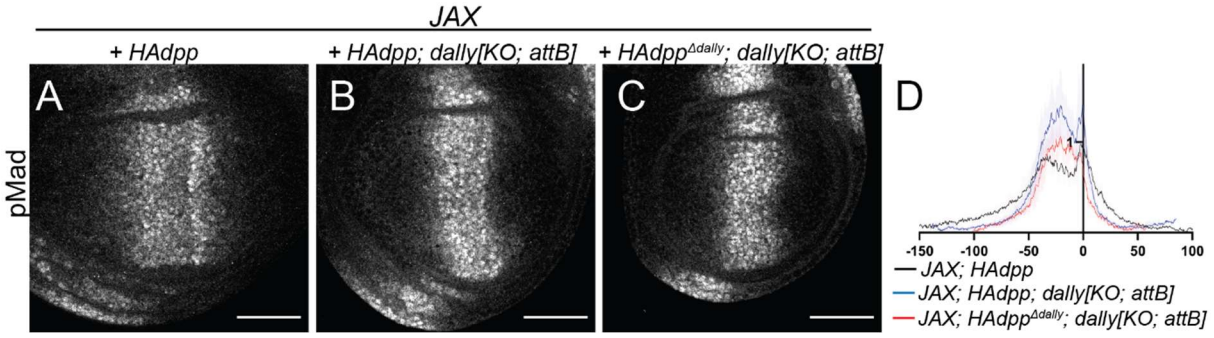


***Figure 7.2.17: JAX;HA-dpp$^{\Delta dally}$ does not rescue the dally mutant phenotype.***
***A,B,C*** *α-pMad staining of JAX;HA-dpp (**A**), JAX;HA-dpp;dally$^{KO}$ (**B**) and JAX;HA-dpp$^{\Delta N}$;dally$^{KO}$ (**C**). **D** Average fluorescence intensity profile of α-pMad staining of JAX;HA-dpp, JAX;HA-dpp;dally$^{KO}$ and JAX;HA-dpp$^{\Delta Dally}$;dally$^{KO}$. Scale bars: 50µm.*

*HA-Dpp$^{\Delta dally}$ can still interact with Dally*

I did not observe the *dally* mutant phenotypes in the *HA-dpp$^{\Delta dally}$* mutant flies. This made me wonder whether HA-Dpp$^{\Delta dally}$ is still able to bind and interact with Dally. To test if there is some binding left, I generated a double tagged *Ollas-HA-Dpp$^{\Delta dally}$* and expressed GFP-HA-Dally in the dorsal compartment using *Hh*-Gal4. When I stained extracellular Ollas-Dpp, I observed high accumulation of Dpp in the dorsal compartment (Fig. 7.1.4H). When the flies expressed the *Ollas-HA-Dpp$^{\Delta dally}$* construct, enhanced Ollas staining was still present when Dally was ectopically expressed (Fig. 7.1.4I). Although the staining intensity was reduced when compared with Ollas-HA-dpp (Fig. 7.1.4H-J), this still demonstrates some, direct or indirect, interaction between Dally and Ollas-HA-Dpp$^{\Delta dally}$.

When I scanned the region around the seven deleted amino acids, I found additional basic amino acids, which could potentially still interact with the HS chains of Dally (Fig. 7.2.18A). I identified five basic amino acids in the area around the deleted region. To see if these basic amino acids are sufficient to interact with Dally, I deleted or changed them to non-basic amino acids and additionally deleted the Dally binding site (HA-Dpp$^{\Delta AA\Delta Dally}$ HA-DppchangedAA$^{\Delta Dally}$)

(Fig. 7.2.18A). Since these additional basic amino acids were part of one of the processing sites of Dpp, I also generated a mutant in which only these basic amino acids were changed, but Dally binding site remained unchanged (HA-DppchangedAA) (Fig. 7.2.18A). The deletion construct seems to be haploinsufficient and I was not able to obtain viable flies of the deletion mutant. However, when combined with JAX, the constructs carrying the changed amino acids were homozygous viable and fertile. The pMad staining in 3$^{rd}$ instar wing discs of these mutants was similar to the staining I observed in *HA-Dpp$^{\Delta dally}$* mutants (Fig. 7.2.18A-F) and the wings did not show any patterning defect (Fig. 7.2.18B'-E'). Anyhow, as observed before in the HA-Dpp$^{\Delta dally}$ wings, the wing size of all three, HA-Dpp$^{\Delta dally}$, HA-DppchangedAA and HA-DppchangedAA$^{\Delta Dally}$ was significantly reduced (Fig. 7.2.18G).

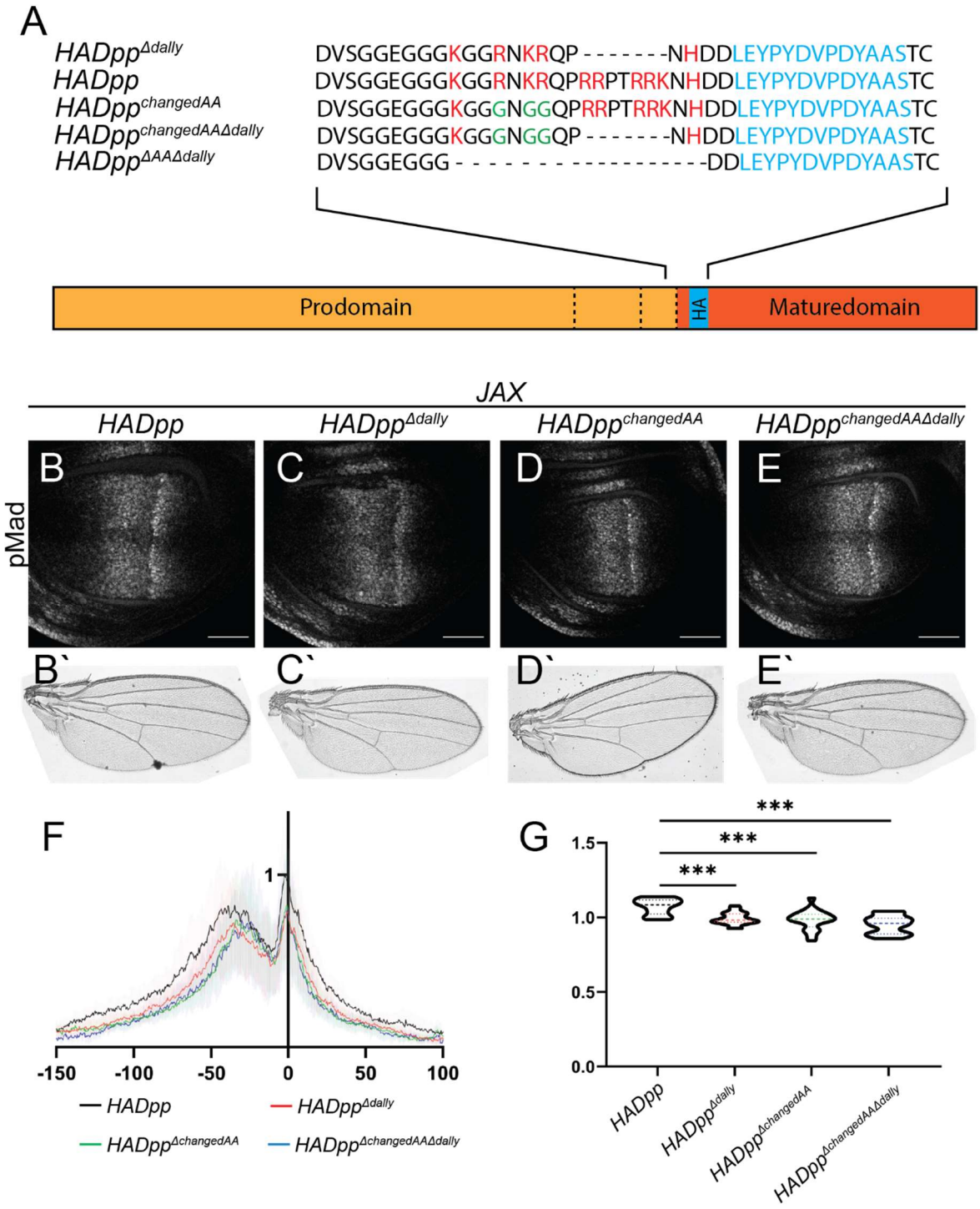


***Figure 7.2.18: Changing all the basic amino acids in the region of the Dally binding side.***
***A*** *N-terminal view of the sequence of HA-Dpp and the different constructs. The basic amino acids are marked in red, the changed ones in yellow and the HA tag in blue.* ***B-E*** *α-pMad stainings in the wing disc of JAX;HA-dpp (**B**), JAX;HA-dppΔdally (**C**), JAX;HA-dppchangedAA (**D**) and JAX;HA-dppchangedAAΔdally (**E**) wing discs.* ***B`-E`*** *Adult wings of the different constructs.* ***F*** *Average intensity profiles of α-pMad staining of JAX;HA-dpp, JAX;HA-dppΔdally, JAX;HA-dppchangedAA and JAX;HA-dppchangedAAΔdally wing discs.* ***G*** *Wing size size comparison of all mutants. Two-tailed unpaired t-test was used for comparison of the wing sizes ($p < 0.0001$). Scale bars: 50µm.*

Since we recently found that the prodomain of Dpp disperses mostly together with the mature domain (unpublished data), I reckon that the prodomain might be able to interact with Dally

and convey the binding to Dally. To see if the prodomain is able to bind to Dally, I expressed a Dpp construct with an Ollas-tagged prodomain and the mature domain tagged with an HA tag, generated in our lab by Milena Bauer. This double-tagged construct allows me to trap the mature domain using the HA-trap expressed with *Hh*-Gal4 and observe the prodomain dispersing in the posterior compartment. When I stained for extracellular Ollas in this condition, I observed high accumulation of the prodomain in the posterior compartment close to the source of Dpp (Fig. 7.2.19A). However, when I additionally expressed GFPHADally in the posterior compartment, I observed higher levels of prodomain accumulation in the posterior compartment (Fig. 7.2.19B,C). It is possible for Dally to antagonize the binding of HA-Dpp to the HA-trap and that is why a larger gradient could be observed when Dally is ectopically expressed. However, this could also be due to an interaction of Dally with the prodomain.

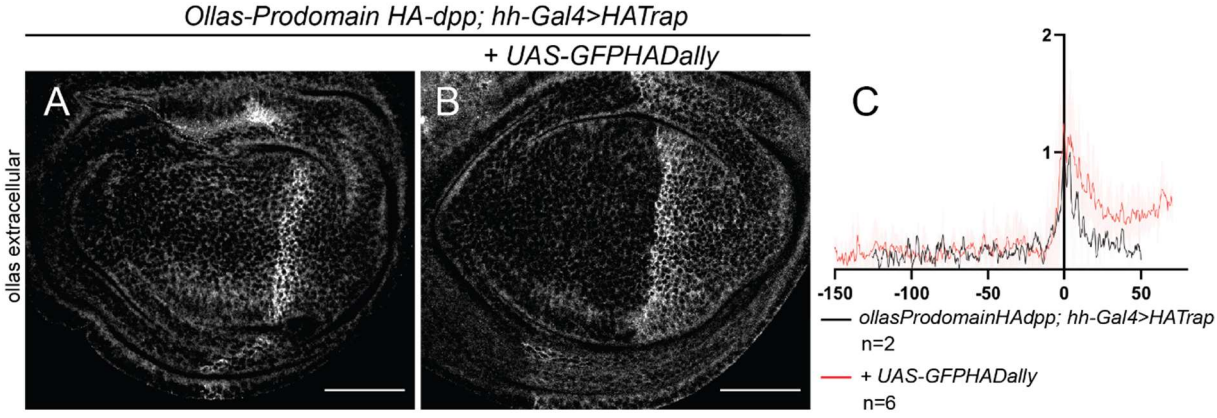


***Figure 7.2.19: Visualizing the Prodomain while trapping the Maturedomain.***
***A*** *Extracellular α-Ollas staining in discs expressing HA-trap in the posterior compartment using Hh-Gal4.* ***B*** *Extracellular α-Ollas staining in discs expressing HA-trap in the posterior compartment and additionally GFPHADally using Hh-Gal4.* ***C*** *Average intensity plots of the trapped OllasProdomain with and without the overexpression of Dally. Scale bars: 50µm.*

To further investigate this possibility, I generated two new constructs with the Dpp prodomain tethered to the membrane through two transmembrane domains and either a wild type mature domain or a Δdally mature domain (TehtProV5DppollasDpp and TehtProV5DppollasDpp$^{\Delta Dally}$). The prodomain was V5-tagged and the mature domain with an Ollas tag. These flies died as early embryos. To be able to observe the wing discs and possible adult phenotypes, these constructs were combined with JAX. Staining for the V5 tag confirmed the prodomain to be tethered to the membrane in the source of Dpp (Fig. 7.2.20A,B). As seen in total stainings of *HA-Dpp$^{\Delta dally}$* before, the intensity of the construct missing the stretch of basic amino acids was stronger than the control (Fig. 7.2.20A,B). When I stained pMad in the

tethered constructs, I could not observe a difference between TehtProV5DppollasDpp and TehtProV5DppollasDpp$^{\Delta Dally}$ (Fig. 7.2.20C-E).

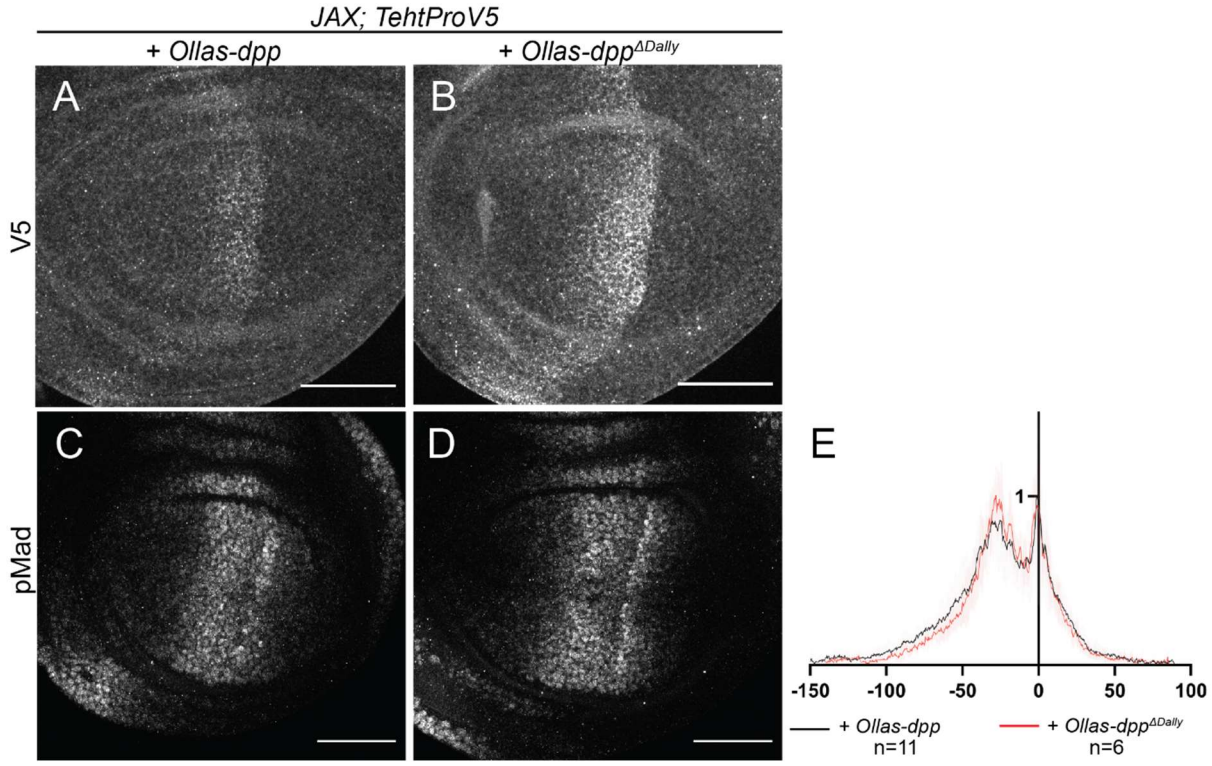


***Figure 7.2.20: pMad staining with a Tethered Prodomain.***
***A,B*** *α-V5 staining in JAX;TehtProV5DppOllasDpp (**A**) and JAX;TehtProV5DppOllasDpp$^{\Delta Dally}$ (**B**) wing discs.* ***C,D*** *α-pMad staining in JAX;TehtProV5DppOllasDpp (**C**) and JAX;TehtProV5DppOllasDpp$^{\Delta Dally}$ (**D**) wing discs.* ***E*** *Average intensity profile of α-pMad staining in JAX;TehtProV5DppOllasDpp and JAX;TehtProV5DppOllasDpp$^{\Delta Dally}$ wing discs. Scale bars: 50µm.*

There are more BMP-like ligands present in the wing disc than just Dpp, and one of them, Gbb, is known to form heterodimers with Dpp, with most of the dimers being heterodimers and only a small amount being homodimers of Dpp (Bauer et al., 2022). Furthermore, a previous study demonstrated the binding of the mammalian Gbb homologue BMP6 to heparin *in vitro* (Billings et al., 2018; Denardo et al., 2021), this allows for the possibility of Gbb interacting with Dally, and via this interaction to rescue the phenotype of *HA-dpp$^{\Delta dally}$* mutants. To investigate the role of Gbb in Dpp-Dally interaction, I expressed *Ollas-HA-dpp$^{\Delta dally}$* together with ectopically expressed GFP-HA-Dally and *gbb*RNAi using *ap*-Gal4. Ollas-HA-Dpp$^{\Delta dally}$ was able to accumulate on overexpressed Dally with the same intensity, when Gbb was present or absent (Fig. 7.2.21A-A''). As demonstrated before, Ollas-HA-Dpp$^{\Delta dally}$ together with overexpressed GFP-HA-Dally was able to enhance the pMad gradient, however, when additionally *gbb*RNAi was expressed, the pMad gradient and intensity was shrunk (Fig.

7.2.21B-B''). These results show that Gbb is important for Dpp signaling but not for Dpp distribution in this condition.

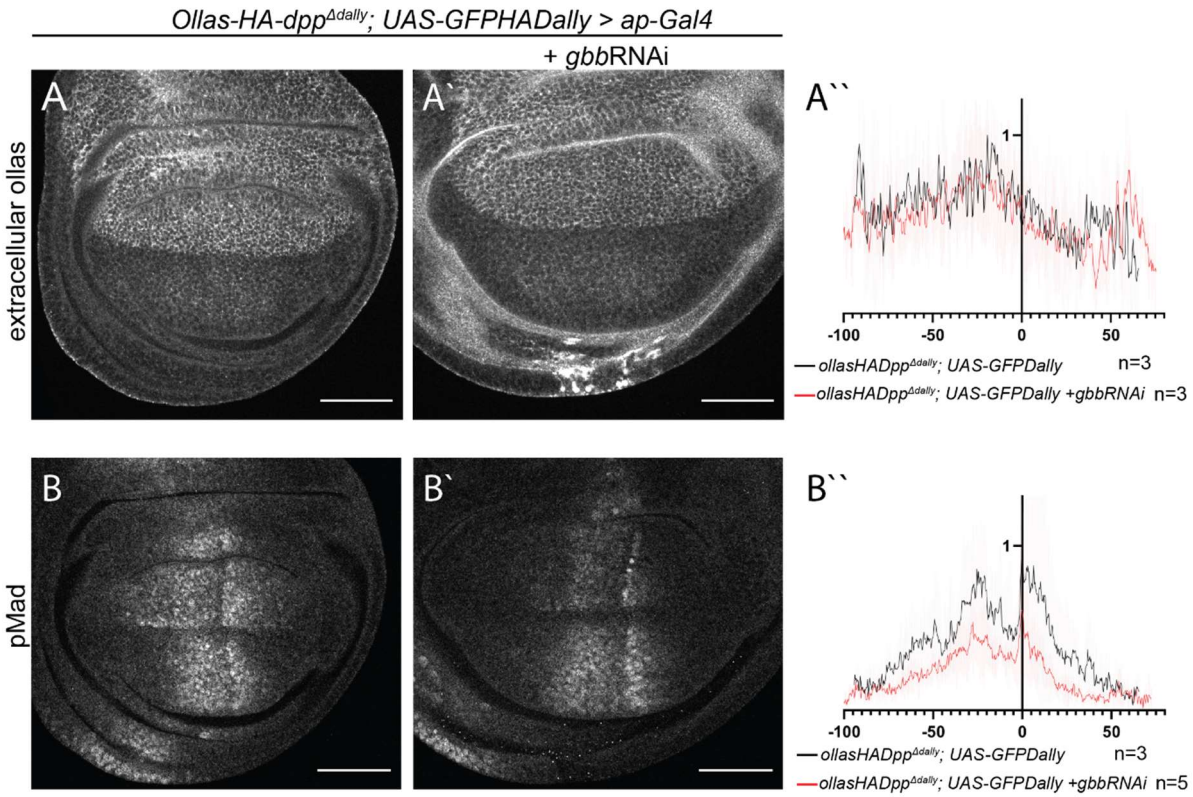


***Figure 7.2.21: JAX;Ollas-HA-dpp$^{\Delta dally}$ together with gbbRNAi can still accumulate on overexpressed Dally.***
***A,A`*** *Extracellular α-Ollas staining of JAX;Ollas-HA-dpp$^{\Delta dally}$,ap-Gal4>;UAS-GFP-HA-Dally (**A**) and JAX;Ollas-HA-dpp$^{\Delta dally}$,ap-Gal4>;UAS-GFP-HA-Dally, gbbRNAi (**A`**) wing discs. **A``** Average intensity profiles of extracellular α-Ollas staining of JAX;Ollas-HA-dpp$^{\Delta dally}$,ap-Gal4>;UAS-GFP-HA-Dally and JAX;Ollas-HA-dpp$^{\Delta dally}$,ap-Gal4>;UAS-GFP-HA-Dally, gbbRNAi wing discs. **B,B`** α-pMad staining of JAX;Ollas-HA-dpp$^{\Delta dally}$,ap-Gal4>;UAS-GFP-HA-Dally (**B**) and JAX;Ollas-HA-dpp$^{\Delta dally}$,ap-Gal4>;UAS-GFP-HA-Dally, gbbRNAi (**B`**) wing discs. **B``** Average intensity profiles of α-pMad staining of JAX;Ollas-HA-dpp$^{\Delta dally}$,ap-Gal4>;UAS-GFP-HA-Dally and JAX;Ollas-HA-dpp$^{\Delta dally}$,ap-Gal4>;UAS-GFP-HA-Dally, gbbRNAi wing discs. Scale bars: 50µm.*

To get more insight into the function of the region including the seven basic amino acids only, I generated a secreted GFP (secGFP) containing these seven basic amino acids (Fig. 7.2.22B'' red region). Modelling of this construct with Alphafold showed that adding the potential interaction domain does not disrupt the folding of the GFP core and the stretch of basic amino acids is easy to access for potential binding partners (Fig. 7.2.22A,'',B''). When this construct is expressed, using *ptc*-Gal4, it can be observed in a central stripe in the wing disc, similar to normal secGFP (Fig. 7.2.22A',B'). However, when I conducted an extracellular staining for GFP, in the secGFP, the GFP signal could be observed uniformly in the whole pouch (Fig 7.2.22A), but in the newly generated construct a stripe of signal could be observed in the centre of the wing disc (Fig. 7.2.22B). As shown in a previous study, cell surface binders for GFP can lead to

a gradient of GFP in the wing imaginal disc (Stapornwongkul et al., 2020). In my experiment I used already existing cell surface molecules and added the binding site to GFP, leading to a GFP gradient. This also demonstrates the ability of the stretch of seven basic amino acids to interact with some cell surface molecule (most likely the HS chains of Dally and Dlp).

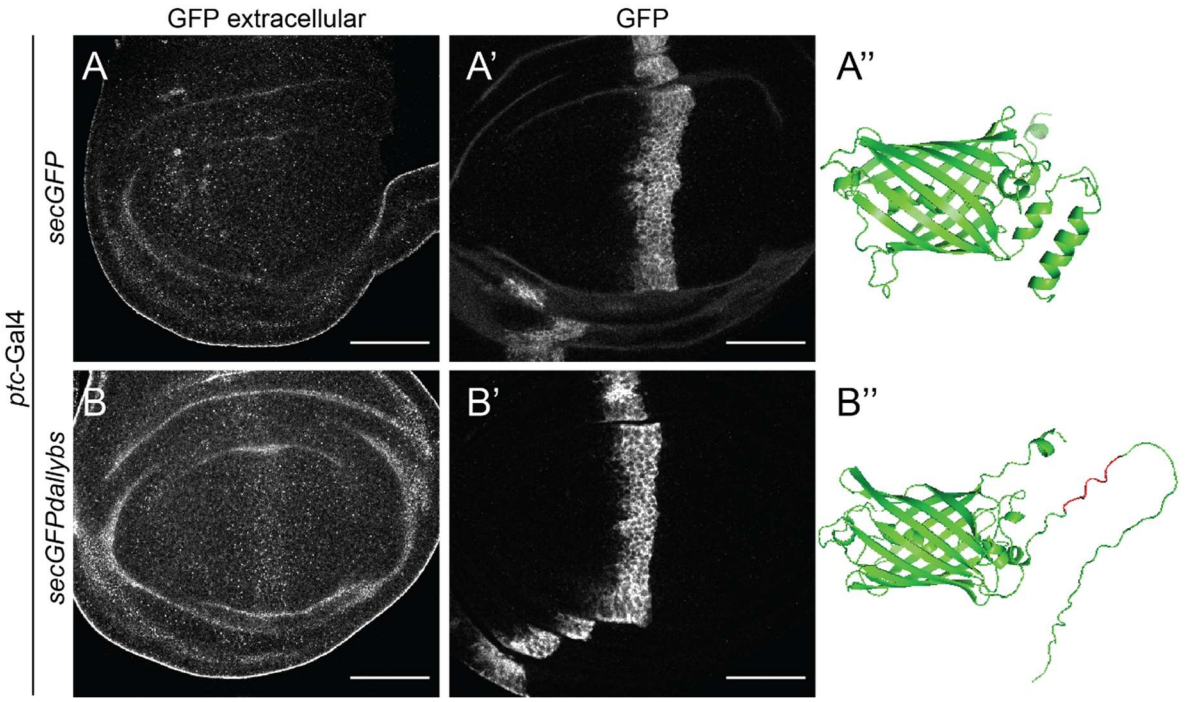


***Figure 7.2.22: secreted GFP with the seven basic amino acids from the Dpp Dally-binding side.***
***A,A'*** *Extracellular (**A**) and conventional (**A'**) α-GFP staining of ptc-Gal4>secGFP wing discs.* ***A''*** *Alphafold predicted structure of secGFP.* ***B,B'*** *Extracellular (**B**) and conventional (**B'**) α-GFP staining of ptc-Gal4>secGFPdallybs wing discs.* ***B''*** *Alphafold predicted structure of secGFPdallybs. Scale bars: 50µm.*

### *7.2.3 Human GPC and BMP*

The human BMP mature domain can only partially function in Drosophila

From a medical point of view, the goal of basic research is to transfer the results from the model organism to humans or, at least, other vertebrates. To see how close human BMP and the Drosophila Dpp are, a previous study generated a construct encoding the Dpp prodomain, but the human BMP4 mature domain (Padgett et al., 1992). In their study, this hybrid DppBMP was ectopically expressed in the Drosophila embryo and it was able to rescue the Dpp function in the Drosophila embryo. However, they were limited by the methods of the time, so I generated two endogenous DppBMP. One construct with the Dally binding site still from Drosophila (DppDallyBMP) (Fig 7.2.23D) and another construct the way it was done in the study before, with the Dally binding site from human BMP4 (DppBMPDally) (Fig. 7.2.23A).

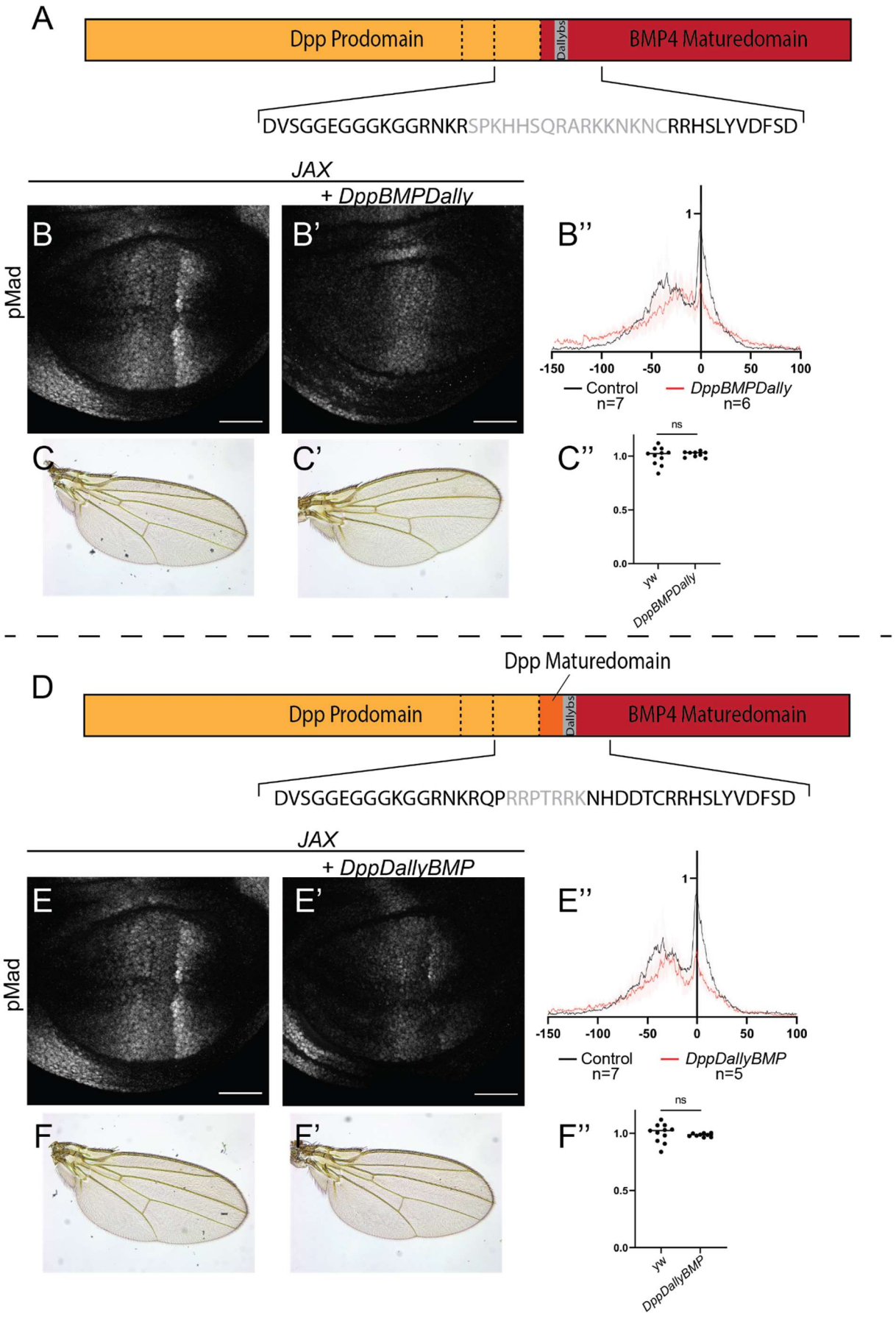


*Figure 7.2.23: JAX;DppBMP shows mild defects in pMad.*

***A** Schematic view of the DppBMPDally construct, with the BMP4 mature domain in red, the Dallybs in grey and the Dpp prodomain in yellow. **B,B'** α-pMad staining in Control (**B**) and JAX;DppBMPDally (**B'**) wing discs. **B''** Average intensity profile of α-pMad staining of DppBMPDally and Control wing discs. **C, C'** Adult wings of yw (**C**) and JAX;DppBMPDally (**C'**) flies. **C''** Adult wing size comparison between yw and JAX;DppBMPDally wings. Two-tailed unpaired t-test was used for comparison of the wing sizes (p=0.5738). **D** Schematic view of the DppDallyBMP construct with the BMP4 mature domain in red, the Dallybs in grey, the Dpp maturedomain in orange and the Dpp prodomain in yellow. **E,E'** α-pMad staining in Control (**E**) and JAX;DppDallyBMP (**E'**) wing discs. **E''** Average intensity profile of α-pMad staining of DppDallyBMP and Control wing discs. **F, F'** Adult wings of yw (**F**) and DppDallyBMP (**F'**) flies. **F''** Adult wing size comparison between yw and JAX;DppDallyBMP wings. Two-tailed unpaired t-test was used for comparison of the wing sizes (p=0.5516). Scale bars: 50µm*

Flies exclusively expressing either one or the other of these endogenous constructs were not homozygous viable and died as embryos.

To overcome this early lethality and investigate the wing discs, I provided the flies with JAX. When combined with JAX, the flies were homozygous viable and fertile. The pMad gradient in the DppBMPDally flies was shrunk and the pMad valley at the anterior/posterior border was gone (Fig. 7.2.23B-B''), similar to *dally* mutants. The pMad gradient in DppDallyBMP was also shrunk and the staining intensity reduced, however, the pMad valley at the anterior/posterior border was present, although with a much lower peak in the posterior compartment along the compartment boundary (Fig. 7.2.23E-E''). The wing size and patterning in adult flies of both constructs was not significantly changed when compared to *yw* control flies (Fig. 7.2.23 C-C''; F-F'').

*Human GPC does not interact with Dpp*

To investigate the effect of human GPC on Dpp in vivo, I used UASGPC3-6 constructs (McGough et al., 2020). When these constructs were expressed using *ap*-Gal4, I could not observe a difference in pMad levels in the dorsal site, when compared to the ventral control (Fig. 7.2.24A-D). However, when I stained for HS, I did observe high accumulation of HS in the dorsal compartment of the wing disc in all four constructs, showing that they were indeed expressed (Fig. 7.2.24I-L).

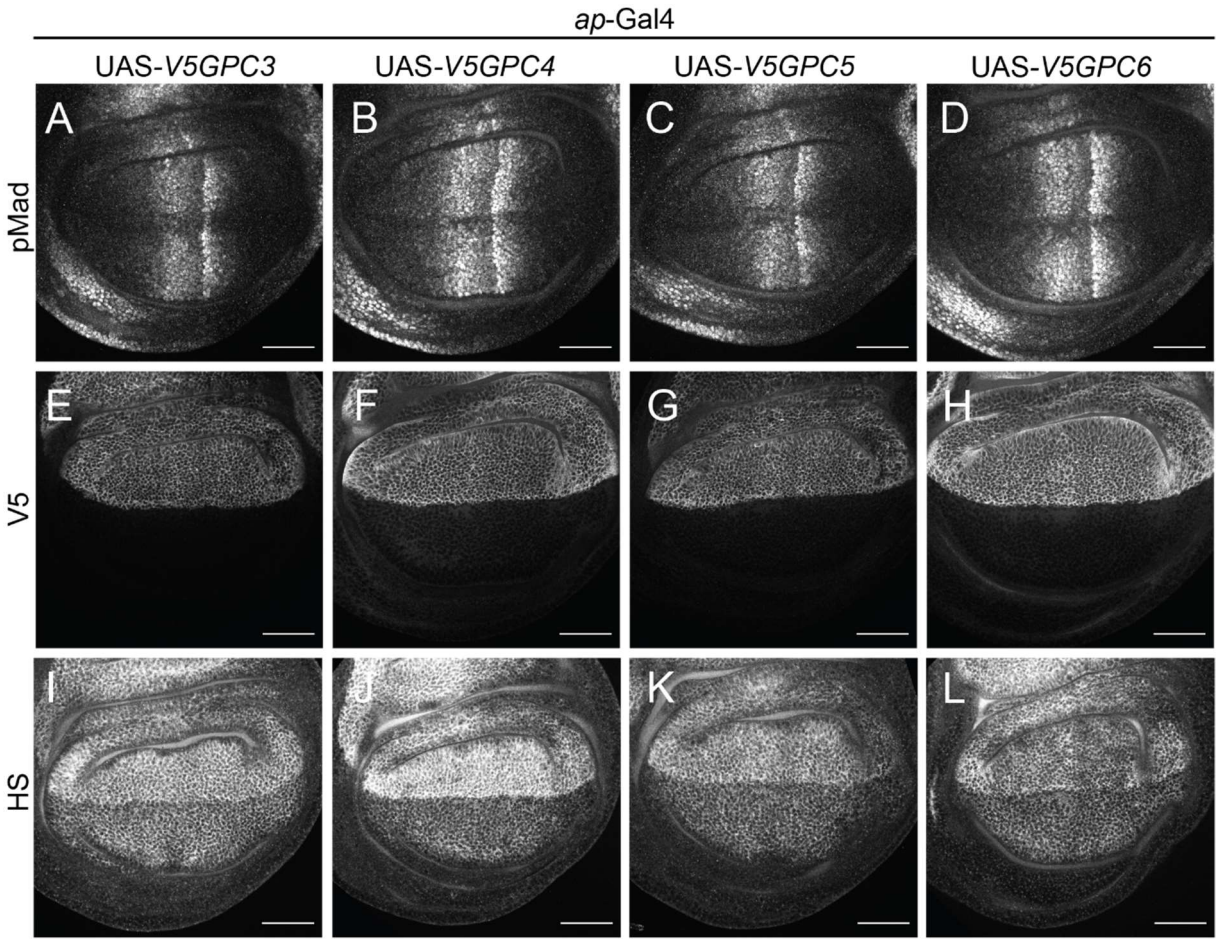


***Figure 7.2.24: Human GPC cannot activate Dpp signaling.***
***A-D*** *α-pMad staining of ap-Gal4>UAS-V5GPC3 (**A**), ap-Gal4>UAS-V5GPC4 (**B**), ap-Gal4>UAS-V5GPC5 (**C**) and ap-Gal4>UAS-V5GPC6 (**D**).* ***E-H*** *α-V5 staining of ap-Gal4>UAS-V5GPC3 (**E**), ap-Gal4>UAS-V5GPC4 (**F**), ap-Gal4>UAS-V5GPC5 (**G**) and ap-Gal4>UAS-V5GPC6 (**H**).* ***I-L*** *α-HS staining of ap-Gal4>UAS-V5GPC3 (**I**), ap-Gal4>UAS-V5GPC4 (**J**), ap-Gal4>UAS-V5GPC5 (**K**) and ap-Gal4>UAS-V5GPC6 (**L**). Scale bars: 50µm.*

Furthermore, I did not observe any accumulation of Ollas-Dpp when the two human Dally homologues, GPC3 and GPC5 were expressed and an extracellular staining was carried out (Fig. 7.2.25).

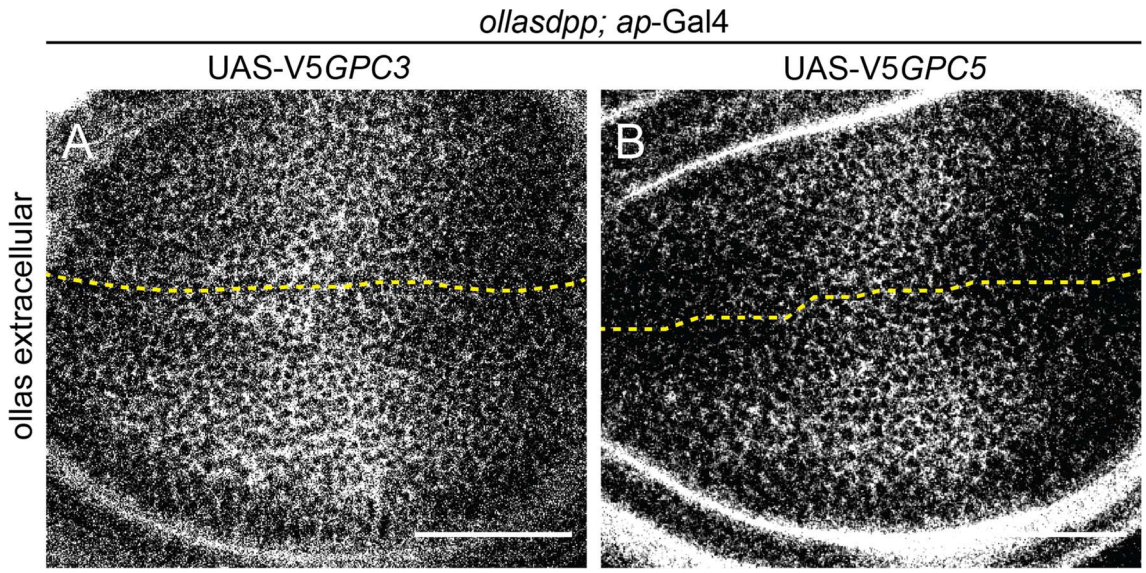


***Figure 7.2.25: Human GPC3 and GPC5 cannot accumulate Dpp.***
***A,B*** *Extracellular α-Ollas staining of Ollas-dpp, ap-Gal4>UAS-V5GPC3 (**A**) and of Ollas-dpp, ap-Gal4>UAS-V5GPC5 (**B**). Scale bars: 50µm.*

### *7.2.4* ***Dpp Glycosylation mutants***

Glycosylation of morphogens has been shown to be important for their function, and several enzymes in the N-glycosylation pathway have been reported to impair Drosophila development (Negreiros et al., 2018). For example, N-linked glycosylation restricts the function of Short gastrulation to bind and shuttle BMPs (Tian & Ten Hagen, 2006). Furthermore, Sog glycosylation mutants display increased BMP binding (Negreiros et al., 2018). BMP is known to be glycosylated in at least five sites, with one glycosylation site being in the mature domain (Hang et al., 2014). It is reasonable to think that Dpp glycosylation mutants have effects on Dpp function. To investigate the function of Dpp glycosylation, Shinya Matsuda generated a glycosylation mutant with the glycosylation side of the Dpp mature domain mutated by exchanging the Asparagin (N) in position 529 to a Glutamin (Q) (HA-dppN529Q), as it was done in previous studies (Hang et al., 2014). This mutation caused lethality and embryos died in early stages. To overcome this early lethality, I combined this mutant with JAX. The combined mutants were viable and survived until adulthood. The pMad in the wing discs of these mutants was reduced when compared to JAX;HA-dpp flies (Fig. 7.2.26A-C). The size and intensity of the extracellular gradient in these mutants was unchanged compared to JAX;HA-dpp flies (Fig. 7.2.26D-F). Anyhow, the adult wings were significantly smaller ($p < 0.0001$) and showed wing vein defects in vein L4 which was partially missing (Fig. 7.2.26G-I). The normal Dpp distribution and the changed pMad levels indicate some problems in signaling in these mutants, while the Dpp distribution is undisturbed.

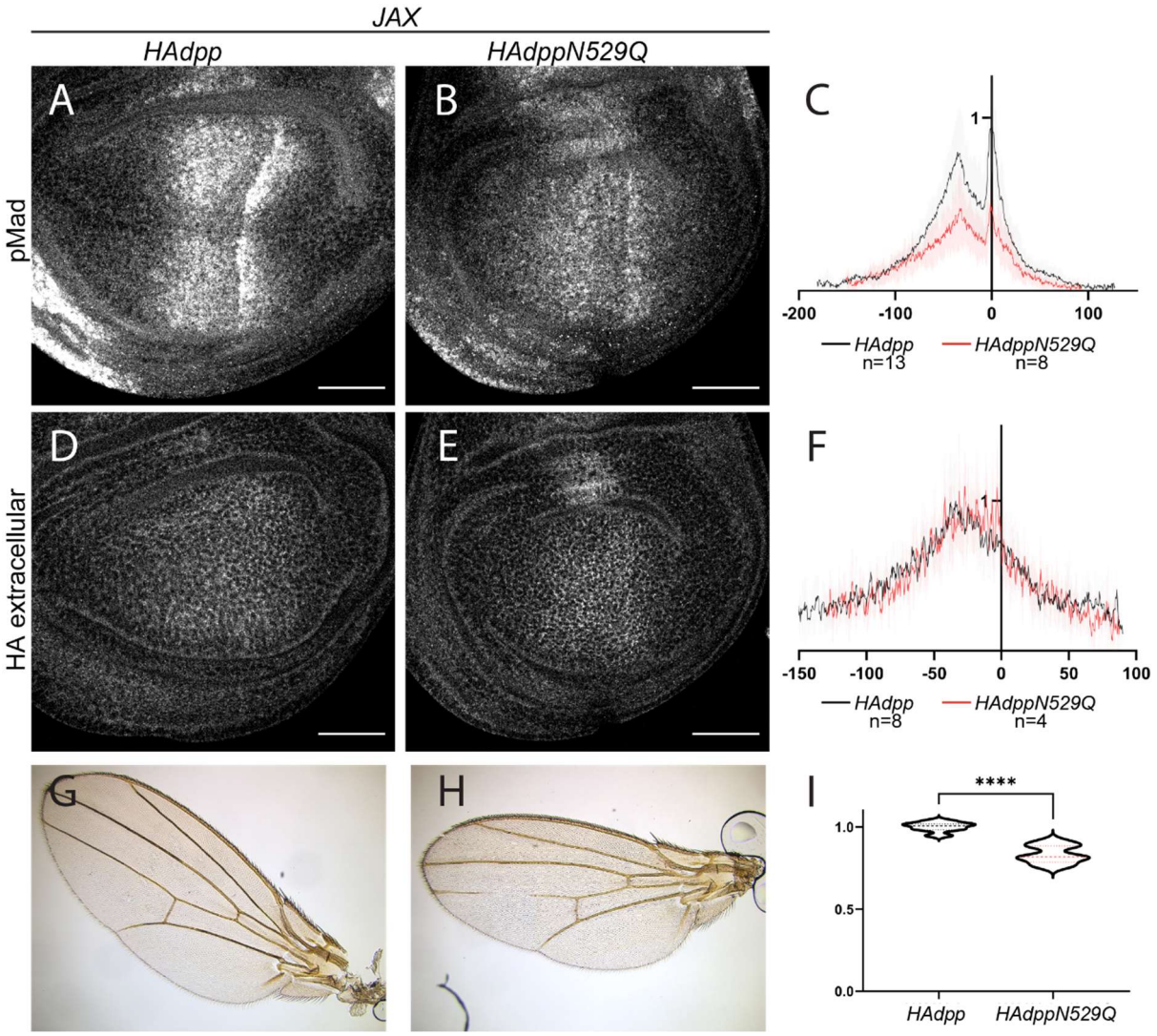


***Figure 7.2.26: Dpp Glycosylation mutants display mild phenotypes in signaling.***
***A,B*** *α-pMad staining of JAX;HA-dpp (**A**) and JAX;HA-dppN529Q (**B**) wing discs.* ***C*** *Average intensity profile of α-pMad staining of JAX;HA-dpp and JAX;HA-dppN529Q wing discs.* ***D,E*** *Extracellular α-HA staining of JAX;HA-dpp (**D**) and JAX;HA-dppN529Q (**E**) wing discs. F Average intensity profile of extracellular α-HA staining of JAX;HA-dpp and JAX;HA-dppN529Q wing discs.* ***G,H*** *Adult wings of JAX;HA-dpp and JAX;HA-dppN529Q flies.* ***I*** *Adult wing size comparison. Two-tailed unpaired t-test was used for comparison of the wing sizes ($p < 0.0001$). Scale bars: 50µm.*

### *7.2.5* ***About the luminal signal in extracellular stainings***

When extracellular stainings were carried out, at times a strong signal could be observed in the lumen of the discs. To investigate this phenomenon and make sure that it is no phenotype, but rather a secondary effect of the staining, caused by antibody entering the lumen, I conducted an extracellular HA staining in *yw* and *HA-dpp* flies. In both these genotypes, wing discs with high accumulation of signal in the lumen could be found (Fig. 7.2.27), demonstrating non-specific luminal signal to exist and being undistinguishable from potential real luminal signal from HA-dpp in the lumen.

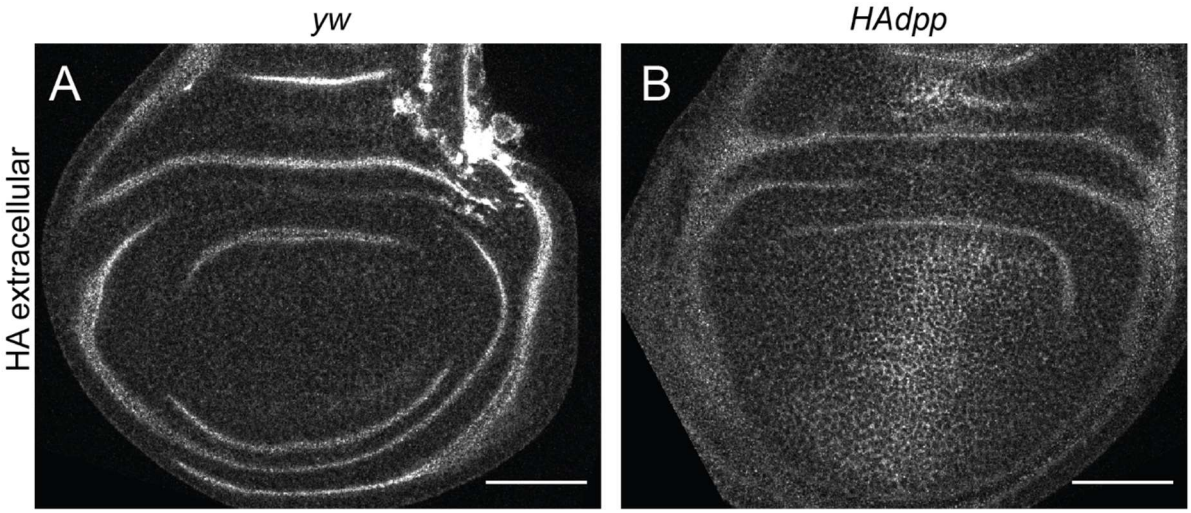


***Figure 7.2.27: Luminal staining in discs stained extracellularly for HA.***
***A*** *Extracellular α-HA staining in yw wing disc.* ***B*** *Extracellular α-HA staining in HA-dpp wing disc. Scale bars: 50µm.*

# Discussion

# 8 Discussion

Summary of the results

Although Dpp is one of the best and longest studied morphogens, the way it disperses through the tissue remains unclear. Depending on the type of tissue, the mode of Dpp dispersal might be different (Hamaratoglu et al., 2014). In this thesis, my focus was on the wing imaginal disc and how Dpp forms a concentration gradient in this specific tissue. Previous studies proposed that Dpp interacts with HSPGs to signal and form a gradient (Akiyama et al., 2008; Dejima et al., 2011; Fujise, 2003; Jackson et al., 1997b). To answer the question of how glypicans control Dpp dispersal and signaling during development of the wing imaginal disc, I used novel methods.

By expressing Dally and Dlp in the dorsal compartment of the wing imaginal disc and looking at pMad levels, I demonstrated that Dally and Dlp do have different functions with regard to Dpp signaling. Furthermore, I also found that the extracellular distribution of Dpp is different in Dally- and Dlp -overexpressing discs. These differences were confirmed when I looked at the knock-out mutants of Dally and Dlp.

Previous studies showed the importance of the glypican GAG chains for Dpp signaling (Bornemann et al., 2004). When I observed a *dally* mutant lacking the HS chains, I was able to confirm their importance for Dpp signaling and distribution (Fig. 7.1.3). However, when this mutant protein was ectopically expressed in the dorsal compartment, Dpp did still accumulate at high levels, illustrating the possibility that Dpp interacts directly with the core protein of Dally (Fig. 7.1.3). Yet, the HS chains appeared to be crucial for Dpp signaling (Fig. 7.1.3). To further investigate the role of the core protein for Dpp signaling and dispersal, I generated different constructs encoding Dally core protein deletions. These deleted versions of Dally were not able to accumulate Dpp anymore. However, when the majority of the core protein was deleted, the HS chains were also absent, indicating some importance of the core protein beyond the known GAG attachment site for HS chain assembly (Fig. 7.2.11).

To further investigate the role of Dally on Dpp dispersal, I induced clones expressing the HA-trap to trap Ollas-HA-Dpp and observe its distribution when Dally was present or in a *dally*RNAi condition (Fig. 7.1.5). Here, I observed less Dpp trapped in the HA-trap clones when Dally was absent, demonstrating some importance of Dally for Dpp distribution. In order to figure out

the mechanism behind this, I stained extracellular Ollas-Dpp when *dally*RNAi and *tkv*RNAi were expressed at the same time using *ap*Gal4. This lead to a normal sized gradient of Dpp in the dorsal compartment, leading to the assumption that Dally acts to prevent Tkv induced internalization of Dpp.

Previous studies identified the HS binding site in BMP/Dpp (Akiyama et al., 2008; Ohkawara et al., 2002; Ruppert et al., 1996), but these studies were not able to investigate mutations abolishing HS interaction under endogenous conditions *in vivo*. I looked at an endogenously expressed *HA-dpp*$^{\Delta Dally}$. In this condition, the pMad and extracellular staining was slightly reduced (Fig. 7.1.4), although *dally* mutants showed more severe phenotypes. Furthermore, this mutant protein was still able to accumulate on overexpressed Dally, indicating either some other regions in Dpp binding to Dally, or some indirect binding to Dally. Although I generated different mutations in Dpp to remove the basic amino acids around the presumed Dally binding site, I did not observe a phenotype similar to the *dally* mutant phenotype. Furthermore, a binding of the prodomain to Dally was excluded by expressing a construct where the prodomain is tethered to the plasma membrane and only the HA-Dpp$^{\Delta Dally}$ or HA-Dpp mature domains are able to disperse. In these conditions, both, the HA-Dpp$^{\Delta Dally}$ and the HA-Dpp mature domain showed similar gradients and intensities of pMad.

In summary, the results show different roles of the *Drosophila* HSPGs in Dpp signaling, possibly due to a direct interaction of Dpp and the core protein of Dally. Furthermore, the HS chains are important for signaling and dispersal in an endogenous condition; however, overexpression of the core protein alone is sufficient to bind Dpp.

*Dally and Dlp have distinct roles in morphogen functions*

The different experiments I performed showed a functional difference between Dally and Dlp. The glypicans Dally and Dlp are thought to control Dpp through the HS chains (Fujise, 2003). However, the relative contributions are not known and studies showing the differences side by side were missing before my work.

Both of these glypicans have HS chains attached to the core protein. If they act only through these HS chains, Dally and Dlp should have the same roles for a given morphogen. Of course, the possibility remains that the HS chains are different. A study showed different HS clusters on glypicans with N-sulfo-rich (NS) and N-acetyl-rich (NA) clusters. It was demonstrated that

Gpc5, the vertebrate Dally homologue possess mostly NS, yet Gpc4, the vertebrate Dlp homologue, possess both NS and NA clusters (Mii et al., 2017). Whether these distinct modifications exist in Drosophila and how they would influence the function and interaction with morphogens remains unknown and to be examined in future studies.

Also in my experiments I confirmed the presence of HS chains on the expressed human GPCs in Drosophila, yet no accumulation of Dpp was observed upon expression of these constructs. This again is a sign that the core protein is important for glypican function. Additionally, previous studies showed that the Dlp core protein interacts with Wg (McGough et al., 2020; Yan, 2012), demonstrating the possibility of the glypican core protein to be involved in morphogen function.

I did not only show the difference of the glypicans in Dpp function, but also in Wg, with reduced Wg accumulation in both *dally*$^{KO}$ and *dlp*$^{KO}$ mutants. However, when Dally and Dlp were overexpressed individually, Wg was affected upon Dlp, but not upon Dally overexpression.

Furthermore, overexpression of Dlp not only affected Wg, but also extracellular Dpp by reducing the gradient width. Since Pent is known to bind directly to HS chains (Norman et al., 2016) and Pent is known to expand the Dpp gradient (Ben-Zvi et al., 2011), Pent bound to the HS chains of Dlp might no longer be functional for its role in Dpp gradient formation, leading to a reduced gradient when Dlp is overexpressed. When overexpressing a glypican, it is also possible that the high amounts of core protein occupy or trap the HS modifying enzymes, taking them away from Dally, leading to less HS-modified Dally on the cell surface. However, these are just assumptions and their testing would need further experiments.

*The Dally core protein can accumulate Dpp*

Dally and Dpp are co-immunoprecipitated from S2 tissue culture cells, suggesting them to form a complex (Kirkpatrick et al., 2006). However, whether this complex is formed through interactions with HS chains or with the core protein is unknown. FGF binding to Dally is mediated by HS chains, but it was shown that BMP4 binding does not entirely depend on HS chains (Kirkpatrick et al., 2006). Furthermore, the same study, using surface plasmon resonance, showed that binding of BMP4 to Dally is not completely abrogated when Dally lacks the HS chains (Kirkpatrick et al., 2006). These results are in support of my results, showing that Dpp accumulates on overexpressed Dally$^{\Delta HS}$ (Fig. 7.1.3). Yet, for Mad to be

phosphorylated, HS chains are required (Fig. 7.1.3). Also, the extracellular Dpp gradient in the presence of Dally$^{\Delta HS}$ mimics the gradient seen in Dally$^{KO}$ (Fig. 7.1.3). Maybe enough core protein is present in the overexpression condition to bind and accumulate Dpp, but in the endogenous condition there is not enough core protein to stabilize Dpp. Also there might be a portion of Dpp escaping the wing disc, this might be prevented by more core protein on the cell surface which binds Dpp and helps to retain it.

However, overexpression of Dally$^{\Delta HS}$ does not enhance pMad, it rather decreases pMad staining intensity in the expressed area. The HS chains are important for Dpp signaling and the Dally core protein binds to Dpp, the core protein without the HS chains is still able to accumulate Dpp, but it is not able to signal. In this case, Dpp bound to the core protein of Dally$^{\Delta HS}$ is taken out of the signaling pool, reducing the amount of pMad formed. Using the core protein deletion construct I made, I did see that the core protein most likely interacts with at least one of the HS modifying enzymes. Since a lot of core protein, to which the HS modifying enzymes can potentially bind, is present upon overexpression of Dally$^{\Delta HS}$, these enzymes or the substrates they are using to synthesise the HS chains might be taken away from wild-type Dally, leading to less Dally with HS chains on the cell surface and, since the HS chains have been shown to be crucial for Dpp signaling, to less pMad.

My findings suggest that the Dally HS chains are important for Dpp signaling and Dpp stability in an endogenous condition. However, they are not the only way for Dpp to bind to Dally.

My results demonstrated that in overexpressed *dally*, Dpp is high in the whole pouch, yet pMad does not reach the very lateral edges. If Dpp activates signaling wherever it is present in the wing disc, we would expect high levels of pMad in the entire wing pouch. It may be possible for the signaling response to take some time, ultimately leading to a graded pMad distribution. Another possibility could be an involvement of Pent. It is known that Pent is able to bind HS chains, since Pent does accumulate on overexpressed Dally, but not on overexpressed Dally$^{\Delta HS}$ (Norman et al., 2016). Furthermore, overexpression of Pent reduced pMad (Zhu et al., 2020), but expanded the Dpp gradient (Vuilleumier et al., 2010). If Pent is blocking the HS or the receptor binding of Dpp, Dpp cannot bind to the receptor anymore and disperses further. Higher amounts of Pent in the lateral sides of the wing pouch lead to less signaling. Furthermore, overexpression of *dally* leads to a wider pMad gradient, while overexpression of *dally* in a *pent* mutant leads to a reduced pMad gradient (Vuilleumier et al., 2010). The extracellular Dpp gradient is not much affected in *pent* mutants, yet the stability

seems to be reduced (Vuilleumier et al., 2010). Also, reduced Tkv levels suppress both, the pMad phenotypes and the adult defects of *pent* mutants and genetic removal of dally does not enhance the *pent* phenotype, suggesting them to act together or in line, demonstrating a role of Pent together with Dally in Dpp stability, most likely through Tkv.

*The role of Dally on Dpp signaling and distribution*

Dally and Tkv have opposite effects on Dpp gradient formation; Dally expands the gradient and Tkv shrinks the gradient. However, when it comes to Dpp signaling, they share the function in that they are both required for signaling, yet in different ways. While Tkv enhances the intensity, Dally mostly enhances its range. Tkv can enhance Dpp signaling cell-autonomously and Dally only enhance signaling in a distance. When the Dpp mature domain was tethered to the cell surface, higher amounts of Dally even reduced the signaling intensity (Fig. 7.2.6). Additionally, the intensity of the pMad signal in Dally-expressing cells is not much higher than in cells expressing Dally at an endogenous level, showing that signal enhancement of Dally is mostly cell-nonautonomous. It has been proposed that Dally stabilize Dpp by inhibiting Tkv-mediated endocytosis and degradation (Akiyama et al., 2008; Entchev et al., 2000; Teleman & Cohen, 2000). Akiyama further described that they observed Dally to colocalize with Tkv and Dpp in the cell (Akiyama et al., 2008). Dally/Tkv/Dpp/Gbb/Punt might form a signaling complex. However, this remains an assumption and it would be nice to solve the structure of this complex in the future and see the potential interaction sites. Along this line, pre-incubation of BMP with its GPC produced a complex which was dissolved by adding BMPR1A (Kirkpatrick et al., 2006), demonstrating a kind of competition between GPC and the receptor for BMP ligand binding, matching the idea of Dally inhibiting Dpp to be endocytosed.

The Dpp gradient is significantly expanded when Tkv is absent and, significantly shrunk when Dally is not present. However, when both, Dally and Tkv are absent, the gradient is only restored to the wild type shape and not expanded such as seen in the *tkv* mutant. This indicates some additional role for Dally in gradient formation, other than enhancement of Dpp stability through Tkv. The difference observed between the Dpp gradient seen in dallyRNAi compared to tkv/dallyRNAi is due to the fraction of Dpp which is endocytosed and degraded. However, the difference observed between tkv/dallyRNAi and tkvRNAi alone, is due to some other effect of Dally on the gradient. There are plenty of possibilities for this other effect, such as keeping Dpp in the disc and stopping it from escaping, or some part of Dpp disperses

through facilitated diffusion, or uptake through other receptor such as Sax or Punt. Or maybe the RNAi is not perfect and some Tkv remains on the cell surface. Unfortunately, to test all these prospects would exceed this Thesis, without a guarantee to find the correct answer.

The finding that the formation of the extracellular Dpp gradient is not much affected in the absence of both Dally and Tkv indicates that at least a portion of Dpp rather freely disperses or disperses with the help of some molecule other than Dally. Furthermore, there might be other cell surface molecules which bind Dpp, enabling Dpp to remain on the cell surface. One possibility for this is Saxophon, the receptor for Gbb. Since in our lab we recently found that Dpp disperses as a heterodimer together with Gbb, these heterodimers could be bound to the receptor of Gbb and by that be able to remain and be visualized on the cell surface. In the future it would be nice to test this idea by additionally removing *sax* and see whether the Dpp gradient is still detectable.

Is the effect of Dally on Tkv direct or not? From the experiments done here, I cannot tell whether Dally binds directly to Tkv or not. As descripted earlier in this paragraph, Akiyama discussed a signaling complex of Dpp, Tkv and Dally in one of his papers (Akiyama et al., 2008). However, since Dpp might not bind to HS and the HS seem to act mostly on Tkv to facilitate Dpp signaling, a direct interaction between Dally core protein and Tkv is unlikely; an interaction between Dally HS chains and Tkv, however, is very much possible. A study demonstrated the binding of Heparin to both, BMP-2 and the BMP receptor (Kanzaki et al., 2008), raising the possibility that Dally HS chains also bind the receptor of Dpp directly. In the future, biochemical assays might help to determine potential binding of Dally and Tkv. Furthermore, treatment with heparin might reduce the binding of Dally to Tkv, since the potential binding sites would be blocked. Under this condition, pMad signaling should be reduced, if HS chains are directly interacting with Tkv.

Dally, together with Boi, was shown to aid Hh recycling for Hh release on the basolateral membrane (Bilioni et al., 2013). Maybe Dally is also involved in Dpp recycling. A recent study showed that recycling of Dpp to the cell surface might be an important factor for gradient formation (Romanova-Michaelides et al., 2022). Maybe Dally also manages a release of Dpp from the receptor after the complex is already internalized and, by that, aids Dpp recycling to the cell surface and form a gradient. However, in my experiments I did observe an enhanced

extracellular gradient of Dpp in wing discs expressing tkvRNAi together with Dally$^{KO}$, making this model very unlikely.

*On the role of HS chains and the core protein for Dally function*

I observed that Dpp accumulates on overexpressed YFP-Dally, and YFP-Dally$^{\Delta HS}$. To be able to tell the importance of the binding to the core protein vs the HS chains, I removed a part of the core protein and no more interaction was found. But also the HS chains were absent on the altered proteins, although they were secreted from the cell and present on the cell surface. A lack of the HS chains indicates some function of the core protein for HS chain synthesis. The known HS chain attachment site of Ser-GIy-X-GIy remained unchanged in my mutant proteins, yet the HS chains seem to be absent. A study on amyloid precursor-like protein, a heparin chain-containing human protein, demonstrated the importance of acidic residues in close proximity of the known GAG attachment site for GAG assembly (Thinakaran et al., 1995). Since Xylosyltransferase initiates the GAG formation, this enzyme presumably needs to interact with the core protein directly. However, this is just a guess and further confirmation is needed. To do so, biochemical assays might be interesting to determine binding of Xylosyltransferase with Dally.

The smaller deletion constructs showed no more binding, too. Either the binding site of Dpp to Dally core protein is in between these deletion constructs, or, more likely, deleting these regions of the core protein disrupts core protein folding and by that the interaction. When the structure was predicted using alphafold, different folding patterns were observed for the deletions when compared to the one seen for wild type Dally, supporting this idea.

*Dpp$^{\Delta Dally}$*

In the embryo, the *Dpp$^{\Delta dally}$* mutant is lethal. This embryonic lethality is unlikely to be caused by the failure of Dpp to bind to HSPGs, since HSPGs are absent during the first three hours of embryonic development when the Dpp gradient is established (Bornemann et al., 2008). Other studies suggest the Dally and the Collagen binding site in Dpp are identical and the 7 amino acids we deleted would represent the binding site for both, Dally and Collagen (Akiyama et al., 2008; Lawrence et al., 2008; Sawala et al., 2012). In the embryo, Dpp forms a gradient from the dorsal to the ventral side, brought about by a shuttling mechanism (Sawala et al., 2012). This shuttling complex requires Dpp to bind to Collagen. Indeed, the stripe of dorsal pMad was

absent in the *Dpp$^{\Delta dally}$* mutants, supporting this model of Dpp gradient formation in the embryo. To further confirm this model, it would be good to directly analyse the extracellular Dpp in the embryo. However, this is technically challenging and the extracellular stainings conducted by me did not lead to interpretable results, due to weak and inconsistent stainings. By using novel labelling techniques such as the insertion of the stronger fluorescent protein Greenlantern into the *dpp* locus, it might be possible to look at the extracellular Dpp and Dpp$^{\Delta dally}$ in the embryo.

In combination with JAX, the *Dpp$^{\Delta dally}$* mutants were viable, survived until adulthood and showed only a mild phenotype with slightly reduced pMad and extracellular distribution in the wing imaginal disc. This is different from *dally* mutants, where the extracellular gradient is strongly affected. If Dpp interacts with Dally only through these seven amino acids, and direct Dpp-Dally interaction is important, this deletion mutant should mimic the *dally* mutant. Also, the *dpp$^{\Delta dally}$* mutant protein was still able to accumulate on overexpressed GFP-Dally, albeit less than wt Dpp. This might be because Dpp binds the core protein and also partially the HS chains. Removing the HS chain binding site leads to less stable binding. However, when the HS chains were removed in a previous experiment, Dpp accumulated on the core protein alone as strongly as on Dally carrying HS chains. Also in *dally*/*HA-dpp$^{\Delta Dally}$* double mutants, the pMad gradient is shrunk just like in the *dally* mutant; however, the intensity is reduced like in the *Dpp$^{\Delta dally}$* mutant. With these results in mind, it seems more likely that the mechanism which causes the mild phenotypes of *Dpp$^{\Delta dally}$* is independent of Dally. And indeed, when I stained total HA-Dpp$^{\Delta dally}$, I saw high accumulation of HA-Dpp$^{\Delta Dally}$ in the source, indicating some issue with secretion or degradation in these mutants. If secretion would be affected, one would expect to observe less extracellular Dpp, which is the case in *HA-Dpp$^{\Delta Dally}$* mutants. I could not observe a higher amount of total Dpp in *dally* mutants. This demonstrates that the effect of Dpp$^{\Delta Dally}$ on total Dpp is independent of Dally, yet the cause for this phenotype remains unclear.

*In vitro* experiments in a previous study showed normal stability and signaling activity of Dpp$^{\Delta N}$ (Akiyama et al., 2008), consistent with my results. However, overexpressed Dpp$^{\Delta N}$ showed less stability *in vivo* (Akiyama et al., 2008). It is possible that the overexpressed Dpp$^{\Delta N}$ oversaturates the system by blocking all the binding sites on the Dally core protein. In wild-type Dpp, additional Dpp might bind to the Dally HS chains, leading to higher stability. To test

the stability of endogenous HA-Dpp$^{\Delta Dally}$, a suitable approach to be taken in the future could be a pulse-chase experiment.

Of course it is possible that Dpp$^{\Delta Dally}$ still binds to and interacts with the HS chains either through some other binding site or indirect through some other molecule. To investigate this possibility, I tested three different ideas of how this binding could still occur. First, I changed additional basic amino acids in the region of the Dally binding site to non-basic amino acids. A previous study tested such mutant proteins in a biochemical assay and found the binding to heparin to be gone (Denardo et al., 2021). Since some of these basic amino acids are located in one of the Dpp processing sites, I also mutated only the basic amino acids in the processing site to see if possible phenotypes are due to a disruption of Dpp processing. Interestingly, the phenotypes of the mutated processing site, and the mutated Dally binding site were similar, with reduced pMad and smaller wing sizes, raising the possibility of the deleted Dally binding site might affect the processing of Dpp in some way.

For the second way to disrupt possible residual binding to HS chains, I wanted to get rid of the prodomain, which could also interact with the HS chains. To do so, I tethered the prodomain to the membrane. The Dpp$^{\Delta Dally}$ maturedomain showed a similar phenotype to the wild-type maturedomain, indicating no involvement of the prodomain in Dpp-HS interaction.

Another BMP-type ligand in the Drosophila imaginal wing disc is Gbb. Gbb is known to form heterodimers and disperse together with Dpp (Bauer et al., 2022). Furthermore, a recent study demonstrated the ability of the mammalian Gbb homologue, BMP6, to bind to heparin through a N- and C-terminal stretch of basic amino acids (Denardo et al., 2021), raising the possibility that Gbb interacts with the HS chains of Dally, and rescues the *dpp$^{\Delta Dally}$* mutant. In a study recently conducted in our lab (Bauer et al., 2022), it was shown that the knochdown of the Gbb receptor Sax leads to a significant reduction in pMad levels, indicating Gbb and Sax to be more important for Dpp signaling than initially thought. These and my results suggest that Gbb is dispensable for Dpp gradient formation when Dally is overexpressed, but essential for proper Dpp signaling.

*HA trap clones accumulate less Dpp when dallyRNAi is expressed*

When the HA trap was expressed in small clones of cells in the posterior compartment, Ollas-HA-Dpp accumulated on these cells. However, when additionally dallyRNAi was expressed in

the entire compartment, less Ollas-HA-Dpp accumulated on these cells. This might be due to a role of Dally in actively helping Dpp to disperse or stabilize on the cell surface. Another possibility explaining these findings is that there is less Dpp to start with. Previous studies demonstrated a role for Dally in Hh signaling (Ayers et al., 2010; Eugster et al., 2007) and Hh signaling being important for Dpp expression (Tanimoto et al., 2000). When I looked at the amount of Dpp trapped in the posterior compartment, I saw less Dpp when dallyRNAi was expressed in the posterior compartment. This might be caused by reduced Dpp production through affected Hh function or by less stability of trapped Dpp by the HA trap in the absence of *dally*, leading to reduced Dpp on the cell surface.

Furthermore, high amounts of YFP-Dally, produced by trapping it in the posterior compartment, lead to higher posterior and anterior levels of pMad. It has been shown before that ectopic expression of Dally in the posterior compartment gives rise to an increased domain of cells expressing Dpp anteriorly. This is due to a higher activity of Hh. Since in my experiment, YFP-Dally is highly accumulated where the morphotrap is expressed, this might act as an overexpression condition, causing higher Hh activity and, consequently, a broader Dpp expression domain. Anyhow, more Hh leads to a reduction of the levels of Tkv, which would consequently lead to reduced pMad levels at the A/P border; however, this is not the case. Maybe cytonemes with a lot of Dally reach into the anterior compartment and modify Dpp stability and signaling, causing higher amounts of pMad.

DppBMP and human GPC

Interestingly, GPC seem to have the opposite function in Xenopus than Dally has in the wing disc. A truncated form of BMP4, which cannot bind to HS (similar to $Dpp^{\Delta dally}$), migrated further in *Xenopus*. Additionally, when the *Xenopus* embryo was treated with heparinase, the BMP gradient was enlarged (Ohkawara et al., 2002). These results are opposite to what I observed in the *Drosophila* wing disc where in *dally* and $dpp^{\Delta dally}$ mutants the pMad levels and the dpp gradient were reduced, albeit at different levels.

In general, it is possible to come up with three different reasons explaining why ligands might fail to form a proper gradient in the extracellular space. First, they may escape the tissue and disperse away from it to act somewhere else; second, they may be degraded by extracellular proteases, or third, they are endocytosed and degraded intracellularly (Akiyama, 2008). Of course, a mixture of all these processes could also occur. However, the exact mechanism

highly depends on the extracellular environmental conditions of the corresponding tissue. Certain tissues might contain more extracellular proteases, others might endocytose faster or slower. Therefore, the observed difference between *Xenopus* and *Drosophila* Glypican and BMP interaction might not be caused by the difference of the interaction itself, but rather by external effects, causing a mutant BMP to move further in a frog, but the same mutant form of Dpp to be hardly affected in Drosophila. In my experiments, in which I overexpressed the human GPC3-6, I could not detect any accumulation of Dpp, in contrast to the experiments in which I overexpressed Dally. This might be due to the different core protein of the GPC and Dally, but it could also be due to the different extracellular environments causing the GPC not to be functional. To test this, a future experiment could be the combination of my DppBMP constructs with the human GPC constructs in the same wing imaginal disc. If the GPC were fully functional in *Drosophila*, they should be able to interact with the DppBMP construct and a higher pMad accumulation should be observed. Yet, the ideal experiment would be to combine the human GPC with a tagged version of DppBMP and look at the extracellular distribution.

# 9 Conclusions

How morphogens disperse in tissues to form a concentration gradient has been under immense discussion since their initial description. It still remains under discussion how one of the best studied morphogens, Dpp, disperses and forms a gradient in the *Drosophila melanogaster* wing imaginal disc. Previous studies showed an importance of glypicans for Dpp gradient formation.

In order to unravel how Dpp forms a gradient, I used new tools and found that Dally, but not Dlp, is required for Dpp stability on the cell surface through antagonizing Tkv-mediated internalization, and by that supporting gradient formation. This function of Dally is mediated by its HS chains; however, direct interaction of Dally and Dpp seemed to be dispensable. The different Dpp signaling and distribution phenotypes observed between *dally* and *dlp* mutants suggests that each of the two glypicans have distinct ligand preference which is mediated by the core protein and not through the HS chains. By removing different parts of the Dally cpre protein I also demonstrated a role of the core protein for HS modification.

These results demonstrate that the spreading mechanism of Dpp is independent of Dally, ruling out the facilitated transport and hindered diffusion model through Dally as a model for Dpp dispersal. Furthermore, my observations demonstrate that the role of Dally in Dpp function is to stabilize Dpp on the cell surface by antogonizing receptor-mediated endocytosis. This function is not through direct interaction of Dally with Dpp, but rather indirect. However, from this study it is not possible to decipher the molecular mechanism behind this function.

In my studies many experiments relied on the extracellular staining of differently tagged Dpp molecules. These antibody stainings are very susceptible to subtle changes in the protocol and can have a high variability, making it necessary to repeat the experiment multiple times to err on the side of caution. In this thesis, I also investigated the phenotypes of *dpp* mutants lacking a stretch of seven amino acids known as the binding site to HS. In these mutants, the phenotypes I observed are mild and do not mimic the *dally* mutant phenotypes. Of course, this might be due to some residual binding of $Dpp^{\Delta Dally}$ to Dally, which is why I tested different possibilities, such as the Prodomain or Gbb binding. However, the possibility of

residual binding between $Dpp^{\Delta Dally}$ and Dally remains and can hardly be ever excluded. The binding of the Dally core protein to Dpp was only observed when Dally was overexpressed, leading to high amounts of Dally on the cell surface. In the endogenous $Dally^{\Delta HS}$ mutants, no proper Dpp gradient was formed. Overexpression of proteins is always a very artificial condition, and the results obtained should be viewed with caution.

To test the binding of Dpp to the Dally core protein, a binding assay would be helpful to use in future experiments. In a biochemical setup, it should be possible to compare binding affinities of Dpp with Dally and $Dally^{\Delta HS}$. Furthermore, the binding between Dally and the Dpp receptor Tkv could be determined. If binding were to be detected between these proteins, solving the structures of these complexes would be the next step, bringing us closer to a better understanding of the relationship of Dpp and Dally for Dpp function. Also, to further assess the stability function of Dally on Dpp, a pulse-chase experiment should be done in the future, using endogenously tagged extracellular Dpp with and without Dally. These experiments could be conducted using a newly tagged version of Dpp, developed by Shinya Matsuda, which already showed promising results to improve the extracellular stainings of Dpp.

My work helps to gain a deeper understanding of how glypicans function in morphogen gradient formation and signaling. However, to fully understand the role of glypicans in Dpp spreading and gradient formation, additional experiments and the use of new methodologies will be fundamental.

# 10 References

Adelman H.B. (1967): The Embryological Treatises of Hieronymus Fabricius of Aquapendente: The Formation of the Egg and of the Chick (De Formatione Ovi et Pulli), The Formed Fetus (De Formato Foetu), Band 1. Cornell University Press, Ithaca, New York, S. 147–191

Akiyama, T., & Gibson, M. C. (2015). Decapentaplegic and growth control in the developing Drosophila wing. *Nature*, *527*(7578), 375–378. https://doi.org/10.1038/nature15730

Akiyama, T., Kamimura, K., Firkus, C., Takeo, S., Shimmi, O., & Nakato, H. (2008). Dally regulates Dpp morphogen gradient formation by stabilizing Dpp on the cell surface. *Developmental Biology*, *313*(1), 408–419. https://doi.org/10.1016/j.ydbio.2007.10.035

Alcedo, J., Ayzenzon, M., Von Ohlen, T., Noll, M., & Hooper, J. E. (1996). The Drosophila smoothened gene encodes a seven-pass membrane protein, a putative receptor for the hedgehog signal. *Cell*, *86*(2), 221–232. https://doi.org/10.1016/S0092-8674(00)80094-X

Alexandre, C., Baena-Lopez, A., & Vincent, J.-P. (2014). Patterning and growth control by membrane-tethered Wingless. *Nature*, *505*(7482), 180–185. https://doi.org/10.1038/nature12879

Almuedo-Castillo, M., Bläßle, A., Mörsdorf, D., Marcon, L., Soh, G. H., Rogers, K. W., Schier, A. F., & Müller, P. (2018). Scale-invariant patterning by size-dependent inhibition of Nodal signalling. *Nature Cell Biology*, *20*(9), 1032–1042. https://doi.org/10.1038/s41556-018-0155-7

Annaval, T., Wild, R., Crétinon, Y., Sadir, R., Vivès, R. R., & Lortat-Jacob, H. (2020). Heparan sulfate proteoglycans biosynthesis and post synthesis mechanisms combine few enzymes and few core proteins to generate extensive structural and functional diversity. *Molecules*, *25*(18). https://doi.org/10.3390/molecules25184215

Aristotle and Peck, (1965). History of Animals. Loeb Classical Library 437. ISBN 9780674994812

Ashique, A. M., Fu, K., & Richman, J. M. (2002). Signalling via type IA and type IB bone morphogenetic protein receptors (BMPR) regulates intramembranous bone formation, chondrogenesis and feather formation in the chicken embryo. *The International Journal of Developmental Biology*, *46*(2), 243–253. https://doi.org/10.1387/ijdb.011535

Ayers, K. L., Gallet, A., Staccini-Lavenant, L., & Thérond, P. P. (2010). The Long-Range Activity of Hedgehog Is Regulated in the Apical Extracellular Space by the Glypican Dally and the

Hydrolase Notum. *Developmental Cell*, *18*(4), 605–620. https://doi.org/10.1016/j.devcel.2010.02.015

Baeg, G. H., Lin, X., Khare, N., Baumgartner, S., & Perrimon, N. (2001). Heparan sulfate proteoglycans are critical for the organization of the extracellular distribution of Wingless. *Development*, *128*(1), 87–94. https://doi.org/10.1242/dev.128.1.87

Balemans, W., & Van Hul, W. (2002). Extracellular Regulation of BMP Signaling in Vertebrates: A Cocktail of Modulators. *Developmental Biology*, *250*(2), 231–250. https://doi.org/10.1006/dbio.2002.0779

Bangi, E., & Wharton, K. (2006). Dpp and Gbb exhibit different effective ranges in the establishment of the BMP activity gradient critical for Drosophila wing patterning. *Developmental Biology*, *295*(1), 178–193. https://doi.org/10.1016/j.ydbio.2006.03.021

Bauer, M., Aguilar, G., Wharton, K. A., Matsuda, S., & Affolter, M. (2022). Heterodimerization-dependent secretion of BMPs in Drosophila. *BioRxiv*.

Belenkaya, T. Y., Han, C., Yan, D., Opoka, R. J., Khodoun, M., Liu, H., & Lin, X. (2004). Drosophila Dpp morphogen movement is independent of dynamin-mediated endocytosis but regulated by the glypican members of heparan sulfate proteoglycans. *Cell*, *119*(2), 231–244. https://doi.org/10.1016/j.cell.2004.09.031

Bellaiche, Y., The, I., & Perrimon, N. (1998). Tout-velu is a Drosophila homologue of the putative tumour suppressor EXT-1 and is needed for Hh diffusion. *Nature*, 85–88.

Ben-Zvi, D., Pyrowolakis, G., Barkai, N., & Shilo, B. Z. (2011). Expansion-repression mechanism for scaling the Dpp activation gradient in drosophila wing imaginal discs. *Current Biology*, *21*(16), 1391–1396. https://doi.org/10.1016/j.cub.2011.07.015

Biehs, B., Sturtevant, M., & Bier, E. (1998). Boundaries in the Drosophila wing imaginal disc organize vein-specific genetic programs. *Development (Cambridge, England)*, *125*, 4245–4257. https://doi.org/10.1242/dev.125.21.4245

Bilioni, A., Sánchez-Hernández, D., Callejo, A., Gradilla, A. C., Ibáñez, C., Mollica, E., Carmen Rodríguez-Navas, M., Simon, E., & Guerrero, I. (2013). Balancing Hedgehog, a retention and release equilibrium given by Dally, Ihog, Boi and shifted/DmWif. *Developmental Biology*, *376*(2), 198–212. https://doi.org/10.1016/j.ydbio.2012.12.013

Billings, P. C., Yang, E., Mundy, C., & Pacifici, M. (2018). Domains with highest heparan sulfate-binding affinity reside at opposite ends in BMP2/4 versus BMP5/6/7:Implications for function. *Journal of Biological Chemistry*, *293*(37), 14371–

14383. https://doi.org/10.1074/jbc.RA118.003191

Bornemann, D. J., Duncan, J. E., Staatz, W., Selleck, S., & Warrior, R. (2004). *Abrogation of heparan sulfate synthesis in Drosophila disrupts the Wingless , Hedgehog and Decapentaplegic signaling pathways*. 1927–1938. https://doi.org/10.1242/dev.01061

Bornemann, D. J., Park, S., Phin, S., & Warrior, R. (2008). A translational block to HSPG synthesis permits BMP signaling in the early Drosophila embryo. *Development*, *135*(6), 1039–1047. https://doi.org/10.1242/dev.017061

Bosch, P. S., Ziukaite, R., Alexandre, C., Basler, K., & Vincent, J. P. (2017). Dpp controls growth and patterning in Drosophila wing precursors through distinct modes of action. *ELife*, *6*, 1–16. https://doi.org/10.7554/eLife.22546

Briscoe, J., Chen, Y., Jessell, T. M., & Struhl, G. (2001). A hedgehog-insensitive form of Patched provides evidence for direct long-range morphogen activity of Sonic hedgehog in the neural tube. *Molecular Cell*, *7*(6), 1279–1291. https://doi.org/10.1016/S1097-2765(01)00271-4

Brummel, T. J., Twombly, V., Marqués, G., Wrana, J. L., Newfeld, S. J., Attisano, L., Massagué, J., O'Connor, M. B., & Gelbart, W. M. (1994). Characterization and relationship of Dpp receptors encoded by the saxophone and thick veins genes in Drosophila. *Cell*, *78*(2), 251–261. https://doi.org/10.1016/0092-8674(94)90295-x

Callejo, A., Culi, J., & Guerrero, I. (2008). Patched, the receptor of Hedgehog, is a lipoprotein receptor. *Proceedings of the National Academy of Sciences of the United States of America*, *105*(3), 912–917. https://doi.org/10.1073/pnas.0705603105

Canalis, E., Economides, A. N., & Gazzerro, E. (2003). Bone morphogenetic proteins, their antagonists, and the skeleton. *Endocrine Reviews*, *24*(2), 218–235. https://doi.org/10.1210/er.2002-0023

Capurro, M. I., Xiang, Y.-Y., Lobe, C., & Filmus, J. (2005). Glypican-3 promotes the growth of hepatocellular carcinoma by stimulating canonical Wnt signaling. *Cancer Research*, *65*(14), 6245–6254. https://doi.org/10.1158/0008-5472.CAN-04-4244

Capurro, M. I., Xu, P., Shi, W., Li, F., Jia, A., & Filmus, J. (2008). Glypican-3 inhibits Hedgehog signaling during development by competing with patched for Hedgehog binding. *Developmental Cell*, *14*(5), 700–711. https://doi.org/10.1016/j.devcel.2008.03.006

Capurro, M., Martin, T., Shi, W., & Filmus, J. (2014). Glypican-3 binds to Frizzled and plays a direct role in the stimulation of canonical Wnt signaling. *Journal of Cell Science*, *127*(7),

1565–1575. https://doi.org/10.1242/jcs.140871

Caussinus, E., Kanca, O., & Affolter, M. (2011). Fluorescent fusion protein knockout mediated by anti-GFP nanobody. *Nature Structural & Molecular Biology*, *19*(1), 117–121. https://doi.org/10.1038/nsmb.2180

Chauvois, L., William H., (1957) His Life and Times, His Discoveries, His Methods. New York: Philosophical Library.

Chen, D., & McKearin, D. M. (2003). A discrete transcriptional silencer in the bam gene determines asymmetric division of the Drosophila germline stem cell. *Development*, *130*(6), 1159–1170. https://doi.org/10.1242/dev.00325

Chen, W., Huang, H., Hatori, R., & Kornberg, T. B. (2017). Essential basal cytonemes take up hedgehog in the Drosophila wing imaginal disc. *Development (Cambridge)*, *144*(17), 3134–3144. https://doi.org/10.1242/dev.149856

Chen, Y., & Struhl, G. (1996). Dual roles for patched in sequestering and transducing Hedgehog. *Cell*, *87*(3), 553–563. https://doi.org/10.1016/S0092-8674(00)81374-4

Cook, O., Biehs, B., & Bier, E. (2004). Brinker and optomotor-blind act coordinately to initiate development of the L5 wing vein primordium in Drosophila. *Development*, *131*(9), 2113–2124. https://doi.org/10.1242/dev.01100

Crick, F. (1970). Diffusion in embryogenesis. *Nature*, *225*(5233), 671. https://doi.org/10.1038/225671b0

Dejima, K., Kanai, M. I., Akiyama, T., Levings, D. C., & Nakato, H. (2011). Novel contact-dependent bone morphogenetic protein (BMP) signaling mediated by heparan sulfate proteoglycans. *Journal of Biological Chemistry*, *286*(19), 17103–17111. https://doi.org/10.1074/jbc.M110.208082

Denardo, A., Elli, S., Federici, S., Asperti, M., Gryzik, M., Ruzzenenti, P., Carmona, F., Bergese, P., Naggi, A., Arosio, P., & Poli, M. (2021). BMP6 binding to heparin and heparan sulfate is mediated by N-terminal and C-terminal clustered basic residues. *Biochimica et Biophysica Acta - General Subjects*, *1865*(2), 129799. https://doi.org/10.1016/j.bbagen.2020.129799

Denzer, K., Kleijmeer, M. J., Heijnen, H. F. G., Stoorvogel, W., & Geuze, H. J. (2000). Exosome: From internal vesicle of the multivesicular body to intercellular signaling device. *Journal of Cell Science*, *113*(19), 3365–3374. https://doi.org/10.1242/jcs.113.19.3365

Diaz de la Loza, M. C., & Thompson, B. J. (2017). Forces shaping the Drosophila wing.

*Mechanisms of Development*, *144*, 23–32. https://doi.org/10.1016/j.mod.2016.10.003

Dobell, C. (1932). Antony van Leeuwenhoek and his „little animals“. S. 353–354. DOI: 10.1007/978-3-642-82396-1_6

Driesch, H. (1891). "Entwicklungsmechanische Studien: I. Der Werthe der beiden ersten Furchungszellen in der Echinogdermenentwicklung. Experimentelle Erzeugung von Theil- und Doppelbildungen. II. Über die Beziehungen des Lichtez zur ersten Etappe der thierischen Form-bildung." Zeitschrift für wissenschaftliche Zoologie 53: 160–84.

Driever, W., & Nüsslein-Volhard, C. (1995). The bicoid protein determines position in the Drosophila embryo in a concentration-dependent manner. *Cell*, *54*(1), 1988. http://www.sciencedirect.com/science/article/pii/0092867488901833

Du, L., Sohr, A., Yan, G., & Roy, S. (2018). Feedback regulation of cytoneme-mediated transport shapes a tissue-specific FGF morphogen gradient. *ELife*, *7*, 1–35. https://doi.org/10.7554/eLife.38137

Dyson, S., & Gurdon, J. B. (1998). The interpretation of position in a morphogen gradient as revealed by occupancy of activin receptors. *Cell*, *93*(4), 557–568. https://doi.org/10.1016/S0092-8674(00)81185-X

Eldar, A., Rosin, D., Shilo, B. Z., & Barkai, N. (2003). Self-enhanced ligand degradation underlies robustness of morphogen gradients. *Developmental Cell*, *5*(4), 635–646. https://doi.org/10.1016/S1534-5807(03)00292-2

Entchev, E. V., Schwabedissen, A., & González-Gaitán, M. (2000). Gradient formation of the TGF-β homolog Dpp. *Cell*, *103*(6), 981–992. https://doi.org/10.1016/s0092-8674(00)00200-2

Escobar, Galvis, M. L., Jia, J., Zhang, X., Jastrebova, N., Spillmann, D., Gottfridsson, E., Van Kuppevelt, T. H., Zcharia, E., Vlodavsky, I., Lindahl, U., & Li, J. P. (2007). Transgenic or tumor-induced expression of heparanase upregulates sulfation of heparan sulfate. *Nature Chemical Biology*, *3*(12), 773–778. https://doi.org/10.1038/nchembio.2007.41

Eugster, C., Panáková, D., Mahmoud, A., & Eaton, S. (2007). Lipoprotein-Heparan Sulfate Interactions in the Hh Pathway. *Developmental Cell*, *13*(1), 57–71. https://doi.org/10.1016/j.devcel.2007.04.019

Filmus, J., Capurro, M., & Rast, J. (2009). Glypicans. *Genome Biology*, *9*(5), 5–10. https://doi.org/10.1186/gb-2008-9-5-224

Franch-Marro, X., Marchand, O., Piddini, E., Ricardo, S., Alexandre, C., & Vincent, J. P. (2005).

Glypicans shunt the Wingless signal between local signalling and further transport. *Development*, *132*(4), 659–666. https://doi.org/10.1242/dev.01639

Fujise, M. (2003). Dally regulates Dpp morphogen gradient formation in the Drosophila wing. *Development*, *130*(8), 1515–1522. https://doi.org/10.1242/dev.00379

Glise, B., Miller, C. A., Crozatier, M., Halbisen, M. A., Wise, S., Olson, D. J., Vincent, A., & Blair, S. S. (2005). Shifted, the Drosophila ortholog of Wnt inhibitory factor-1, controls the distribution and movement of hedgehog. *Developmental Cell*, *8*(2), 255–266. https://doi.org/10.1016/j.devcel.2005.01.003

González-Gaitán, M., & Jäckle, H. (1999). The range of spalt-activating Dpp signalling is reduced in endocytosis-defective Drosophila wing discs. *Mechanisms of Development*, *87*(1), 143–151. https://doi.org/https://doi.org/10.1016/S0925-4773(99)00156-2

González-Méndez, L., Seijo-Barandiarán, I., & Guerrero, I. (2017). Cytoneme-mediated cell-cell contacts for hedgehog reception. *ELife*, *6*, 1–24. https://doi.org/10.7554/eLife.24045

Gorfinkiel, N., Sierra, J., Callejo, A., Ibañez, C., & Guerrero, I. (2005). The Drosophila ortholog of the human Wnt inhibitor factor shifted controls the diffusion of lipid-modified hedgehog. *Developmental Cell*, *8*(2), 241–253. https://doi.org/10.1016/j.devcel.2004.12.018

Greco, V., Hannus, M., & Eaton, S. (2001). Argosomes: A potential vehicle for the spread of morphogens through epithelia. *Cell*, *106*(5), 633–645. https://doi.org/10.1016/S0092-8674(01)00484-6

Gross, G. G., Junge, J. A., Mora, R. J., Kwon, H.-B., Olson, C. A., Takahashi, T. T., Liman, E. R., Ellis-Davies, G. C. R., McGee, A. W., Sabatini, B. L., Roberts, R. W., & Arnold, D. B. (2013). Recombinant probes for visualizing endogenous synaptic proteins in living neurons. *Neuron*, *78*(6), 971–985. https://doi.org/10.1016/j.neuron.2013.04.017

Häcker, U., Lin, X., & Perrimon, N. (1997). The Drosophila sugarless gene modulates Wingless signaling and encodes an enzyme involved in polysaccharide biosynthesis. *Development (Cambridge, England)*, *124*(18), 3565–3573. https://doi.org/10.1242/dev.124.18.3565

Häcker, U., Nybakken, K., & Perrimon, N. (2005). Heparan sulphate proteoglycans: The sweet side of development. *Nature Reviews Molecular Cell Biology*, *6*(7), 530–541. https://doi.org/10.1038/nrm1681

Hama, C., Ali, Z., & Kornberg, T. B. (1990). Region-specific recombination and expression are directed by portions of the Drosophila engrailed promoter. *Genes & Development*, *4*(7), 1079–1093. https://doi.org/10.1101/gad.4.7.1079

Hamaratoglu, F., Affolter, M., & Pyrowolakis, G. (2014). Dpp/BMP signaling in flies: From molecules to biology. *Seminars in Cell and Developmental Biology*, *32*(May 2014), 128–136. https://doi.org/10.1016/j.semcdb.2014.04.036

Han, C., Belenkaya, T. Y., Wang, B., & Lin, X. (2004). Drosophila glypicans control the cell-to-cell movement of Hedgehog by a dynamin-independent process. *Development*, *131*(3), 601–611. https://doi.org/10.1242/dev.00958

Han, C., Yan, D., Belenkaya, T. Y., & Lin, X. (2005). Drosophila glypicans Dally and Dally-like shape the extracellular Wingless morphogen gradient in the wing disc. *Development*, *132*(4), 667–679. https://doi.org/10.1242/dev.01636

Hang, Q., Zhou, Y., Hou, S., Zhang, D., Yang, X., Chen, J., Ben, Z., Cheng, C., & Shen, A. (2014). Asparagine-linked glycosylation of bone morphogenetic protein-2 is required for secretion and osteoblast differentiation. *Glycobiology*, *24*(3), 292–304. https://doi.org/10.1093/glycob/cwt110

Harmansa, S., Alborelli, I., Bieli, D., Caussinus, E., & Affolter, M. (2017). A nanobody-based toolset to investigate the role of protein localization and dispersal in Drosophila. *ELife*, *6*, 1–22. https://doi.org/10.7554/eLife.22549

Harmansa, S., Hamaratoglu, F., Affolter, M., & Caussinus, E. (2015). Dpp spreading is required for medial but not for lateral wing disc growth. *Nature*, *527*(7578), 317–322. https://doi.org/10.1038/nature15712

Harris, R. E., & Ashe, H. L. (2011). Cease and desist: Modulating short-range Dpp signalling in the stem-cell niche. *EMBO Reports*, *12*(6), 519–526. https://doi.org/10.1038/embor.2011.80

Hawley, S. H. B., Wünnenberg-Stapleton, K., Hashimoto, C., Laurent, M. N., Watabe, T., Blumberg, B. W., & Cho, K. W. Y. (1995). Disruption of BMP signals in embryonic Xenopus ectoderm leads to direct neural induction. *Genes and Development*, *9*(23), 2923–2935. https://doi.org/10.1101/gad.9.23.2923

Heldin, C. H., Miyazono, K., & ten Dijke, P. (1997). TGF-beta signalling from cell membrane to nucleus through SMAD proteins. *Nature*, *390*(6659), 465–471. https://doi.org/10.1038/37284

Heyman, R. A., Mangelsdorf, D. J., Dyck, J. A., Stein, R. B., Eichele, G., Evans, R. M., & Thaller, C. (1992). 9-cis retinoic acid is a high affinity ligand for the retinoid X receptor. *Cell*, *68*(2), 397–406. https://doi.org/10.1016/0092-8674(92)90479-V

Hoffmann, F. M., & Goodman, W. (1987). Identification in transgenic animals of the Drosophila decapentaplegic sequences required for embryonic dorsal pattern formation. *Genes & Development*, *1*(6), 615–625. https://doi.org/10.1101/gad.1.6.615

Hsiung, F., Ramirez-Weber, F. A., David Iwaki, D., & Kornberg, T. B. (2005). Dependence of Drosophila wing imaginal disc cytonemes on Decapentaplegic. *Nature*, *437*(7058), 560–563. https://doi.org/10.1038/nature03951

Hufnagel, L., Kreuger, J., Cohen, S. M., & Shraiman, B. I. (2006). On the role of glypicans in the process of morphogen gradient formation. *Developmental Biology*, *300*(2), 512–522. https://doi.org/https://doi.org/10.1016/j.ydbio.2006.08.076

Inoue, H., Imamura, T., Ishidou, Y., Takase, M., Udagawa, Y., Oka, Y., Tsuneizumi, K., Tabata, T., Miyazono, K., & Kawabata, M. (1998). Interplay of signal mediators of decapentaplegic (Dpp): Molecular characterization of Mothers against dpp, Medea, and Daughters against dpp. *Molecular Biology of the Cell*, *9*(8), 2145–2156. https://doi.org/10.1091/mbc.9.8.2145

Jackson, S. M., Nakato, H., Sugiura, M., Jannuzi, a, Oakes, R., Kaluza, V., Golden, C., & Selleck, S. B. (1997a). dally, a Drosophila glypican, controls cellular responses to the TGF-beta-related morphogen, Dpp. *Development (Cambridge, England)*, *124*, 4113–4120. https://doi.org/10.1016/0092-8674(87)90452-1

Jackson, S. M., Nakato, H., Sugiura, M., Jannuzi, A., Oakes, R., Kaluza, V., Golden, C., & Selleck, S. B. (1997b). dally, a Drosophila glypican, controls cellular responses to the TGF-β-related morphogen, Dpp. *Development*, *124*(20), 4113–4120. https://doi.org/10.1242/dev.124.20.4113

Jasuja, R., Allen, B. L., Pappano, W. N., Rapraeger, A. C., & Greenspan, D. S. (2004). Cell-surface heparan sulfate proteoglycans potentiate chordin antagonism of bone morphogenetic protein signaling and are necessary for cellular uptake of chordin. *Journal of Biological Chemistry*, *279*(49), 51289–51297. https://doi.org/10.1074/jbc.M408129200

Jaźwińska, A., Kirov, N., Wieschaus, E., Roth, S., & Rushlow, C. (1999). The Drosophila gene brinker reveals a novel mechanism of Dpp target gene regulation. *Cell*, *96*(4), 563–573.

https://doi.org/10.1016/s0092-8674(00)80660-1

Kakugawa, S., Langton, P. F., Zebisch, M., Howell, S. A., Chang, T. H., Liu, Y., Feizi, T., Bineva, G., O'Reilly, N., Snijders, A. P., Jones, E. Y., & Vincent, J. P. (2015). Notum deacylates Wnt proteins to suppress signalling activity. *Nature*, *519*(7542), 187–192. https://doi.org/10.1038/nature14259

Kanzaki, S., Takahashi, T., Kanno, T., Ariyoshi, W., Shinmyouzu, K., Tujisawa, T., & Nishihara, T. (2008). Heparin inhibits BMP-2 osteogenic bioactivity by binding to both BMP-2 and BMP receptor. *Journal of Cellular Physiology*, *216*(3), 844–850. https://doi.org/10.1002/jcp.21468

Kerszberg, M., & Wolpert, L. (1998). Mechanisms for positional signalling by morphogen transport: A theoretical study. *Journal of Theoretical Biology*, *191*(1), 103–114. https://doi.org/10.1006/jtbi.1997.0575

Kerszberg, M., & Wolpert, L. (2007). Specifying Positional Information in the Embryo: Looking Beyond Morphogens. *Cell*, *130*(2), 205–209. https://doi.org/10.1016/j.cell.2007.06.038

Kicheva, A., Pantazis, P., Bollenbach, T., Kalaidzidis, Y., Bittig, T., Jülicher, F., & González-Gaitán, M. (2007). Kinetics of morphogen gradient formation. *Science*, *315*(5811), 521–525. https://doi.org/10.1126/science.1135774

Kirkpatrick, C. A., Knox, S. M., Staatz, W. D., Fox, B., Lercher, D. M., & Selleck, S. B. (2006). The function of a Drosophila glypican does not depend entirely on heparan sulfate modification. *Developmental Biology*, *300*(2), 570–582. https://doi.org/10.1016/j.ydbio.2006.09.011

Kornberg, T. B., & Roy, S. (2014). Cytonemes as specialized signaling filopodia. *Development (Cambridge)*, *141*(4), 729–736. https://doi.org/10.1242/dev.086223

Koziel, L., Kunath, M., Kelly, O. G., & Vortkamp, A. (2004). Ext1-dependent heparan sulfate regulates the range of Ihh signaling during endochondral ossification. *Developmental Cell*, *6*(6), 801–813. https://doi.org/10.1016/j.devcel.2004.05.009

Kruse, K., Pantazis, P., Bollenbach, T., Jülicher, F., & González-Gaitán, M. (2004). Dpp gradient formation by dynamin-dependent endocytosis: Receptor trafficking and the diffusion model. *Development*, *131*(19), 4843–4856. https://doi.org/10.1242/dev.01335

Künnapuu, J., Björkgren, I., & Shimmi, O. (2009). The Drosophila DPP signal is produced by cleavage of its proprotein at evolutionary diversified furin-recognition sites.

*Proceedings of the National Academy of Sciences of the United States of America*, *106*(21), 8501–8506. https://doi.org/10.1073/pnas.0809885106

Lawrence, R., Olson, S. K., Steele, R. E., Wang, L., Warrior, R., Cummings, R. D., & Esko, J. D. (2008). Evolutionary differences in glycosaminoglycan fine structure detected by quantitative glycan reductive isotope labeling. *Journal of Biological Chemistry*, *283*(48), 33674–33684. https://doi.org/10.1074/jbc.M804288200

Lecuit, T., Brook, W. J., Ng, M., Calleja, M., Sun, H., & Cohen, S. M. (1996). Two distinct mechanisms for long-range patterning by Decapentaplegic in the Drosophila wing. In *Nature* (Vol. 381, Issue 6581, pp. 387–393). https://doi.org/10.1038/381387a0

Lecuit, T., & Cohen, S. M. (1998). Dpp receptor levels contribute to shaping the Dpp morphogen gradient in the Drosophila wing imaginal disc. *Development (Cambridge, England)*, *125*(24), 4901–4907. https://doi.org/10.1242/dev.125.24.4901

Li, S., Li, S., Wang, B., & Jiang, J. (2018). Hedgehog reciprocally controls trafficking of Smo and Ptc through the Smurf family of E3 ubiquitin ligases. *Science Signaling*, *11*(516). https://doi.org/10.1126/scisignal.aan8660

Lin, X., & Perrimon, N. (1999). Dally cooperates with Drosophila Frizzled 2 to transduce Wingless signalling. *Nature*, *400*(6741), 281–284. https://doi.org/10.1038/22343

Litwack, E. D., Ivins, J. K., Kumbasar, A., Paine-Saunders, S., Stipp, C. S., & Lander, A. D. (1998). Expression of the heparan sulfate proteoglycan glypican-1 in the developing rodent. *Developmental Dynamics : An Official Publication of the American Association of Anatomists*, *211*(1), 72–87. https://doi.org/10.1002/(SICI)1097-0177(199801)211:1<72::AID-AJA7>3.0.CO;2-4

Ma, H., Zhao, H., Liu, F., Zhao, H., Kong, R., Shi, L., Wei, M., & Li, Z. (2019). Heparan sulfate negatively regulates intestinal stem cell proliferation in Drosophila adult midgut. *Biology Open*, *8*(10), 1–11. https://doi.org/10.1242/bio.047126

Mandaravally Madhavan, M., & Schneiderman, H. A. (1977). Histological analysis of the dynamics of growth of imaginal discs and histoblast nests during the larval development ofDrosophila melanogaster. *Wilhelm Roux's Archives of Developmental Biology*, *183*(4), 269–305. https://doi.org/10.1007/BF00848459

Martín-Castellanos, C., & Edgar, B. A. (2002). A characterization of the effects of Dpp signaling on cell growth and proliferation in the Drosophila wing. *Development*, *129*(4), 1003–1013. https://doi.org/10.1242/dev.129.4.1003

Martinez-Arias, A., & Lawrence, P. A. (1985). Parasegments and compartments in the Drosophila embryo. *Nature*, *313*(6004), 639–642. https://doi.org/10.1038/313639a0

Marty, T., Müller, B., Basler, K., & Affolter, M. (2000). Schnurri mediates Dpp-dependent repression of brinker transcription. *Nature Cell Biology*, *2*(10), 745–749. https://doi.org/10.1038/35036383

Matsuda, S., & Affolter, M. (2017). Dpp from the anterior stripe of cells is crucial for the growth of the Drosophila wing disc. *ELife*, *6*, 1–9. https://doi.org/10.7554/eLife.22319

Matsuda, S., Harmansa, S., & Affolter, M. (2016). BMP morphogen gradients in flies. *Cytokine and Growth Factor Reviews*, *27*, 119–127. https://doi.org/10.1016/j.cytogfr.2015.11.003

Matsuda, S., Schaefer, J. V., Mii, Y., Hori, Y., Bieli, D., Taira, M., Plückthun, A., & Affolter, M. (2021). Asymmetric requirement of Dpp/BMP morphogen dispersal in the Drosophila wing disc. *Nature Communications*, *12*(1), 1–18. https://doi.org/10.1038/s41467-021-26726-6

Mattes, B., Dang, Y., Greicius, G., Kaufmann, L. T., Prunsche, B., Rosenbauer, J., Stegmaier, J., Mikut, R., Özbek, S., Nienhaus, G. U., Schug, A., Virshup, D. M., & Scholpp, S. (2018). Wnt/PCP controls spreading of Wnt/β-catenin signals by cytonemes in vertebrates. *ELife*, *7*, 1–28. https://doi.org/10.7554/eLife.36953

McGough, I. J., Vecchia, L., Bishop, B., Malinauskas, T., Beckett, K., Joshi, D., O'Reilly, N., Siebold, C., Jones, E. Y., & Vincent, J. P. (2020). Glypicans shield the Wnt lipid moiety to enable signalling at a distance. *Nature*, *585*(7823), 85–90. https://doi.org/10.1038/s41586-020-2498-z

McLellan, J. S., Yao, S., Zheng, X., Geisbrecht, B. V, Ghirlando, R., Beachy, P. A., & Leahy, D. J. (2006). Structure of a heparin-dependent complex of Hedgehog and Ihog. *Proceedings of the National Academy of Sciences of the United States of America*, *103*(46), 17208–17213. https://doi.org/10.1073/pnas.0606738103

Mertens, G., Van der Schueren, B., van den Berghe, H., & David, G. (1996). Heparan sulfate expression in polarized epithelial cells: the apical sorting of glypican (GPI-anchored proteoglycan) is inversely related to its heparan sulfate content. *The Journal of Cell Biology*, *132*(3), 487–497. https://doi.org/10.1083/jcb.132.3.487

Micchelli, C. A., & Perrimon, N. (2006). Evidence that stem cells reside in the adult Drosophila midgut epithelium. *Nature*, *439*(7075), 475–479.

https://doi.org/10.1038/nature04371

Mii, Y., Nakazato, K., Pack, C.-G., Ikeda, T., Sako, Y., Mochizuki, A., Taira, M., & Takada, S. (2021). Quantitative analyses reveal extracellular dynamics of Wnt ligands in \textit{Xenopus} embryos. *ELife*, *10*, e55108. https://doi.org/10.7554/eLife.55108

Mii, Y., Yamamoto, T., Takada, R., Mizumoto, S., Matsuyama, M., Yamada, S., Takada, S., & Taira, M. (2017). Roles of two types of heparan sulfate clusters in Wnt distribution and signaling in Xenopus. *Nature Communications*, *8*(1), 1–19. https://doi.org/10.1038/s41467-017-02076-0

Milán, M., & Cohen, S. M. (2000). Temporal regulation of Apterous activity during development of the Drosophila wing. *Development*, *127*(14), 3069–3078. https://doi.org/10.1242/dev.127.14.3069

Mizutani, C. M., Nie, Q., Wan, F. Y. M., Zhang, Y.-T., Vilmos, P., Sousa-Neves, R., Bier, E., Marsh, J. L., & Lander, A. D. (2005). Formation of the BMP Activity Gradient in the Drosophila Embryo. *Developmental Cell*, *23*(1), 1–7. https://doi.org/10.1016/j.devcel.2005.04.009.Formation

Molnar, C., Ruiz-Gómez, A., Martín, M., Rojo-Berciano, S., Mayor, F., & de Celis, J. F. (2011). Role of the drosophila non-visual ß-arrestin kurtz in hedgehog signalling. *PLoS Genetics*, *7*(3). https://doi.org/10.1371/journal.pgen.1001335

Morimura, S., Maves, L., Chen, Y., & Hoffmann, F. M. (1996). decapentaplegic overexpression affects Drosophila wing and leg imaginal disc development and wingless expression. *Developmental Biology*, *177*(1), 136–151. https://doi.org/10.1006/dbio.1996.0151

Muller, P., Rogers, K. W., Yu, S. R., Brand, M., & Schier, A. F. (2013). Morphogen transport. *Development*, *140*(8), 1621–1638. https://doi.org/10.1242/dev.083519

Nakato, H., Fox, B., & Selleck, S. B. (2002). dally, a Drosophila member of the glypican family of integral membrane proteoglycans, affects cell cycle progression and morphogenesis via a cyclin A-mediated process. *Journal of Cell Science*, *115*(1), 123–130. https://doi.org/10.1242/jcs.115.1.123

Nakato, H., Futch, T. A., & Selleck, S. B. (1995). The division abnormally delayed (daily) gene: A putative integral membrane proteoglycan required far cell division patterning during postembryonic development of the nervous system in Drosophila. *Development*, *121*(11), 3687–3702. https://doi.org/10.1242/dev.121.11.3687

Needham, J. (1942): Biochemistry and Morphogenesis: Biochemistry and Morphogenesis.

785 pages. Cambridge: At The University Press. New York: The Macmillan Company.

Negreiros, E., Herszterg, S., Kang, K.-H., Câmara, A., Dias, W. B., Carneiro, K., Bier, E., Todeschini, A. R., & Araujo, H. (2018). N-linked glycosylation restricts the function of Short gastrulation to bind and shuttle BMPs. *Development (Cambridge, England)*, *145*(22). https://doi.org/10.1242/dev.167338

Nellen, D., Burke, R., Struhl, G., & Basler, K. (1997). Direct and Long-Range Action of a DPP Morphogen Gradient. *Cell*, *85*(3), 1–12. papers2://publication/uuid/BB1BA745-0AE6-429F-B788-0919A11A9C33

Neumann, C. J., & Cohen, S. M. (1997). Long-range action of Wingless organizes the dorsal-ventral axis of the Drosophila wing. *Development*, *124*(4), 871–880. https://doi.org/10.1242/dev.124.4.871

Nohe, A., Keating, E., Knaus, P., & Petersen, N. O. (2004). Signal transduction of bone morphogenetic protein receptors. *Cellular Signalling*, *16*(3), 291–299. https://doi.org/10.1016/j.cellsig.2003.08.011

Norman, M., Vuilleumier, R., Springhorn, A., Gawlik, J., & Pyrowolakis, G. (2016). Pentagone internalises glypicans to fine-tune multiple signalling pathways. *ELife*, *5*(JUNE2016), 1–20. https://doi.org/10.7554/eLife.13301

Nusse, R., & Varmus, H. E. (1982). Many Tumors Induced by the Mouse Mammary Tumor Virus Contain a Provirus Integrated in the Same Region of the Host Genome. *Cell*, *31*(8), 99–109.

Nüsslein-Volhard, C., & Wieschaus, E. (1980). Mutations affecting segment number and polarity in Drosophila. *Nature*, *287*(2), 787–790.

O'Connor, M. B., Umulis, D., Othmer, H. G., & Blair, S. S. (2006). Shaping BMP morphogen gradients in the Drosophila embryo and pupal wing. *Development*, *133*(2), 183–193. https://doi.org/10.1242/dev.02214

Ohkawara, B., Iemura, S., Dijke, P., & Ueno, N. (2002). *Action Range of BMP Is Defined by Its N-Terminal Basic Amino Acid Core*. *12*(01), 205–209.

Ohkawara, B., Yamamoto, T. S., Tada, M., & Ueno, N. (2003). Role of glypican 4 in the regulation of convergent extension movements during gastrulation in Xenopus laevis. *Development (Cambridge, England)*, *130*(10), 2129–2138. https://doi.org/10.1242/dev.00435

Ornitz, D. M., & Itoh, N. (2001). Fibroblast growth factors. *Genome Biology*, *2*(3),

reviews3005.1-3005.12. http://genomebiology.com/2001/2/3/reviews/3005

Padgett, R. W., Wozneyt, J. M., & Gelbart, W. M. (1992). Human BMP sequences can confer normal dorsal-ventral patterning in the Drosophila embryo. *Developmental Biology*, *90*(April), 1–5. papers2://publication/uuid/E5478749-4B6C-4441-A0BB-2420557BA68E

Paine-Saunders, S., Viviano, B. L., & Saunders, S. (1999). GPC6, a novel member of the glypican gene family, encodes a product structurally related to GPC4 and is colocalized with GPC5 on human chromosome 13. *Genomics*, *57*(3), 455–458. https://doi.org/10.1006/geno.1999.5793

Panáková, D., Sprong, H., Marois, E., Thiele, C., & Eaton, S. (2005). Lipoprotein particles are required for Hedgehog and Wingless signalling. *Nature*, *435*(7038), 58–65. https://doi.org/10.1038/nature03504

Pani, A. M., & Goldstein, B. (2018). Direct visualization of a native Wnt in vivo reveals that a long-range Wnt gradient forms by extracellular dispersal. *ELife*, *7*, e38325. https://doi.org/10.7554/eLife.38325

Park, P. W., Reizes, O., & Bernfield, M. (2000). Cell surface heparan sulfate proteoglycans: Selective regulators of ligand-receptor encounters. *Journal of Biological Chemistry*, *275*(39), 29923–29926. https://doi.org/10.1074/jbc.R000008200

Petrášek, Z., & Schwille, P. (2008). Precise measurement of diffusion coefficients using scanning fluorescence correlation spectroscopy. *Biophysical Journal*, *94*(4), 1437–1448. https://doi.org/10.1529/biophysj.107.108811

Pfeiffer, S., Alexandre, C., Calleja, M., & Vincent, J. P. (2000). The progeny of wingless-expressing cells deliver the signal at a distance in Drosophila embryos. *Current Biology*, *10*(6), 321–324. https://doi.org/10.1016/S0960-9822(00)00381-X

Ramírez-Weber, F. A., & Kornberg, T. B. (1999). Cytonemes: Cellular processes that project to the principal signaling center in Drosophila imaginal discs. *Cell*, *97*(5), 599–607. https://doi.org/10.1016/S0092-8674(00)80771-0

Rogers, K. W., & Schier, A. F. (2011a). Morphogen gradients: From generation to interpretation. *Annual Review of Cell and Developmental Biology*, *27*, 377–407. https://doi.org/10.1146/annurev-cellbio-092910-154148

Rogers, K. W., & Schier, A. F. (2011b). Morphogen Gradients: From Generation to Interpretation. *Annual Review of Cell and Developmental Biology*, *27*(1), 377–407. https://doi.org/10.1146/annurev-cellbio-092910-154148

Romanova-Michaelides, M., Hadjivasiliou, Z., Aguilar-Hidalgo, D., Basagiannis, D., Seum, C., Dubois, M., Jülicher, F., & Gonzalez-Gaitan, M. (2022). Morphogen gradient scaling by recycling of intracellular Dpp. *Nature*, *602*(7896), 287–293. https://doi.org/10.1038/s41586-021-04346-w

Rothbauer, U., Zolghadr, K., Tillib, S., Nowak, D., Schermelleh, L., Gahl, A., Backmann, N., Conrath, K., Muyldermans, S., Cardoso, M. C., & Leonhardt, H. (2006). Targeting and tracing antigens in live cells with fluorescent nanobodies. *Nature Methods*, *3*(11), 887–889. https://doi.org/10.1038/nmeth953

Roubinet, C., Tsankova, A., Pham, T. T., Monnard, A., Caussinus, E., Affolter, M., & Cabernard, C. (n.d.). Spatio-temporally separated cortical flows and spindle geometry establish physical asymmetry in fly neural stem cells. *Nature Communications*, 1–15. https://doi.org/10.1038/s41467-017-01391-w

Roux, W. (1888). Beiträge zur Entwicklungsmechanik des Embryo. Nr. 5. Über diekünstliche Hervorbringung “halber” Embryonen durch Zerstörung einer der beiden ersten Furchungszellen, sowie über die Nachentwickelung (Postgeneration) der fehlenden Körperhälfte. Virchows Archiv,CXIV, S. 133–153, 246–291.

Ruberte, E., Marty, T., Nellen, D., Affolter, M., & Basler, K. (1995). An absolute requirement for both the type II and type I receptors, punt and thick veins, for Dpp signaling in vivo. *Cell*, *80*(6), 889–897. https://doi.org/10.1016/0092-8674(95)90292-9

Ruppert, R., Hoffmann, E., & Sebald, W. (1996). Human bone morphogenetic protein 2 contains a heparin-binding site which modifies its biological activity. *European Journal of Biochemistry*, *237*(1), 295–302. https://doi.org/10.1111/j.1432-1033.1996.0295n.x

Sagner, A., & Briscoe, J. (2017). Morphogen interpretation: concentration, time, competence, and signaling dynamics. *Wiley Interdisciplinary Reviews: Developmental Biology*, *6*(4), 1–19. https://doi.org/10.1002/wdev.271

Saha, K., & Schaffer, D. V. (2006). Erratum: Signal dynamics in Sonic hedgehog tissue patterning (Development vol. 133 (889-900)). *Development*, *133*(7), 1411. https://doi.org/10.1242/dev.02337

Sanders, T. A., Llagostera, E., & Barna, M. (2013). Specialized filopodia direct long-range transport of SHH during vertebrate tissue patterning. *Nature*, *497*(7451), 628–632. https://doi.org/10.1038/nature12157

Saremba, S., Nickel, J., Seher, A., Kotzsch, A., Sebald, W., & Mueller, T. D. (2008). Type I

receptor binding of bone morphogenetic protein 6 is dependent on N-glycosylation of the ligand. *FEBS Journal*, *275*(1), 172–183. https://doi.org/10.1111/j.1742-4658.2007.06187.x

Sarrazin, S., Lamanna, W. C., & Esko, J. D. (2011). Heparan sulfate proteoglycans. *Cold Spring Harbor Perspectives in Biology*, *3*(7), 1–33. https://doi.org/10.1101/cshperspect.a004952

Sawala, A., Sutcliffe, C., & Ashe, H. L. (2012). Multistep molecular mechanism for Bone morphogenetic protein extracellular transport in the Drosophila embryo. *Proceedings of the National Academy of Sciences*, *109*(28), 11222–11227. https://doi.org/10.1073/pnas.1202781109

Schwank, G., Dalessi, S., Yang, S. F., Yagi, R., de Lachapelle, A. M., Affolter, M., Bergmann, S., & Basler, K. (2011). Formation of the long range Dpp morphogen gradient. *PLoS Biology*, *9*(7). https://doi.org/10.1371/journal.pbio.1001111

Schwank, G., Restrepo, S., & Basler, K. (2008). Growth regulation by Dpp: an essential role for Brinker and a non-essential role for graded signaling levels. *Development*, *135*(24), 4003–4013. https://doi.org/10.1242/dev.025635

Serpe, M., Umulis, D., Ralston, A., Chen, J., Olson, D. J., Avanesov, A., Othmer, H., O'Connor, M. B., & Blair, S. S. (2008). The BMP-Binding Protein Crossveinless 2 Is a Short-Range, Concentration-Dependent, Biphasic Modulator of BMP Signaling in Drosophila. *Developmental Cell*, *14*(6), 940–953. https://doi.org/10.1016/j.devcel.2008.03.023

Shi, Y., & Massagué, J. (2003). Mechanisms of TGF-β signaling from cell membrane to the nucleus. *Cell*, *113*(6), 685–700. https://doi.org/10.1016/S0092-8674(03)00432-X

Shieh, Y. E., Wells, D. E., & Sater, A. K. (2014). Zygotic expression of exostosin1 (Ext1) is required for BMP signaling and establishment of dorsal-ventral pattern in Xenopus. *International Journal of Developmental Biology*, *58*(1), 27–34. https://doi.org/10.1387/ijdb.130257as

Shimmi, O., Umulis, D., Othmer, H., & O'Connor, M. B. (2005). Facilitated transport of a Dpp/Scw heterodimer by Sog/Tsg leads to robust patterning of the Drosophila blastoderm embryo. *Cell*, *120*(6), 873–886. https://doi.org/10.1016/j.cell.2005.02.009

Sieber, C., Kopf, J., Hiepen, C., & Knaus, P. (2009). Recent advances in BMP receptor signaling. *Cytokine and Growth Factor Reviews*, *20*(5–6), 343–355. https://doi.org/10.1016/j.cytogfr.2009.10.007

Singh, A., & Morris, R. J. (2010). The Yin and Yang of bone morphogenetic proteins in cancer. *Cytokine & Growth Factor Reviews*, *21*(4), 299–313. https://doi.org/10.1016/j.cytogfr.2010.06.003

Song, X., Wong, M. D., Kawase, E., Xi, R., Ding, B. C., McCarthy, J. J., & Xie, T. (2004). Bmp signals from niche cells directly repress transcription of a differentiation-promoting gene, bag of marbles, in germline stem cells in the Drosophila ovary. *Development*, *131*(6), 1353–1364. https://doi.org/10.1242/dev.01026

Spemann, H., & Mangold, H. (1924). über Induktion von Embryonalanlagen durch Implantation artfremder Organisatoren. *Archiv Für Mikroskopische Anatomie Und Entwicklungsmechanik*, *100*(3–4), 599–638. https://doi.org/10.1007/BF02108133

Spencer, F. A., Hoffmann, F. M., & Gelbart, W. M. (1982). Decapentaplegic: A gene complex affecting morphogenesis in Drosophila melanogaster. *Cell*, *28*(3), 451–461. https://doi.org/10.1016/0092-8674(82)90199-4

Sprague, B. L., Pego, R. L., Stavreva, D. A., & McNally, J. G. (2004). Analysis of binding reactions by fluorescence recovery after photobleaching. *Biophysical Journal*, *86*(6), 3473–3495. https://doi.org/10.1529/biophysj.103.026765

Stapornwongkul, K. S., de Gennes, M., Cocconi, L., Salbreux, G., & Vincent, J. P. (2020). Patterning and growth control in vivo by an engineered GFP gradient. *Science*, *370*(6514), 321–327. https://doi.org/10.1126/science.abb8205

Strigini, M., & Cohen, S. M. (1996). A Hedgehog activity gradient contributes to AP axial patterning of the Drosophila wing. *Cell*, *124*(22), 4697–4705. https://doi.org/10.1242/dev.124.22.4697

Takada, R., Mii, Y., Krayukhina, E., Maruyama, Y., Mio, K., Sasaki, Y., Shinkawa, T., Pack, C. G., Sako, Y., Sato, C., Uchiyama, S., & Takada, S. (2018). Assembly of protein complexes restricts diffusion of Wnt3a proteins. *Communications Biology*, *1*(1), 1–14. https://doi.org/10.1038/s42003-018-0172-x

Takeo, S., Akiyama, T., Firkus, C., Aigaki, T., & Nakato, H. (2005). Expression of a secreted form of Dally, a Drosophila glypican, induces overgrowth phenotype by affecting action range of Hedgehog. *Developmental Biology*, *284*(1), 204–218. https://doi.org/10.1016/j.ydbio.2005.05.014

Tanimoto, H., Itoh, S., ten Dijke, P., & Tabata, T. (2000). Hedgehog Creates a Gradient of DPP Activity in Drosophila Wing Imaginal Discs. *Molecular Cell*, *5*(1), 59–71.

https://doi.org/https://doi.org/10.1016/S1097-2765(00)80403-7

Teleman, A. A., & Cohen, S. M. (2000). Dpp gradient formation in the drosophila wing imaginal disc. *Cell*, *103*(6), 971–980. https://doi.org/10.1016/S0092-8674(00)00199-9

The, I., Bellaiche, Y., & Perrimon, N. (1999). Hedgehog movement is regulated through tout velu-dependent synthesis of a heparan sulfate proteoglycan. *Molecular Cell*, *4*(4), 633–639. https://doi.org/10.1016/S1097-2765(00)80214-2

Thinakaran, G., Slunt, H. H., & Sisodia, S. S. (1995). Novel regulation of chondroitin sulfate glycosaminoglycan modification of amyloid precursor protein and its homologue, APLP2. *Journal of Biological Chemistry*, *270*(28), 16522–16525. https://doi.org/10.1074/jbc.270.28.16522

Tian, E., & Ten Hagen, K. G. (2006). Expression of the UDP-GalNAc: polypeptide N-acetylgalactosaminyltransferase family is spatially and temporally regulated during Drosophila development. *Glycobiology*, *16*(2), 83–95. https://doi.org/10.1093/glycob/cwj051

Tickle, C., & Towers, M. (2017). Sonic hedgehog signaling in limb development. *Frontiers in Cell and Developmental Biology*, *5*(FEB), 1–19. https://doi.org/10.3389/fcell.2017.00014

Topczewski, J., Sepich, D. S., Myers, D. C., Walker, C., Amores, A., Lele, Z., Hammerschmidt, M., Postlethwait, J., & Solnica-Krezel, L. (2001). The Zebrafish Glypican Knypek Controls Cell Polarity during Gastrulation Movements of Convergent Extension. *Developmental Cell*, *1*(2), 251–264. https://doi.org/10.1016/S1534-5807(01)00005-3

Toyoda, H., Kinoshita-Toyoda, A., Fox, B., & Selleck, S. B. (2000). Structural analysis of glycosaminoglycans in animals bearing mutations in sugarless, sulfateless, and tout-velu:Drosophila homologues of vertebrate genes encoding glycosaminoglycan biosynthetic enzymes. *Journal of Biological Chemistry*, *275*(29), 21856–21861. https://doi.org/10.1074/jbc.M003540200

Traister, A., Shi, W., & Filmus, J. (2008). Mammalian Notum induces the release of glypicans and other GPI-anchored proteins from the cell surface. *The Biochemical Journal*, *410*(3), 503–511. https://doi.org/10.1042/BJ20070511

Tsuda, M., Kamimura, K., Nakato, H., Archer, M., Staatz, W., Fox, B., Humphrey, M., Olson, S., Futch, T., Kaluza, V., Siegfried, E., Stam, L., & Selleck, S. B. (1999). The cell-surface proteoglycan Dally regulates Wingless signalling in Drosophila. *Nature*, *400*(6741), 276–280. https://doi.org/10.1038/22336

Tsuneizumi, K., Nakayama, T., Kamoshida, Y., Kornberg, T. B., Christian, J. L., & Tabata, T. (1997). Daughters against dpp modulates dpp organizing activity in Drosophila wing development. *Nature*, *389*(6651), 627–631. https://doi.org/10.1038/39362

Turing, A. M. (1990). The chemical basis of morphogenesis. *Bulletin of Mathematical Biology*, *52*(1–2), 153–197. https://doi.org/10.1007/BF02459572

Umulis, D. M. (2009). Analysis of dynamic morphogen scale invariance. *Journal of the Royal Society Interface*, *6*(41), 1179–1191. https://doi.org/10.1098/rsif.2009.0015

Urist, M. R., Strates, B. S., & Brand, R. A. (2009). The classic: Bone morphogenetic protein. *Clinical Orthopaedics and Related Research*, *467*(12), 3051–3062. https://doi.org/10.1007/s11999-009-1068-3

Vallet, S. D., Clerc, O., & Ricard-Blum, S. (2021). Glycosaminoglycan–Protein Interactions: The First Draft of the Glycosaminoglycan Interactome. *Journal of Histochemistry and Cytochemistry*, *69*(2), 93–104. https://doi.org/10.1369/0022155420946403

Van der Horst, D. J., & Ryan, R. O. (2005). Lipid Transport. *Comprehensive Molecular Insect Science*, *4–6*, 225–246. https://doi.org/10.1016/B0-44-451924-6/00055-7

Veugelers, M., De Cat, B., Ceulemans, H., Bruystens, A. M., Coomans, C., Dürr, J., Vermeesch, J., Marynen, P., & David, G. (1999). Glypican-6, a new member of the glypican family of cell surface heparan sulfate proteoglycans. *The Journal of Biological Chemistry*, *274*(38), 26968–26977. https://doi.org/10.1074/jbc.274.38.26968

Vitale, A., & Denecke, J. (1999). *Vitale, A_The Endoplasmic Reticulum—Gateway of the secretory pathway_the plant cell_1999.pdf*. *11*(April), 615–628.

Von Bubnoff, A., & Cho, K. W. Y. (2001). Intracellular BMP signaling regulation in vertebrates: Pathway or network? *Developmental Biology*, *239*(1), 1–14. https://doi.org/10.1006/dbio.2001.0388

Von Ohlen, T., Lessing, D., Nusse, R., & Hooper, J. E. (1997). Hedgehog signaling regulates transcription through cubitus interruptus, a sequence-specific DNA binding protein. *Proceedings of the National Academy of Sciences of the United States of America*, *94*(6), 2404–2409. https://doi.org/10.1073/pnas.94.6.2404

Vuilleumier, R., Affolter, M., & Pyrowolakis, G. (2011). Pentagone patrolling BMP morphogen signaling. *Fly*, *5*(3), 210–214. https://doi.org/10.4161/fly.5.3.15311

Vuilleumier, R., Springhorn, A., Patterson, L., Koidl, S., Hammerschmidt, M., Affolter, M., & Pyrowolakis, G. (2010). Control of Dpp morphogen signalling by a secreted feedback

regulator. *Nature Cell Biology*, *12*(6), 611–617. https://doi.org/10.1038/ncb2064

Waghmare, I., & Page-Mccaw, A. (2021). Glypicans and cytonemes unite to distribute wnt ligands. *Journal of Cell Biology*, *220*(12), 1–2. https://doi.org/10.1083/jcb.202110033

Wang, Y., & Huang, S. (2017). Golgi structure formation, function, and post-translational modifications in mammalian cells. *F1000Research*, *6*, 1–13. https://doi.org/10.12688/f1000research.11900.1

Wartlick, O., Kicheva, A., & González-Gaitán, M. (2009). Morphogen gradient formation. *Cold Spring Harbor Perspectives in Biology*, *1*(3), 1–22. https://doi.org/10.1101/cshperspect.a001255

Willert, K., Brown, J. D., Danenberg, E., Duncan, A. W., Weissman, I. L., Reya, T., Yates, J. R. 3rd, & Nusse, R. (2003). Wnt proteins are lipid-modified and can act as stem cell growth factors. *Nature*, *423*(6938), 448–452. https://doi.org/10.1038/nature01611

Williams, J. A., Bell, J. B., & Carroll, S. B. (1991). Control of Drosophila wing and haltere development by the nuclear vestigial gene product. *Genes and Development*, *5*(12 PART B), 2481–2495. https://doi.org/10.1101/gad.5.12b.2481

Williams, J. A., Paddock, S. W., & Carroll, S. B. (1993). Pattern formation in a secondary field: A hierarchy of regulatory genes subdivides the developing Drosophila wing disc into discrete subregions. *Development*, *117*(2), 571–584. https://doi.org/10.1242/dev.117.2.571

Wiweger, M. I., Zhao, Z., van Merkesteyn, R. J. P., Roehl, H. H., & Hogendoorn, P. C. W. (2012). HSPG-deficient zebrafish uncovers dental aspect of multiple osteochondromas. *PLoS ONE*, *7*(1). https://doi.org/10.1371/journal.pone.0029734

Wodarz, A., & Nusse, R. (1998). Mechanisms of Wnt signaling in development. *Annual Review of Cell and Developmental Biology*, *14*, 59–88. https://doi.org/10.1146/annurev.cellbio.14.1.59

Wolpert, L. (1969). Positional information and the spatial pattern of cellular differentiation, Journal of Theoretical Biology, Volume 25, Issue 1, 1969, Pages 1-47, ISSN 0022-5193, https://doi.org/10.1016/S0022-5193(69)80016-0

Yan, D. (2012). *The core protein of glypican Dally-like determines its biphasic activity in Wingless morphogen signaling*. *17*(4), 470–481. https://doi.org/10.1016/j.devcel.2009.09.001.The

Yao, S., Lum, L., & Beachy, P. (2006). The Ihog Cell-Surface Proteins Bind Hedgehog and

Mediate Pathway Activation. *Cell*, *125*(2), 343–357. https://doi.org/10.1016/j.cell.2006.02.040

Yu, S. R., Burkhardt, M., Nowak, M., Ries, J., Petráek, Z., Scholpp, S., Schwille, P., & Brand, M. (2009). Fgf8 morphogen gradient forms by a source-sink mechanism with freely diffusing molecules. *Nature*, *461*(7263), 533–536. https://doi.org/10.1038/nature08391

Zecca, M., Basler, K., & Struhl, G. (1995). Sequential organizing activities of *engrailed*, *hedgehog* and *decapentaplegic* in the *Drosophila* wing. *Development (Cambridge, England)*, *121*(8), 2265–2278. http://www.ncbi.nlm.nih.gov/pubmed/7671794

Zhou, S., Lo, W. C., Suhalim, J. L., Digman, M. A., Gratton, E., Nie, Q., & Lander, A. D. (2012). Free extracellular diffusion creates the Dpp morphogen gradient of the Drosophila wing disc. *Current Biology*, *22*(8), 668–675. https://doi.org/10.1016/j.cub.2012.02.065

Zhu, Y., Qiu, Y., Chen, W., Nie, Q., & Lander, A. D. (2020). Scaling a Dpp Morphogen Gradient through Feedback Control of Receptors and Co-receptors. *Developmental Cell*, *53*(6), 724-739.e14. https://doi.org/10.1016/j.devcel.2020.05.029